Analysing polyubiquitin chain signalling by means of tailor-made ubiquitin ligases

Dissertation

Zur Erlangung des Grades

“Doktor der Naturwissenschaften”

(Dr. rer. nat.)

am Fachbereich Biologie

der Johannes Gutenberg-Universität Mainz

Kirill Petriukov

geboren am 30.05.1995 in Sankt Petersburg

JOHANNES GUTENBERG UNIVERSITÄT MAINZ

JG|U

Juli 2023

Dekan:

1st examiner:

2nd examiner:

Date: 11.01.2024

Declaration

I, Kirill Petriukov, confirm that the work presented in this thesis is my own. Where information has been derived from other sources, I confirm that it has been indicated in the thesis.

Abstract

Ubiquitylation is a widespread posttranslational modification involved in all major cellular pathways. Ubiquitin can be attached to target proteins as a single moiety or form conjugates of higher complexity, creating unique interaction surfaces on the substrates, called the 'ubiquitin code'. DNA sliding clamp PCNA is one of the substrates for which mono- and polyubiquitylation have been shown to perform different functions during replication over damaged DNA. Monoubiquitylation of PCNA recruits translesion synthesis polymerases, whereas modification of PCNA with a K63-linked polyubiquitin chain activates an error-free damage bypass pathway in a mechanistically poorly characterised manner.

To explore the roles of PCNA polyubiquitylation in human cells, tailor-made ubiquitin ligases were designed and applied to create ubiquitin chains on PCNA independently of the responsible cellular enzymes. These tailor-made enzymes harbour a PCNA-interaction motif combined with linkage-specific ubiquitin ligase domains, designed to create M1-, K63- and K48-linked ubiquitin chains. By applying tailor-made ligases in human cells, I demonstrate that unscheduled modification of PCNA with K63-linked polyubiquitin chains leads to global replication collapse. Mass spectrometry-based analysis identifies the ubiquitin-dependent segregase VCP as the responsible effector. By performing a series of independent *in vitro* and *in vivo* assays, I demonstrate that K63-linked chains on PCNA are further modified by the E2 enzyme UBE2K with K48 linkages, leading to the recruitment of VCP, PCNA degradation and checkpoint activation. I further demonstrate that the build-up of branched K63-K48 chains is not an artefact of tailor-made enzymes but is a general cellular pathway, which takes place upon replication over damaged DNA and underlies the synthetic lethality between the tumour suppressor BRCA1 and the deubiquitylating enzyme USP1.

Finally, I describe the 'Ubiquiton' technology recently designed in our laboratory. It allows inducible polyubiquitylation of any protein of interest with M1-, K63- and K48-linked chains. By applying this technology to human histone H2B, I demonstrate the feasibility of this approach in human cells. Altogether, this work focuses on two protein engineering technologies, which allowed to explore the functions of PCNA polyubiquitylation and provides the basis for a study of ubiquitin signalling on other substrates.

Zusammenfassung

Die Ubiquitinierung ist eine weit verbreitete posttranslationale Modifikation, die an allen wichtigen zellulären Signalwegen beteiligt ist. Ubiquitin kann als einzelnes Molekül an das Zielprotein angehängt werden oder Konjugate in höherer Komplexität bilden, die als 'Ubiquitin-Code' bezeichnet werden. Einige Substrate wie beispielsweise das DNA-Ringklemmenprotein PCNA üben je nach Ubiquitinierungsstatus unterschiedliche Funktionen aus. Während der Replikation beschädigter DNA dient die Monoubiquitinierung von PCNA als Rekrutierungssignal für Transläsionspolymerasen, während die Modifikation von PCNA mit einer K63-verknüpften Polyubiquitinkette, auf noch mechanistisch unzureichend charakterisierte Weise, den fehlerfreien ‘Template Switching’ Signalweg aktiviert.

Um die Rollen der PCNA-Polyubiquitinierung in menschlichen Zellen zu erforschen, wurden maßgeschneiderte Ubiquitin-Ligasen entworfen und angewendet, welche unabhängig von den verantwortlichen zellulären Enzymen Ubiquitinketten auf PCNA synthetisieren. Diese maßgeschneiderten Enzyme enthalten ein PCNA-Interaktionsmotiv kombiniert mit verknüpfungsspezifischen Ubiquitin-Ligase-Domänen, die so konzipiert sind, dass sie M1-, K63- und K48-verknüpfte Ubiquitinketten erzeugen. In der vorliegenden Arbeit werden die maßgeschneiderten Ubiquitin-Ligasen verwendet um die Rollen der PCNA-Polyubiquitinierung in menschlichen Zellen zu untersuchen. Ich weise nach, dass eine außerplanmäßige Modifikation von PCNA mit K63-verknüpften Polyubiquitinketten zum Zusammenbruch der Replikation führt. Eine Massenspektrometrie-basierte Analyse identifizierte die Ubiquitin-Segregase VCP als Interaktor von polyubiquitiniertem PCNA *in vivo*. Durch eine Reihe von unabhängigen *in vitro* und *in vivo* Assays zeige ich, dass K63-verknüpfte Ketten auf PCNA durch das E2-Enzym UBE2K mit K48-Verknüpfungen weiter modifiziert werden. Dies resultiert in der Rekrutierung von VCP, dem Abbau von PCNA und der Aktivierung des Checkpoints. Darüber hinaus zeige ich weiter, dass der Aufbau verzweigter K63-K48-Ketten kein Artefakt der maßgeschneiderten Enzyme ist, sondern vielmehr ein allgemeiner zellulärer Prozess, der bei der Replikation geschädigter DNA abläuft und der der synthetischen Letalität zwischen dem Tumorsuppressor BRCA1 und der Deubiquitinase USP1 zugrunde liegt.

Abschließend beschreibe ich die kürzlich in unserem Labor entwickelte Technologie namens 'Ubiquiton', die eine induzierbare Polyubiquitinierung jedes beliebigen Proteins mit M1-, K63- oder K48-verknüpften Ketten ermöglicht. Indem ich diese Technologie bei dem menschlichen Histon H2B einsetze, demonstriere ich die Anwendbarkeit dieses Systems in menschlichen Zellen. Insgesamt konzentriert sich diese Arbeit auf zwei Technologien des Protein-Engineerings, die es ermöglichen, die Funktionen der PCNA-Polyubiquitinierung zu erforschen und die zusätzlich die Grundlage für die Untersuchung der Ubiquitin-Signale anderer Substrate schaffen.

Acknowledgements

Contents

List of figures

List of tables

Chapter 1

Introduction

1.1 The Ubiquitin system

1.1.1 Ubiquitin as a posttranslational modifier

Protein-protein interactions form the basis of life. Whereas some proteins tend to interact with each other constitutively, many protein-protein interactions emerge or disappear as a response to certain stimuli. Regulation of protein interactions often occurs at a posttranslational level through protein modification, as it does not require time-consuming *de novo* protein synthesis. Modification of a protein can change its interactome, stability or subcellular localisation and may initiate or terminate cellular pathways. More than 400 posttranslational modifications (PTMs) are known, affecting side chains of amino acids as well as N- and C-termini of proteins (Khoury *et al.,* 2011). Many PTMs are small modifications of amino acids: typical examples are phosphorylation, methylation or acetylation. The addition of a modification changes the charge distribution and spatial characteristics of a given amino acid, thereby affecting corresponding interactions. Importantly, due to their size, small modifications are recognised in the context of surrounding amino acids: the precise position of a small modification in a protein may drastically change its function. A canonical example is the modification of histone tails: trimethylation of lysines K4 and K9 of histone H3, which are separated by just four amino acids, leads to opposite effects on gene expression (Lu *et al.,* 2018; Bannister and Kouzarides, 2011).

An 8.6 kDa protein Ubiquitin, as well as a family of structurally related proteins, termed ubiquitin-like modifiers (UBLs), can also serve as a posttranslational modification. Attachment of ubiquitin to target proteins occurs via an isopeptide bond between the C-terminal glycine of ubiquitin and the ε-amino group of the substrate lysine. Although lysine is the most common ubiquitylation target, other amino acids such as serine, cysteine, threonine or N-terminal methionine have also been shown to be ubiquitylated (McClellan *et al.,* 2019; Ciechanover, 2005; Ben-Saadon *et al.,* 2004). In striking contrast to small

modifications, ubiquitin is several magnitudes larger and, for small substrates, can be comparable in size to its target proteins. Not surprisingly, the attachment of ubiquitin may result in a conformational change of a region surrounding the attachment site, as suggested by *in silico* simulations for Ubc7 and p19 (Hagai and Levy, 2010). Due to its size, recognition of ubiquitin usually occurs by means of dedicated ubiquitin-binding domains (Husnjak and Dikic, 2012), allowing for certain flexibility in terms of an attachment site (discussed later in **section 1.1.6.3**). The importance of ubiquitin is highlighted by its extremely high conservation: just three amino acids out of 76 differ between yeast and human ubiquitin (Zuin *et al.,* 2014). Being present at approximately 10^8 copies per cell, ubiquitin is one of the most abundant proteins, amounting to up to 5% of all proteins in a cell (Yewdell 2001; Haas and Bright, 1985). The structure of ubiquitin involves a β-sheet, an α-helix and a short 3_{10} helix. It is compact except for the highly flexible C-terminal region, which protrudes from the globular fold (**Figure 1A**) (Vijay-Kumar *et al.,* 1987). A characteristic feature of ubiquitin is the presence of two water-exposed hydrophobic patches: the I44 patch (L8-I44-V70) and the I36 patch (I36-L71-L73). Most known ubiquitin-binding domains interact with hydrophobic patches (Grabbe and Dikic, 2009), although for several types of ubiquitin-binding domains the non-hydrophobic D58 patch (R54-T55-S57-D58) and F4 patch (Q2-F4-T14) have the highest impact on the interaction (**Figure 1B**) (Lee *et al.,* 2006; Sato *et al.,* 2011; Wright *et al.,* 2016).

There are multiple ways in which ubiquitin can modify a target protein. The first one is monoubiquitylation – attachment of a single ubiquitin moiety. This type of modification has been observed for PCNA, histones, RAD18, CENP-A and other substrates and typically plays signalling non-degradative roles (Hicke 2001; Hoege *et al.,* 2002; Stelter and Ulrich, 2003; Zeman *et al.,* 2014; Niikura *et al.,* 2019). A substrate can also carry several monoubiquitin moieties (multi-monoubiquitylation) (Lai *et al.,* 2001; Haglund *et al.,* 2003). Importantly, ubiquitin itself can be a target for ubiquitylation, with seven internal lysines (K6, K11, K27, K29, K33, K48, K63) or the N-terminal methionine of ubiquitin acting as attachment sites (**Figure 1C**). Therefore, 8 linkage types between two ubiquitin moieties are possible, all detected in mammalian cells (discussed in detail in **section 1.1.3**). Furthermore, multiple lysine residues of a single ubiquitin can be ubiquitylated, giving rise to branched ubiquitin chains. Given that ubiquitin itself can be posttranslationally modified and considering the existence of non-lysine ubiquitylation,

ubiquitin can form a great variety of structures with different topologies. This phenomenon has been called the 'Ubiquitin code' (**Figure 1D**) (Komander and Rape, 2012).

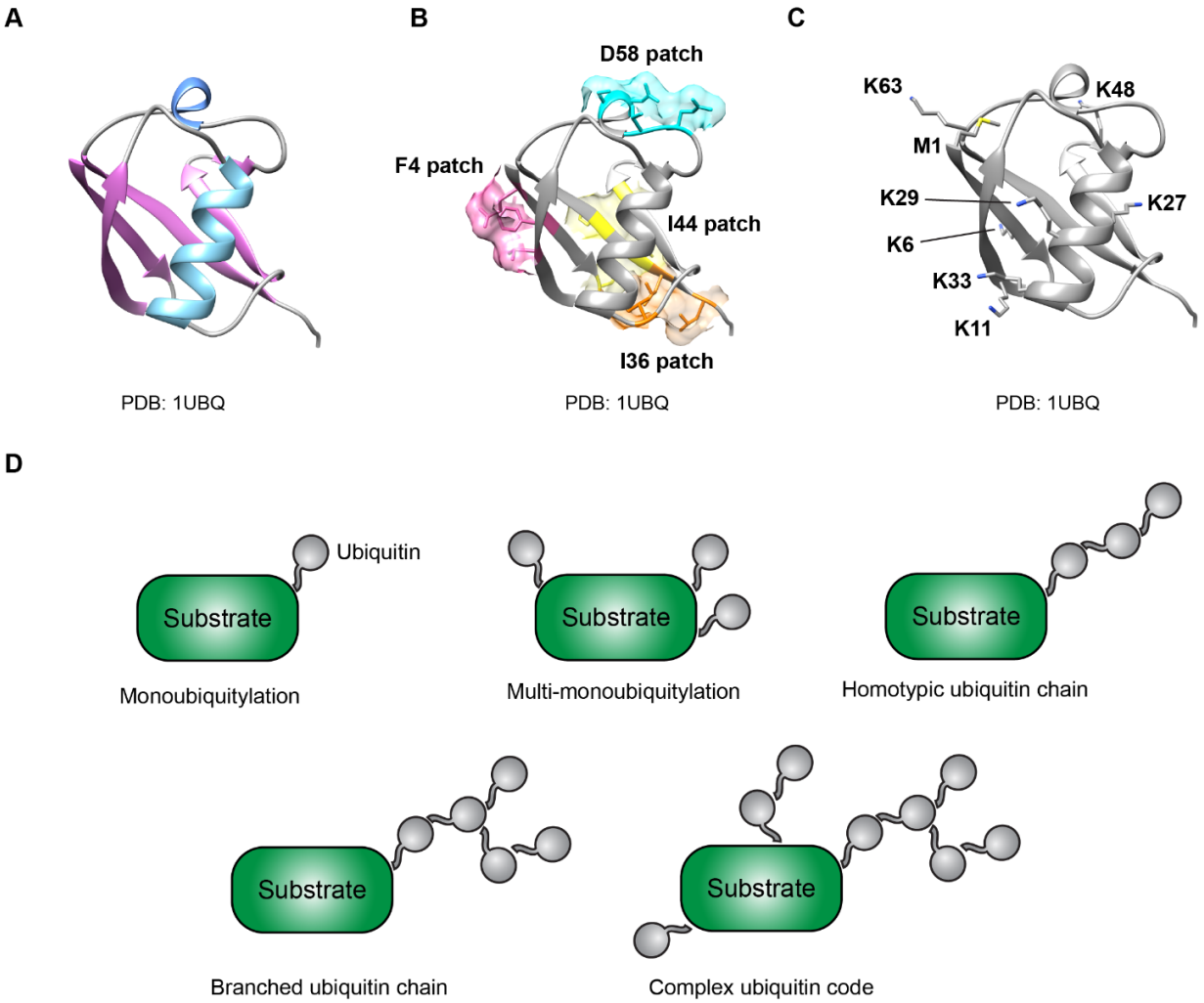

Figure 1: Ubiquitin as a posttranslational modifier. (A) Crystal structure of ubiquitin in cartoon representation (PDB: 1UBQ). Highlighted are the following secondary structure elements: β-sheet (pink), α-helix (light blue) and 3_{10} helix (dark blue). **(B)** Crystal structure of ubiquitin as in (A) with highlighted interaction patches: I44 patch (yellow), I36 patch (orange), D58 patch (light blue) and an F4 patch (pink). **(C)** Crystal structure of ubiquitin as in (A) with highlighted N-terminal methionine and lysine residues. **(D)** Different modes of protein ubiquitylation.

1.1.2 Enzymatic core of the ubiquitin system

Attachment of ubiquitin to the target proteins takes place via a cascade of enzymatic reactions involving ubiquitin-activating enzymes (E1), ubiquitin-conjugating enzymes (E2) and ubiquitin ligases (E3), which mediate the final step and are responsible for the choice of a substrate (Stewart *et al.,* 2016; Zheng and Shabek, 2017). Human cells

possess 2 E1, at least 38 E2 and at least 600 E3 enzymes. E1 enzymes couple the C-terminus of ubiquitin to their active site via a thioester bond, followed by a transfer of ubiquitin to the catalytic site of E2 enzymes. The next step in the ubiquitylation cascade highly depends on the type of E3 enzymes. There are three different classes of ubiquitin ligases: RING/U-box, HECT and RING-between-RING (RBR). Ligases of the RING-type mediate interactions between E2 enzymes and substrates: ubiquitin is directly transferred from the E2 enzyme onto the substrate. As the E3 enzyme does not directly participate in the ubiquitin transfer, the linkage type in the case of RING-type E3s is determined by the E2 enzyme. On the contrary, HECT-type E3s first load ubiquitin on their catalytic cysteine and then transfer it onto the substrate. In this case, the linkage type is dependent on the E3 enzyme. RBR-type E3 enzymes can be considered RING-HECT hybrids, as they possess two RING domains, one interacting with the ubiquitin-charged E2 and the other accepting ubiquitin from the E2. As for HECT-type E3s, the linkage type in the case of RBR enzymes is determined by the E3 enzyme itself (**Figure 2**).

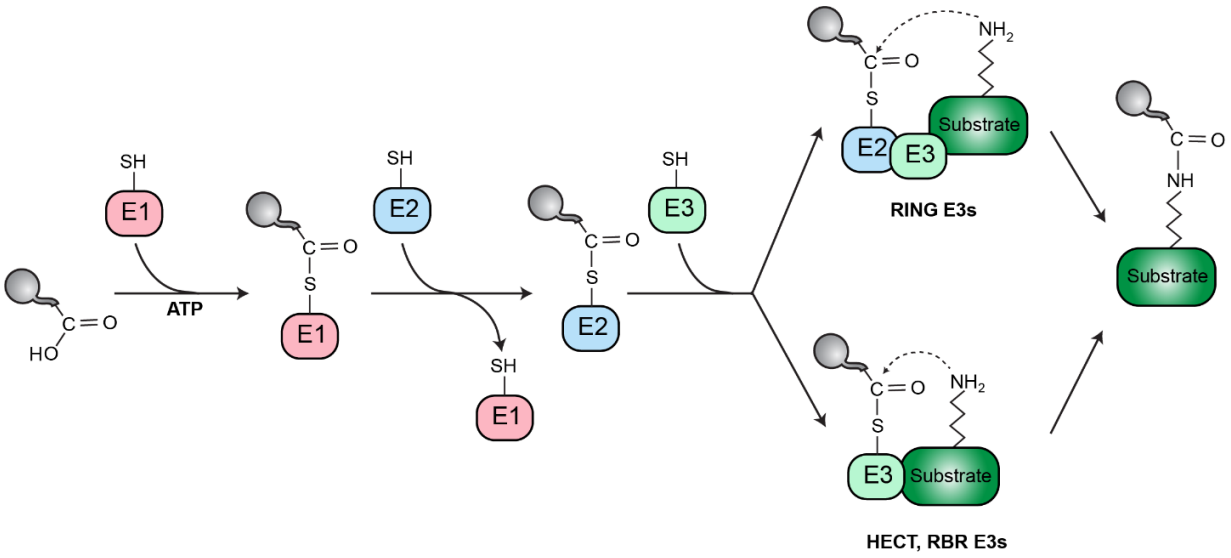

Figure 2: Enzymatic machinery of the ubiquitin system. Schematic representation of the ubiquitylation cascade starting from the free ubiquitin and resulting in a ubiquitylated substrate.

1.1.3 Ubiquitin chains

As introduced in **section 1.1.1**, two ubiquitins in a chain can be connected with at least 8 linkage types. Whereas certain linkage types have been shown to fulfil specific functions in a cell, for many chain types the significance of the linkage remains unexplored. Here I summarise the known functions of ubiquitin chains, starting with the best and finishing with the least well-characterised ones, as well as describe functions of the known ubiquitin structures of higher complexity.

1.1.3.1 K48-linked ubiquitin chains

K48 linkages are the most abundant linkage type in a cell, representing a canonical signal for protein degradation by the proteasome (**section 1.1.4**) (Pickart, 1997). This pathway is indispensable for cell viability, as expression of the K48R mutant of ubiquitin cannot compensate for the loss of ubiquitin genes (Finley *et al.,* 1994). Whereas a minimum chain length of 4 ubiquitin units has been initially suggested to be a signal for proteasomal degradation, later findings suggest that high local ubiquitin concentration is more important than chain length: two di-ubiquitin K48-linked chains on a cyclin B1 represent a stronger degradation signal than a single tetra-ubiquitin chain of the same linkage type (Thrower *et al.,* 2000; Lu *et al.,* 2015). Despite their predominant role in protein degradation, several reports indicate that K48-linked chains may fulfil regulatory non-degradative functions. An example is the transcriptional factor Met4, which binds K48-linked chains with high specificity. This interaction competes with the binding of the transcription machinery to the same region, thereby repressing the transcriptional activity of Met4 (Villamil *et al.,* 2022; Li *et al.,* 2019). Another example is the translesion polymerase kappa, which has been shown to associate with K48-linked ubiquitin chains on PCNA upon conditions of nucleotide starvation. However, the relevance of chain linkage on PCNA as well as its functions need to be clarified (Tonzi *et al.,* 2018).

1.1.3.2 K63-linked ubiquitin chains

K63-linked polyubiquitylation performs a variety of predominantly non-degradative functions in a cell. Assembly of these chains by RING-type ubiquitin ligases often depends on the E2 enzyme UBC13. It possesses unique linkage specificity due to its obligatory interaction with the catalytically inactive E2 variant MMS2. In yeast, Ubc13 functions with

ubiquitin ligases Rad5 and Pib1, whereas its human homologue has a broader spectrum of cognate E3s, including HLTF, SHPRH, TRAF6, RNF8, CHFR and CHIP (Hodge *et al.,* 2016).

Modification of the DNA sliding clamp PCNA with K63-linked chains is indispensable for error-free damage bypass and fork reversal in yeast and human cells, respectively (**section 1.2.3.5)**, and modification of histones with this chain type is required for the proper DNA damage response during repair of double-strand breaks (Schwertman *et al.,* 2016; Stelter and Ulrich, 2003; Vujanovic *et al.,* 2017). In the latter case, the responsible reader is RAP80, which brings the BRCA1A complex to the site of damage. The binding of K63-linked chains by RAP80 occurs via its highly linkage-selective tandem ubiquitin-binding motifs, which served as a basis for the design of K63-linked polyubiquitin sensor probes (Sims and Cohen, 2009; Sims *et al.,* 2012). K63-linked chains, assembled by ubiquitin ligases TRAF6, cIAP1 and cIAP2, are also crucial for inflammation and immune responses via the recruitment of TAB2 and promoting NF-κB activation (Deng *et al.,* 2000; Wajant and Scheurich, 2011). Functions of K63-linked ubiquitin chains in membrane trafficking are demonstrated by the strict requirement of this chain type for the endocytosis of yeast uracil permease Fur4; a similar pathway has also been observed for mammalian proteins, such as epidermal growth factor receptor EGFR or dopamine transporter DAT (Galan and Haguenauer-Tsapis, 1997; Vina-Vilaseca and Sorkin, 2010).

K63-linked chains have also been shown to be modified with K48 linkages, resulting in the formation of branched ubiquitin chains, which can be assembled by the ubiquitin ligases UBE2K, HUWE1 and UBR5 and fulfil both degradative and non-degradative functions in a cell (Ohtake *et al.,* 2018; Ohtake *et al.,* 2016; Pluska *et al.,* 2021). A recent proteomics-based study identifies a number of proteins, which selectively bind to branched K63-K48 chains, but not to homotypic K63- or K48-linked ones (Lange *et al.,* 2023).

1.1.3.3 M1-linked (linear) ubiquitin chains

In *S. cerevisiae*, M1 linkages between ubiquitins are not produced enzymatically and are only present in the product of the UBI4 gene, which is a head-to-tail fusion of 5 ubiquitins. In higher eukaryotes, M1-linked chains are produced by the LUBAC complex, which is, up until now, the only E3 ligase complex known to synthesise linear ubiquitin

chains. The LUBAC complex consists of three components: ubiquitin ligases HOIL1 and HOIP, as well as the structural component SHARPIN. HOIL1 mainly participates in the transfer of the first ubiquitin to the substrate (lysine, serine or threonine residues), whereas HOIP extends ubiquitins on the substrate into an M1-linked chain (Kelsall *et al.,* 2019; Smit *et al.,* 2013). Several substrates for linear ubiquitylation (RIPK1/2, TRADD, TNFR1, etc.), as well as readers of linear ubiquitin chains (ABIN1-3, Optineurin, A20, etc.), have been reported (Fennell *et al.,* 2018; Dittmar and Winklhofer, 2019). Interestingly, NF-κB essential modulator NEMO is both a selective reader of linear ubiquitin chains and a substrate of linear polyubiquitylation. Functions of linear ubiquitin chains mainly involve inflammation and immune responses. However, the role of linear polyubiquitylation in the ubiquitin fusion degradation pathway in human cells has also been reported (Tokunaga and Iwai, 2012; Kirisako *et al.,* 2006). In addition to homotypic linear chains, mixed M1/K63 chains have been implicated in the IKK activation pathway (Emmerich *et al.,* 2013). M1-linked chains were also found on the TRAF6 proteins in combination with K48 and K63 linkages, suggesting the presence of a complex ubiquitin code on this substrate (Ohtake *et al.,* 2016).

1.1.3.4 K11-linked ubiquitin chains

K11-linked chains have been most extensively characterised in the context of branched chains generated by the APC/C complex. The E2 enzyme UBE2S assembles K11 linkages on top of the substrates, pre-ubiquitylated by the UBE2C enzyme with K63, K48 and K11 linkages. Branched K11/K48 conjugates have been shown to possess a unique interface, increasing their affinity to p97/VCP and the proteasome receptor S5a and facilitating faster degradation of the APC/C substrates (Boughton *et al.,* 2020; Meyer and Rape, 2014). Branched K11/K48 chains have also been found on misfolded nascent proteins. Their formation depends on the ubiquitin ligases UBR4 and UBR5 (Yau *et al.,* 2017). Another example is the degradation of the secretory factor EVI/WLS, which is dependent on VCP activity and ubiquitin-conjugating enzymes UBC13, UBE2K and UBE2J2. Ubiquitin code on EVI/WLS includes K48, K63 and K11 linkages. High linkage specificity of UBC13 (K63) and UBE2K (K48) suggests that UBE2J2 might be the enzyme that builds K11 chains on the EVI/WLS substrate. Similar ubiquitin architecture, namely a combination of K63, K48 and K11 linkages, is triggered by K63-linked polyubiquitylation

in mammalian cells. This pathway has been employed to create a new class of PROTACs, which rely on K63 ubiquitylation (Akizuki *et al.,* 2023). Apart from a role in protein turnover, several non-degradative roles of K11-linked chains have also been proposed. cIAP1/UBCH5-dependent polyubiquitylation of RIP1 with K11 linkages promotes NF-κB activation upon TNFα signalling (Dynek *et al.,* 2010). Indirect evidence, based on depletion of the K11-selective DUB Cezanne, suggests that K11 chains are assembled on top of K63-linked chains during DNA damage response, limiting recruitment of RAP80/BRCA1-A complex to the sites of DNA damage (Wu *et al.,* 2019).

1.1.3.5 K27-linked ubiquitin chains

Ubiquitin replacement strategy revealed that K27 linkages, along with K63 ones, are essential for the proper activation of the DNA damage response upon double-strand break induction. Ubiquitin ligase RNF168 was shown to be responsible for the polyubiquitylation of chromatin proteins with K27-linked chains, and a mass spectrometry-based approach revealed histones as the main targets (Gatti *et al.,* 2015). Another area where K27-linked chains were shown to be highly important is immune signalling. In response to cytoplasmic DNA accumulation, ubiquitin ligase AMFR modifies STING with K27-linked ubiquitin chains. This modification is crucial for recruiting the TBK1 kinase and downstream activation of the immune response (Wang *et al.,* 2014). K27-linkages have also been found as a component of complex ubiquitin conjugates involving K6, K29 and K48 linkages (Zucchelli *et al.,* 2010; Ben-Saadon *et al.,* 2006). Apart from that, K27-linked ubiquitin dimers possess one additional interesting characteristic – compared to other linkages, they are resistant to cleavage by several linkage non-selective DUBs (Ubp6, USP5, USP2) – physiological relevance of this phenomenon remains to be understood.

1.1.3.6 K29-linked ubiquitin chains

K29-linked chains have been implicated in the ubiquitin fusion degradation (UFD) pathway, which is responsible for the degradation of proteins C-terminally fused to an uncleavable ubiquitin moiety. Ufd4 builds a K29-linked on a ubiquitin moiety of a UFD substrate. This chain is further modified with K48 linkages by Ufd2, leading to the degradation of the substrate (Johnson *et al.,* 1995; Koegl *et al.,* 1999). UFD pathway is generally conserved in human cells. Ubiquitin ligase TRIP12, which is a human

homologue of Ufd4, assembles K29-linked chains *in vitro* and *in vivo* and is involved in the degradation of UFD substrates (Park *et al.,* 2009). Together with CRL2, TRIP12 is also involved in the formation of branched K29/K48 chains during PROTAC-induced degradation of BRD4, suggesting that roles of K29-linked polyubiquitylation by TRIP12 extend beyond the UFD pathway (Kaiho-Soma *et al.,* 2021).

The only well-characterised example of non-proteolytic K29-linked polyubiquitylation is ubiquitylation of AXIN1 by Smurf1. This modification inhibits the interaction of AXIN1 with LRP5/6, leading to the repression of the Wnt/β-catenin pathway (Fei *et al.,* 2013).

1.1.3.7 K6-linked ubiquitin chains

Mass-spectrometry analysis revealed enrichment of K6 linkages after UV treatment but not after ionising radiation (Elia *et al.,* 2015). BRCA1/BARD1 complex was shown to build K6-linked chains as a response to replication stress (Morris and Solomon, 2004). However, the targets and readers of K6-linked ubiquitylation in these conditions are not yet identified. Another condition that leads to a build-up of K6 linkages is the depolarisation of mitochondria – in this case, the responsible ligase is Parkin. Ubiquitin replacement strategy reveals that K6-linked ubiquitylation in this condition is crucial for the timely initiation of mitophagy (Ordureau *et al.,* 2015). HUWE1 is another ligase that creates K6-linked chains *in vitro* and *in vivo* (Michel *et al.,* 2017). Mitochondrial membrane protein MFN2 is a target of HUWE1-dependent K6-linked polyubiquitylation, however, the existence of other HUWE1 substrates is not excluded. Recently, K6-linked ubiquitylation has been linked to the quality control pathway at the stalled ribosomes, with RFN14 being the responsible ubiquitin ligase (Oltion *et al.,* 2023). Finally, proteomic analysis reveals a unique behaviour of K6-linked chains with respect to VCP and proteasome inhibition: whereas K48 linkages accumulate in a cell upon inhibition of either VCP or proteasome, the abundance of K6 linkages significantly increases upon VCP inhibition but remains rather unchanged upon inhibition of proteasome (Heidelberger *et al.,* 2018). This pinpoints K6 linkages as VCP substrates and, at the same time, highlights the non-degradative role of these linkages.

1.1.3.8 K33-linked ubiquitin chains

Similar to K6-linked chains, K33 linkages accumulate in mammalian cells upon UV but not ionising irradiation (Elia *et al.,* 2015). One of the described substrates of K33-linked polyubiquitylation is XRCC1. Once allosterically activated by 5-hydroxymethylcytosine, ubiquitin ligase UHRF2 polyubiquitylates XRCC1 with K33 linkages, leading to the recruitment of RAD23B and activating base excision repair pathway (Liu *et al.,* 2021). Apart from DNA damage, K33-linked polyubiquitylation occurs during T-cell activation, AMPK family kinase signalling and post-Golgi trafficking (Yuan *et al.,* 2014; Al-Hakim *et al.,* 2008; Huang *et al.,* 2010). Recently developed split GFP-based polyubiquitin imaging approach PolyUB-FC revealed that the autophagosome cargo protein SQSTM1/p62 interacts with K33-linked chains via its UBA binding domain, promoting the transport of K33-polyubiquitylated cargo to the autophagosomes (Nibe *et al.,* 2018).

1.1.4 The ubiquitin-proteasome system

Together with autophagy, the ubiquitin-proteasome system (UPS) is a key regulator of cellular metabolism, accounting for 80-90% of total protein degradation (Lee and Goldberg, 1998). The discovery of the UPS resulted in the award of the 2004 Nobel Prize to A. Ciechanover, A. Hershko and I. Rose (Ciechanover *et al.,* 1980; Hershko *et al.,* 1980). The main enzyme complex of the UPS is the 26S proteasome, which consists of the 20S core protease subunit and two regulatory 19S particles. 20S proteasome has a cylindrical shape, resulting from the stacking of two α-rings and two β-rings, each consisting of seven subunits. Proteolysis is performed by β1, β2 and β5 subunits, which cleave peptide bonds after acidic, basic and hydrophobic amino acids, respectively. 19S regulatory subunits cap the 20S proteasome on one or both sides (**Figure 3A**). Their primary role is to recognise polyubiquitylated substrates, unfold them and translocate them into the proteasome inner chamber, where the hydrolysis of peptide bonds takes place (Tanaka, 2009). Although the 26S proteasome possesses intrinsic ubiquitin receptors (Martinez-Fonts *et al.,* 2020), several factors have been shown to bind polyubiquitylated substrates and shuttle them to the proteasome. An example is RAD23, which, on the one hand, selectively binds K48-linked chains and, on the other hand,

interacts with proteasome via its ubiquitin-like domain (Liang *et al.,* 2014; Chen and Madura, 2002). As a part of the 19S regulatory particles, several deubiquitinating enzymes are associated with the 26S proteasome - USP14, RPN11, and UCH37. They remove ubiquitin moieties from polyubiquitylated substrates upon binding to the proteasome, protecting ubiquitin from degradation and replenishing the cellular ubiquitin pool (Shin *et al.,* 2020).

In some instances, direct shuttling of polyubiquitylated proteins to the proteasome is impossible. This happens, for example, when proteins reside in the membranes or are tightly bound to DNA. In this case, polyubiquitylated proteins undergo unfolding by the ATPase VCP/p97 concomitantly with their extraction from the corresponding cellular compartments (Meyer and Weihl, 2014; Meyer *et al.,* 2012). VCP is a highly conserved protein, which belongs to type II AAA+ ATPase family due to the presence of two tandem ATPase domains (D1 and D2) and a large N-terminal domain, which mediates interactions of VCP with its substrates. VCP exists as a homohexamer, although two VCP hexamers can interact tail-to-tail and form a dodecamer: interaction between the subunits is promoted by ATP binding to the D1 domain (Wang *et al.,* 2003) (**Figure 3B**). Unfolding of the substrates by VCP occurs via a hand-over-hand mechanism: sequential ATP hydrolysis by subunits leads to a conformational change and a step-by-step translocation of the substrate polypeptide chain through the central pore (Cooney *et al.,* 2019). Although VCP can directly interact with and unfold a subset of its targets, typical VCP substrates are conjugated to ubiquitin (Ahlstedt *et al.,* 2022). Recognition of polyubiquitylated proteins by VCP takes place with the help of its multiple adaptors. Interestingly, whereas some adaptors (UFD1, NPLOC4, UBXN1) prefer to bind K48-linked and K48-K11 branched ubiquitin chains, marked preference for branched K63-K48 chains was observed for the VCP-associated proteins ZFAND2B, ATXN3 and RHBDD1 (Yau *et al.,* 2017; Lange *et al.,* 2023).

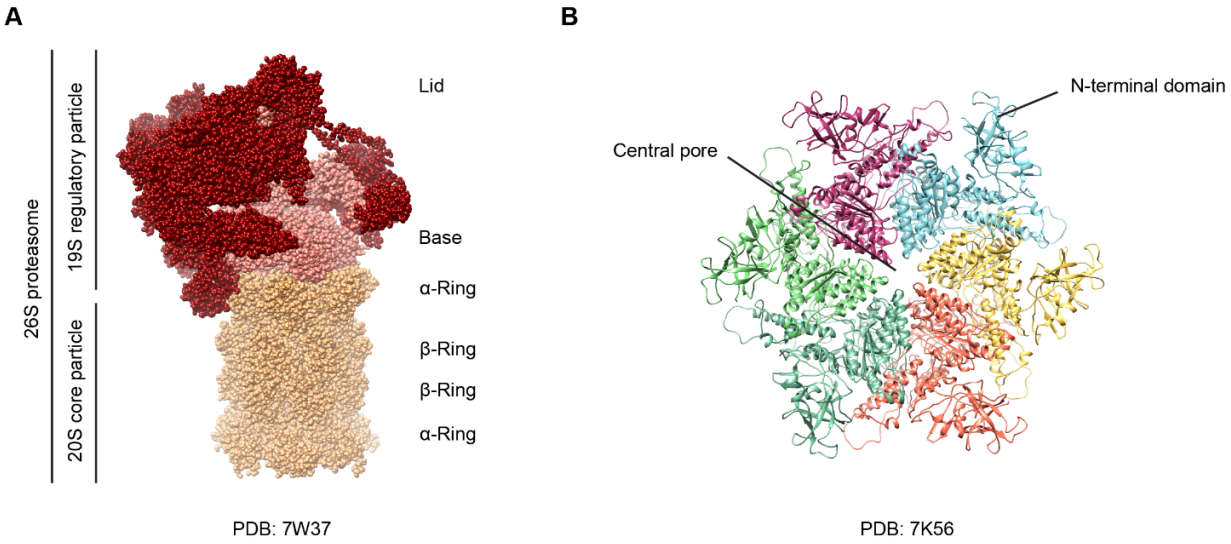

Figure 3: Structure of 26S proteasome and VCP. (A) Structure of a human 26S proteasome, obtained by electron microscopy, in spheres representation (Zhang *et al.,* 2022). **(B)** Structure of human VCP, obtained by electron microscopy, in cartoon representation. Different colours correspond to different subunits of a hexamer (Yu *et al.,* 2021).

1.1.5 Deubiquitylating enzymes

Attachment of ubiquitin to target proteins can be reverted by the action of ubiquitin-specific hydrolases, or deubiquitylating enzymes (DUBs). The activity of DUBs results in the termination of ubiquitin signalling (including prevention of protein degradation) and replenishment of the free ubiquitin pool. Human cells have ~100 DUBs, which can be roughly divided into two classes: cysteine proteases, which use cysteine as a catalytic residue, and metalloproteases, which employ a catalytic serine and zinc as a cofactor. Like E3 enzymes, many DUBs have their preferred substrates and linkage types. For example, USP1 removes monoubiquitin moiety from PCNA and FANCD2 (Huang *et al.,* 2006; Nijman *et al.,* 2005); AMSH and OTUB1 are selective towards K63- and K48-linked polyubiquitin chains, respectively (McCullough *et al.,* 2006; Wang *et al.,* 2009). Deubiquitylating enzyme A20/TNFAIP3 is the only known protein that has ubiquitin ligase activity, deubiquitylating activity and binds to polyubiquitin chains. Interestingly, these three functions are directed towards different chain types: A20 selectively binds to linear ubiquitin chains, cleaves K63-linked and synthesises K48-linked ubiquitin chains (Tokunaga *et al.,* 2012; Wertz *et al.,* 2004). All these functions are essential for the NF-κB

activation, highlighting the complexity of the ubiquitin code in this pathway (Bai *et al.,* 2022).

1.1.6 Tools to study the ubiquitin system

1.1.6.1 Mass spectrometry

Detection of protein ubiquitylation by mass spectrometry relies on the specific signature that ubiquitin leaves on the substrate after trypsin digestion: ubiquitin is removed from the substrate via cleavage of the peptide bond between R74 and G75, leaving two C-terminal glycine residues of ubiquitin attached to the substrate via an isopeptide bond. Detection of such peptides by mass spectrometry allows to identify those residues of the substrate, which had been ubiquitylated. Early proteomics approaches to study ubiquitylation relied on the expression of tagged ubiquitin, which allows isolating and identifying ubiquitylated proteins by means of affinity chromatography or immunoprecipitation (Peng *et al.,* 2003). Development of the monoclonal antibody against GG dipeptide coupled via an isopeptide bond to a lysine allowed to identify global ubiquitylation profile of a cell in unperturbed conditions, i.e. without overexpression of tagged ubiquitin (Kim *et al.,* 2011; Wagner *et al.,* 2011). Absolute quantification of ubiquitin linkages became possible with the development of AQUA (absolute quantification) mass spectrometry, where synthesised isotope-labelled ubiquitin peptides are used as an internal standard. This method allowed direct quantification of ubiquitin linkages on the cyclin B1, which is heavily ubiquitylated by the anaphase-promoting complex: rather surprisingly, K48, K63 and K11 linkages amount up to 40% of total ubiquitin forms, the rest being monoubiquitylation events (Kirkpatrick *et al.,* 2006). Detection of ubiquitin chain branching by mass spectrometry is more challenging: during trypsin digestion, the majority of the ubiquitin peptides, originating from branched chains and therefore containing two diGly remnants at the same time, will be cleaved between the two ubiquitylation sites. This makes it later impossible to understand whether these remnants originate from the same ubiquitin molecule. An interesting approach to overcome this problem was used to prove the presence of branched K63-K48 chains *in vivo*: R54, the only residue between K48 and K63 that leads to trypsin cleavage, was mutated to alanine. Tryptic digestion of this ubiquitin mutant produces peptides, which contain both K48 and K63 residues, allowing

to simultaneously monitor their ubiquitylation. Combining this approach with AQUA technology revealed that nearly one-fifth of all K63 linkages are branched via K48. The amount of branched K63-K48 linkages increases upon proteasome inhibition, suggesting their role in protein degradation (Ohtake *et al.,* 2016).

1.1.6.2 High-affinity binders to polyubiquitin chains

Different conformations of ubiquitin linkages underlie the existence of high-affinity binders, which prefer one linkage type over the others. The first class of binders is linkage-selective antibodies, which are available for all linkage types (Matsumoto *et al.,* 2010; Matsumoto *et al.,* 2012; Newton *et al.,* 2008). Linkage-selective antibodies allow the detection of their cognate linkages by western blotting or immunofluorescence. However, their use *in vivo* is limited due to the complex maturation process required for the correct antibody folding. The use of non-antibody binders can overcome this limitation. A major class of binders to ubiquitin linkages is based on the existing linkage-selective ubiquitin-binding domains. For example, the NZF domain of TAB2 and the UBAN domain of NEMO have been used as sensors for K63-linked and linear ubiquitin chains, respectively (Qin *et al.,* 2022). Linkage selectivity of these domains is achieved due to their binding to the interface between two ubiquitin moieties around the (iso)peptide bond. Another approach relies on combining several weak ubiquitin-interacting motifs separated by appropriate linkers. As demonstrated for tandem ubiquitin-interacting motifs (tUIMs) of RAP80 and Ataxin-3, linker length determines the linkage selectivity of the domain. Whereas high-avidity binding to K63-linked chains by RAP80 tUIMs requires 7 amino acid linkers between ubiquitin-binding entities, 2 amino acid linkers are optimal for binding to more compact K48-linked chains by Ataxin-3 (Sims and Cohen, 2009). Varying the type of ubiquitin-binding modules and amino acid composition of the linkers allows to create binders with different affinities toward desired linkages (Sims *et al.,* 2012).

Apart from adapting naturally occurring ubiquitin-binding domains, a number of artificial protein binders to ubiquitin linkages have been developed. These binders are typically based on a specific protein frame with several variable regions, which dictate specificity to a target. Existing high-throughput screening platforms allow the selection of binders by screening a library of peptide fragments incorporated in the variable regions. One example is affimers, ~12 kDa proteins based on a cystatin fold with two variable

regions that dictate their specificity (Tiede *et al.,* 2017). An affimer developed for the K6 linkage has found widespread use and revealed the involvement of K6-linked polyubiquitylation in the DNA damage response and VCP metabolism, as well as led to the identification of proteins ubiquitylated with this linkage type (Michel *et al.,* 2017; Heidelberger *et al.,* 2018). Another example is nanobodies – single-chain camelid antibodies, which have found use in fundamental science and also have therapeutic applications (Salvador *et al.,* 2019). Selection of nanobodies on high-throughput display platforms *in vitro* bypasses the need of animal immunisation. Nanobodies have been developed not only for pure K48 and K63 linkages, but also for K63-K48 branched ubiquitin chains (Gonzalez-Santamarta *et al.,* 2023; Lange *et al.,* 2023). The latter nanobody was used to confirm the degradative function of branched K63-K48 linked chains and identify the previously underestimated role of these linkages in DNA damage response.

1.1.6.3 Protein engineering approaches

As discussed in **section 1.1.1**, recognition of ubiquitylated substrates by effector proteins differs from the recognition of small modifications, such as phosphate or methyl groups. Affinity to ubiquitylated substrates is often achieved by combining separate substrate-binding and ubiquitin-binding domains. It allows for certain conformational flexibility both for the modified substrate and the effector protein. Moreover, ubiquitin is attached to the substrate via its flexible C-terminus, contributing to the conformational freedom of the product. Indeed, X-ray scattering analysis and molecular simulations confirm the conformational flexibility of ubiquitylated PCNA (Powers *et al.,* 2018). This is further supported by the fact that the formation of a complex between ubiquitylated PCNA and its reader protein – polymerase eta – involves significant rotation of the ubiquitin moiety (Lau *et al.,* 2015). Therefore, a natural approach to mimic the ubiquitylation at the native lysine is to fuse a ubiquitin moiety N- or C-terminally to the substrate. Notably, the design of the fusion proteins should include removal or mutation of the terminal GG peptide, as it may lead to cleavage by DUBs in case of N-terminal fusions or uncontrolled conjugation to cellular proteins via its C-terminus in case of C-terminal fusions (Qian *et al.,* 2002; Qin *et al.,* 2016). If the flexibility of the effector protein and ubiquitin-substrate

fusion allows their interaction, linear fusions to ubiquitin can rescue the phenotypes that originate from the loss of a target lysine residue or the responsible ubiquitin ligases. The number of known cases when linear fusions can substitute for the native ubiquitylation events is surprisingly high: for more than 20 proteins, linear fusions to ubiquitin or ubiquitin-like modifiers can functionally replace modifications at the native lysine residues (Asimaki *et al.,* 2022). These known substrates belong to entirely different cellular pathways: DNA damage response (PCNA, RAD18, FANCD2), regulation of chromatin structure (H2A, H2B), endocytosis (EGFR, EEA1), immune response and related signalling pathways (RIP1, NEMO, p53). An interesting alternative approach has been used to mimic PCNA ubiquitylated at K164: PCNA was split between residues 163 and 164, followed by an attachment of ubiquitin to the N-terminus of the second fragment (Freudenthal *et al.,* 2010). The resulting fusion protein resembles PCNA ubiquitylated at K164: it forms stable trimers and supports translesion synthesis *in vitro* and *in vivo*.

Unlike monoubiquitylation, there are only a few described attempts to mimic polyubiquitin chains using linear fusions. As fusions of multiple ubiquitins in-frame represent a linear chain, this approach may accurately represent linear and, in some cases, conformationally similar K63-linked chains, whereas their ability to mimic differently linked chains remains questionable. Linear fusion of three ubiquitins was successfully used to mimic a K63-linked chain on the yeast membrane transporter Ypq1 in the approach termed RapiDeg (Rapamycin-induced degradation). Recruitment of the chain to Ypq1 by means of the FKBP-FRB dimerisation system resulted in its rapid internalisation and degradation. Thus, a linear fusion of three ubiquitins can successfully mimic endogenous K63-linked ubiquitin chains in the membrane trafficking pathways (Zhu *et al.,* 2017). Another example comes from the mitophagy field: linear tetraubiquitin fusions harbouring the S65D phospho-mimicking mutation are proficient in recruiting phospho-mimetic Parkin (Okatsu *et al.,* 2015). This approach directly targets the ubiquitin chain to the outer mitochondrial membrane via a mitochondrial targeting domain. Therefore, a phosphorylated ubiquitin chain can lead to Parkin recruitment independently of the substrate to which it is attached. Significantly, targeting linear di-, tetra-, or hexa-ubiquitin chains to the mitochondrial outer membrane induces mitophagy independently of Parkin (Yamano *et al.,* 2020). A third example is PCNA polyubiquitylation: Unlike native K63-linked chains, linear polyubiquitin fusions to PCNA do not support error-free damage

bypass in *S. cerevisiae* (Zhao and Ulrich, 2010). At the same time, an extension of a ubiquitin moiety of a ubiquitin-PCNA fusion protein in a K63-linked manner supports error-free damage bypass, even if chain length is limited to a single K63 linkage (Takahashi *et al.,* 2020). This may reflect that combining a non-native linkage type with a non-native attachment site results in the fusion protein not being recognised by the endogenous effector(s) of polyubiquitylated PCNA.

1.2 Genome stability

Maintenance of genetic information is essential to sustain an organism's life and ensure the lives of the next generations. Endogenous and exogenous factors constantly threaten the integrity of DNA – the carrier of the entire genetic information of a cell. In this section, I will describe the most common sources of DNA damage and the mechanisms a cell can employ to maintain genetic information in challenging conditions.

1.2.1 Types of DNA damage

1.2.1.1 Base oxidation

Reactive oxygen species (ROS) constantly threaten DNA as they are produced during cellular respiration due to ionising radiation or other pathways (Markkanen, 2017). Among all four DNA bases, guanine oxidation at position C8 (8-oxoG) (**Figure 4A**) is one of the most well-known examples of oxidative DNA damage, the other common ones being thymine glycol and 8-hydroxy adenine. Typical agents used to induce oxidative damage of DNA are hydrogen peroxide (H_2O_2) and hydroxyurea (HU). The latter affects cells in at least two different ways, depleting the dNTP pool and leading to the formation of H_2O_2 and oxidative damage of DNA (Sakano *et al.,* 2001). Repair of oxidised bases typically includes their removal from DNA by OGG1 and MYH DNA glycosylases and subsequent abasic site repair (**section 1.2.1.6**).

1.2.1.2 Base alkylation

Alkylation of DNA bases (predominantly methylation of purine bases) is another prominent type of DNA damage. The most common methylated DNA bases are N7-methylguanine (**Figure 4B**), O6-methylguanine and N3-methyladenine. Methylmethanesulfonate (MMS) and N-methyl-N′-nitro-N-nitrosoguanidine (MNNG) are

two DNA methylating drugs widely used to study the cellular response to DNA alkylation. Cellular enzymes can directly demethylate several methylated bases. For example, O6-methylguanine can be directly demethylated by E. coli Ogt or mammalian MGMT (Dolan *et al.,* 1990; Sedgwick and Lindahl, 2002). Methylated bases can be also excised by DNA glycosylases (Bjelland *et al.,* 1993; Singer and Hang, 1997), leading to the formation of abasic sites (**section 1.2.1.6**).

1.2.1.3 Bulky adducts

This term applies to large (polycyclic) aromatic compounds covalently attached to DNA bases. The main difference between small base modifications (oxidation, methylation) and bulky adducts is that the latter significantly distort the DNA helix (Gómez-Pinto *et al.,* 2004). A typical example of a bulky DNA adduct is benzo[a]pyrene and its oxidised derivative BPDE, which efficiently modifies the N2 position of guanine (Hess *et al.,* 1997) (**Figure 4C**). Repair of bulky adducts typically includes the excision of a damaged DNA strand with the subsequent filling of the resulting ~30 nt gap (nucleotide excision repair, NER) (Schärer, 2013). Importantly, DNA duplex distortion is a critical step in the NER-dependent repair of bulky adducts, as the distorted helix is recognised by the XPC–RAD23B complex, favouring the nucleotide excision repair pathway (Sugasawa, 2001).

1.2.1.4 UV photoproducts

UVB (280-315 nm) and UVC (<280 nm) light can lead to DNA damage via the formation of cyclobutane pyrimidine dimers and (6-4) photoproducts (**Figure 4D** and **3E**). Both lesions induce distortion of the DNA helix, which is more prominent in the case of (6-4) photoproducts. Although certain organisms possess enzymes that can directly repair both types of photoproducts (photolyases) (Zhang *et al.,* 2017), their repair in human cells takes place via nucleotide excision repair (Tornaletti and Pfeifer 1996). The importance of this pathway for the repair of UV-induced lesions is highlighted by the fact that mutations in the members of the NER machinery are associated with severe photosensitive genetic diseases in humans: *Xeroderma pigmentosum*, Cockayne syndrome and trichothiodystrophy (Bergoglio and Magnaldo, 2006).

1.2.1.5 Interstrand crosslinks

Interstrand crosslinks (ICLs) represent a lesion where two complementary DNA strands become covalently linked. Unlike all described above types of lesions, interstrand crosslinks affect both DNA strands simultaneously, which makes their repair more challenging. Furthermore, the covalent linkage of two DNA strands poses a roadblock for transcription and replication machinery. This ability of ICLs to cause severe problems in cellular metabolism is reflected by the widespread use of ICL-inducing agents, such as cisplatin or oxaliplatin, as potent chemotherapeutic drugs (**Figure 4F**). Apart from the mentioned platinum-based compounds, ICLs can be induced by nitrogen mustards, mitomycin C, psoralen in combination with UVA light exposure and many other chemicals (Deans and West, 2011). Repair of ICLs involves the coordinated action of multiple enzymes, including structure-specific nucleases, DNA helicases and polymerases. Mutation of the components of the ICL repair system results in a rare genetic disorder, Fanconi anaemia (Moreno *et al.,* 2021), which gives rise to the name of the repair mechanism (Fanconi anaemia pathway).

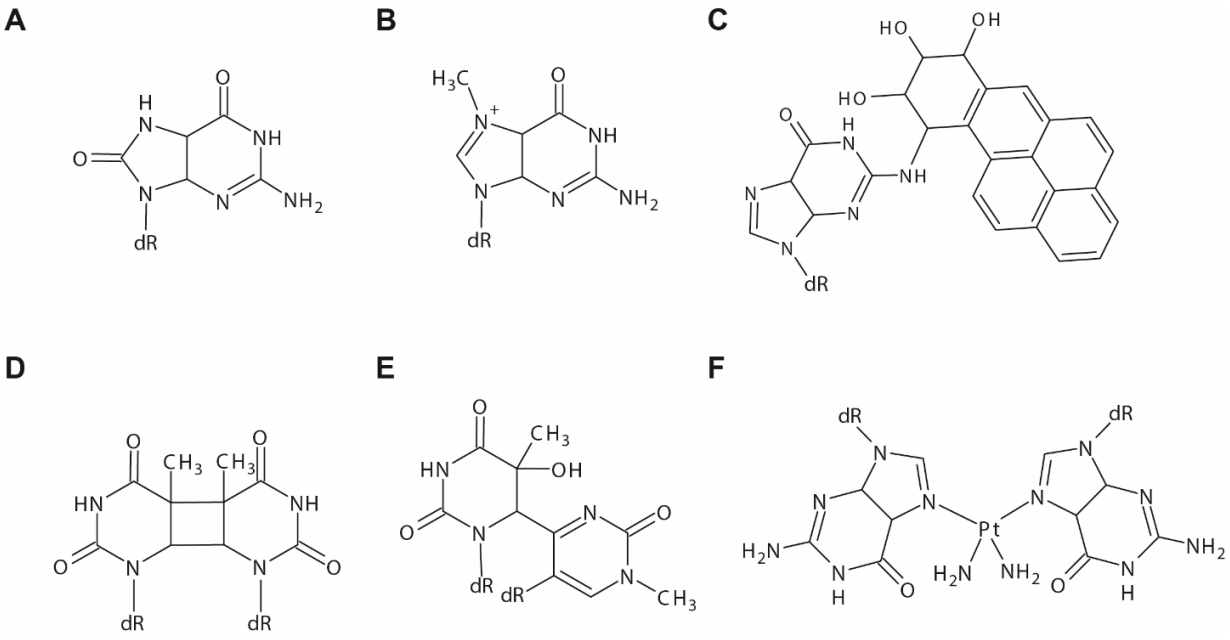

Figure 4: Different types of DNA lesions. **(A)** 8-oxoguanine. **(B)** N7-methylguanine. **(C)** Adduct of guanine to BPDE. **(D)** Thymidine dimer. **(E)** 6-4 photoproduct formed by adjacent thymidines. **(F)** DNA crosslink, formed by cis-platin between two guanine residues.

1.2.1.6 Abasic sites

Abasic sites can be considered as an extreme form of base modification, as the whole nitrogen base is lost from the nucleotide due to the hydrolysis of the glycosidic bond – a process termed depurination (for A and G bases) or depyrimidination (for C and T bases). Cleavage of a glycosidic bond can happen spontaneously (An *et al.,* 2014) or as a result of the enzymatic activity of DNA glycosylases. Abasic sites in DNA can contribute to genomic instability in multiple ways. First, losing a nitrogen base at a specific position in DNA means losing genetic information, and bypassing abasic sites by translesion synthesis polymerases (TLS) can be mutagenic (Chan *et al.,* 2013). Second, the ribose ring in the absence of a base resides in equilibrium with its aldehyde form and can therefore react with amino groups of neighbouring proteins, such as histones, leading to the formation of DNA-protein crosslinks (**Figure 5**) (Sczepanski *et al.,* 2010). Although crosslinking of abasic sites to HMCES protein was shown to serve a protective role (Nowotny, 2019), nonspecific crosslinking to chromatin proteins may pose a serious threat to transcription and replication. Hydrolysis of a glycosidic bond *in vivo* is an irreversible process, and repair of abasic sites requires base excision repair - excision of the deoxyribose, filling of the gap and ligation of DNA strands (Krokan and Bjørås, 2013).

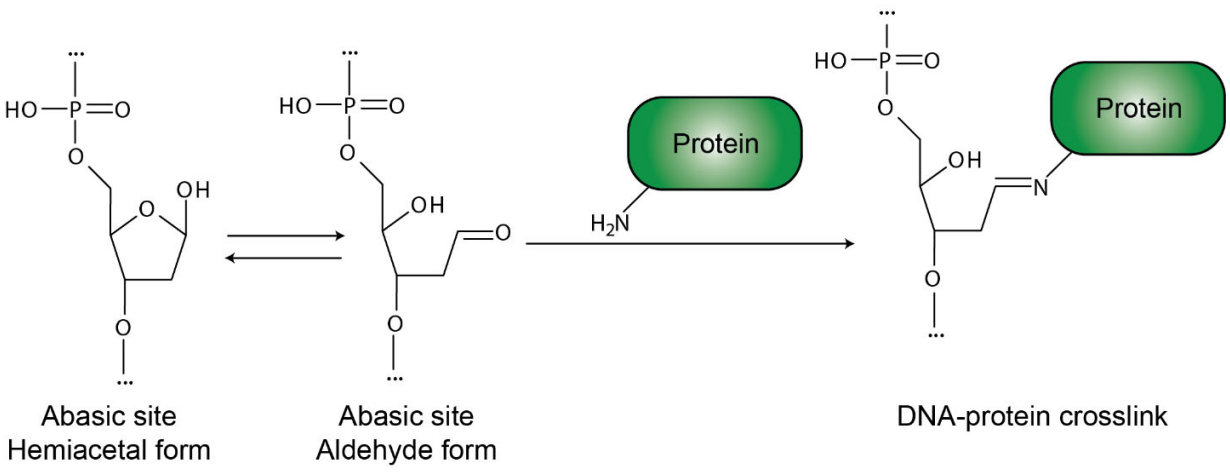

Figure 5. Structure of an abasic site and the mechanism of its conversion into a DNA-protein crosslink.

1.2.1.7 DNA-protein crosslinks

DNA-protein crosslinks (DPCs) represent a broad class of modifications where a protein is covalently attached to a DNA base or backbone. Aldehydes represent one class of potent DPC-inducing substances: a formyl group can sequentially react with two nucleophiles, ultimately linking them together via a methylene bridge. A DPC is formed if these nucleophiles are represented by DNA bases (typically amino- and imino-groups) and proteins (typically N-terminus and several amino acid side chains). The high crosslinking activity of formaldehyde led to the development of the chromatin immunoprecipitation (ChIP) technique, which enables the identification of DNA-binding profiles of any proteins of interest (Orlando, 2000). Another source of DNA-protein crosslinks is the enzymatic activity of certain enzymes, such as topoisomerases I and II. These enzymes create single- and double-strand breaks in the DNA duplex, respectively, while being attached to the DNA backbone via a transient covalent bond between the phosphate group in DNA and a tyrosine residue in the enzymes (Champoux, 2001). While the normal enzymatic cycle of topoisomerases I and II involves rejoining of the DNA ends with the simultaneous release of the enzyme, inhibition of topoisomerases (for example, by camptothecin and etoposide, respectively) results in the enzyme remaining covalently attached to DNA. The repair of DPCs highly depends on the nature of the attached protein. It may involve direct reversal of a crosslink (for topoisomerase adducts), cleavage of the trapped protein by SPRTN/Wss1 protease, conversion of DPCs into clean double-strand breaks, nucleotide excision repair and other pathways (Stingele *et al.,* 2017).

1.2.1.8 Single-strand breaks

Together with abasic sites, single-strand breaks (SSBs) or nicks represent one of the most common types of DNA insults. They can arise due to ROS activity towards the DNA backbone, as an intermediate of the BER pathway or TOP1 activity, and they are naturally present during DNA replication due to discontinuous synthesis of the lagging strand. When not being timely repaired, SSBs result in highly poisonous one-ended double-strand breaks during DNA replication. Typical ways to induce SSB formation in cells include H_2O_2 and MMS as damaging agents, which trigger SSBs due to BER activation. However, the spectrum of lesions for these drugs is quite diverse. Inhibition of TOP1 also results in SSBs concomitantly with the formation of DPCs. A much cleaner way

to create SSBs relies on the activity of the D10A mutant of Cas9 (Ren *et al.,* 2014), which inactivates one of two nuclease domains of Cas9 and therefore turns its DSB-inducing activity into a nickase one. Repair of SSBs is initiated by the poly (ADP-ribose) polymerase PARP1, which binds to and is activated by DNA breaks (Ali *et al.,* 2012). PARP1 activity results in the accumulation of single-strand break repair proteins, which include DNA end processing factors and DNA ligases, leading to the sealing of the DNA nick (Caldecott, 2008).

1.2.1.9 Double-strand breaks

Double-strand breaks, which occur when two strands of a DNA duplex are simultaneously broken, represent highly deleterious structures: a single DSB can be sufficient to kill a cell (Cui and Bikard, 2016). DSBs can arise from two adjacent SSBs in the opposite DNA strands or exposure to ionising radiation or certain chemicals (neocarzinostatin, zeocin). Inhibition of human DNA topoisomerase TOP2 by etoposide also leads to the formation of DSBs. However, DNA ends in this case remain covalently attached to the enzyme. The primary pathway of DSB repair in human cells is non-homologous end joining (NHEJ), which involves the processing of DNA ends and their ligation by DNA ligase IV and operates throughout the cell cycle. In the case of defective NHEJ machinery, DNA ends can be joined via an alternative end-joining pathway, which relies on microhomology and often involves base insertions by DNA polymerase theta (Chang *et al.,* 2017). During S and G2 phases, when a sister chromatid is available, DSBs can be repaired by homologous recombination: resection of DNA ends leads to an invasion of RAD51-coated ssDNA into a sister chromatid, DNA synthesis on a sister chromatid template and resolution of Holliday-junction intermediates (Wright *et al.,* 2018). Pathway choice is highly dependent on the cell cycle stage and includes multiple layers of regulation involving phosphorylation and ubiquitin signalling (Yun and Hiom, 2009; Schwertman *et al.,* 2016; Ceccaldi *et al.,* 2016).

1.2.2 Replication stress

The time a cell spends between two divisions is called a cell cycle and can be subdivided into distinct stages. During the G1 phase, the primary goal of a cell is to grow and accumulate sufficient nutrients for DNA replication. The S phase is defined by

replication and finishes once the genome information has been duplicated. During the following G2 phase, a cell prepares for division in the subsequent M phase. Two daughter cells, which appear after mitosis, enter the G1 phase, and the cell cycle repeats. The S phase is the most critical for preserving genetic information: mistakes during DNA replication in the form of mutations or genomic rearrangements are propagated to following generations. Replication starts from discrete genomic regions – replication origins – and involves a series of events called 'origin licencing', which is necessary to initiate replication. It includes loading the origin recognition complex (ORC) onto double-stranded DNA, followed by recruitment of CDT1, CDC6 and MCM2-7 double hexamers. This complex is further converted into bidirectional replication forks upon activation by DDK and CDK kinases (Parker *et al.,* 2017). Processive DNA synthesis is carried out by the replisome – a multiprotein complex involving the helicase, replicative polymerases Polε and Polδ, primase Polα, replication sliding clamp PCNA and other factors. *In vitro* reconstitution of a human replisome requires 43 proteins, and more proteins may be involved *in vivo* (Baris *et al.,* 2022). As DNA synthesis by polymerases occurs exclusively in the 5'-3' direction, two DNA strands are replicated differently: one strand is replicated continuously by Polε in the 5'-3' direction (leading strand) and the other discontinuously in small patches (lagging strand). These patches, termed Okazaki fragments, originate from ~35 nucleotide-long RNA primers, which Polδ extends into ~200 nucleotide-long fragments. Maturation of the lagging strand, which is one of the most common DNA metabolic processes, requires removing the RNA primer and ligating the neighbouring Okazaki fragments (Maga *et al.,* 2001; Raducanu *et al.,* 2022). When DNA replication is complete, converging replication forks meet and are disassembled in a VCP-dependent manner (Dewar and Walter, 2017).

Replication stress is defined as a condition which leads to the slowdown or stalling of individual replication forks or global DNA synthesis (Zeman and Cimprich, 2014). The primary source of replication stress is damaged DNA bases, which often stall replicative DNA polymerases (**section 1.2.1**). Ribonucleotides, often incorporated in DNA by Polε and Polδ, can also block processive DNA synthesis (Dalgaard, 2012). Another source of replication stress arises from DNA sequences prone to form non-B form secondary structures. These typically involve hairpins, DNA triplexes and G-quadruplexes. Secondary structures can lead to replication stress by inhibiting helicase-dependent DNA

unwinding or stalling DNA polymerases if they are formed by ssDNA after the helicase unwinding (Sharma, 2011). Transcription-replication conflicts (TRCs) can also lead to replication stress as collisions with transcription machinery prevent DNA synthesis by DNA polymerases. TRCs are a common source of genomic instability in highly transcribed DNA regions, such as ribosomal DNA (Lindström *et al.*, 2018; Murakumo *et al.,* 2001). Depletion of the cellular nucleotide pool is another common trigger of replication stress. Hydroxyurea is a commonly used replication stress-inducing drug, which leads to dNTP pool depletion by inhibiting ribonucleotide reductase (Turner *et al.,* 1966). Nucleotide depletion can also occur due to the excessive number of origins being fired simultaneously and is often a consequence of oncogene overexpression (Beck *et al.*, 2012; Srinivasan *et al.*, 2013; Jones *et al.*, 2013).

Replication stress often leads to persistent exposure of single-stranded DNA, which appears due to the unwinding of the parental DNA duplex by the replicative helicase after the polymerase has stalled. Single-stranded DNA stretches are bound and protected by ssDNA-binding protein complex RPA. The protective role of RPA is demonstrated by the fact that replication collapse upon substantial replication stress is often dependent on RPA levels and can be prevented by RPA overexpression (Toledo *et al.*, 2013). The regions where dsDNA of the newly synthesised duplex turns into the exposed ssDNA – also called primer-template junctions – have been shown to activate checkpoint signalling, involving the Ataxia telangiectasia and Rad3 related (ATR) kinase (MacDougall *et al.,* 2007).

One pathway to cope with replication stress relies on the regulation of origin firing. In order to control the distribution of resources, such as dNTPs, not all the origins are fired at the same time, and a significant proportion of the origins is not fired at all during the unperturbed S phase (dormant origins). However, in the presence of replication stress, firing of dormant origins increases the number of active replication forks, allowing to complete replication in time despite the stress conditions. Importantly, firing of new origins is the primary pathway that allows the completion of replication upon long-term replication block (Petermann *et al.,* 2010). Nevertheless, stressed forks do not always have to rely on the neighbouring forks and are often able to sustain replication in the presence of DNA damage without removing DNA lesions. This involves a series of pathways, which will be discussed in detail in the following sections.

1.2.3 DNA damage bypass

As two DNA strands are complementary, either of them contains all the genetic information of the cell. A lesion in one DNA strand can be eliminated and replaced with a correct nucleotide using the second DNA strand as a template. However, in a number of cases, a second DNA strand is not available. This can happen when an interstrand crosslink affects complementary DNA bases or during DNA replication when DNA strands are unwound by the MCM2-7 helicase. The latter situation is hazardous, as the excision of damaged nucleotides from single-stranded DNA regions during DNA replication results in single-ended double-strand breaks, which may lead to cell death if not timely repaired. Therefore, cells have developed a series of pathways that allow the completion of DNA replication in the presence of DNA damage without repairing the damaged bases. This series of pathways is collectively termed 'DNA damage bypass'. In the following sections, I will describe the critical components of the damage bypass system in yeast and mammalian cells and how they are coordinated to enable the faithful completion of DNA replication.

1.2.3.1 Translesion synthesis

High fidelity of the replicative DNA polymerases ε and δ is achieved by the structure of their catalytic pockets, which can only accommodate a perfect Watson-Crick base pair, as well as by their ability to proofread and replace wrongly incorporated bases utilising the 3'-5' exonuclease activity (Bębenek and Ziuzia-Graczyk, 2018). Translesion synthesis (TLS) polymerases have more relaxed catalytic pockets and therefore reduced requirements for an incoming base pair. On the one hand, this allows them to catalyse DNA synthesis over damaged DNA. On the other hand, less strict control of base pairing and the lack of exonuclease activity can result in a higher mutagenesis rate than that of replicative polymerases. Whereas there are three TLS polymerases in *S. cerevisiae* (Polζ, Polη and Rev1), their number increases to 10 in human cells, at least 5 of which can function in DNA damage bypass. These are Polζ and the members of a so-called Y family of polymerases - Polη, Polκ, Polι and REV1. Unique structural features allow these polymerases to bypass specific lesions in an error-free manner. For example, Polη can perform error-free DNA synthesis over CPDs, making this polymerase crucial for the cellular response to UV damage (Hendel *et al.,* 2008). In line with this, levels of Polη

drastically increase after UV irradiation in a p53-dependent manner, increasing cellular resistance to UV light (Lerner *et al.,* 2017). Polκ can insert correct bases opposite of benzo[a]pyrene adducts and thymine glycol (Jha *et al.,* 2016; Yoon *et al.,* 2010). Although there are examples of an error-free mode of action of TLS polymerases, certain lesions, such as (6-4) photoproducts or abasic sites, tend to be bypassed by TLS polymerases in a mutagenic way. However, the danger of increased mutagenesis is often lower than that of the persistent replication blockade, as the latter may result in fork collapse, double-strand breaks and, ultimately, cell death. TLS polymerase REV1 is quite different from other Y-family members: in addition to performing TLS synthesis, it acts as a scaffold for the recruitment of other TLS polymerases, including Polη, Polκ, Polι and Polζ (Ohashi *et al.,* 2004; Murakumo *et al.,* 2001). At least for Polκ and Polζ, it has been shown that their recruitment to the UV-damaged chromatin depends on REV1, confirming its scaffolding role (Gallina *et al.,* 2021). For many DNA lesions, their bypass by TLS polymerases results in imperfectly paired bases, unable to be extended by replicative DNA polymerases. B-family TLS polymerase Polζ, consisting of a catalytic (REV3) and structural (REV7) subunits, has been shown to efficiently elongate unpaired primer termini, suggesting a two-step lesion bypass mechanism: dependent on the type of DNA damage, the first TLS polymerase inserts a base opposite the lesion, followed by an extension step by Polζ (Shachar *et al.,* 2009; Martin and Wood, 2019). Similar to Polη, expression of REV3 increases after DNA damage in a p53-dependent manner, representing an adaptive response to replication stress (Krieg *et al.,* 2006).

1.2.3.2 Template switching

In some instances, stalled primer terminus can use a sister chromatid as a template for extension in a DNA damage bypass pathway called template switching. In budding yeast, template switching is activated by K63-linked PCNA polyubiquitylation by Rad5/Ubc13/Mms2, although the effectors of this modification are unknown. Many steps of template switching resemble those from the homologous recombination pathway of DSB repair: following DNA unwinding and resection by Pif1 and Exo1, respectively, the formation of Rad51 filaments leads to the annealing of the ssDNA to the complementary strand of the homologous sister chromatid. Following branch migration and DNA synthesis based on the sister chromatid template, the resolution of Holliday structure-like

intermediates by Sgs1-Top3-Rmi1 complex completes the pathway, resulting in the error-free bypass of the lesion (**Figure 6**) (García-Rodríguez *et al.,* 2018b; García-Rodríguez *et al.,* 2018a; Branzei and Szakal, 2016). The proposed mechanism was confirmed by means of two-dimensional gel electrophoresis and electron microscopy of the pathway intermediates (Giannattasio *et al.,* 2014; Branzei *et al.,* 2008). Despite being best characterised in budding yeast, template switching also operates in human cells, as was shown for the bypass of UV photoproducts and bulky adducts (Izhar *et al.,* 2013; Piberger *et al.,* 2020).

In budding yeast, template switching is initiated by PCNA polyubiquitylation with K63-linked chains. The responsible E3 enzyme, Rad5, in addition to ubiquitin ligase activity, can catalyse fork regression and recruit the TLS polymerase Rev1 (Blastyák *et al.,* 2007; Gallo *et al.,* 2019). However, all three activities of Rad5 are genetically separable and, therefore, may be necessary in different physiological circumstances (Choi *et al.,* 2015).

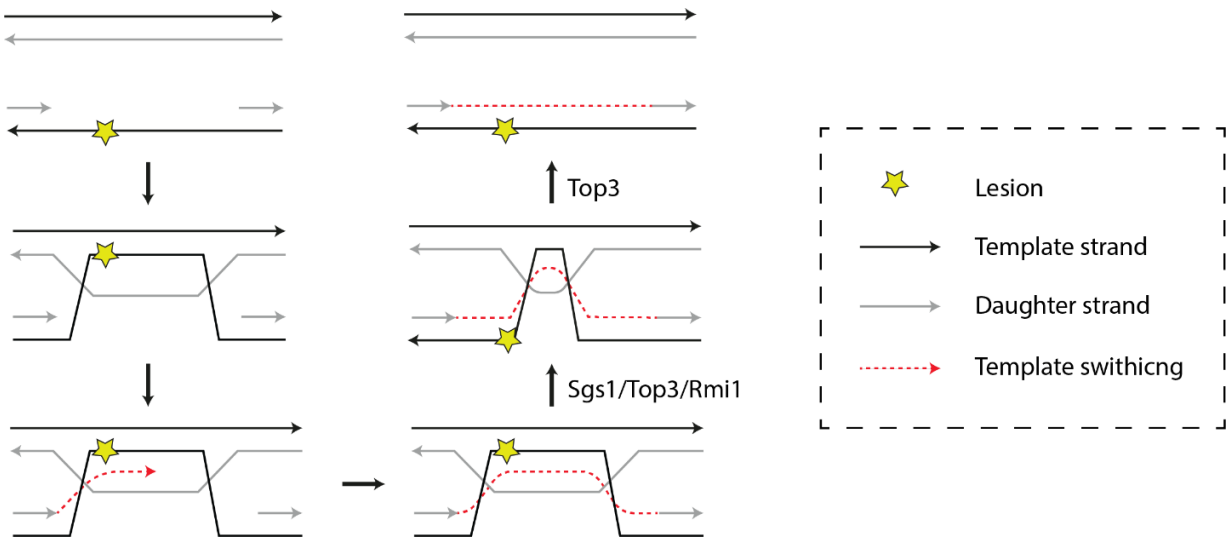

Figure 6: Schematic representation of the template switching pathway. Main steps are depicted, including gap invasion into the sister chromatid, DNA synthesis on a sister chromatid template and resolution of the Holliday junction-like intermediates.

1.2.3.3 Fork reversal

One of the mechanisms activated when a replisome encounters a DNA lesion or stalls due to other reasons is a transformation of a replication fork into a Holliday junction structure – a process termed replication fork reversal (**Figure 7**). Detection of reversed forks became possible due to advances in electron microscopy techniques, which allow direct visualisation of these replication intermediates. In budding yeast, fork reversal is a rare event: in cells treated for 30 min with HU, only 1.5% of replication forks appear to be reversed. Their number, however, increases if checkpoint kinase Rad53 is absent, rising to 11,2% (Sogo *et al.,* 2002). In striking contrast to yeast, replication fork reversal in mammalian cells is considered one of the main pathways initiated as a response to replication stress. Electron microscopy experiments, which allow direct visualisation of reversed forks, revealed that 15-30% of forks are reversed after treating human cells with 10 common DNA-damaging agents (Zellweger *et al.,* 2015).

The roles of the replication fork reversal and whether it can be considered a mode of damage bypass is a matter of debate. On the one hand, fork reversal transfers a damaged nucleotide into the parental DNA duplex, where it can be faithfully repaired. On the other hand, if the 5'-DNA overhang in the regressed arm is longer than the 3' one, it can serve as a template for DNA synthesis and thus lead to damage bypass. This pathway, however, lacks experimental evidence. Alternatively, cleavage of a reversed fork by structure-specific nucleases results in a double-strand break, which can be repaired by a break-induced replication (BIR) pathway (Hanada *et al.,* 2007; Donnianni and Symington, 2013). Another role for fork reversal has been recently proposed by Mutreja and colleagues (Mutreja *et al.,* 2018). Using immunolabelling of individual ICLs, the authors demonstrate that not only those forks that encountered the lesion undergo reversal, but global ATR-dependent fork reversal takes place as a response to replication stress. The fact that even unaffected forks undergo reversal suggests that the formation of reversed forks may be a protective mechanism which slows down global replication, thereby providing stressed forks more time to deal with the damage.

Several enzymes can regress replication forks *in vivo* and *in vitro*, among which SMARCAL1, HLTF and ZRANB3 are the best-characterised ones. SMARCAL1 is targeted to replication forks via RPA and reanneals DNA strands, which were unwound by the

helicase. HLTF performs a dual function: it promotes fork remodelling via its HIRAN domain and polyubiquitylates PCNA, leading to ZRANB3 recruitment. Importantly, these three translocases are not redundant *in vivo*, suggesting they participate in different stages of fork regression (Halder *et al.* 2022; Achar *et al*. 2015; Motegi *et al.* 2008; Ciccia *et al*. 2012). Recent studies also suggest that fork reversal is a two-step pathway: coordinated activity of SMARCAL1, HLTF and ZRANB3 leads only to initial steps of fork remodelling, leading to DNA supercoiling, sumoylation of TOP2B and recruitment of the DNA translocase PICH, which catalyses extensive fork reversal (Tian *et al*. 2021).

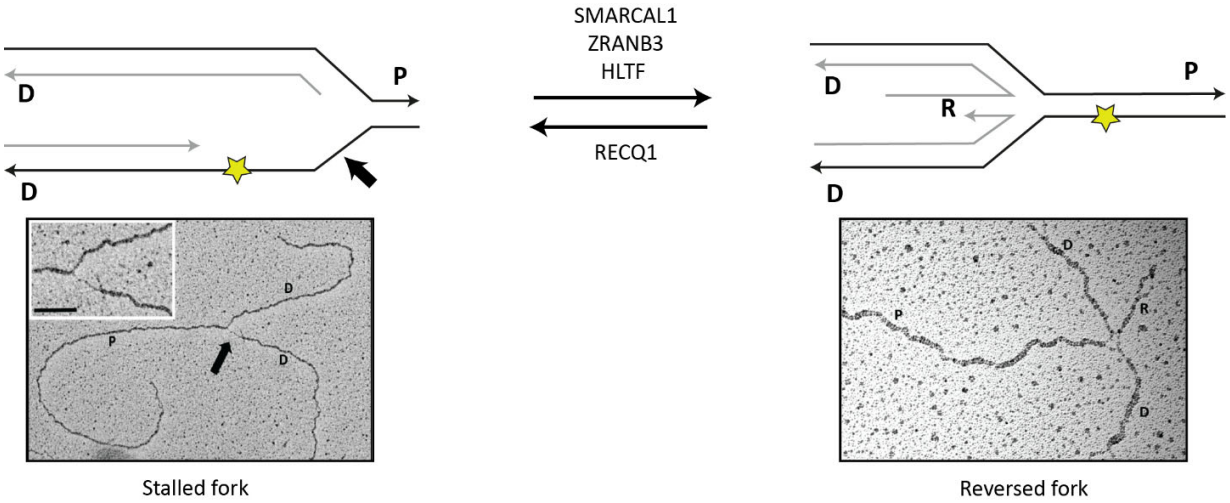

Figure 7: Fork reversal. Schematic representation of a fork reversal pathway. Electron microscopy images of a stalled and reversed fork are adapted from (Zellweger *et al.,* 2015).

Replication fork reversal is responsible for the nascent DNA degradation phenotype: depletion of certain factors, termed replication fork protectors, leads to degradation of newly synthesised DNA. Some of the best-characterised fork protectors are BRCA1 and BRCA2 (Lemaçon *et al*. 2017). Prolonged replication stress in the absence of these factors leads to MRE11 and EXO1-dependent DNA degradation, dependent on fork remodellers SMARCAL1, HLTF and ZRANB3, and thus likely originating from reversed replication forks (Taglialatela *et al*. 2017). Depletion of another fork protector, WRNIP1, also leads to nascent DNA degradation. However, in this case, it is dependent on the nuclease DNA2. WRNIP1 has been proposed to directly bind Holliday junctions of reversed replication forks and protect them from SLX4-dependent cleavage and formation of double-strand breaks (Porebski *et al.* 2019). Thus, nascent DNA

degradation may result from DNA2-dependent resection of double-strand breaks. Interestingly, nuclease CtIP and the cytoskeleton motor protein MYO6 behave similarly to WRNIP1 regarding fork protection (Przetocka *et al.,* 2018; Shi *et al.,* 2023). In all the abovementioned cases, nascent DNA degradation depends on all three major fork reversal enzymes (**Figure 8**). However, there is one exception to this pattern, which will be discussed in **section 1.2.3.5**.

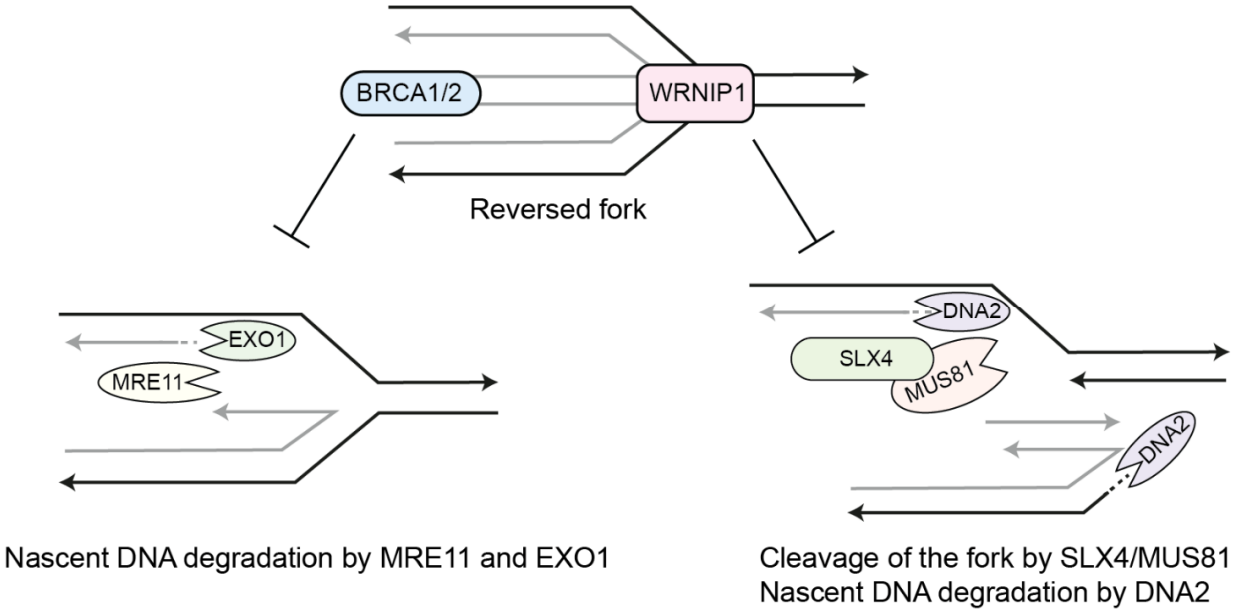

Figure 8: Nascent DNA degradation. Schematic representation of the two major pathways of fork protection. BRCA1/2 prevent resection of a reversed fork by the nucleases MRE11 and EXO1, whereas WRNIP1 protects the Holliday junction from the activity of structure-specific nucleases with subsequent DSB resection.

1.2.3.4 Repriming

Another pathway cells often utilise when a replication fork encounters a lesion is reinitiation of DNA synthesis downstream of the lesion. As replicative polymerases cannot start DNA synthesis on the blank ssDNA template and require the presence of a short primer, this pathway is often referred to as repriming. Repriming is an essential part of unperturbed replication of the lagging strand due to its discontinuous mode of synthesis. However, it is not typical for the leading strand in the absence of replication stress. Repriming downstream of a lesion results in a daughter-strand gap, essentially a region of ssDNA flanked by dsDNA. These postreplicative gaps differ from single-strand gaps

that appear during nucleotide excision repair, as they contain a lesion in the ssDNA stretch (**Figure 9A**). The presence of postreplicative gaps after replication over damaged DNA has been proven by single-molecule techniques, such as electron microscopy and DNA fibre assays (**Figure 9B**).

In budding yeast, Polα is responsible for repriming downstream of a lesion (Fumasoni *et al.,* 2015). In contrast, human cells have an additional enzyme, PRIMPOL, which is targeted to stressed replication forks by RPA and can initiate DNA synthesis on the leading strand ~14 nucleotides past the lesion (Guilliam *et al.,* 2017). Repriming neither repairs DNA damage nor leads to damage bypass but merely allows the replication fork to continue DNA replication past the lesion, which needs to be repaired later in a postreplicative manner via translesion synthesis or template switching. Significantly, postreplicative damage bypass can be separated from bulk DNA replication: yeast cells that lack Rad18, which is essential for damage bypass, are able to complete the S phase even in the presence of DNA damage, accumulating gaps behind the replication forks. Subsequent re-expression of Rad18 in the G2 phase leads to gap filling, which can be visualised by microscopy as short DNA stretches scattered along the bulk DNA. Interestingly, whereas both TLS and TS pathways can fill postreplicative gaps, for the UV-induced lesions, TLS by Rev1 and Polζ is a dominant pathway of gap filling, with template switching acting as a backup (Daigaku *et al.,* 2010). It was further demonstrated that damage bypass can occur in a postreplicative manner in Rad18-proficient cells. The loci where it takes place are visualised by RPA foci, resulting from repriming and gap expansion (Wong *et al.,* 2020). Evidence for the postreplicative gap filling has also been found for mammalian cells: bypass of BPDE-induced bulky adducts requires repriming by PRIMPOL and homologous recombination at gaps in a postreplicative manner (Piberger *et al.,* 2020).

Although repriming allows the cells to continue replication after encountering DNA lesions, extensive use of this pathway can be detrimental to cell viability. The formation of daughter-strand gaps has been identified as an underlying pathway for the sensitivity of BRCA-deficient cells to chemotherapeutic drugs (Panzarino *et al.,* 2021). Furthermore, hyperaccumulation of daughter-strand gaps can lead to elevated mutagenesis rates due to the increased use of TLS in gap filling (Somyajit *et al.,* 2021).

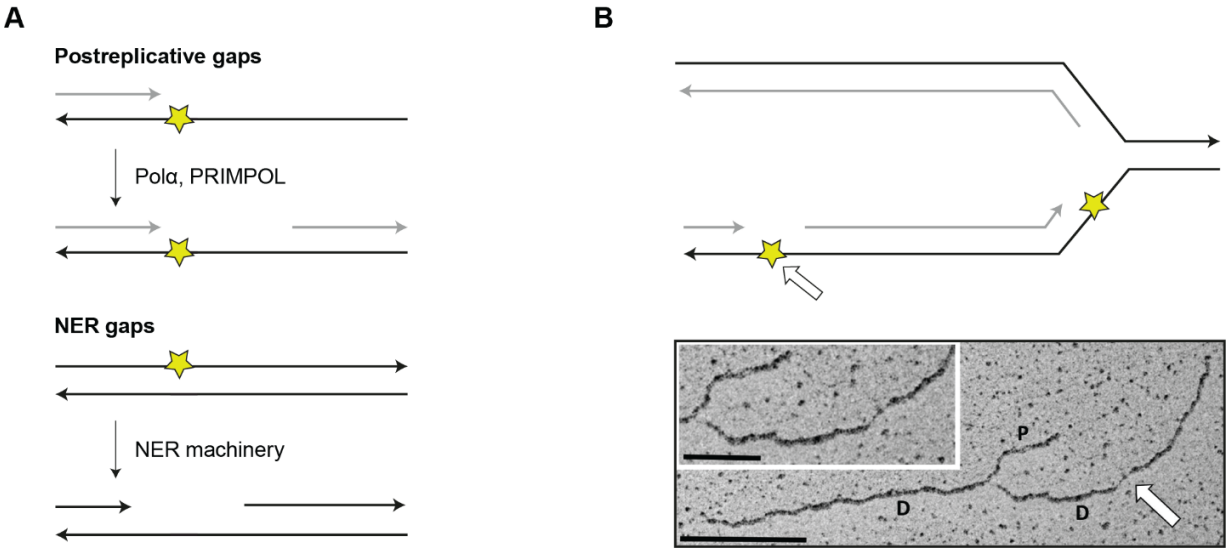

Figure 9: Daughter-strand gaps. (A) Schematic representation of daughter-strand gaps and their comparison to NER-dependent gaps. Note that lesion is not eliminated from DNA upon daughter-strand gap formation. **(B)** Electron microscopy image of a ssDNA gap behind the fork, adapted from (Zellweger *et al.,* 2015). P: parental DNA duplex; D: daughter DNA strands. The arrow indicates a daughter-strand gap.

Finally, it should be noted that once a replication fork encounters the lesion, there is competition between repriming, fork reversal and translesion synthesis. HLTF knockout cells, which lack a functional fork reversal pathway, do not slow down replication in the presence of low-dose HU due to PRIMPOL-dependent repriming. Conversely, increased expression of PRIMPOL interferes with fork reversal and prevents nascent DNA degradation in BRCA1-deficient cells. At the same time, mutation of the HLTF HIRAN domain, which is responsible for fork reversal, leads to unrestrained fork progression dependent on the TLS polymerase REV1 (Bai *et al.,* 2020). There are multiple other examples of the interplay between the discussed pathways, extensively reviewed in (Quinet *et al.,* 2021).

1.2.3.5 Roles of ubiquitylated PCNA in DNA damage bypass

DNA sliding clamp PCNA is subject to multiple posttranslational modifications, including phosphorylation, acetylation, sumoylation and ubiquitylation. Among these, mono- and polyubiquitylation of PCNA play an essential role in the cellular response to DNA damage and replication stress (**Figure 10**). PCNA monoubiquitylation, carried out

by the E3 enzyme RAD18, is a signal for the recruitment of TLS polymerases in yeast and human cells. A common feature of TLS polymerases is their interaction with PCNA and ubiquitin: REV1 has two ubiquitin-binding motifs and a PCNA-interacting BRCT domain; Polη – two PCNA-interacting peptides and a ubiquitin-binding zinc finger; Polκ - two PCNA-interacting peptides and two ubiquitin-binding UBZ domains (Guo *et al.,* 2006; Yoon *et al.,* 2014; Acharya *et al.,* 2008). In yeast, monoubiquitylation of PCNA is essential for TLS, as damage-induced mutagenesis is completely abolished in strains harbouring the PCNA K164R mutation (Stelter and Ulrich, 2003). In human cells, PCNA monoubiquitylation favours TLS, but appears to be not essential for it (Temviriyanukul *et al.,* 2012). Interestingly, in avian DT40 cells, recruitment of the TLS polymerase REV1 requires PCNA monoubiquitylation at gaps but not at replication forks (Edmunds *et al.,* 2008). In addition to TLS polymerases, metalloprotease Spartan has been shown to bind ubiquitylated PCNA via a combination of a PIP box and a UBZ domain (Centore *et al.,* 2012). By recruiting VCP, Spartan promotes the removal of Polη from the damage site, preventing excessive mutagenesis (Davis *et al.,* 2012). Finally, a combination of a PIP box and a UBZ domain was found in a nuclease SNM1A (Yang *et al.,* 2010). In the context of alternative telomere lengthening, ubiquitylated PCNA recruits SNM1A, initiating resection and template-switching pathway at damaged telomeres (Zhang *et al.,* 2023).

A ubiquitin moiety on PCNA can be further extended into a K63-linked polyubiquitin chain. In budding yeast, the responsible E3 is Rad5, which operates with highly K63-specific E2 Ubc13/Mms2. Although human cells possess two Rad5 homologs, HLTF and SHPRH, they are not essential for PCNA polyubiquitylation. Recent findings implicate E3 ligase RFWD3 in promoting this PCNA modification. However, it needs to be clarified whether RFWD3 directly polyubiquitylates PCNA or it recruits other E3 ligases to the damage site. In *S. cerevisiae*, PCNA polyubiquitylation activates an error-free branch of the damage bypass by means of template switching (**section 1.2.3.2**). This pathway seems to be conserved in higher eukaryotes, as K63-linked polyubiquitylation was shown to protect human cells against TLS-induced mutations. Interestingly, whereas K63-linked polyubiquitylation in yeast is vital for cell survival after MMS and UV damage, human cell lines with K63R mutant as the only source of ubiquitin are sensitive to cisplatin, but not to UV irradiation unless Polη is co-depleted (Chiu *et al.,* 2006). This implies a high level of redundancy for the TS and TLS in the bypass of UV-induced photoproducts in human

cells. In addition to the activation of template switching, K63-linked PCNA polyubiquitylation is essential in human cells for the replication fork reversal, where it acts as a recruitment signal for the DNA translocase ZRANB3 (Ciccia *et al.,* 2012). Another possible effector of polyubiquitylated PCNA is the TLS polymerase Polζ. K63-linked PCNA polyubiquitylation is essential for Polζ-dependent lesion bypass during replication in *X. laevis* egg extracts (Gallina *et al.,* 2021). Consistent with these data, the S phase gap-filling pathway in human cells relies on UBC13 and REV1-Polζ (Tirman *et al.,* 2021).

PCNA polyubiquitylation in human cells has recently been linked to the replication fork protection pathway: prolonged replication stalling in PCNA polyubiquitylation-deficient cells leads to DNA2-dependent nascent DNA degradation (Thakar *et al.,* 2020). Interestingly, this pathway is substantially different from the “BRCA1” and “WRNIP1” pathways, as it depends entirely on SMARCAL1, only partially on ZRANB3 and is independent of HLTF. This suggests that PCNA polyubiquitylation may be important to protect replication intermediates that originate from SMARCAL1 and ZRANB3 but not HLTF activity, underlining differential roles of these enzymes in fork regression.

Finally, PCNA is also decorated with K48-linked polyubiquitin chains upon hydroxyurea-induced fork stalling. K48-linked polyubiquitylated PCNA was shown to interact with Polκ, implicating this modification in the pathway of fork restart (Tonzi *et al.,* 2018). However, the writers of this modification, as well as its functions, are currently unknown.

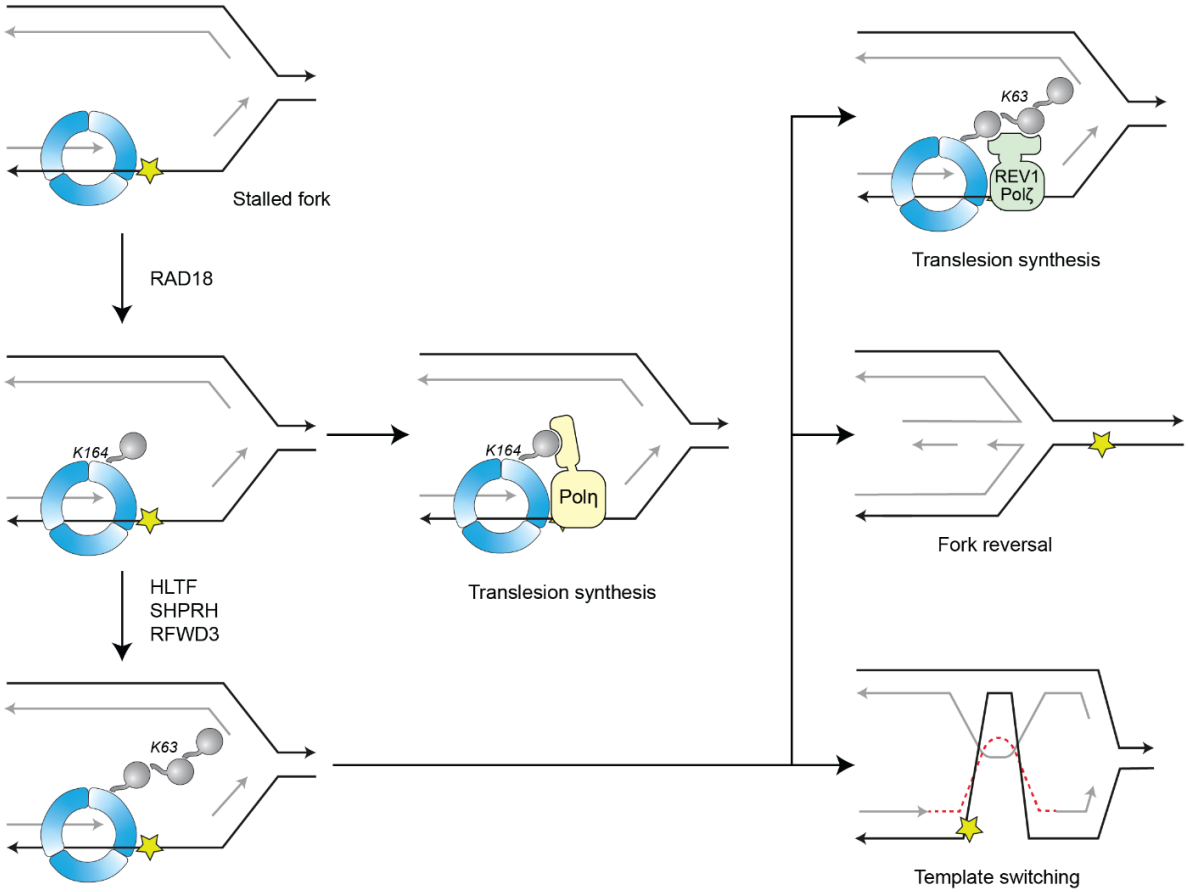

Figure 10: Roles of PCNA ubiquitylation in DNA damage tolerance. Depicted are only the best characterised pathways: translesion synthesis, template switching and fork reversal. For the details see main text.

1.3 Aims of this work

Among all posttranslational modifications, ubiquitylation is one of the most complex due to the variety of topologies that ubiquitin units may adopt on a given substrate. At least 8 different ubiquitin linkages, branched chains and multi-ubiquitylation events create distinctive interaction surfaces on the modified proteins, determining their interaction profiles. PCNA polyubiquitylation is unique among other instances of protein polyubiquitylation: although the fact that PCNA is subject to modification with K63-linked chains is known for more than 20 years, responsible readers of this modification are yet not characterised. Even though human cells possess the enzyme ZRANB3, which binds to polyubiquitylated PCNA, several cellular pathways in human cells cannot be mechanistically explained if ZRANB3 is assumed to be the only effector of polyubiquitylated PCNA.

This work aims to provide a better understanding of the pathways acting downstream of PCNA polyubiquitylation in human cells. For this purpose, artificial tailor-made enzymes are used to build a K63-linked polyubiquitin chain on PCNA in the absence of exogenous DNA damage. This technology, which has previously been implemented in *S. cerevisiae*, allows to mechanistically separate ubiquitin signalling on PCNA from other damage-induced pathways. Furthermore, exchanging the K63-specific enzyme with a K48-specific one allows direct comparison of differently linked polyubiquitin chains on PCNA. Finally, the expression of artificial enzymes will be compared to physiological scenarios where excessive PCNA polyubiquitylation takes place.

Chapter 2

Materials and methods

2.1 Reagents

2.1.1 Chemicals and recombinant proteins

Unless indicated differently, chemicals and recombinant proteins used in this study were purchased from Sigma Aldrich or Thermo Fisher Scientific. Chemicals purchased from other companies are listed below.

Carl Roth:	Ethanol 96% and 99.5%, isopropanol, acetic acid glacial, guanidine hydrochloride, imidazole, urea
Macherey-Nagel:	NucleoBond Xtra Midi Plus
MedChemExpress:	ML-323
New England Biolabs:	Restriction endonucleases, 10x CutSmart buffer
Takara Bio:	2x DNA ligation kit
Polyscience:	Polyethyleneimine linear (Molecular weight ~ 25000 g/mol)
Promega:	FUGENE HD transfection reagent
QIAGEN:	QIAquick gel extraction kit, FlexiTube siRNA solutions, Ni-NTA agarose

Recombinant proteins for the *in vitro* ubiquitylation assay (**section 2.13**) were generously provided by Sabrina Wegmann (former member of Helle Ulrich laboratory).

Recombinant proteins for the ubiquitin chain restriction assay (**section 2.12.3**) were generously provided by Christian Renz (a member of Helle Ulrich laboratory).

2.1.2 Antibodies

Table 1: List of primary antibodies used in this study. Unless otherwise indicated, the dilutions refer to western blotting.

ID	Name	Species	Source	Dilution
11	BrdU (BU1/75)	Rat mAb	Abcam ab6326	DNA fibre assay: 1:50
38	EXO1	Rabbit pAb	GeneTex GTX109891	1:1000
42	Flag (M2)	Mouse mAb	Sigma Aldrich F1804	1:2500
72	HLTF	Rabbit pAb	Alexandra Belayew, UMONS (Belgium)	1:1000
122	PCNA (PC10)	Mouse mAb	IMB PPCF	1:5000
125	PCNA	Rabbit pAb	Abcam ab18197	1:2500
133	γH2AX (JBW301)	Mouse mAb	Millipore 05-636-I	1:1000
153	POLH	Rabbit pAb	Abcam ab17725	1:1000
167	RAD18 (79B1048)	Mouse mAb	Abcam ab12007	1:1000
199	RPA32 (12F3.3)	Mouse mAb	Abcam ab12320	1:2500
261	Ubiquitin (VU1)	Mouse mAb	Tebu-bio VU101	1:1000
262	Ubiquitin (K48-selective, Apu2)	Rabbit mAb	Millipore 05-1307	1:1000
263	Ubiquitin (K63-selective, HWA4C4)	Mouse mAb	Enzo BML-PW-0600	1:1000
265	Ubiquitin (P4D1)	Mouse mAb	CST 3936	1:5000
272	VSV (P5D4)	Mouse mAb	Roche 11667351001	1:2500
276	ZRANB3	Rabbit pAb	Bethyl A303-033A	1:1000
324	Phospho-RPA S4-S8	Rabbit pAb	Biomol A300-245A	1:2500
334	Phospho-RPA S33	Rabbit pAb	Biomol A300-246A	1:2500
335	Phospho-RPA T21	Rabbit pAb	R&D Systems AF6654	1:2500
339	CHK1 (2G1D5)	Mouse mAb	CST 2360	1:1000
340	Phosho-CHK1 S345	Rabbit pAb	CST 2341	1:1000
372	H2B (53H3)	Mouse mAb	CST 2934	1:2500
392	Linear Ubiquitin (LUB9)	Mouse mAb	Merck MABS451	1:1000
395	WRNIP1	Rabbit pAb	Bethyl A301-389A-T	1:1000
402	SMARCAL1	Mouse mAb	Santa Cruz sc-376377	1:1000
404	GAPDH	Goat pAb	Novus Biologicals NB300-320	1:10000
408	RAP80	Rabbit pAb	Novus Biologicals NBP1-87156	1:1000

417	HUWE1	Rabbit pAb	ThermoFisher PA5-20374	1:1000
423	BrdU (B44)	Mouse mAb	BD Bio 347580	DNA fibre assay: 1:50 IF: 1:500
425	PCNA-Ub (D5C7P)	Rabbit mAb	CST 13439	1:2000
436	UBE2K/HIP2 (H-6)	Mouse mAb	Santa Cruz sc-390339	1:2000
442	Ubiquitin 1002A	Rabbit mAb	Bio-Techne MAB8595	1:2500

Table 2: A list of secondary antibodies used in this thesis. Unless otherwise indicated, the dilutions refer to western blotting.

ID	Name	Species	Source	Dilution
86	Mouse Alexa Fluor 488	Goat	Life A-11001	IF: 1:500
88	Mouse Alexa Fluor 647	Goat	Life A-21236	DNA fibre assay 1:100
93	Mouse HRP	Goat	Pierce	1:10000
156	Rabbit HRP	Goat	Pierce	1:10000
186	Rat Alexa Fluor 488	Goat	Invitrogen A-11006	DNA fibre assay 1:100

2.2 Media and solutions

2.2.1 Media for bacteria

All *E. coli* strains were grown in liquid Luria Broth (LB) medium or on LB-agar plates. If needed, liquid medium was supplemented with 100 µg/ml ampicillin or 30 µg/ml kanamycin, or antibiotic-containing LB-agar plates were used. Liquid LB medium, LB-agar plates and stock solutions of antibiotics were prepared by the IMB Media Laboratory.

2.2.2 Media for mammalian cells

HEK 293T and MDA-MB-436 cells were maintained in Dulbecco's Modified Eagle Medium (DMEM) supplemented with 2 mM L-glutamine, 100 U/ml penicillin, 100 µg/ml streptomycin and 10% (v/v) Fetal bovine serum (FBS). RPE1 hTERT cells were cultured in RPMI 1640 medium with the same supplements as stated for the DMEM medium. If indicated, 2 µg/ml puromycin, 100 µg/ml blasticidin, 100 µg/ml zeocin or 400 µg/ml G418 were added to the medium.

2.2.1 Solutions

Following solutions were prepared by IMB Media Laboratory: 5x PBS, 1M Tris-HCl pH 6.3, 1M Tris-HCl pH 7.5, 1M Tris-HCl pH 8.0, 1M KCl, 2M $MgCl_2$, 0.5 M EDTA pH 8.0, 5M NaCl, 10x TBE, 10x wet transfer buffer.

Blocking buffer for DNA fibre assay: 2% (w/v) BSA in PBST

Blocking buffer for immunofluorescence: 3% (w/v) BSA in PBST

Blocking buffer for western blotting: 5% (w/v) skim milk powder in PBST

Buffer A for denaturing pulldown: 6M Gua-HCl, 50 mM NaH_2PO_4, 50 mM Na_2HPO_4, 10 mM Tris-HCl pH 8.0, 0.1% Tween 20

Buffer B for denaturing pulldown: 8M Gua-HCl, 80 mM NaH_2PO_4, 20 mM Na_2HPO_4, 10 mM Tris-HCl pH 6.3, 0.1% Tween 20

Cell fractionation buffer: 10 mM HEPES pH 7.5, 10 mM KCl, 1.5 mM $MgCl_2$, 350 mM sucrose, 10% glycerol

Cell lysis buffer for DNA fibre assay: 200 mM Tris-HCl pH 7.5, 50 mM EDTA, 0.5% SDS

Dilution buffer for immunoprecipitation: 20 mM HEPES pH 7.5, 125 mM KOAc, 1.5 mM $MgCl_2$, 10% glycerol

Elution buffer for denaturing pulldown: 2x NuPAGE LDS sample buffer (Thermo Fisher Scientific), 200 mM imidazole, 10 mM DTT

MES running buffer: 50 mM MES hydrate, 50 mM Tris, 0.1% SDS, 1mM EDTA

MOPS running buffer: 50 mM MOPS, 50 mM Tris, 0,1 % (v/v) SDS, 1 mM EDTA

PBST: 1x PBS, 0.1% (v/v) Tween 20

PI staining buffer: 1x PBS, 20 µg/ml RNAse A (Sigma Aldrich), 100 µg/ml propidium iodide (PI)

Ponceau S solution: 0.1% (w/v) Ponceau S in 5% (v/v) acetic acid

Pre-extraction buffer for immunofluorescence: 100 mM PIPES pH 6.8, 1 mM EGTA, 100 mM NaCl, 300 mM sucrose, 0,5% Triton X-100

RIPA buffer: 50 mM Tris-HCl pH 7.5, 150 mM NaCl, 1% IGEPAL CA-630, 0.5% sodium deoxycholate, 0.1% SDS, 2.5 mM $MgCl_2$

Trans-Blot Turbo buffer: 1x Trans-Blot Turbo buffer (Bio-Rad), 20% ethanol

Ubiquitylation buffer: 40 mM HEPES pH 7.4, 8 mM magnesium acetate, 50 mM NaCl

Wet transfer buffer: 192 mM glycine, 25 mM Tris-HCl pH 8.3, 15% (v/v) methanol

2.3 DNA oligonucleotides

Table 3: A list of DNA oligonucleotides used in this thesis.

ID	Name	Sequence
3343	Ub-K63R-fw	CCCTGTCTGACTACAACATCCAGAGAGAGTCCACCCTGCACCTG
3344	Ub-K63R-rev	CAGGTGCAGGGTGGACTCTCTCTGGATGTTGTAGTCAGACAGGG
4455	Ub-K48R-fw	GATTGATCTTTGCCGGTCGACAGCTAGAAGACGGTAGAAC
4456	Ub-K48R-rev	GTTCTACCGTCTTCTAGCTGTCGACCGGCAAAGATCAATC
4457	Ub-K63R-fwII	GTCTGATTACAACATTCAGCGAGAGTCCACCTTACATCTTG
4458	Ub-K63R-revII	CAAGATGTAAGGTGGACTCTCGCTGAATGTTGTAATCAGAC
4950	Ubc7-His_6-NotI-rev	GCAAGCGGCCGCTTAGTGATGGTGATGGTGATGAG
5085	VSV-fw	TACACTGACATCGAAATGAATAGATTG
5086	$E3^{63}$-NotI-rev	GCAAGCGGCCGCTTAAAAAACCGCATCGTGAAATG
5194	Ube2G2-NotI-rev	GCAAGCGGCCGCTCACAGTCCCAGAGACTTCTG
5196	Ubc7-NcoI-fw	GACCACCATGGGATCGAAAACCGCTCAGAAACG
5197	Ube2G2-NcoI-fw	GACCACCATGGCGGGGACCGCGCTCAAGAG
5285	Flag-NotI-rev	GCAAGCGGCCGCTTACTTGTCGTCGTCATCCTTGTAG
5288	hcoUbc7-ATG-fw	AGCAAGACCGCCCAGAAGCG
5289	hcoUbc7-NotI-rv	GCAAGCGGCCGCTCAGAAGCCCAGGCTCTTCAG
5305	hcoCue1-SmaI-fw	CGATCCCGGGGCAGAGCAACCAGCACCCAAG
5436	$E3^{63}$ I227A-fw	GAGTGTCCTGCGTGTTTTGAAAACATGG
5437	$E3^{63}$ I227A-rev	TTCAAAACACGCAGGACACTCTTTAATAGC
5438	$E3^{63}$-fw	AATCTCCTTGTCTCAAGCACTAATAG
5439	VSV-rev	CTTCCCCAATCTATTCATTTCGATGTC

5447	E3^{63}RINGdel-rev	CTCTTTAATAGCGTTATCAGTCGTG
5448	E3^{63}RINGdel-fw	GATGCGGTTTTTTAAGCGGC
5454	^{hco}E3^{1} RBR-N-BglII-fw	CAGTAGATCTGCTAGCGGTGCTGGAGG
5455	^{hco}E3^{1} RBR-N-SbfI-rev	TTCTCCTGCAGGTACATGGCCAGGCC
5456	^{hco}E3^{1} RBR-C-SbfI-fw	TGTACCTGCAGGAGAACGGCATCGACTG
5457	^{hco}E3^{1} RBR-C-NotI-rev	GAGTGCGGCCGCCTACTTGCGGCGGCGAGGG
5799	^{hco}Ubc7-P2A-PacI-fw	GATCTTAATTAACGGAAGCGGAGCCACGAACTTC TCTCTGTTAAAGCAAGCAGGAGACGTGGAAGAAA ACCCCGGTCCTGACTACAAAGACCATGACGGT
5880	Ub-K48R-fwII	CAGCAGAGGTTGATCTTTGCTGGGAGACAGCTGG AAGATGGACGC
5881	Ub-K48R-revII	GCGTCCATCTTCCAGCTGTCTCCCAGCAAAGATC AACCTCTGCTG
5896	His-Ub-HindIII-fw	GCATAAGCTTCGGGCTGCAGATGCATCACC
5897	Ub-NotI-rev	GCATGCGGCCGCTCACCCACCTCTGAGACGGAG G
5981	HOIP-C885A-fw	CGCCCTGGCCCGAGGAGGCGCTATGCACTTTCA CTGTACCC
5982	HOIP-C885A-rev	GGGTACAGTGAAAGTGCATAGCGCCTCCTCGGG CCAGGGCG
6000	His$_{8}$-H2B-HindIII-fw	GCATAAGCTTACCATGCATCACCATCACCATCAC CATCACATGCCAGAGCCAGCGAAGTCTGCTC
6002	H2B-BamHI-rev	CGATGGATCCCTTAGCGCTGGTGTACTTGGTG
6006	P2A-mutagenesis-fw	CGTGGAAGAAAAACTCGCTTCTGACTACAAAGAC
6007	P2A-mutagenesis-rev	GTCTTTGTAGTCAGAAGCGAGTTTTTCTTCCACG
6008	Ub-K11R-fw	GAAGACCCTGACTGGTAGGACCATCACTCTCGAA G
6009	Ub-K11R-rev	CTTCGAGAGTGATGGTCCTACCAGTCAGGGTCTT C
6060	Ub-K6R-fw	GGCATGCAGATCTTCGTGCGGACCCTGACTGGT
6061	Ub-K6R-rev	ACCAGTCAGGGTCCGCACGAAGATCTGCATGCC
6062	Ub-K27R-K29R-K33R-fw	GACACCATTGAGAATGTCAGGGCAAGAATCCAAG ACCGGGAAGGCATCCCTCCTGAC
6063	Ub-K27R-K29R-K33R-rev	GTCAGGAGGGATGCCTTCCCGGTCTTGGATTCTT GCCCTGACATTCTCAATGGTGTC
6100	H2B-GA-fw	ATGCCAGAGCCAGCGAAG
6101	H2B-GA-rev	CTTAGCGCTGGTGTACTTGGTG
6102	H2B-FRB*-GA-rev	GACTTCGCTGGCTCTGGCATACTAGTCTTGCTGA TGCGGCG
6103	H2B-His$_{8}$-GA-fw	CACCAAGTACACCAGCGCTAAGCATCACCATCAC CATCACCATCACTAAGCGGCCGCTCGAGTCTAGA G
6165	PIP box-fw	CATGGGCATGAAGCAAAGCTCATTGCTGTCATTC TTTTG
6166	PIP box-rev	GATCCAAAAGAATGACAGCAATGAGCTTTGCTTC ATGCC

6167	OTUB1 C91S-fw	CAGGCCTGACGGCAACTCTTTCTATCGGGCTTTC
6168	OTUB1 C91S-rev	GAAAGCCCGATAGAAAGAGTTGCCGTCAGGCCT G
6187	His_6-HindIII-fw	AGCTTATGCATCACCATCACCATCACA
6188	His_6-HindIII-rev	AGCTTGTGATGGTGATGGTGATGCATA
6219	yUbc13hco-HindIII-fw	GATCAAGCTTCCACCATGGCCAGCCTGCCCAAGC
6220	yUbc13hco-NotI-rev	CGATGCGGCCGCTCACTCGGGCTTCTTCTTGGC
6221	yMMS2 hco-HindIII-fw	GATCAAGCTTCCACCATGAGCAAGGTGCCCCGCA AC
6222	yMMS2 hco-NotI-fw	CGATGCGGCCGCTCAGAACGTCTCGCCCTCTTTG
6264	His_6-NUbo-ATG mutagenesis-fw	CACCATCACCATCACAAGCTTGGGCAGATCTTCG TGAAGACCC
6265	His_6-NUbo-ATG mutagenesis-rev	GGGTCTTCACGAAGATCTGCCCAAGCTTGTGATG GTGATGGTG

2.4 RNA oligonucleotides

Table 4: A list of RNA oligonucleotides used in this thesis. Information is provided for the sense (5'-3') strand of the duplex.

Name	**Sequence 5'-3'**	**Source**
siHLTF	GCGAAAUGACUUAUACUAUTT	Life Technologies
siHUWE1	GGUCUAAUCAUGCCGCAGATT	Life Technologies
siRAD18#1	GUUCAGACAUCAUAAGAGATT	Life Technologies
siRAD18#2	GGAUUAUCUAUUCAAGGAATT	Life Technologies
siRAP80#1	GAUACAGUAUUGACUCGGATT	Life Technologies
siRAP80#2	GGGUUGCAGAAAACGAAGATT	Life Technologies
siSMARCAL1	CAGCUUUGACCUUCUUAGCAA	Qiagen
siUBE2K	ACAGGAUGCUGUAGUAGCAAA	Qiagen
siWRNIP1#1	CCAAGGCUGUCAUUUUAUATT	Life Technologies
siWRNIP1#2	GAAACAUAGCAUAAGGUUUTT	Life Technologies
siZRANB3#1	CCGGAUUCACAUCUAUACUAA	Qiagen
siZRANB3#2	UGCCAGUGUAUGACACCUUAA	Qiagen

2.5 Plasmids

Table 5: A list of plasmids created in this study

ID	Name	Construction	Use
4528	pENTR4-Ubc7-His_6	Ubc7-His_6 was amplified from p3365 with o5196 + o4950. PCR product was cloned into pHU1788 via NcoI/NotI	Gateway cloning
4596	pENTR4-VSV-PIP-$E3^{63}$	VSV-PIP-$E3^{63}$ was amplified with o5085 + o5086 from a G-block (IDT). PCR product was cloned into p1788 via NcoI/NotI	Gateway cloning
4599	pDEST/FRT/TO-Flag-VSV-PIP-$E3^{63}$	Gateway LR recombination between p4596 and p3543.	Overexpression of Flag-VSV-PIP-$E3^{63}$ in mammalian cells; creation of FlpIn cell lines
4635	pENTR4-VSV-PIP-$E3^{48}$-Flag	$E3^{48}$ sequence was amplified from a G-block (IDT) with o5305 + o5285. PCR product was cloned into pHU4597 via XmaI/NotI	Gateway cloning
4645	pENTR4-hcoUbc7	^{hco}Ubc7 sequence was amplified from a G-block (IDT) with o5288 + o5289. PCR product was cloned into pHU1788 via NcoI/NotI	Gateway cloning
4650	pENTR4-Ube2G2	Ube2G2 sequence was amplified from p4393 with o5194 + o5197. PCR product was cloned into pHU1788 via NcoI/NotI	Gateway cloning
4651	pDEST-3xFlag-Ube2G2	Gateway LR recombination between p4650 and p1804	Overexpression of 3xFlag-Ube2G2 in mammalian cells
4660	pDEST-3xFlag-^{hco}Ubc7	Gateway LR recombination between p4645 and p1804	Overexpression of 3xFlag-^{hco}Ubc7 in mammalian cells
4715	pDEST/FRT/TO-Flag-VSV-PIP-$E3^{63}$ (I227A)	PCR with 5'-phosphorylated o5436 + o5437 on pHU4599. Self-ligation of the PCR product	Overexpression of Flag-VSV-PIP-$E3^{63}$ (I227A) in mammalian cells; creation of FlpIn cell lines

4720	pDEST/FRT/TO-Flag-VSV-E3^{63}	PCR on p4599 with 5'-phosphorylated oligos o5438 + o5439. Self-ligation of the PCR product	Overexpression of Flag-VSV-E3^{63} (I227A) in mammalian cells; creation of FlpIn cell lines
4756	pDEST/FRT/TO-Flag-VSV-PIP-E3^{63}ΔRING	PCR on p4599 with 5'-phosphorylated oligos o5447 + o5448. Self-ligation of the PCR product	Overexpression of Flag-VSV-PIP-E3^{63}ΔRING in mammalian cells; creation of FlpIn cell lines
4894	pLentiCMV/Tre/3G Neo -VSV-PIP-E3^{63}	Gateway LR recombination between p4893 and p4596	Creation of stable cell lines with inducible overexpression of VSV-PIP-E3^{63}
5109	pENTR4-VSV-PIP-^{hco}E3^{1}	Ligation of three DNA fragments: 1. PCR on the G-block (IDT) with o5454 + o5455, digested with BglII/SbfI 2. PCR on the G-block (IDT) with o5456 + o5457, digested with NotI/SbfI 3. p4510 digested with NotI/BglII	Gateway cloning
5110	pDEST/FRT/TO-Flag-VSV-PIP-E3^{1}	Gateway LR recombination between p3543 and p4510	Overexpression of Flag-VSV-PIP-E3^{1} in mammalian cells
5111	pDEST/FRT/TO-Flag-VSV-PIP-^{hco}E3^{1}	Gateway LR recombination between p3543 and p5109	Overexpression of Flag-VSV-PIP-^{hco}E3^{1} in mammalian cells
5112	pDEST/FRT/TO-Flag-VSV-PIP-E3^{48}-Flag	Gateway LR recombination between p3543 and p4635	Overexpression of Flag-VSV-PIP-E3^{48}-Flag in mammalian cells; creation of FlpIn cell lines

5136	pDEST/FRT/TO-Flag-VSV-PIP-E3^{48}-Flag-P2A-3xFlag-^{hco}Ubc7	3xFlag-Ubc7 was amplified from p4660 with o5799 + o5289. PCR product was cloned into p5112 backbone via PacI/NotI	Overexpression of Flag-VSV-PIP-E3^{48}-Flag-P2A-3xFlag-^{hco}Ubc7 in mammalian cells; creation of FlpIn cell lines
5242	pDEST-His$_{10}$-Ubiquitin	p2685 was amplified with o5896 + o5897 and cloned into p4530 via NotI/HindIII	Overexpression of His$_{10}$-Ubiquitin in mammalian cells
5340	pDEST-His$_{10}$-Ubiquitin (K48R)	Site-directed mutagenesis on p5242 with o5880 + o5881	Overexpression of His$_{10}$-Ubiquitin (K48R) in mammalian cells
5341	pDEST-His$_{10}$-Ubiquitin (K63R)	Site-directed mutagenesis on p5242 with o3343 + o3344	Overexpression of His$_{10}$-Ubiquitin (K63R) in mammalian cells
5342	pDEST-His$_{10}$-Ubiquitin (K48R K63R)	Site-directed mutagenesis on p5340 with o3343 + o3344	Overexpression of His$_{10}$-Ubiquitin (K48R K63R) in mammalian cells
5346	pDEST-His$_{10}$-Ubiquitin (K11R K48R K63R)	Site-directed mutagenesis on p5342 with o6008 + o6009	Overexpression of His$_{10}$-Ubiquitin (K11R K48R K63R) in mammalian cells
5347	pDEST-His$_{10}$-Ubiquitin (K11R K48R)	Site-directed mutagenesis on p5340 with o6008 + o6009	Overexpression of His$_{10}$-Ubiquitin (K11R K48R) in mammalian cells
5351	pDEST/FRT/TO-Flag-VSV-PIP-^{hco}E3^{48}-P2A*-3xFlag-^{hco}Ubc7	Site-directed mutagenesis on p5136 with o6006 + o6007	Overexpression of Flag-VSV-PIP-^{hco}E3^{48}-P2A*-3xFlag-^{hco}Ubc7 in mammalian cells
5370	pcDNA5/FRT/TO-His$_8$-H2B-FKBP-CUb	H2B sequence was amplified from p3234 with o6000 + o6002 and cloned into p5049 via HindIII/BamHI	Overexpression of His$_8$-H2B-FKBP-CUb in mammalian cells
5372	pcDNA5/FRT/TO-His$_8$-H2B-FKBP-CUb(K48R)	Site-directed mutagenesis on p5370 with o4455 + o4456	Overexpression of His$_8$-H2B-FKBP-CUb(K48R) in mammalian cells

5374	pcDNA5/FRT/TO-His_8-H2B-FKBP-CUb(K63R)	Site-directed mutagenesis on p5370 with o4457 + o4458	Overexpression of His_8-H2B-FKBP-CUb(K63R) in mammalian cells
5379	pDEST-His_{10}-Ubiquitin (K6R K11R K48R)	Site-directed mutagenesis on p5347 with o6060 + o6061	Overexpression of His_{10}-Ubiquitin (K6R K11R K48R) in mammalian cells
5380	pDEST-His_{10}-Ubiquitin (K63-only)	Site-directed mutagenesis on p5379 with o6062 + o6063	Overexpression of His10-Ubiquitin (K63-only) in mammalian cells
5381	pDEST-His_{10}-Ubiquitin (K0)	Site-directed mutagenesis on p5380 with o3343 + o3344	Overexpression of His_{10}-Ubiquitin (K0) in mammalian cells
5382	pcDNA5/FRT/TO-NUa-HA-FRB*-H2B-His_8	Gibson assembly for: 1. PCR on p5046 with o6102 + o6103 2. PCR on p5370 with o6100 + o6101	Overexpression of NUa-HA-FRB*-H2B-His_8 in mammalian cells
5425	pENTR4 PIP-OTUB1	p3457 was digested with NotI/BamHI and ligated with the annealed oligos o6165 + o6166	Gateway cloning
5431	pENTR4 PIP-OTUB1 (C91S)	Site-directed mutagenesis on p5425 with o6167 + o6168	Gateway cloning
5457	pDEST/FRT/TO-Flag-PIP-OTUB1	Gateway LR recombination between p3543 and p5425	Overexpression of Flag-PIP-OTUB1 in mammalian cells
5458	pDEST/FRT/TO-Flag-PIP-OTUB1 (C91S)	Gateway LR recombination between p3543 and p5431	Overexpression of Flag-PIP-OTUB1 (C91S) in mammalian cells
5477	pcDNA5/FRT/TO-y^{hco}UBC13	y^{hco}UBC13 sequence was amplified from a G-block (IDT) with o6219 + o6220. PCR product was cloned into p4636 backbone via HindIII/NotI	Overexpression of y^{hco}UBC13 in mammalian cells
5478	pcDNA5/FRT/TO-y^{hco}MMS2	y^{hco}UBC13 sequence was amplified from a G-block (IDT) with o6221 + o6222. PCR product was cloned into p4636 backbone via HindIII/NotI	Overexpression of y^{hco}MMS2 in mammalian cells

5703	pcDNA5/FRT/TO-Myc-^{hco}E3^{1}(C885A)-L20-FKBP-CUb	Site-directed mutagenesis on p5236 with o5981 + o5982	Overexpression of Myc-^{hco}E3^{1}(C885A)-L20-FKBP-CUb in mammalian cells
5706	pcDNA5/FRT/TO-His$_6$-NUa-HA-FRB*-H2B-His$_8$	p5382 was digested with HindIII and ligated with the annealed oligos o6187 + o6188, followed by site-directed mutagenesis with o6264 + o6265	Overexpression of His$_6$-NUa-HA-FRB*-H2B-His$_8$ in mammalian cells

Table 6: A list of plasmids generated by others and used in this study.

ID	Name	Use	Source/Received from
1788	pENTR4	Gateway cloning	Simon Boulton
1804	pDEST/N-3xFLAG/FRT	Gateway cloning	Stephen West
1809	pOG44	Creation of stable cell lines	Simon Boulton
3543	pDEST/TO/FLAG FRT Puro	Gateway cloning	Martin Möckel
3457	pENTR4-OTUB1	Gateway cloning	Stephanie Nick
4636	pcDNA5/FRT/TO	Overexpression in mammalian cells; creation of stable cell lines	Petra Beli laboratory
4693	pcDNA5/FRT/TO-Nua-HA-FRB*-E3^{48}-Flag	Overexpression in mammalian cells	Evrydiki Asimaki
4892	pLenti CMV rtTAE3 Blast	Lentiviral vector for the expression of the reverse tetracycline transactivator rtTAE3	Vassilis Roukos laboratory
4893	pLentiCMV/Tre/3G Neo Dest	Gateway cloning	Vassilis Roukos laboratory
5046	pcDNA5/FRT/TO-Nua-HA-FRB*-E3^{63}-Flag	Overexpression of Nua-HA-FRB*-E3^{63}-Flag in mammalian cells	Evrydiki Asimaki
5236	pcDNA5/FRT/TO-Myc-^{hco}E3^{1}-L20-FKBP-CUb	Overexpression of Myc-^{hco}E3^{1}-L20-FKBP-Cub in mammalian cells	Evrydiki Asimaki

2.6 Strains and cell lines

2.6.1 Bacterial strains

Table 7: A list of the *E. coli* strains used in this study

ID	Strain	Genotype	Use	Source
14	Top Ten	F-*mcrA* Δ(*mrr-hsd*RMS-*mcr*BC) Φ80*Lac*ZΔM15 Δ *Lac*X74 *rec*A1 *ara*D139 Δ(*araleu*) 7697 *gal*U *gal*K *rps*L (StrR) *end*A1 *nup*G	Cloning	Invitrogen
18	ccdB Survival 2	F^{-}*mcr*A Δ(*mrr-hsd*RMS-*mcr*BC) Φ80*lac*ZΔM15 Δ*lac*X74 *rec*A1 *ara*Δ139 Δ(*ara-leu*)7697 *gal*U *gal*K *rps*L (Str^{R}) *end*A1 *nup*G *fhu*A::*IS2*	Cloning of ccdB-containing vectors	Invitrogen

2.6.2 Mammalian cell lines

Table 8: A list of the mammalian cell lines used in this study

ID	Cell line	Antibiotics	Source
120	RPE1 hTERT FlpIn TREX	Blasticidin, Zeocin, G418	Jonathon Pines laboratory
157	HEK 293T		Merck
249	RPE1 hTERT FlpIn TREX Flag-VSV-PIP-E3^{63}	Blasticidin, Puromycin, G418	This study
257	RPE1 hTERT FlpIn TREX Flag-VSV-E3^{63}	Blasticidin, Puromycin, G418	This study
258	RPE1 hTERT FlpIn TREX Flag-VSV-PIP-E3^{63} (I227A)	Blasticidin, Puromycin, G418	This study
259	RPE1 hTERT FlpIn TREX Flag-VSV-PIP-E3^{63} (ΔRING)	Blasticidin, Puromycin, G418	This study
268	HEK 293T WT/PCNA K164R		George-Lucian Moldovan laboratory
269	HEK 293T PCNA K164R		George-Lucian Moldovan laboratory
270	RPE1 hTERT WT		Anja-Katrin Bielinsky laboratory
271	RPE1 hTERT		Anja-Katrin Bielinsky laboratory
273	RPE1 hTERT WT Tet-On VSV-PIP-E3^{63}	Blasticidin, G418	This study

274	Rpe1 hTERT PCNA K164R clone 2B10 Tet-On VSV-PIP-E3^{63}	Blasticidin, G418	This study
275	HEK 293T Tet-On VSV-PIP-E3^{63}	Blasticidin, G418	This study
277	HEK 293T WT/PCNA K164R Tet-On VSV-PIP-E3^{63}	Blasticidin, G418	This study
278	HEK 293T PCNA K164R Tet-On VSV-PIP-E3^{63}	Blasticidin, G418	This study
308	RPE1 hTERT FlpIn TREX Flag-VSV-PIP-E3^{48}	Blasticidin, Puromycin, G418	This study
313	RPE1 hTERT FlpIn TREX Flag-VSV-PIP-E3^{48}-P2A-3xFlag-^{hco}Ubc7	Blasticidin, Puromycin, G418	This study
391	MDA-MB-436		Petra Beli laboratory

2.7. General methods for DNA manipulation

2.7.1 Measurement of DNA concentration

Concentration of DNA in solution was measured with the Nanodrop 2000 spectrophotometer (Thermo Scientific) or with the DeNovix DS-11 spectrophotometer (Biozym).

2.7.2 Agarose gel electrophoresis

Agarose gels were prepared by dissolving 1% (w/v) agarose in 1x TBE buffer, supplemented with SYBR Safe DNA stain (Invitrogen). DNA was mixed 5:1 with 6x DNA loading dye, loaded on a 1% agarose gel and run at 100 V until the desired separation of DNA bands took place. 1 kbp or 100 bp New England Biolab DNA ladder was used as a size standard.

2.8 Methods for molecular cloning

2.8.1 Polymerase chain reaction (PCR)

DNA amplification by polymerase chain reaction (PCR) was performed using HF polymerase (IMB Protein production core facility). 1-10 ng of DNA were mixed with 5 µl of 10x HF buffer, 2.5 µl of 10 µM forward and reverse oligonucleotides, 1 µl of 10 mM dNTPs and 0.5 µl of HF polymerase (2 cU/µl) in a total volume of 50 µl. The reaction was performed in a Professional TRIO cycler (Biometra). PCR protocol included a denaturation

step at 98°C for 30 s followed by 30 cycles of 98°C for 10 s (denaturation), 50-72°C (depending on the melting temperatures of the oligonucleotides) for 30 s (annealing) and 72°C for 30 s per kbp of the amplified DNA fragment (extension). PCR was completed by a final extension step at 72 °C for 10 min.

2.8.2 Site-directed mutagenesis

In order to introduce point mutations in a plasmid, a PCR with primers containing the desired mutations was performed as described in **section 2.8.1** with the following modifications. The annealing temperature was set to 42°C during the first 3 cycles and increased to 58°C during the next 18 cycles. The total number of cycles was 21, and the extension time was 9 min. After the completion of a PCR, 5.5 µl of 10x CutSmart buffer (New England Biolabs) and 0.5 µl DpnI restriction nuclease (20 U/µl) were added, followed by overnight incubation at 37°C. PCR product was purified with a GeneJET PCR purification kit (Thermo Fisher Scientific) and transformed into chemically competent *E. coli* cells (**section 2.10.2**). Mutations were analysed by DNA sequencing of plasmid DNA isolated from individual bacterial colonies.

2.8.3 Gibson assembly

DNA fragments containing ~20 nt long overlapping ends were mixed 1:1 (molar ratio) in a total volume of 10 µl, followed by the addition of 10 µl of the 2x Gibson assembly master mix (IMB Protein Production Core Facility). The reaction mix was incubated at 50°C for 1 h and transformed into chemically competent *E. coli* cells (**section 2.10.2)**. Individual bacterial clones were analysed for the presence of the desired plasmid by DNA sequencing.

2.8.4 Gateway cloning

100 ng of a Gateway entry vector was mixed with 100 ng of a Gateway destination vector in a total volume of 7.5 µl. 2.5 µl of the 4x LR clonase mix (IMB Protein Production Core Facility) were added to the mix, followed by incubation at room temperature for 1 h. 2 µg of Proteinase K were added to the reaction mix and incubated at 37°C for 10 min. The reaction mix was transformed into chemically competent *E. coli* cells (**section 2.10.2)**, and the presence of the desired plasmid DNA was analysed in individual bacterial clones by DNA sequencing.

2.8.5 Restriction cloning

For DNA digestion with endonucleases, 1-2 µg of plasmid DNA or PCR product were digested in 1x CutSmart buffer with 10-20 U of the desired endonuclease overnight at 37°C. DNA fragments were separated by agarose gel electrophoresis, and the desired fragment was purified using the QIAquick Del Extraction kit (Qiagen).

For DNA ligation, vector (backbone) and insert DNA fragments were combined in a 1:3 molar ratio in a total volume of 10 µl. 10 µl of the 2x DNA Ligation mix (Takara) were added, and the reaction mix was incubated at 16°C for 30 min. Ligation mix was transformed into chemically competent *E. coli* cells (**section 2.10.2).** Plasmid DNA was isolated from individual bacterial clones, and the fragments of interest were sequenced.

2.8.6 DNA sequencing

400-700 ng of plasmid DNA were mixed with 1 µl of 10 µM DNA primer in a total volume of 7 µl and sent for sequencing to StarSEQ GmbH.

2.9 Methods for protein manipulation

2.9.1 SDS polyacrylamide gel electrophoresis

SDS polyacrylamide gel electrophoresis was performed using 4-12% NUPAGE gels (Life Technologies). Protein samples were mixed 3:1 (v/v) with 4x NUPAGE LDS Sample buffer (Thermo Fisher), supplemented with 100 mM DTT, and incubated at 95°C for 5 min. After loading on a gel, the samples were run at 140V in 1x MOPS buffer for 60-90 min. Prestained PageRuler (Thermo Fisher Scientific) was used as a size marker. For the detection of free ubiquitin and low-molecular-weight ubiquitin chains,1x MES buffer was used.

2.9.2 Western blotting

In most cases, semi-dry transfer with Trans-Blot Turbo Transfer System (Bio-Rad) was used. Filter paper stacks and nitrocellulose membranes were equilibrated in 1x Trans-Blot Turbo buffer for 1 min. A filter paper stack was placed at the anode (bottom) part of

a Trans-Blot cassette, followed by a membrane, a gel, and another stack of filter paper. Air bubbles were rolled out, the cassette was closed, and a constant voltage of 15 V was applied for 12 min, with the maximum allowed current being 1.3A. Following the transfer, membranes were optionally stained with Ponceau S solution to visualise the efficiency of the transfer, and the membranes were further incubated in the blocking buffer for 1-2 h at room temperature with constant shaking. Membranes were incubated with primary antibodies overnight at 4°C with constant shaking. Following 4× 5 min washes with PBST, secondary antibodies were applied for 1-2 h at room temperature. Membranes were then washed again 4× 5 min with PBST and developed with Amersham's ECL Prime or Select Western blotting detection reagent. Chemiluminescence signal was recorded on a Fusion FX system (Vilber).

For the detection of PCNA polyubiquitylation, wet transfer in a Mini Trans-Blot Cell (Bio-Rad) was used. The technique was similar to the one described above, with the exception of buffer composition (Wet blot buffer) and transfer conditions (100 V, 100 min).

For the detection of free ubiquitin in the UBICREST assay with VU1 anti-Ubiquitin antibody (**section 3.5.3.1**), after Trans-Blot Turbo transfer, membranes were washed 2× 5 min with PBS and incubated with 0.5% glutaraldehyde solution in PBS, followed by a 2 h incubation in the blocking buffer at room temperature. Subsequent steps were identical to the ones described above.

2.10 Methods for *E. coli*

2.10.1 Cultivation of *E. coli*

All *E. coli* strains were cultured in liquid LB medium or on LB-agar plates supplemented with the appropriate antibiotic at 37°C.

2.10.2 Transformation of chemically competent *E. coli* cells

An aliquot of chemically competent *E. coli* Top Ten cells was thawed on ice, mixed with ~100 ng plasmid DNA or up to 10% (v/v) of a ligation mix and incubated for 20 min on ice. Following 45 sec of heat shock at 42°C, cells were diluted with 1 ml of LB medium, incubated for 45 min at 37°C with constant shaking and plated on an agar plate with the

respective antibiotic. In case ampicillin was used, cells were plated on an agar plate directly after the heat shock.

2.10.3 Isolation of plasmid DNA

To isolate plasmid DNA for sequencing or genetic manipulations, a single *E. coli* colony was incubated in 5 ml of LB medium with the respective antibiotic and grown overnight at 37°C with constant shaking (200 rpm). Bacteria were pelleted by centrifugation for 10 min at 4500 ×g, followed by plasmid DNA isolation with the GeneJET Plasmid Miniprep kit (Thermo Fisher Scientific) according to the manufacturer's instructions. For the preparation of transfection-grade DNA, a single *E. coli* colony was inoculated in 5 ml of LB medium with the respective antibiotic for 8 h, then diluted 1:1000 into 220 ml of the antibiotic-containing LB medium and grown overnight at 37°C with constant shaking (200 rpm). DNA was subsequently isolated with the NucleoBond Xtra Midi Plus kit (Macherey-Nagel) according to the manufacturer's instructions.

2.11 Methods for mammalian cells

2.11.1 Cell thawing and freezing

For cell thawing, a cryovial with frozen cells was transferred from the -150°C freezer into a water bath pre-warmed to 37°C. After thawing, cell suspension was added dropwise to a petri dish containing the respective cell medium. Cells were allowed to adhere to the dish overnight, and the following day the media was exchanged.

For cell freezing, exponentially grown cells were washed once with pre-warmed to 37°C Dulbecco's Phosphate-Buffered Saline (DPBS) (Gibco) and incubated with 0.05% Trypsin-EDTA-Phenol red (Gibco) until complete cell detachment. Cell suspension was mixed with complete DMEM or RPMI 1640 medium, followed by centrifugation at 300 ×g for 3 min. Cell pellet was resuspended in freezing medium (90% complete growth medium, 10% DMSO), distributed in cryovials and transferred to the -80°C freezer in a CoolCell Freezing Container. The next day cryovials were transferred to the -150°C freezer for long-term storage.

2.11.2 Cell passaging

Cells were passaged once they reached ~90-100% confluency. After washing with DPBS, pre-warmed to 37°C, cells were incubated with 0.05% Trypsin-EDTA-Phenol red until complete cell detachment. Trypsin was inactivated by the addition of the complete growth medium, and cells were transferred to a new dish in a 1:8 to 1:10 dilution. Due to their slow growth rate, MDA-MB-436 cells were typically split in a 1:4 dilution.

2.11.3 Cell harvesting

In case cell lysates were needed, cells were washed on the plate once with DPBS, collected with a cell scraper in 1-2 ml of ice-cold DPBS and centrifuged at 300 ×g for 3 min. DBPS was removed, and cell pellets were stored at -80°C until further processing. Cell harvesting for flow cytometry is described in **section 2.11.11**.

2.11.4 Cell counting

The number of cells in a cell suspension after trypsinisation was determined with a TC20 Automated Cell Counter (BioRad) according to the manufacturer's instructions.

2.11.5 Transient transfection of DNA

HEK 293T cells were transfected with polyethyleneimine (PEI) and RPE1 hTERT cells with the Fugene HD (Promega) reagent.

2.11.5.1 Cell transfection with polyethyleneimine

For transfection in 6-well plates, $2*10^5$-$5*10^5$ HEK 293T cells were plated 24 h prior to transfection. 1.5 µg of plasmid DNA was mixed with 6 µl of PEI solution (1 mg/ml) in 250 µl of DMEM media without FBS but with all other aforementioned supplements, vortexed and incubated for 10 min at room temperature. 750 µl of full DMEM media was then added to the DNA-PEI mix and the resulting 1 ml of the transfection mix was added to cells. For the transfection of larger cell plates, the amounts of reagents were scaled up accordingly.

2.11.5.2 Cell transfection with Fugene HD

For transfection in 10-cm dishes, $1-2*10^6$ RPE1 hTERT cells were plated 24 h prior to transfection. 3 µg of plasmid DNA were mixed with 9 µl of the Fugene HD reagent in

510 µl of Opti-MEM medium (Life Technologies) and incubated for 10 min at room temperature. Cell medium was replaced with 10 ml of fresh full RPMI 1640, followed by the dropwise addition of the transfection mix. The medium was replaced 24 h after transfection.

2.11.6 Transient transfection of siRNA

Transient cell transfection with siRNA duplexes was performed with the Lipofectamine RNAiMAX reagent (Thermo Fisher Scientific). For transfection in 10-cm dishes, 1-2*10^6 RPE1 hTERT cells were plated 24 h prior to the transfection. 10 µl of siRNA duplex solution was mixed with 25 µl of the Lipofectamine RNAiMAX reagent in 1 ml of Opti-MEM medium and incubated for 20 min at room temperature. Cell medium was exchanged with 4 ml of Opti-MEM, pre-warmed to 37°C, followed by dropwise addition of the transfection mix. For RPE1 hTERT cells, medium was exchanged 8 h, for MDA-MB-436 cells – 4 h after transfection. Functional experiments were performed 72 h after siRNA transfections.

2.11.7 Creation of stable cell lines via Flp-In integration

2.7 µg of the Flp-recombinase expression vector (pOG44, ID 1809) was mixed with 0.3 µg of the target plasmid and transfected in RPE1 hTERT FlpIn TREX cells (ID 120) as described in **section 2.12.6**. 24 h after transfection, cell medium was replaced, and 48 h after the transfection puromycin was added to the final concentration of 2 µg/ml. During the following 2 weeks, the medium was replaced every 2-3 days until bulk cell death took place and colonies of puromycin-resistant cells appeared. Surviving cells were trypsinised, pooled and further cultured with the standard cell culture techniques.

2.11.8 Lentiviral transduction

All manipulations that included lentiviral particles were conducted in the IMB S2 laboratory. Recipient cells were plated in 10-cm dishes 24 h prior to transduction at 5*10^5 (for RPE1 hTERT) or 2*10^6 (for HEK 293T) cells per plate. For the generation of lentiviral particles, lentiviral packaging plasmids (ID 3805, 3806 and 3807) were co-transfected in HEK 293T cells together with the rtTAE3-expressing vector (ID 4892) or the target transfer plasmid (based on the pLENTI CMV vector, ID 4894), as described in **section 2.11.5.1**. For each transfection, 4*10^6 of HEK 293T cells, 2,5 µg of each packaging plasmid and 4

µg of rtTAE3-expressing vector or the target plasmid were used. 7 h after transfection, the medium was changed with 10 ml of full DMEM, and cells were allowed to express the proteins for 24 h. After that, supernatants containing rtTAE3 and target plasming-containing viral particles were combined, mixed with 16 µl polybrene (10 mg/ml stock solution), filter-sterilised and added to the cells-recipients. Media was replaced 24 h after transduction. 48 h after transduction, 100 µg/ml blasticidin and 400 µg/ml G418 were added to the medium. During the following 2 weeks of selection, cell medium was changed every 2-3 days, and cells were split 1:5 if they reached confluency.

2.11.9 DNA fibre assay

Cells were incubated with 50 µM CldU, washed 3× with pre-warmed to 37°C DPBS, followed by labelling with 50 µM IdU. The exact labelling times are described in the figure legends. If indicated, hydroxyurea was added during or after the second pulse, as described in the figure legends. After labelling, cells were washed 3× with ice-cold DPBS, trypsinised for 2-3 min at 37°C, diluted with complete cell media, centrifuged for 3 min at 300 ×g, resuspended in DPBS, counted and diluted to the concentration of $1.75*10^5$ cells/ml. 7,5 µl of the lysis buffer were mixed with 4 µl of the cell suspension directly on the surface of a SuperFrost Ultra Plus Gold adhesion slide (Thermo Fisher Scientific). Cells were lysed on the slide at room temperature for 8.5 min. After that, the slide was tilted, allowing the drop to run down. The precise angle at which the slide was tilted depended on the temperature and the humidity of the air and was adjusted for every experiment in a way that it took at least 1 min for each drop to reach the end of the slide. The slides were air-dried for 30 min and fixed overnight in a fixation solution. Next day, the slides were washed 2× 3 min in PBS, dipped in water and denatured in 2,5M HCl for 1,5 h at room temperature. Slides were washed with PBS 6× 2,5 min and blocked with a blocking solution for 40 min at room temperature. After that, the slides were incubated with primary antibodies (anti-BrdU ID 11 and 423) for 2,5h at room temperature, washed 3× 5 min in PBST, followed by the incubation with the secondary antibodies (ID 88 and 186) for 1 h at room temperature in the dark. The slides were washed 3× 5 min in PBST, 2× 1 min in water, air-dried and mounted in ProLong Diamond Antifade Mountant (Thermo Fisher Scientific). Images of DNA fibres were acquired with a Widefield Fluorescence Microscope (Thunder, LASX software, Leica) (magnification: 63x, NA 1.44 HC PL APO oil

immersion objective; LED illumination and the corresponding emission filters: 635 nm, 642/80 and 475 nm, 535/70). Lengths of DNA fibres were quantified manually using the Fiji/ImageJ software.

2.11.10 Preparation of cell lysates

Cells were collected with a cell scraper in ice-cold PBS, centrifuged at 1000 ×g for 3 min, the cell pellet was resuspended in RIPA buffer, supplemented with 1x cOmplete™ protease inhibitor cocktail (Roche) and Sm nuclease (0.625 cU/ µl), and incubated for 1 h on ice. Lysates were centrifuged at 21500 ×g for 10 min, and the supernatant was transferred to a new tube. Protein concentration was determined with the Protein Assay Dye Reagent (Bio-Rad) according to the manufacturer's instructions.

2.11.11 Cell cycle analysis by flow cytometry

For cell cycle analysis by flow cytometry, cells were washed once on a plate with DPBS, pre-warmed to 37°C, and incubated with 0.05% Trypsin-EDTA-Phenol red (Gibco) until complete cell detachment. Trypsin was inactivated by addition of complete cell media, cells were centrifuged at 300 ×g for 5 min, washed once with PBS and centrifuged again at 300 ×g for 5 min. The supernatant was discarded, and the cell pellet was resuspended in 50 µl of ice-cold PBS. 1 ml of 70% ethanol, pre-cooled to -20°C, was added dropwise to the cell suspension with constant vortexing. Cell suspension was stored overnight at 4°C and then transferred to -20°C until further processing. For the propidium iodide (PI) staining, cells were centrifuged at 1000 ×g for 10 min, washed once with 1 ml of ice-cold PBS and centrifuged again at 1000 ×g for 10 min. The supernatant was discarded, cells were resuspended in 500-1000 µl of PI staining buffer and incubated for 30 min at room temperature. Cells were analysed on the BD LSRFortessa SORP system (BD Biosciences) equipped with the BD FACSDIVA software. Data were analysed with the Flow Jo software.

For 2D cell cycle analysis, 10 µl of EdU were added to cell medium 30 min before harvest. Coupling of the AlexaFluor 647 fluorophore was performed with Click-IT™ 647 Flow Cytometry Assay kit (Thermo Fisher Scientific) according to the manufacturer's instructions. Analysis of cells by flow cytometry was performed as described above.

2.11.12 Detection of single-stranded DNA by immunofluorescence

RPE1 hTERT cells were plated in 6-well plates with coverslips (Carl Roth) at 650000 cells/well and cultured in the presence of 10 μM BrdU for 24 h. Next, cells were treated as described in the respective figure legend, coverslips were transferred to a 24-well plate, washed once briefly with ice-cold PBS and incubated for 5 min with pre-extraction buffer on ice. Following another wash with PBS, cells were incubated with 4% formaldehyde in PBS for 10 min at room temperature and permeabilised with 0.3% Triton X-100 in PBS for 15 min at room temperature. Coverslips were then washed again in PBS and incubated in the blocking buffer for 1 h. Primary anti-BrdU antibody (clone B44, ID) solution was applied overnight at 4°C. Coverslips were washed 3× 5 min in PBST, incubated with secondary antibody (ID 86) for 1 h at room temperature, washed again 3× 5 min in PBST and incubated with 1 μg/ml Hoechst 33342 (Thermo Fisher Scientific) in PBS for 5 min at room temperature for total DNA staining. Image acquisition and analysis were performed as described in **section 2.11.9**.

2.11.13 SILAC labelling of cells

For the analysis of the interactome of polyubiquitylated PCNA, stable isotope labelling by amino acids in cell culture (SILAC) mass spectrometry-based approach was used (Ong and Mann 2006). HEK 293T were labelled with ‘light’ (Lys-0, Arg-0), ‘medium’ (Lys-4, Arg-6) or ‘heavy’ (Lys-8, Arg-10) amino acids for 2 weeks and transfected as described in **section 2.11.5.1**. PCNA was immunoprecipitated as described in **section 2.12.1**. During the last wash, beads from different samples belonging to the one replicate were pooled. Downstream processing and data analysis were performed by Ivan Mikicic (Petra Beli laboratory).

2.11.14 Cell viability assay

Cells were transfected with siRNAs as described in **section 2.11.6** and, after 24 h, plated on a 96-well plate at 2000 cells per well. Next day, cell medium was replaced, and cells were treated as indicated in the respective figure legend for 72 h. Viability of cells was assessed with the MTT Cell Viability Assay Kit (Sigma Aldrich) according to the manufacturer’s instructions.

2.12 Detection of protein ubiquitylation

2.12.1 Detection of PCNA ubiquitylation by PCNA immunoprecipitation

Cells (typically 1 sub-confluent 15-cm plate per condition) were treated as indicated in the respective figure legends and collected with a cell scraper in ice-cold PBS. Cells were centrifuged at 1000 ×g for 3 min, the cell pellet was resuspended in the cell fractionation buffer, supplemented with 1× cOmplete™ protease inhibitor cocktail (Roche), and incubated for 15 min on ice. The suspension was then centrifuged at 1300 ×g for 5 min, the supernatant was discarded, and cell pellets were frozen at -80°C for at least 30 min. Pellets were then resuspended in 1 ml of ice-cold RIPA buffer, supplemented with 1x cOmplete™ protease inhibitor cocktail (Roche) and Sm nuclease (0.625 cU/ µl), followed by incubation for 45 min on ice. 60 µl of 5M NaCl was added to the lysates, which were briefly vortexed and incubated on ice for 15 min. Lysates were centrifuged at 21500 ×g for 10 min, supernatants were transferred to new tubes, and protein concentration was determined with the Protein Assay Dye Reagent (Bio-Rad) according to the manufacturer's instructions. Equal amounts of proteins for different conditions were mixed with RIPA buffer to make the total volume up to 1 ml, and 300 µl of dilution buffer for immunoprecipitation were added. 13 µl of each sample were taken out, mixed with 5 µl of 4x NUPAGE LDS Sample buffer (Thermo Fisher), supplemented with 100 mM DTT, incubated at 95°C for 5 min and later used as the 'input' samples. 1.5 µg of monoclonal PC10 were added to each sample except for the negative control, and the samples were incubated for 2 h at 4°C. 40 µl of 50% Protein A-agarose slurry per sample were washed once with 500 µl of RIPA buffer and added to the cell lysates, followed by an overnight incubation at 4°C. Beads were then centrifuged at 1000 ×g for 3 min, the supernatant was discarded, and the beads were washed 6× 5 min with 1 ml of RIPA buffer at 4°C. After the last wash, the supernatant was removed completely with a syringe, and proteins were eluted in 60 µl of 2× NUPAGE LDS Sample buffer (Thermo Fisher), supplemented with 50 mM DTT, at 95°C for 15 min. Beads were then centrifuged at 1000 ×g for 3 min, and the eluate was used for SDS-PAGE and western blotting (**sections 2.9.1** and **2.9.2**).

2.12.2 Detection of protein ubiquitylation by denaturing Ni-NTA pulldown

HEK 293T cells were plated at $5*10^6$ cells per 10-cm plate (for the pulldown of His-tagged histone H2B, 48 h prior to harvest) or at $2.5*10^6$ cells per 10-cm plate (for the pulldown of his-tagged ubiquitin, 72 h prior to harvest) and transfected with the required constructs 24 h after plating. On the day of harvest, cells were optionally treated as indicated in the respective figure legends and collected in ice-cold PBS with a cell scraper. After centrifugation at 1000 ×g 3 min, the cell pellet was lysed in 1.5 ml of buffer A. Lysates were sonified with the Branson Ultrasonics sonifier (2-3 pulses at the lowest intensity) to reduce the viscosity. 22.5 µl of 1M imidazole and 40 µl of 50% Ni-NTA slurry were added to each sample and incubated overnight on a rotation wheel at 4°C. Beads were washed 4× 5 min buffer A and 2× 5 min buffer B at room temperature, followed by incubation with 50 µl elution buffer for 10 min at 95°C. Beads were centrifuged for 5 min at 1000 ×g, eluates were collected and analysed by SDS-PAGE and western blotting (**sections 2.9.1** and **2.9.2**)

2.12.3 Ubiquitin chain restriction assay (UBICREST)

For the *in vitro* ubiquitin chain restriction assay (UBICREST), PCNA was immunoprecipitated from mammalian cells as described in **section 2.12.1** before the elution step. Beads were additionally washed 2 times with 500 µl of 1x ubiquitylation buffer, and after the last wash, the supernatant was completely removed with a syringe. Beads were resuspended in 80 µl of the 1x ubiquitylation buffer. If indicated, AMSH, OTUB1 or USP2cc were added to the final concentrations of 3 µM, 10 µM and 1 µM, respectively. Beads were incubated at 37°C for 1 h with constant shaking and manually vortexed every 10 min. Beads were then centrifuged for 5 min at 1000 ×g, 60 µl of the supernatant were mixed with 20 µl of 4x NUPAGE LDS Sample buffer (Thermo Fisher), supplemented with 100 mM DTT, and incubated at 95°C for 5 min ('Supernatant' fraction). The remaining supernatant was completely removed from the beads with a syringe, and proteins were eluted from the beads with 60 µl of 2x NUPAGE LDS Sample buffer (Thermo Fisher), supplemented with 50 mM DTT, at 95°C for 15 min. Beads were centrifuged at 1000 ×g for 3 min, and the eluate was collected ('Elution' fraction). The presence of ubiquitin chains on ubiquitylated proteins in the 'Supernatant' and 'Elution' fractions was analysed by SDS-PAGE and western blotting (**sections 2.9.1** and **2.9.2**).

2.13 *In vitro* ubiquitylation assay

In vitro ubiquitylation assay was performed in 1x ubiquitylation buffer supplemented with 100 µM ATP in a 10 µl scale. 2 µM PCNA or $PCNA^{Ub}$(K164), 5 µM ubiquitin, 0.1 µM Uba1, 0.2 µM Ubc13 or UBE2N, 0.2 µM Mms2 or UBE2V2 and 1 µM PIP-E3[63] were incubated at 30°C for 40 min. The reaction was stopped by the addition of 3 µl of 4x NUPAGE LDS Sample buffer (Thermo Fisher) and analysed by SDS-PAGE and western blotting (**sections 2.9.1** and **2.9.2**).

Chapter 3

Results

3.1 Basis of the study. Design of PCNA-selective linkage-specific ubiquitin ligases

DNA repair mechanisms are essential to preserve the integrity of genomic information and to sustain life at both cellular and organismal levels. DNA damage can be hazardous for cells during DNA replication, as it may lead to incorrect duplication of the genetic information and, ultimately, cell death or the development of cancer. To minimise possible devastating effects of DNA lesions during S phase, cells have developed a series of pathways, collectively termed “DNA damage bypass”. They allow to complete DNA replication in the presence of DNA lesions, which can be removed in a postreplicative manner once replication has finished. One of the critical layers of DNA damage bypass regulation is posttranslational modifications of the DNA sliding clamp PCNA (Ulrich and Takahashi, 2013). Upon accumulation of replication intermediates due to replication over damaged DNA, PCNA undergoes Rad18-dependent monoubiquitylation – a signal that recruits translesion synthesis polymerases to the sites of DNA damage. Subsequent extension of this monoubiquitin into a K63-linked chain activates an error-free branch of damage bypass. Although K63-linked PCNA polyubiquitylation is a phenomenon known for over 20 years (Hoege *et al.,* 2002; Stelter and Ulrich, 2003), a comprehensive understanding of the pathway is still missing. In mammalian cells, DNA translocase ZRANB3 has been shown to bind polyubiquitylated PCNA via a combination of its PCNA-binding motifs (PIP and APIM) and NZF domain, selective towards K63-linked ubiquitin chains (Ciccia *et al.,* 2012). Recruitment of ZRANB3 to stalled replication forks promotes their transformation into Holliday junctions via a process termed replication fork reversal. However, yeast cells lack a convincing homologue of ZRANB3, and replication fork reversal is a rare event unless checkpoint signalling is deactivated (Sogo *et al.,* 2002), indicating the presence of another reader of PCNA polyubiquitylation. In yeast, PCNA polyubiquitylation is catalysed by the E3 ligase Rad5, which, together with its cognate E2

Ubc13/Mms2, extends monoubiquitin moiety on PCNA into a polyubiquitin chain. As Rad5 is a multi-domain protein that also recruits TLS polymerases and has a helicase activity (Gallo *et al.,* 2019; Blastyák *et al.,* 2007), it was initially not clear whether the presence of a ubiquitin chain on PCNA is sufficient to activate error-free DNA damage bypass in yeast, or ubiquitin-independent functions of Rad5 are also essential for this pathway. Furthermore, the importance of linkage type in this process has not yet been characterised. These biological problems have been successfully solved by replacing Rad5 with artificial enzymes that mimic its ubiquitin ligase activity and are able to create not only native K63 but also other types of polyubiquitin linkages (Wegmann *et al.,* 2022). The catalytic core of these artificial enzymes is based on previously identified and further developed in our laboratory highly linkage-selective ubiquitin ligases. These enzymes have been successfully designed for three chain types, namely K63, K48 and M1 (linear) linkages, and will be addressed further in the text as $E3^{63}$, $E3^{48}$ and $E3^{1}$, respectively. The design of these enzymes is described below and graphically presented in **Figure 11A**.

- K63-linked chains are assembled by an *S. cerevisiae* RING-type ubiquitin ligase Pib1, which, together with its cognate highly K63-selective E2 Ubc13-Mms2, functions in the multivesicular body (MVB) pathway (Renz *et al.,* 2020). In order to keep the ubiquitin ligase activity but abrogate MVB-related functions, the N-terminal phosphatidylinositol 3-phosphate-binding FYVE domain was removed from the protein (Shin *et al.,* 2001).
- K48-linked chains are assembled by a *S. cerevisiae* protein Cue1 that acts as an activator for the highly K48-selective E2 Ubc7 (Bagola *et al.,* 2013). The transmembrane domain of Cue1 was removed in order to prevent its targeting to ER membrane (Ravid and Hochstrasser, 2007).
- M1-linked chains are assembled by the *H. sapiens* RING-Between-RING ubiquitin ligase HOIP, which is a component of the LUBAC complex and is known to function with several E2 enzymes. As HOIP is a large and multi-domain protein, only the catalytic RING-in-between-RING and linear chain determination (LDD) regions were used as an $E3^{1}$ (Smit *et al.,* 2012). Additionally, as HOIP is allosterically activated by ubiquitin (Lechtenberg *et al.,* 2016), two uncleavable (G76L) ubiquitin

moieties together with appropriate linkers were added N-terminally to the catalytic domain (Wegmann *et al.,* 2022).

In order to bring the enzymes to PCNA, a canonical PCNA-interacting motif (PIP-box) from the mismatch repair protein Msh6 was fused N-terminally to the described catalytic domains of the E3s. The resulting enzymes are called PIP-E3^{63}, PIP-E3^{48} and PIP-E3^{1}. To promote the nuclear localisation of PIP-E3^{1}, a nuclear localisation signal (NLS) was added upstream of a PIP box.

High linkage selectivity of the tailor-made E3s implies that they only take a specific ubiquitin lysine as a substrate and therefore cannot initiate a chain on any protein other than ubiquitin (elongation specificity). Thus, Rad18-dependent PCNA monoubiquitylation is a prerequisite for the activity of the enzymes. By expressing the tailor-made E3s in a *rad5* background, one can explore whether PCNA polyubiquitylation is sufficient to initiate error-free damage bypass and which linkages would support this pathway. Strikingly, PIP-E3^{63} is able to reverse the damage sensitivity of a *rad5* strain (Wegmann *et al.,* 2022). Although to a lesser extent, the same holds true for PIP-E3^{1}, which most likely reflects the similar conformation of K63- and linear polyubiquitin chains (Komander *et al.,* 2009). On the contrary, expression of PIP-E3^{48} causes a dominant negative effect: not only is error-free bypass not supported, but also translesion synthesis is inhibited due to the proteasomal degradation of PCNA (**Figure 11B**). These results not only indicate that PCNA polyubiquitylation is sufficient to trigger error-free damage bypass in yeast but also delineate the geometric requirements for ubiquitin chains in this pathway. This experiment was the first example of an *in vivo* manipulation of ubiquitin signalling: depending on the linkage type, differently linked ubiquitin chains, assembled on the same acceptor site of the same substrate, provide different biological outputs.

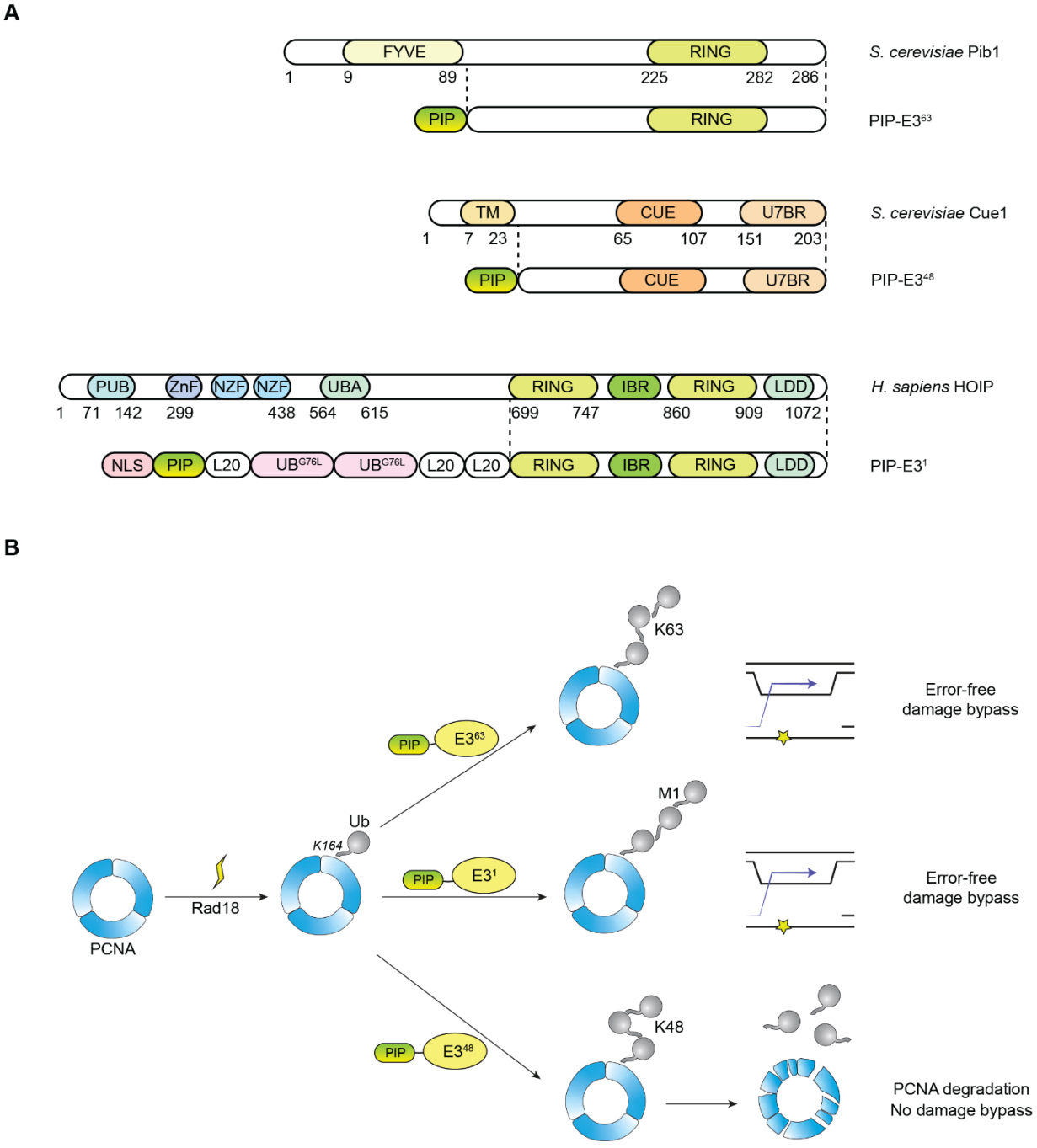

Figure 11: Design and implementation of tailor-made ubiquitin ligases. **(A)** Design of PIP-E3s: domain arrangement of linkage-selective ubiquitin ligases and PIP-E3s that use their catalytic domains. Numbers below the protein schemes indicate amino acid positions in the protein sequence. **(B)** Application of PIP-E3s in *S. cerevisiae* reveals linkage requirements in DNA damage bypass.

The roles of PCNA polyubiquitylation in human cells are even less well understood. Although this signal has been associated with ZRANB3-mediated fork reversal, an accumulating number of cellular pathways that depend on this modification cannot be explained simply assuming that ZRANB3 is the only reader of polyubiquitylated PCNA (Tirman *et al.,* 2021; Thakar *et al.,* 2020). My goal in the present work was to use PIP-E3s in human cells to address the following two questions:

- What are the functional consequences of PCNA polyubiquitylation in human cells?
- How important is K63 linkage in ubiquitin signalling on PCNA in human cells?

In the following sections, I address these questions and discuss the optimisation steps that were needed to transfer the yeast PIP-E3 system into human cells, the effects that are caused by K63-linked PCNA polyubiquitylation, a comparison of K63 versus K48 polyubiquitylation, the physiological relevance of PCNA polyubiquitylation and, finally, further development of tailor-made ubiquitin ligases, which enables their application to other substrates.

3.2 Optimisation of PIP-E3s in mammalian cells

3.2.1 PIP-E3^{63}

The original PIP-E3 constructs contain a canonical PIP-box from yeast Msh6, which interacts with yeast PCNA. Although PCNA is a highly conserved protein - the human and yeast orthologues display 35% identity and 62% similarity - I first tested whether the yeast PIP-E3^{63} can polyubiquitylate human PCNA *in vitro*. As a substrate, I used PCNA pre-monoubiquitylated by UbcH5c at its native lysine K164 (Hibbert and Sixma, 2012). As demonstrated in **Figure 12A**, PIP-E3^{63} readily polyubiquitylates monoubiquitylated PCNA with a similar efficiency for yeast Ubc13-Mms2 pair or their human homologs UBE2N-UBE2V2. In accordance with the elongation specificity of PIP-E3s, no reaction takes place if unmodified PCNA is used as a substrate. Instead, free ubiquitin chains are accumulated in this condition. This justifies the use of the PIP-E3 constructs with the original PIP box in human cells.

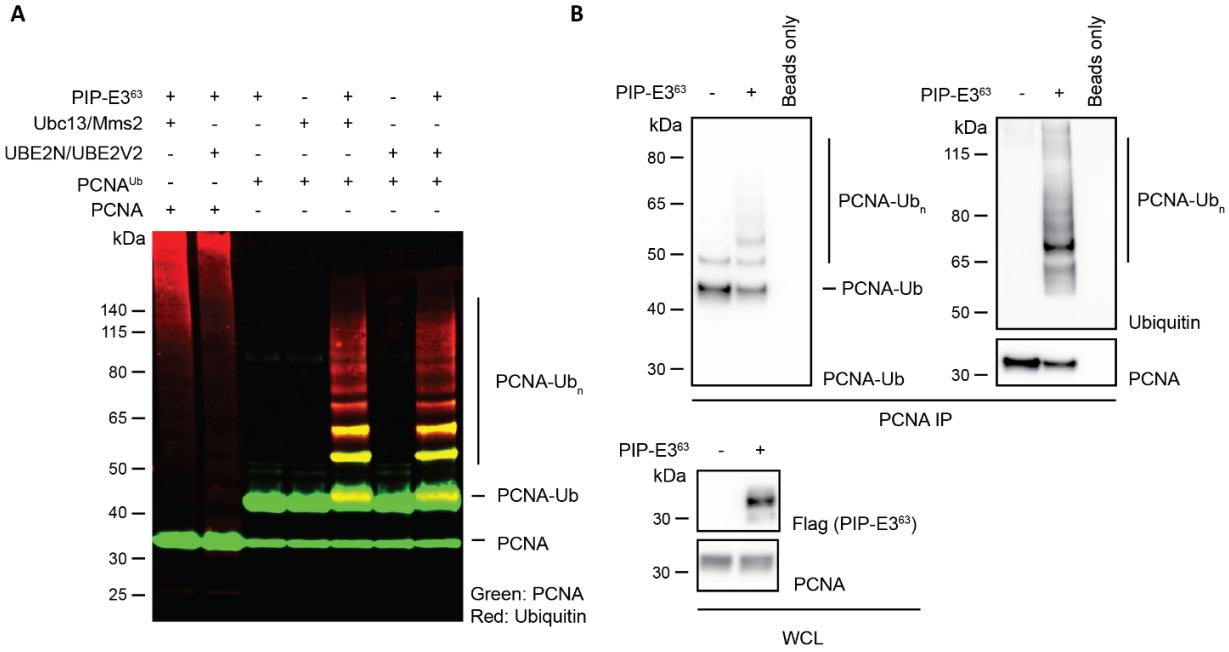

Figure 12: PIP-E3^{63} is active *in vitro* and in human cells. (A) *In vitro* ubiquitylation assay with PCNA and PCNA-Ub(K164) as substrates and PIP-E3^{63} as a ligase. Yeast and human E2s were compared. **(B)** PIP-E3^{63} was expressed in HEK 293T cells for 24 h, followed by PCNA immunoprecipitation from chromatin. PCNA polyubiquitylation was analysed in the immunoprecipitate fraction, and expression of the ligase in whole cell extracts.

In order to proceed with *in vivo* studies, a codon-optimised version of PIP-E3^{63} was cloned under the control of the CMV promoter and, as a proof-of-concept, overexpressed in HEK 293T cells. As shown in **Figure 12B**, expression of PIP-E3^{63} induces robust polyubiquitylation of PCNA, visualised by the anti-Ubiquitin and anti-PCNA-Ub (native K164 linkage) antibody after immunoprecipitation of PCNA from chromatin. Importantly, in striking contrast to yeast, the basal levels of PCNA monoubiquitylation, likely originating from endogenous DNA damage or due to replication over difficult-to-replicate regions (Tubbs and Nussenzweig, 2017), are sufficient to support PIP-E3^{63} activity.

3.2.2 PIP-E3^{48}

Unlike K63-linked, K48-linked ubiquitin chains represent a canonical signal for proteasomal degradation and are rapidly deconjugated upon degradation of a substrate (Shin *et al.,* 2020). Despite strong genetic evidence for PIP-E3^{48} activity *in vivo*, K48-linked chains have not been detected on yeast PCNA, likely because of their transient nature (Wegmann *et al.,* 2022). To overcome this problem, His$_{10}$-tagged ubiquitin was overexpressed in human HEK 293T cells together with codon-optimised PIP-E3^{48}. Subsequent Ni-NTA pulldown under fully denaturing conditions allows the identification of all proteins that have incorporated His-tagged ubiquitin, including PCNA. Furthermore, in order to boost E3 activity, I co-overexpressed PIP-E3^{48} together with the original yeast Ubc7, a codon-optimised version of it (^{hco}Ubc7) or its human homologue UBE2G2. The results of the experiment are shown in **Figure 13A**. If only His-tagged ubiquitin, but no PIP-E3^{48} is transfected, the anti-PCNA antibody detects a single species, likely representing PCNA modified with a single His-tagged ubiquitin. Expression of PIP-E3^{48} results in the formation of higher molecular weight PCNA forms, likely representing K48-linked chains. Co-expression of non-codon-optimised Ubc7 further augments chain formation, and co-expression of UBE2G2 results in longer ubiquitin chains. Strikingly, when the codon-optimised version of Ubc7 is used, I observed the disappearance of monoubiquitylated PCNA concomitantly with the formation of high molecular weight species. This may indicate that the combination of PIP-E3^{48} with codon-optimised Ubc7 leads to very efficient polyubiquitylation of PCNA with K48 linkages and its subsequent rapid degradation. As PIP-E3^{48} is elongation-specific, only monoubiquitylated PCNA

should undergo polyubiquitylation and degradation, which could explain the disappearance of the PCNA-Ub form. These results correlate with the expression levels of the enzymes, shown in **Figure 13B**: while the original yeast Ubc7 is hardly detectable by western blotting, codon optimisation drastically increases its levels. The disappearance of the monoubiquitylated PCNA in total cell extracts upon co-expression of PIP-E3^{48} with ^{hco}Ubc7 correlates with the results of the Ni-NTA pulldown. Taken together, these results show that, depending on the co-expressed E2, PIP-E3^{48} may create chains of different lengths and intensities. The most active combination is PIP-E3^{48} together with ^{hco}Ubc7.

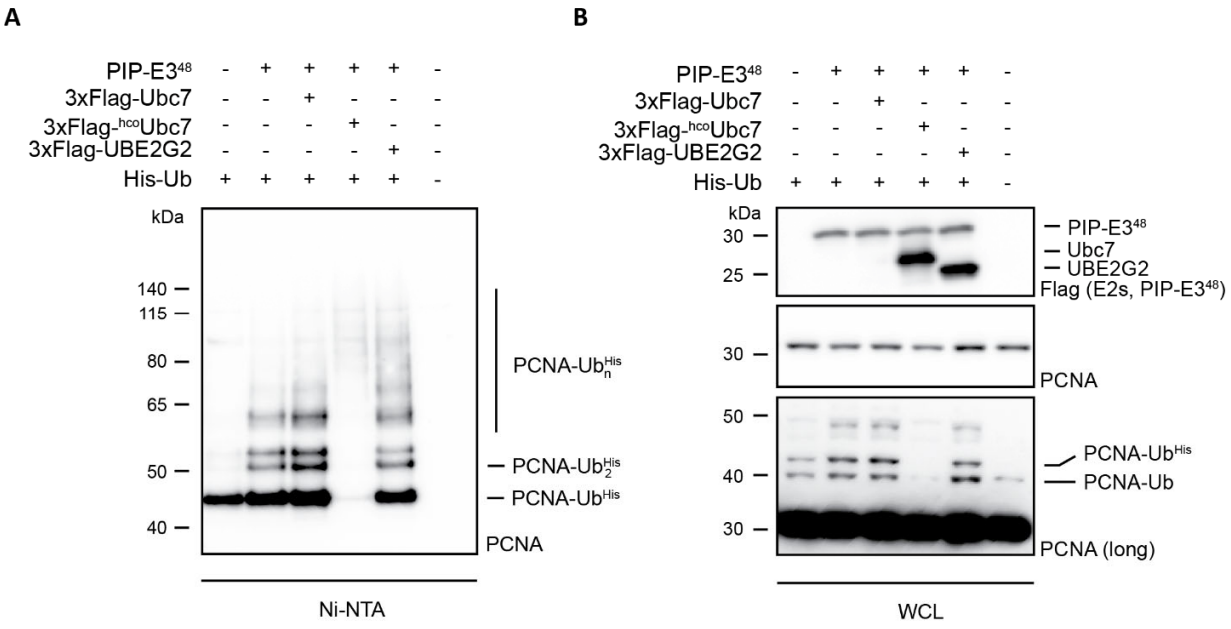

Figure 13: Optimisation of PIP-E3^{48} system in mammalian cells. (A) HEK 293T cells were transfected with the indicated constructs and allowed to express the proteins for 48 h. His-tagged ubiquitin conjugates were isolated via Ni-NTA pulldown and analysed for presence of PCNA by western blotting. **(B)** Expression of the enzymes as well as PCNA ubiquitylation were analysed by western blotting in the lysates of cells that were used for Ni-NTA pulldown.

3.2.3 PIP-E3^{1}

Linear polyubiquitylation by PIP-E3^{1} was investigated analogously. Due to the high repetitiveness and GC content of the full-length PIP-E3^{1}, I was able to optimise the codon usage of this construct only partially (**Figure 14A**). Nevertheless, I detect the activity of

the PIP-E3^{1} on PCNA after performing denaturing pulldown from cells expressing His-tagged ubiquitin (**Figure 14B**). Importantly, unlike K48-linked chains, the incorporation of a His-tagged ubiquitin into a growing M1-linked chain terminates it because its N-terminus is blocked by the His-tag itself. Therefore, it is not surprising to see that, when co-expressed with His-tagged ubiquitin, PIP-E3^{1} predominantly creates di- and tri-ubiquitylated PCNA forms. Interestingly, even though the codon usage of this construct could not be fully optimised, partial optimisation still results in higher expression levels of the enzyme and more potent PCNA polyubiquitylation.

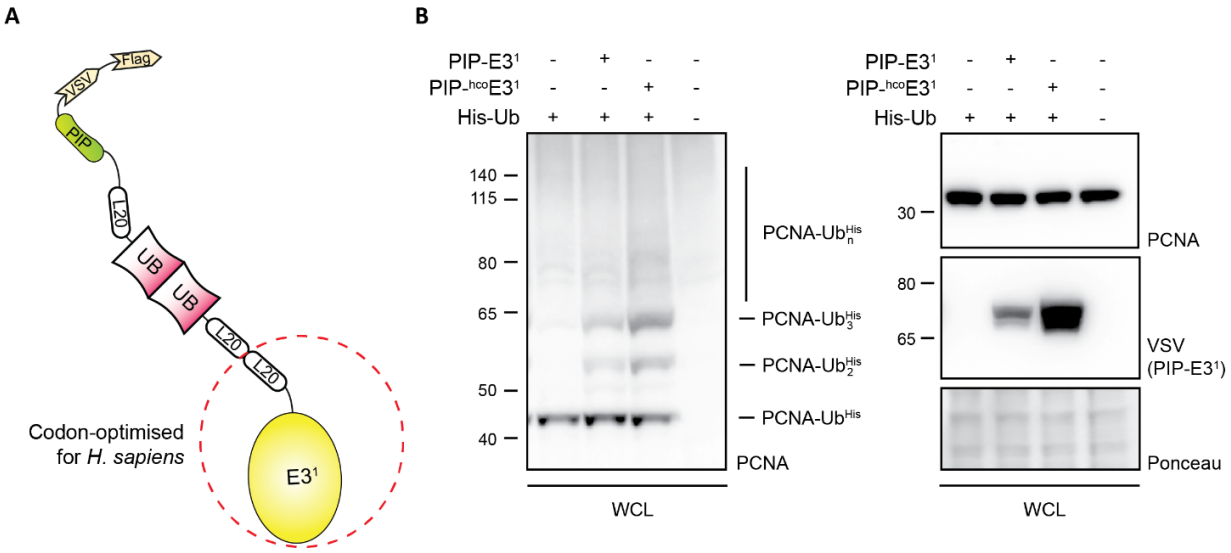

Figure 14: Optimisation of PIP-E3^{1} system in mammalian cells. (A) Schematic representation of the PIP-E3^{1} enzyme. The region that was codon optimised for expression in human cells is encircled with a red dashed line. **(B)** HEK 293T cells were transfected with the indicated constructs and allowed to express the proteins for 48 h. His-tagged ubiquitin conjugates were isolated via Ni-NTA pulldown and analysed for presence of PCNA by western blotting (left). Expression of the enzymes was analysed by western blotting in total lysates from the cells that were used for the Ni-NTA pulldowns.

3.3 Excessive K63-linked PCNA polyubiquitylation results in replication catastrophe

3.3.1 Creation of a cell line with inducible expression of PIP-E3^{63}

Up until now, the DNA damage field has accumulated a lot of data that originate from different model organisms and, particularly, from different human cell lines. As mutations in DNA damage response pathways are one of the key mechanisms employed by cancer cells to achieve immortality, the genetic background of a cell line should be taken into account when interpreting experimental results (Erenpreisa and Cragg, 2013). Importantly, some DNA damage and replication stress-related phenotypes are cell line-specific, and the reasons for this specificity remain unclear (Liu *et al.,* 2020). As a starting point, I chose a human retinal epithelial cell line RPE1 hTERT for two main reasons. First, this cell line is diploid, chromosomally stable and untransformed, immortality being achieved via constitutive telomerase expression. Second, PCNA polyubiquitylation has been shown to be essential for fork protection in these cells (Thakar *et al.,* 2020). Data from the Ulrich laboratory, as well as others (Igoucheva *et al.,* 2006), suggest that the introduction of exogenous double-stranded DNA in mammalian cells via transient transfection leads to activation of DNA damage response, which may be the consequence of lesions present in the transfected DNA. Therefore, in order to carefully analyse the impact of K63-linked PCNA polyubiquitylation on damage signalling, PIP-E3^{63} was stably integrated in RPE1 hTERT FlpIn cells via FRT recombination (**Figure 15A**). In the resulting cell line, hereafter called RPE1 hTERT PIP-E3^{63}, the open reading frame of the ligase was integrated into the genome and placed under the control of a doxycycline-inducible promoter. In this system, two copies of a TetO sequence are placed immediately downstream of a CMV promoter and, in the absence of doxycycline, are tightly bound by the TetR protein expressed in the host line. The addition of doxycycline releases TetR from the DNA, allowing transcription from the CMV promoter. As the initial PIP-E3^{63} construct contained a VSV tag at the N-terminus and the vector for FlpIn recombination provided a Flag tag, the resulting protein expressed in the RPE1 hTERT PIP-E3^{63} cell line carried both tags. As expected, the addition of doxycycline induced robust expression of PIP-E3^{63}, detectable by western blotting with the anti-Flag or anti-VSV antibodies (**Figure 15B**). Furthermore, I observed that expression of the construct begins as early as 2 h after

the addition of doxycycline and gradually increases over time (**Figure 15C**). To analyse whether PIP-E3^{63} expression level, arising from a single-copy integration, is sufficient to induce PCNA polyubiquitylation, I analysed the presence of ubiquitin chains on PCNA after 24 h expression of the enzyme by means of PCNA pulldown from chromatin. Albeit less efficient than after a transient overexpression of PIP-E3^{63} in the HEK 293T cell line, PCNA polyubiquitylation was also induced by adding doxycycline to RPE1 hTERT PIP-E3^{63} cells (**Figure 15D**). Importantly, when PCNA monoubiquitylation was enhanced by UV light treatment, the amount of PIP-E3^{63}-generated chains increased correspondingly. I also observe a decrease in monoubiquitylated PCNA levels after expression of the ligase, consistent with the conversion of PCNA-Ub into polyubiquitylated forms. These data justify the use of an RPE1 hTERT PIP-E3^{63} cell line as a model system to study PCNA polyubiquitylation.

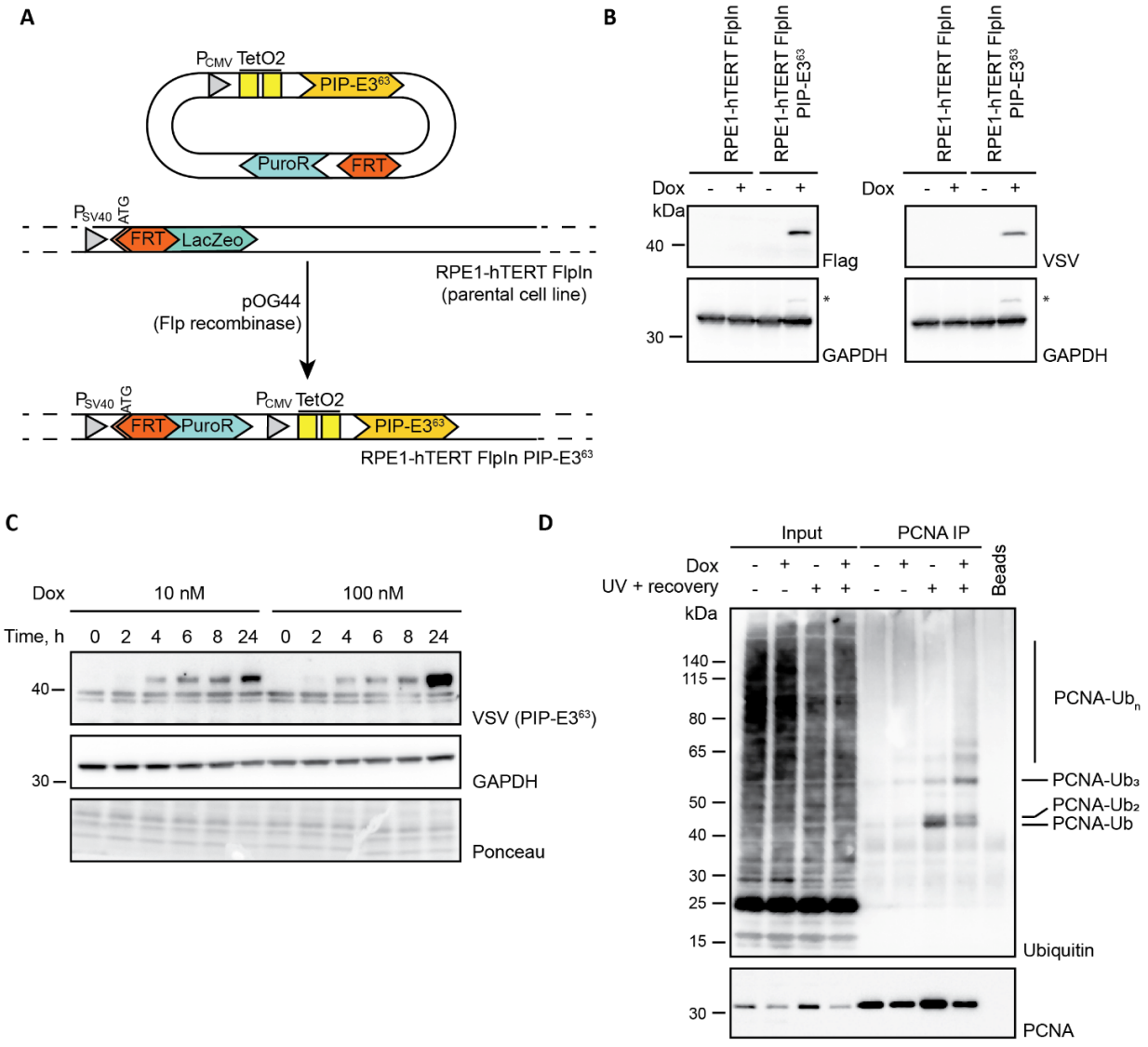

Figure 15: Creation and characterization of an RPE1 hTERT PIP-E3^{63} cell line. (A) Schematic representation of cell line generation based on FRT recombination. **(B)** Indicated cell lines were treated with 1 µg/ml doxycycline for 24 h and expression of PIP-E3^{63} was analysed by western blotting. Asterisks indicate signal remaining from Flag or VSV detection. **(C)** RPE1 hTERT PIP-E3^{63} cells were treated with 10 nM or 100 nM doxycycline for the indicated times, followed by western blotting. **(D)** RPE1 hTERT PIP-E3^{63} cells were treated with 1 µg/ml for 24 h and, if indicated, irradiated with 40 J/m^2 4h prior to cell harvesting. After chromatin fractionation and lysis, PCNA was immunoprecipitated from the lysates and analysed by western blotting with the indicated antibodies.

3.3.2 PIP-E3^{63}-expressing cells activate checkpoint signalling and exhibit S phase arrest

A common hallmark of cells experiencing replication stress or DNA damage is the activation of checkpoint signalling. This involves hyperactivation of certain kinases, typically ATR, ATM and DNA-PK, characterised by increased self-phosphorylation and phosphorylation of substrates such as CHK1, CHK2, RPA, H2AX and many others (Lanz *et al.,* 2019). PCNA polyubiquitylation is also a cellular response to replication stress; however, it is not yet known how a cell would react to this modification if no DNA damage is present. To understand whether polyubiquitylation of PCNA without exposing cells to DNA-damaging agents also induces checkpoint activation in cells, we first analysed the phosphorylation status of the checkpoint kinase CHK1. Surprisingly, we observe strong activation of CHK1 phosphorylation, starting from 6 h post-PIP-E3^{63} induction (**Figure 16A**). Interestingly, while phosphorylated CHK1 peaks at early time points, it almost disappears after 24 h, together with a drop in total CHK1 levels. As phosphorylation of CHK1 has been shown to be a destabilizing modification (You-Wei Zhang *et al.,* 2005), the results suggest that excessive and persistent CHK1 phosphorylation during extensive PIP-E3^{63} expression leads to substantial degradation of this kinase. We also observe phosphorylation of the histone variant H2AX at serine 139 (γH2AX), which is a common marker for the presence of DNA double-strand breaks. Unlike phospho-CHK1, we do not see an increase in γH2AX at the early time points but rather late, suggesting that DNA double-strand breaks occur as a consequence of long-term replication stress induced by PIP-E3^{63}. As CHK1 phosphorylation is carried out by ATR, which is typically activated upon persistent exposure of single-stranded DNA, I analysed RPA phosphorylation at S33 and T21 as a proxy for the presence of single-stranded DNA. Indeed, both phosphorylated RPA forms appear after the expression of PIP-E3^{63}, and the kinetics of this modification is more similar to that of phospho-CHK1 than γH2AX (**Figure 16B**). Interestingly, the extent of checkpoint activation is comparable or even higher, as for the 24 h time point, than that induced by 40J/m^2 UV light, which is considered a high dose of DNA damage. Taken together, these data suggest that expression of PIP-E3^{63} leads to exposure of single-stranded DNA and checkpoint activation, ultimately resulting in DNA double-strand breaks.

As activation of checkpoint signalling slows down cell cycle progression, I analysed the DNA content of RPE1 hTERT cells expressing PIP-E3^{63} for 6–48 h. As shown in **Figure 16C**, expression of PIP-E3^{63} leads to a strong early S-phase arrest: the effect is already noticeable 12 h after the addition of doxycycline and becomes stronger at the later time points.

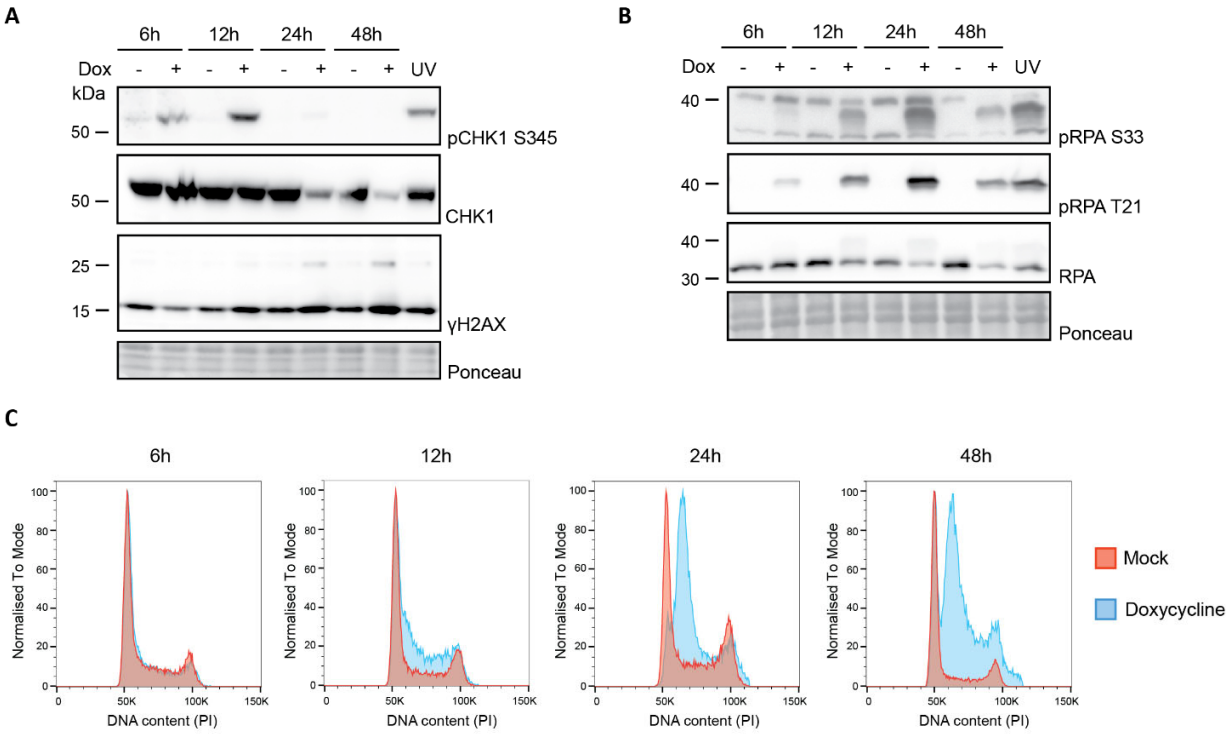

Figure 16: PCNA polyubiquitylation induces checkpoint activation and cell cycle arrest. (A) RPE1 hTERT PIP-E3^{63} cells were treated with 1 µg/ml doxycycline for the indicated time periods and, if indicated, irradiated with 40 J/m^2 4h prior to cell harvesting. Activation of checkpoint signalling was analysed by western blotting with indicated antibodies. Ponceau S staining serves as a loading control. **(B)** RPA phosphorylation was analysed by western blotting for cells treated as in (A). **(C)** RPE1 hTERT PIP-E3^{63} cells were treated as in (A), followed by cell cycle analysis by flow cytometry.

The significant accumulation of PIP-E3^{63}-expressing cells in the S phase suggests they struggle to complete replication. This phenomenon could be caused by lower total replication speed, which can be monitored by nucleotide incorporation. 2D cell cycle analysis reveals a robust decrease in the incorporation of the thymidine analogue EdU 24 h and, even stronger, 48 h after the expression of PIP-E3^{63} (**Figure 17A**). This indicates that PIP-E3^{63}-expressing cells require more time to complete replication, thus explaining their accumulation in the S phase. At the same time, lower EdU incorporation for cells in the S phase can have two main reasons. First – the number of replication forks remains unchanged, but their velocity decreases. Second – the speed of individual forks *per se* is unaffected, but the total number of active replication forks decreases. The second scenario is less likely, as the general response to replication stress involves excessive firing of new origins, leading to more replication forks being active at a given time (Courtot *et al.,* 2018). Nevertheless, one cannot exclude that PCNA polyubiquitylation may permanently stall replication forks, decreasing the number of moving replisomes. In order to discriminate between these two scenarios, I performed a DNA fibre assay, which allows monitoring of replication speed at the level of individual replication forks. This assay involves the treatment of the cells with two different thymidine analogues, CldU and IdU, followed by cell lysis and spreading of the DNA on a glass slide. Subsequent immunofluorescent detection of CldU and IdU allows direct visualisation of replication tracts and analysis of fork speed in given conditions. Importantly, in this assay, ongoing replication results in two-colour tracts, whereas one-colour tracts may represent initiation and termination of replication (depending on the colour) or fork stalling. As shown in **Figure 17B**, expression of PIP-E3^{63} for 12 h results in a massive decrease in replication fork speed, indicating that the first scenario, namely reduced replication speed at the level of individual forks, is responsible for the cell cycle arrest.

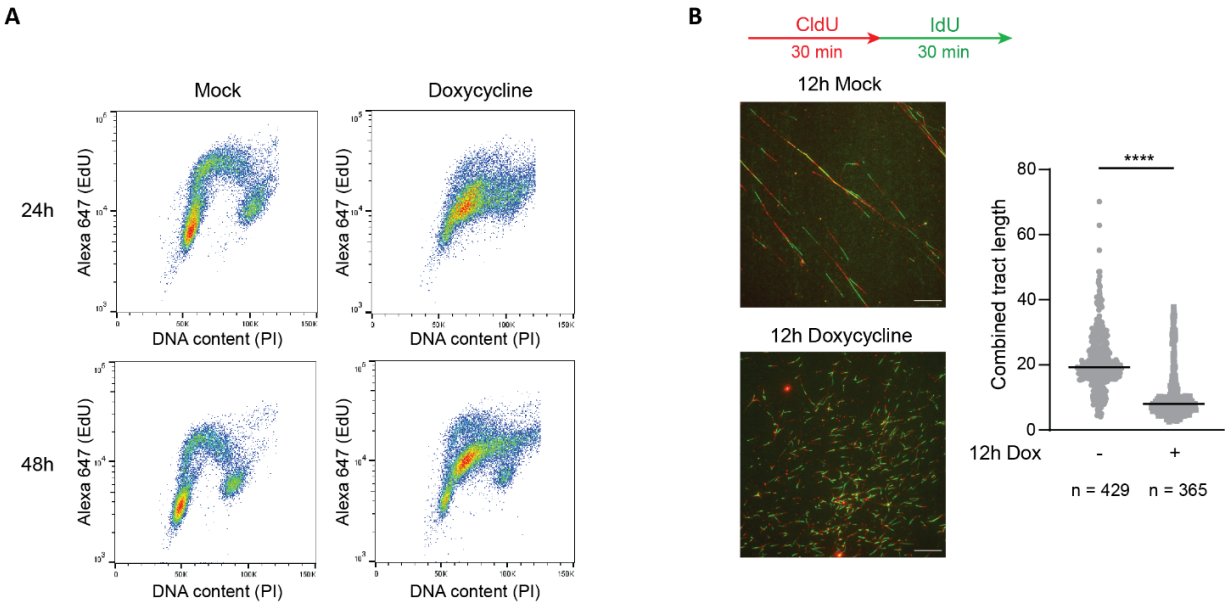

Figure 17: Lower EdU incorporation and replication speed in PIP-E3^{63}-expressing cells. (A) RPE1 hTERT PIP-E3^{63} cells were mock-treated or treated with 1 µg/ml doxycycline for 24 h or 48 h, followed by a treatment with 10 µM EdU for 30 min. Levels of incorporated EdU as well as total DNA content were analysed by flow cytometry. **(B)** DNA fibre assay was performed in RPE1 hTERT PIP-E3^{63} cells that were mock-treated or treated with 1 µg/ml doxycycline for 12 h. Representative images and quantification of total tract lengths are shown. Scale bar corresponds to 30 µm. ****p<0.0001 (Mann-Whitney U test).

3.3.3 ATR inhibition exacerbates effects of PIP-E3^{63}

The above-described data demonstrate that K63-linked PCNA polyubiquitylation by PIP-E3^{63} leads to dramatic consequences for cells: intra-S checkpoint signalling is activated, fork speed decreases, and cells arrest in the S phase. This persistent replication arrest ultimately results in the formation of double-strand breaks. It is known that activation of checkpoint signalling *per se* even in the absence of real DNA damage may inhibit cell cycle progression (Soutoglou and Misteli, 2008). Therefore, I aimed to understand whether inhibition of checkpoint signalling would prevent any long-term adverse effects of PIP-E3^{63} expression. Phosphorylation of CHK1 and RPA at S33 upon expression of PIP-E3^{63} suggests that ATR is one of the kinases responsible for checkpoint generation. Therefore, I reasoned that if ATR activity is the reason for replication collapse after PIP-E3^{63} expression, inhibition of this kinase should prevent the negative effects of PCNA polyubiquitylation, including DSB formation. As shown in **Figure 18**, the addition of the

ATR inhibitor VE-821 essentially prevents CHK1 phosphorylation after PIP-E3^{63} expression. Phospho-RPA T21 levels are partially reduced, and phospho-RPA S4-S8 levels are unaffected, consistent with the known contribution of other checkpoint kinases to the phosphorylation of these residues (Liu *et al.,* 2012). Strikingly, I observe a heavy increase in a γH2AX signal in the conditions where ATR is inhibited on top of PIP-E3^{63} expression. As H2AX phosphorylation is a canonical marker of DNA double-strand breaks, this indicates that ATR activity prevents DNA breakage after prolonged PCNA polyubiquitylation. In this respect, the expression of PIP-E3^{63} is similar to the treatment of cells with the replication stress-inducing agent hydroxyurea (HU). Inhibition of ATR leads to excessive firing of new origins and RPA exhaustion, leading to the formation of single-stranded DNA that is not coated by RPA and therefore prone to breakage (Toledo *et al.,* 2013). ATR has a second known activity that prevents the formation of breaks during HU treatment: it phosphorylates SMARCAL1, preventing excessive fork reversal and SLX4-dependent cleavage of reversed forks (Couch *et al.,* 2013). It is likely that one of these mechanisms is responsible for the observed PIP-E3^{63}-induced γH2AX signalling upon ATR inhibition.

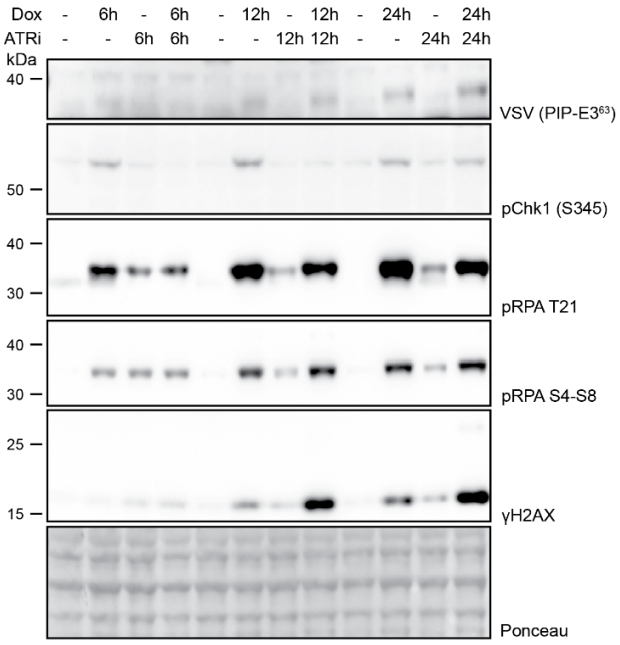

Figure 18: ATR prevents DSB formation upon excessive PCNA polyubiquitylation. RPE1 hTERT PIP-E3^{63} cells were mock-treated or treated with 1 µg/ml doxycycline or 10 µM VE-821 for the indicated time periods. Checkpoint signalling was analysed by western blotting. Ponceau S staining serves as a loading control.

3.3.4 Effects of PIP-E3^{63} expression are dependent on its interaction with PCNA and catalytic activity

To prove that the observed phenotypes are not the result of potential off-target activity of PIP-E3^{63}, I created a panel of mutants of this ligase: 1) lacking the PIP-box (ΔPIP or, alternatively, E3^{63}), 2) containing the point mutation I227A, which has been shown to abolish interaction with Ubc13 in yeast (Renz *et al.,* 2020) or 3) completely lacking the RING domain (ΔRING) (**Figure 19A**). I created RPE1 hTERT-based cell lines that express these mutants of PIP-E3^{63} and compared them to the cell line expressing the original PIP-E3^{63}. As shown in **Figure 19B**, interfering with either PCNA binding or with the catalytic activity of E3 results in no checkpoint activation, although all constructs, except for the probably unstable PIP-E3^{63}ΔRING, were expressed at similar levels. Interestingly, I227A reduces but does not completely abolish the activity of PIP-E3^{63} – nevertheless, this is sufficient to completely abrogate checkpoint signalling. Moreover, the expression of none of these constructs interferes with cell cycle progression either (**Figure 19C**). Therefore, this means that both the interaction with PCNA and the catalytic activity of PIP-E3^{63} are important to induce replication catastrophe in cells.

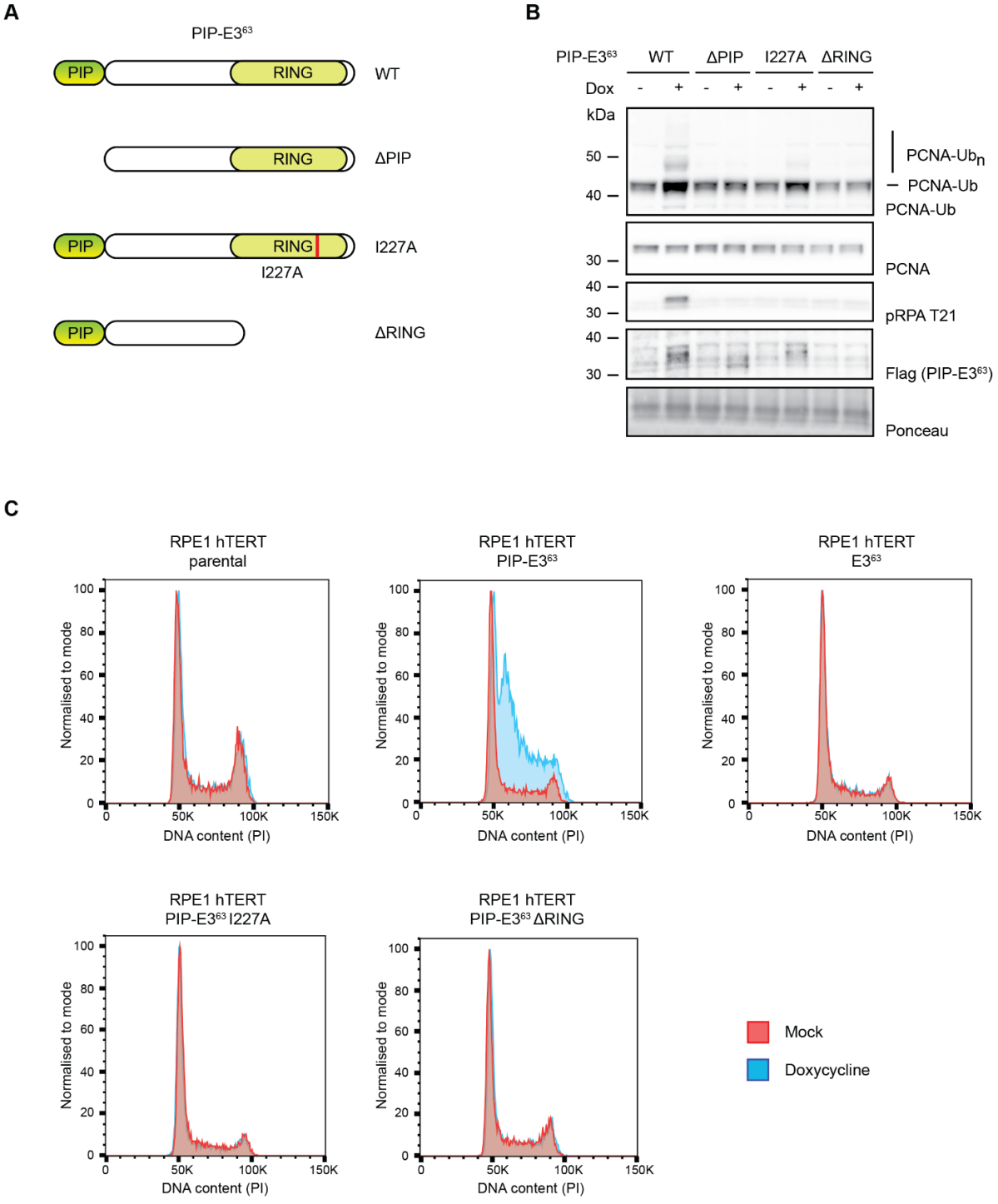

Figure 19: Negative effects of PIP-E3^{63} require interaction with PCNA and catalytic activity. **(A)** Scheme of the PIP-E3^{63} enzyme and its mutant forms: lacking a PIP box, containing an I227A mutation or lacking a RING domain. **(B)** RPE1 hTERT cells carrying doxycycline-inducible PIP-E3^{63} variants described in panel (A) were treated with 1 µg/ml doxycycline for 6 h. Expression of enzymes and checkpoint activation were analysed by western blotting. Ponceau S staining serves as a loading control. **(C)** Cell cycle profiles of cells treated as in (B) but for 24 h.

3.3.5 PCNA monoubiquitylation is a prerequisite for PIP-E3^{63} activity *in vivo*

The findings described earlier show that replication stress induced by PIP-E3^{63} results from its ubiquitin ligase activity in the vicinity of PCNA. However, there is a possibility that our tailor-made E3 extends ubiquitin(s) present on substrates other than PCNA. To test this hypothesis, I integrated PIP-E3^{63} by means of lentiviral transduction in an RPE1 hTERT K164R (KR) mutant cell line, in which K164 of PCNA is mutated to arginine and therefore cannot be ubiquitylated by RAD18 (Thakar *et al.,* 2020). As a control, the corresponding parental RPE1 hTERT (WT) cell line was used. Together with PIP-E3^{63}, TetR was integrated in the same cells in order to make expression of the ligase doxycycline-inducible. Additionally, to confirm that the effects are not cell line-specific, I also used the following panel of HEK 293T-derived cells (Thakar *et al.,* 2020):

1. Wild-type HEK293 (WT)
2. Heterozygous PCNA K164R, in which other PCNA alleles were inactivated. The loss of PCNA levels was compensated by re-expressing wild-type PCNA (WT/KR).
3. Heterozygous PCNA K164R mutant, in which other PCNA alleles were inactivated. Loss of PCNA levels was compensated by re-expressing mutant PCNA (KR/KR).

Figure 20A shows the expression of PIP-E3^{63} and activation of the checkpoint after its integration in the described cell lines. The RPE1 hTERT FlpIn PIP-E3^{63} cell line serves as a positive control (here, the ligase is ~2 kDa heavier due to the presence of an additional Flag tag). Despite having a higher expression of PIP-E3^{63}, the cell lines that harbour the PCNA K164R mutation do not activate checkpoint signalling after expression of the ligase, as demonstrated by the absence of phospho-RPA T21 or γH2AX. In order to show that the K164R mutation abolishes PIP-E3^{63}-induced polyubiquitylation, PCNA was immunoprecipitated from these cell lines after the expression of PIP-E3^{63}. In accordance with PIP-E3s being elongation-specific, polyubiquitylation of PCNA by PIP-E3^{63} is completely abolished when the acceptor lysine is not available (**Figure 20B**). Interestingly, compared to homozygous wild-type cells, we do not observe a decrease in PCNA polyubiquitylation in HEK 293T WT/KR cells. This may be due to the fact that exogenous PCNA is overexpressed in the WT/KR cell line, leading to slightly higher total

PCNA levels and may ultimately interfere with the pathway. Alternatively, it is possible that checkpoint activation by PIP-E3^{63} requires all three subunits of PCNA to be simultaneously monoubiquitylated, which is less likely to be the case in the WT/KR cell line. It has been reported that such simultaneous ubiquitylation of PCNA subunits acts as a switch for the HLTF mode of action (Masuda *et al.,* 2018). It remains to be understood what the underlying molecular mechanism of HLTF activity towards the fully and partially monoubiquitylated PCNA trimers is and whether it can also be applied to the PIP-E3^{63} system.

Consistent with no checkpoint signalling being active in K164R cells, only wild-type, but not mutant RPE1 hTERT cells exhibit cell cycle arrest after PIP-E3^{63} expression (**Figure 20C**). Interestingly, HEK 293T maintain the normal cell cycle progression even when the checkpoint is active, highlighting that the genetic background of a cell line may influence its reaction to replication stress and checkpoint signalling (**Figure 20D**).

To further prove that PIP-E3^{63}-induced effects are specific for PCNA, the E3 was expressed in cells transiently depleted of Rad18 by means of two independent siRNAs. S-phase arrest (**Figure 21A, 11B**) and robust checkpoint activation (**Figure 21C**) were observed only in cells, transfected with control siRNA and were absent upon knock-down of Rad18. Of note, siRNA #1 led to a moderate decrease in expression levels of PIP-E3^{63}; however, this is not the case for siRNA #2 and, altogether, these results place Rad18 upstream of PIP-E3^{63} in the PCNA ubiquitylation cascade.

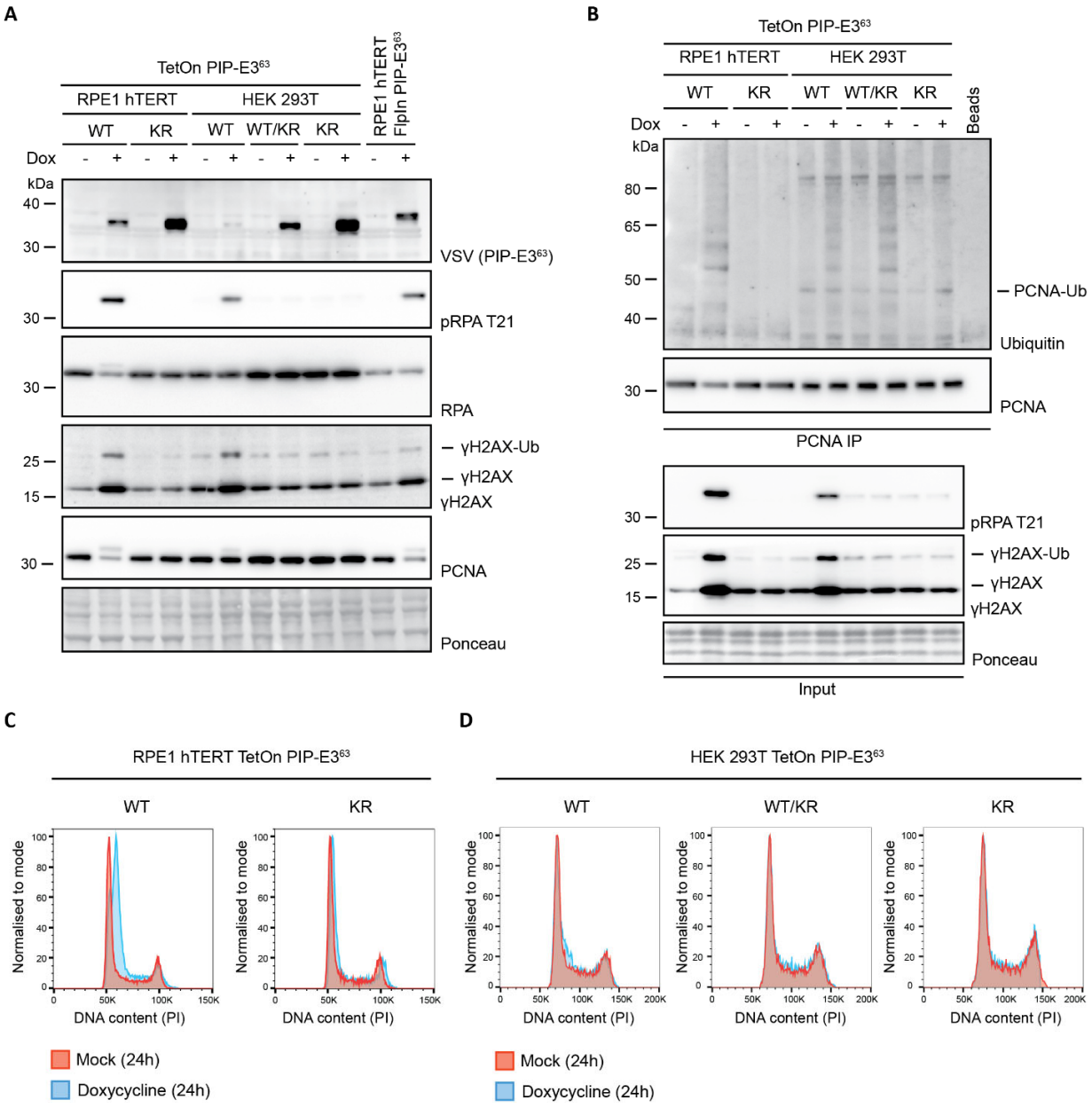

Figure 20: The negative effects of PIP-E3^{63} are dependent on lysine 164 of PCNA. (A) Indicated cell lines with integrated PIP-E3^{63} were treated 1 µg/ml doxycycline for 24 h. Expression of the E3, PCNA levels and checkpoint activation were analysed by western blotting of total cell lysates with the indicated antibodies. Ponceau S staining serves as a loading control. **(B)** Indicated cell lines with integrated PIP-E3^{63} were treated as in panel (A), followed by chromatin isolation, PCNA immunoprecipitation and western blotting with indicated antibodies. **(C)** Cell cycle profiles of wild-type and PCNA K164R RPE1 hTERT TetOn PIP-E3^{63} cells, treated with 1 µg/ml doxycycline for 24 h. **(D)** Cell cycle profiles of wild-type, heterozygous and homozygous PCNA K164R mutant HEK 293T TetOn PIP-E3^{63} cells, treated with 1 µg/ml doxycycline for 24 h.

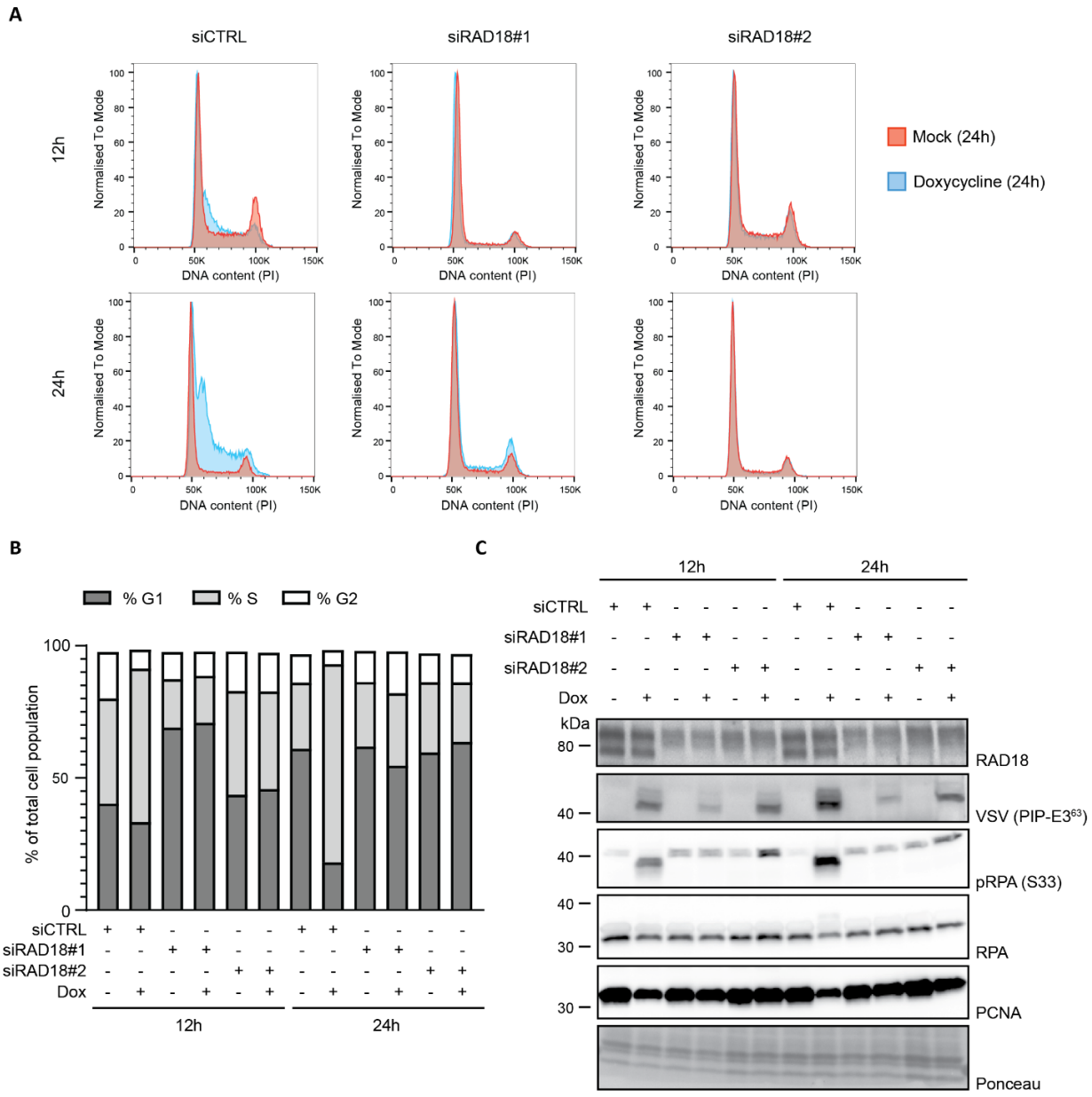

Figure 21: The negative effects of PIP-E3^{63} are dependent of RAD18 activity. (A) Cell cycle profiles of RPE1 hTERT PIP-E3^{63} cells, transfected with control siRNA or 2 independent siRNAs against RAD18 for 72 h and treated with doxycycline during the last 12 h or 24 h. **(B)** Quantification of cell cycle distribution of cells treated as described in (A). **(C)** RPE1 hTERT PIP-E3^{63} cells were treated as described in (A), followed by lysis and western blotting with the indicated antibodies. Ponceau S staining serves as a loading control.

3.3.6 Negative effects of PIP-E3^{63} are independent of known interactors of polyubiquitylated PCNA

To date, two proteins have been reported to interact with polyubiquitylated PCNA. One is the DNA translocase ZRANB3, which catalyses the reversal of replication forks. Therefore, we hypothesised that excessive fork reversal upon PIP-E3^{63} overexpression may cause activation of checkpoint signalling. However, I observed that depletion of ZRANB3 with 2 independent siRNAs does not abolish PIP-E3^{63}-induced checkpoint activation (**Figure 22A**), indicating that the negative effects of the ligase expression are likely ZRANB3-independent. ZRANB3 catalyses fork reversal with at least two other DNA translocases – HLTF and SMARCAL1. Although a link between HLTF and SMARCAL1 recruitment to stalled replication forks and PCNA ubiquitylation, as well as a possible functional redundancy between all three translocases, have not been reported, I tested whether depletion of HLTF and SMARCAL1 would counteract the negative effects of PIP-E3^{63}. Similar to ZRANB3, depletion of HLTF or SMARCAL1 does not significantly change checkpoint activation upon PCNA polyubiquitylation (**Figure 22B**).

As the factors that must act downstream of PCNA polyubiquitylation in the PIP-E3^{63} system do not have to bind to PCNA itself and can merely be general readers of K63-linked chains on chromatin, I hypothesised that the responsible factor could be RAP80. This protein is involved in double-strand break repair by binding to K63-linked chains on histones and recruiting the BRCA1-A complex to damage sites to counteract resection (Hu *et al.,* 2011). However, no change in checkpoint activation is observed when RAP80 is depleted (**Figure 22C**). The same holds for the second known interactor of polyubiquitylated PCNA, WRNIP1 (**Figure 22D**). Thus, the phenotypes observed in the PIP-E3^{63} system suggest the presence of other readers of PCNA polyubiquitylation.

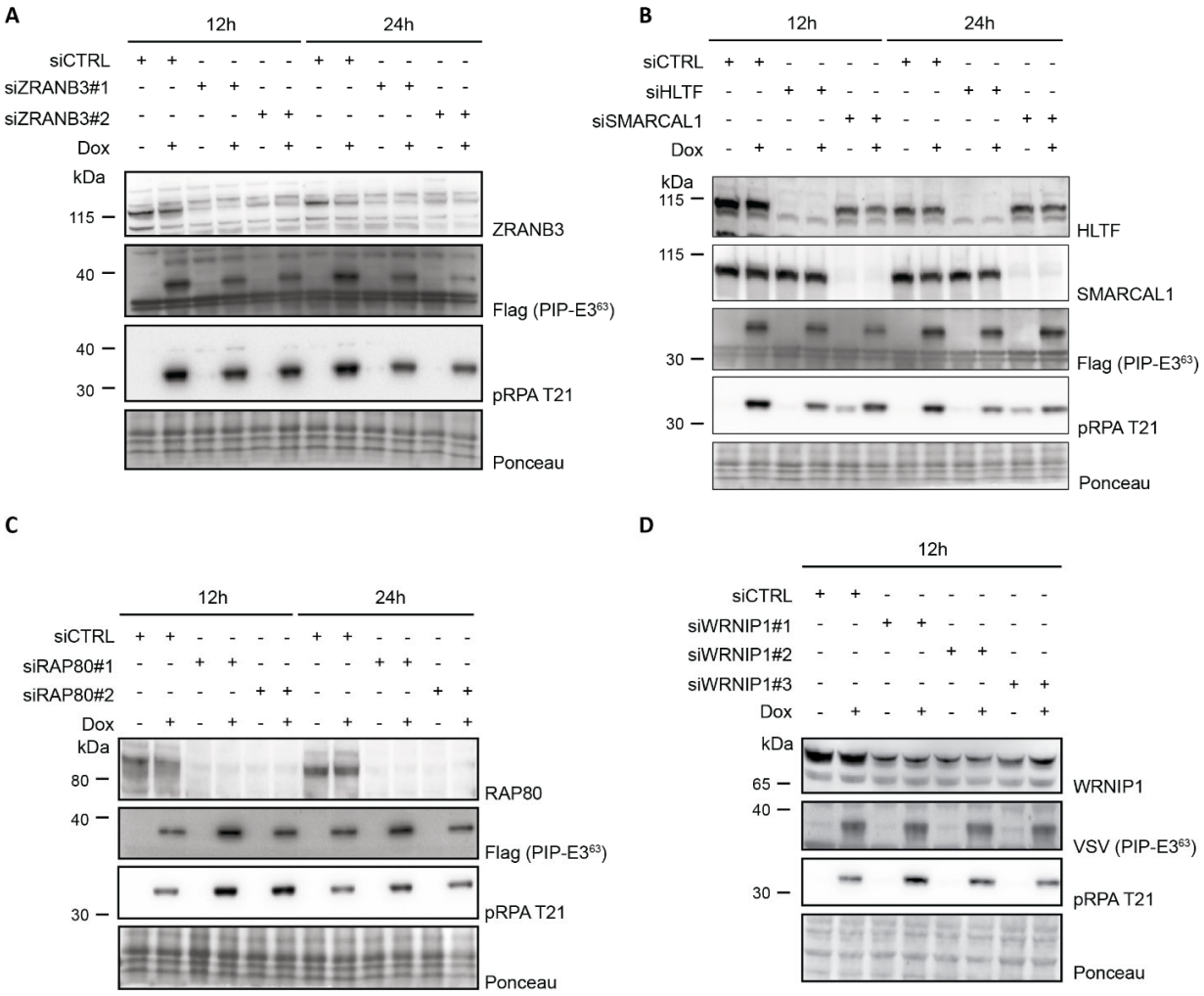

Figure 22: The negative effects of PIP-E3^{63} are independent of fork reversal enzymes, RAP80 and WRNIP1. RPE1 hTERT PIP-E3^{63} cells were transfected with siRNAs against ZRANB3 (A), HLTF (B), SMARCAL1 (B), RAP80 (C) and WRNIP1 (D) for 72 h and treated with doxycycline for 12 h or 24 h. Expression of PIP-E3^{63} and levels of RPA phosphorylation were analysed in total cell lysates by western blotting. Ponceau S staining serves as a loading control.

3.4 Analysing the interactome of polyubiquitylated PCNA

Given that the depletion of putative interactors of polyubiquitylated PCNA did not lead to the rescue of PIP-E3^{63}–induced checkpoint activation, I set out to identify interactors of polyubiquitylated PCNA in an unbiased manner *in vivo* by mass-spectrometry. In order to prove that pulling down PCNA in my experimental setup preserves binding of PCNA to its known interactors, I analysed whether ZRANB3, HLTF, EXO1 and POLH, all of which have been reported to directly interact with PCNA (Ciccia *et al.,* 2012; Seelinger and Otterlei, 2020; Chen *et al.,* 2013; Bienko *et al.,* 2005), co-immunoprecipitate with PCNA. I also compared whether stable or transient overexpression of PIP-E3^{63} influences these interactions.

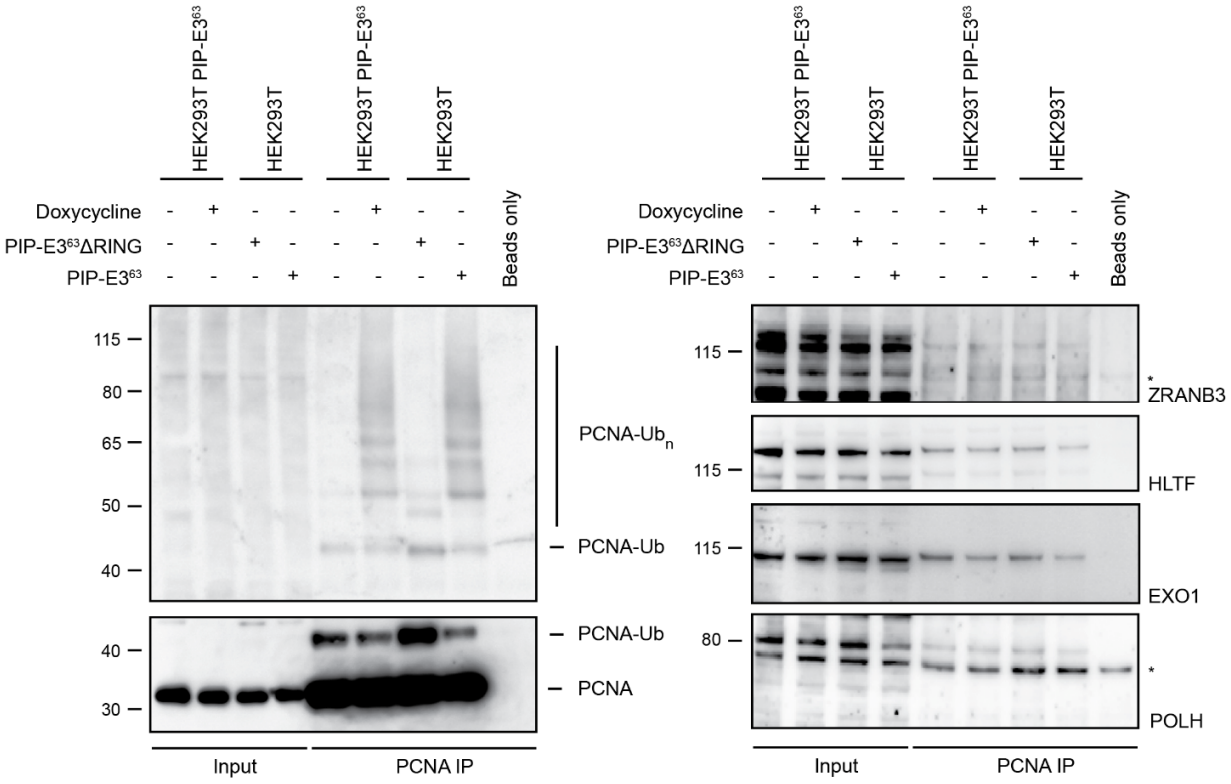

Figure 23: Immunoprecipitation of chromatin-bound PCNA preserves its interactions with a panel of known PCNA binders. PIP-E3^{63} was expressed either in HEK 293T PIP-E3^{63} cells by addition of 1 µg/ml doxycycline for 24 h or via a transient overexpression of PIP-E3^{63} in wild-type HEK 293T cells, followed by chromatin isolation and immunoprecipitation of PCNA. The levels of PCNA ubiquitylation as well as co-immunoprecipitated ZRANB3, HLTF, EXO1 and POLH were analysed by western blotting.

As shown in **Figure 23**, all four factors bind to PCNA. However, these interactions seem to be independent of the ubiquitylation status of PCNA. I also observe that transient overexpression of the enzyme leads to more intense PCNA polyubiquitylation, justifying the use of this method for further MS-based experiments.

To analyse the interactome of polyubiquitylated PCNA in mammalian cells, I performed SILAC labelling in HEK 293T cells with heavy or light amino acids, followed by transient overexpression of PIP-E3^{63} or, as a control, PIP-E3^{63}ΔRING (**Figure 24A**). The experiment was performed in triplicates: twice PIP-E3^{63} was overexpressed in heavy-, and PIP-E3^{63}ΔRING in light-labelled cells, and for the third replicate, a label switch was performed. Preparation of samples for mass-spectrometry, as well as subsequent data analysis, was carried out by Ivan Mikicic (Petra Beli laboratory). **Figure 24B** shows the results of this experiment as a volcano plot; factors that preferentially interact with polyubiquitylated PCNA are shown on the right side. Importantly, we observe WRNIP1 as one of the top interactors. ZRANB3 peptides, on the contrary, were not identified in this experiment, probably due to the transient nature of its interaction with polyubiquitylated PCNA or low expression levels. Somewhat unexpectedly, I observed the preferential binding of VCP (valosin-containing protein, also known as p97 or Cdc48 in yeast) and the proteasomal subunit PSMD4 to polyubiquitylated PCNA. VCP is an ATP-dependent unfoldase that extracts polyubiquitylated proteins from chromatin and other cellular compartments (Meyer and Weihl, 2014). VCP is targeted to its substrates via a set of adaptor proteins (Meyer and van den Boom, 2023); however, a high preference of VCP for K48-linked and branched, but not K63-linked chains has been reported (Yau *et al.,* 2017; Lange *et al.,* 2023). PSMD4 is a ubiquitin receptor of the proteasome, which has been shown to bind both K63 and K48-linked polyubiquitin with a marked preference for longer ubiquitin chains (Wang *et al.,* 2005). Factors that preferentially bind to polyubiquitylated PCNA in the aforementioned interactome analysis also include the ubiquitin ligases HUWE1 and UBR5, both of which have been shown to bind K63-linked ubiquitin chains and to be involved in DNA damage repair pathways in mammalian cells (Ohtake *et al.,* 2016; Choe *et al.,* 2016; Cipolla *et al.,* 2019).

Table 9 contains a list of proteins identified in the interactome analysis that have been implicated either in DNA damage response or in ubiquitin-mediated transactions.

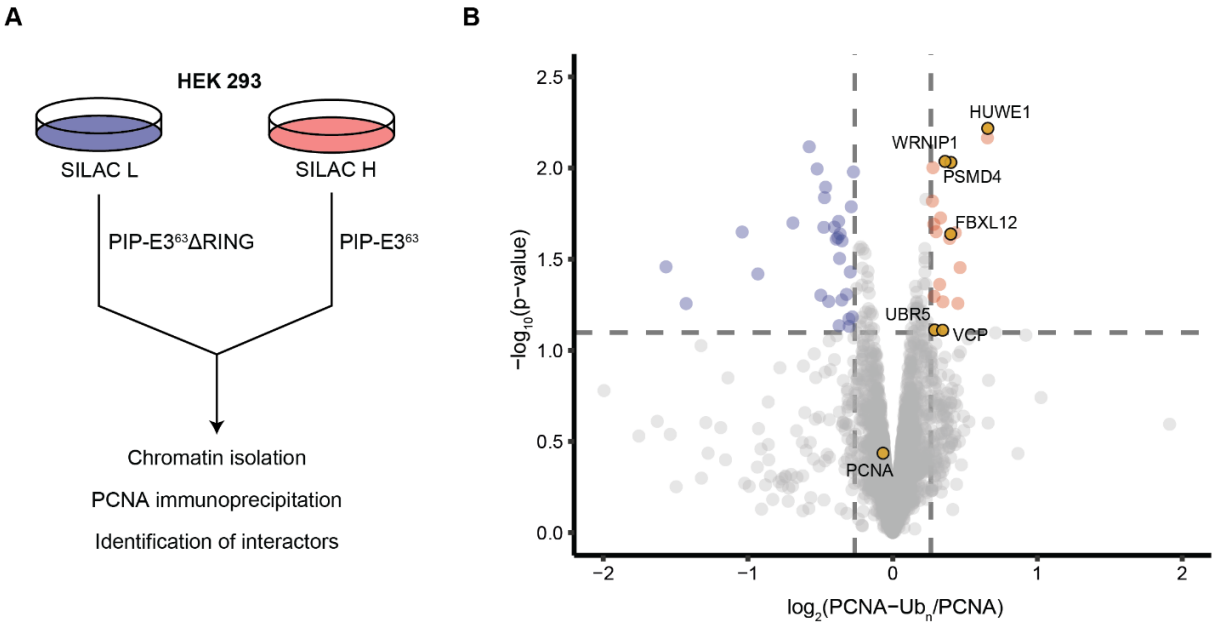

Figure 24: Analysing the interactome of polyubiquitylated PCNA. (A) MS-based experimental approach to identify interactors of polyubiquitylated PCNA. **(B)** Volcano plot of the results of the experiment. Factors that preferentially interact with polyubiquitylated PCNA are highlighted in red.

Table 9: Selected interactors of polyubiquitylated PCNA, identified in the MS experiment

Protein name	Fold change PCNA-Ub$_n$/PCNA	Brief description
HUWE1	1.5763	HECT-type ubiquitin ligase. Interacts with PCNA (Choe *et al.,* 2016), as well as K63-linked polyubiquitin, assembles K48 linkages on top of K63-linked chains (Ohtake *et al.,* 2016).
PSMD4	1.3209	Ubiquitin receptor subunit of the 26S proteasome. Prefers long ubiquitin chains (Wang *et al.,* 2005).
FBXL12	1.3202	Substrate-recognition component of the SCF E3 ubiquitin ligase complex. Mediates ubiquitylation of Ku80 at damage sites (Postow and Funabiki 2013).
WRNIP1	1.2845	Interacts with polyubiquitylated PCNA (Saugar *et al.,* 2012; Kanu *et al.,* 2016). Involved in replication fork protection (Leuzzi *et al.,* 2016; Porebski *et al.,* 2019) and intra-strand crosslink repair (Socha *et al.,* 2020).

VCP	1.2697	VCP/p97 extracts polyubiquitylated proteins from membranes or cellular structures (Meyer and van den Boom 2023). Is involved in many pathways that safeguard genome stability (Vaz *et al.,* 2013)
ERBB2	1.2715	Receptor tyrosine kinase often overexpressed in breast cancers. Modulates repair of certain DNA lesions produced by chemotherapy (Boone *et al.,* 2009)
H1.3	1.2573	Linker histone. Involved in chromatin compaction into higher order structures (Hergeth and Schneider 2015)
UBR5	1.2224	HECT-type ubiquitin ligase. Interacts with the components of replication fork and controls the levels of histone H2A monoubiquitylation (Cipolla *et al.,* 2019). Limits spreading of chromatin ubiquitylation (Gudjonsson *et al.,* 2012). Forms branched K63-K48 ubiquitin chains (Ohtake *et al.,* 2018).

Thus, in the interactome of polyubiquitylated PCNA, I identified several factors that have not been previously known to be associated with this modification. In the following sections, I will analyse several of these factors to unravel the pathway triggered by excessive K63-linked PCNA polyubiquitylation.

3.5 K63-linked chains on PCNA are converted into conjugates of higher complexity *in vivo*

3.5.1 VCP activity underlies PIP-E3^{63}-induced replication collapse

In the interactome of polyubiquitylated PCNA, we observe components of the VCP – proteasome pathway. This is a common mechanism of extraction and degradation of polyubiquitylated substrates; however, the relevance of ubiquitin chain linkage in this context remains underinvestigated. Therefore, I hypothesised that VCP might be one of the factors that mediated checkpoint activation following the expression of PIP-E3^{63}. Since VCP is an essential protein and its knockdown can lead to heavy alterations of cellular metabolism, I set out to inhibit its activity via allosteric inhibition with NMS-873 (hereafter referred to as VCPi) (Magnaghi *et al.,* 2013). Regardless of how long either PIP-E3^{63} is expressed, or VCP is inhibited, blocking VCP activity prevents checkpoint activation by PIP-E3^{63} (**Figure 25A**). As inhibition of VCP for 12 h leads to a reduction of the ligase levels, probably due to a toxic effect of the compound, only shorter (6 h) times of VCP inhibition are used for future experiments. Consistent with the role of VCP in the turnover of ubiquitylated proteins, VCP inhibition leads to the accumulation of a high molecular weight ubiquitin smear. Yet, interestingly, the pool of free ubiquitin seems to be unaffected by this treatment. Concomitantly with an abrogation of checkpoint signalling, VCP inhibition leads to the accumulation of polyubiquitylated PCNA on the chromatin (**Figure 25B**). I also observe that long polyubiquitin conjugates on PCNA are more efficiently extracted from chromatin than shorter forms, as demonstrated by stronger enrichment of high molecular weight smear upon VCP inhibition.

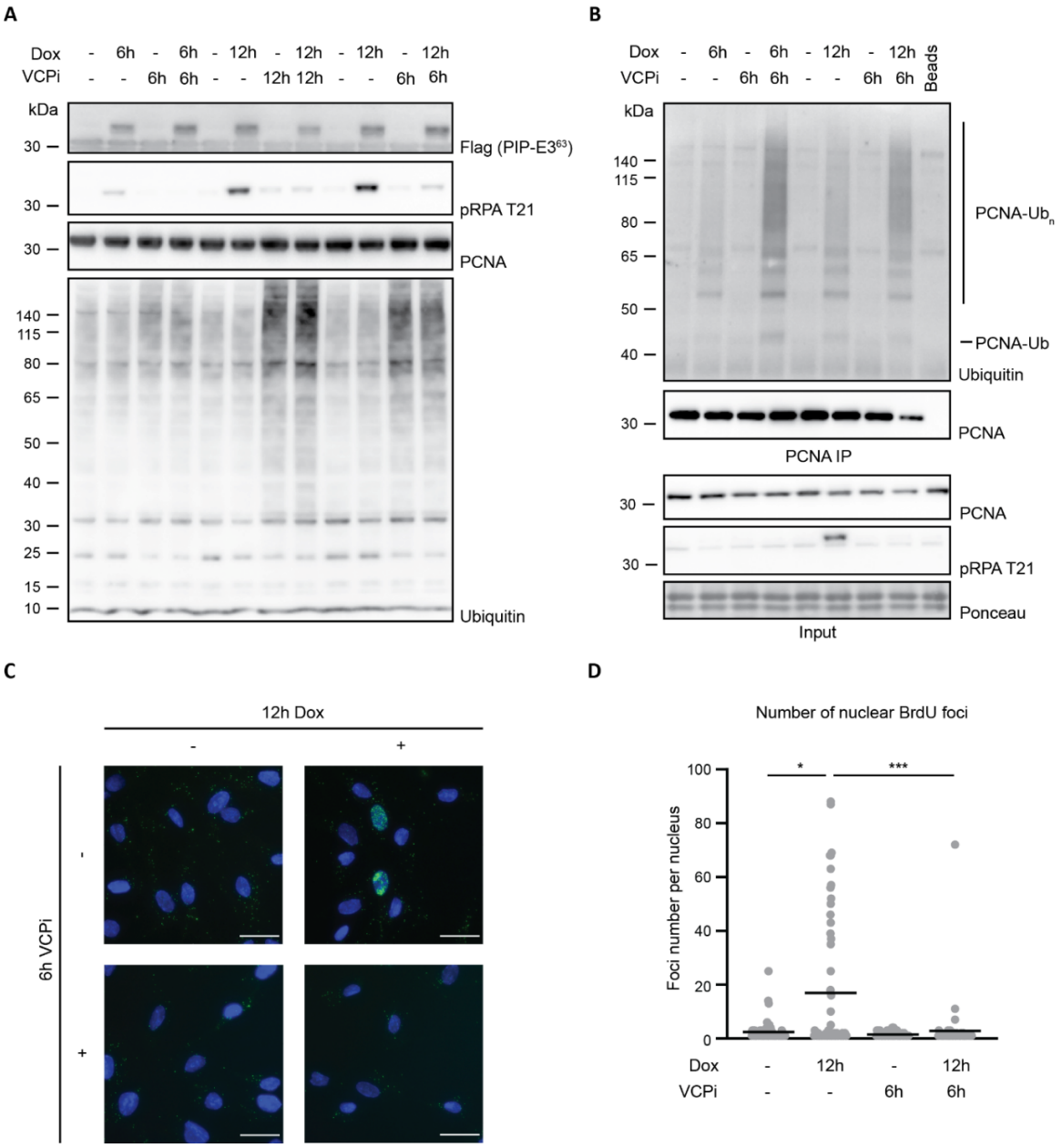

Figure 25: VCP activity mediates the toxic effects of PIP-E3^{63} expression. (A) RPE1 hTERT PIP-E3^{63} cells were treated with 1 µg/ml doxycycline or 5 µM NMS-873 (VCPi) for the indicated time periods, followed by western blotting with the indicated antibodies. **(B)** RPE1 hTERT PIP-E3^{63} cells were treated as described in (A), followed by chromatin isolation, PCNA immunoprecipitation and western blotting with the indicated antibodies. **(C)** RPE1 hTERT PIP-E3^{63} cells were labelled with 10 µM BrdU for 24 h, treated as described in panel (A) followed by immunofluorescence staining against BrdU in non-denaturing conditions. Images represent an overlay of DAPI (blue) and BrdU (green) signals. The scale bar corresponds to 30 µm. **(D)** Quantification of the experiment described in (C). Graph represents the number of nuclear foci per nucleus in cells that have at least one nuclear focus. *p<0.05; ***p<0.001 (Mann-Whitney test).

Expression of PIP-E3^{63} induces replication catastrophe, which is characterised by activation of checkpoint signalling, exposure of single-stranded DNA and cell cycle arrest. To exclude the possibility that VCP inhibition acts similarly to ATR inhibition - reducing the checkpoint signalling without affecting the other adverse effects of PIP-E3^{63} expression - I analysed the exposure of single-stranded DNA upon expression of PIP-E3^{63} and inhibition of VCP. This was achieved by labelling the cells with BrdU and performing immunofluorescence staining in non-denaturing conditions: only BrdU carried within single-stranded DNA can be visualised by this method. As shown in **Figure 25C, D**, expression of PIP-E3^{63} induces massive exposure of single-stranded DNA; however, this is largely prevented by VCP inhibition. These data indicate that multiple negative effects of PIP-E3^{63} overexpression rely on the removal of polyubiquitylated PCNA from chromatin by VCP.

Next, I wanted to understand whether the observed activity of VCP towards polyubiquitylated PCNA is specific to the PIP-E3^{63} system or is also present when PCNA polyubiquitylation is induced by replication stress. Therefore, I induced replication stress in wild-type RPE1 hTERT cells by means of three DNA-damaging agents – HU, MMS and UV, and analysed the impact of VCP inhibition on PCNA polyubiquitylation in these conditions. All three genotoxins create polymerase-stalling base lesions, and HU additionally leads to fork stalling due to the depletion of the free nucleotide pool. As shown in **Figure 26A**, PCNA polyubiquitylation is induced by all three treatments. Inhibition of VCP increases the intensity of chromatin-bound PCNA polyubiquitylation, the effect being the strongest for HU and MMS. To make sure that all ubiquitin-reactive species observed in the PCNA IP/western blot depend on PCNA K164 monoubiquitylation and do not correspond to *de novo* PCNA ubiquitylation events on other residues, I analysed PCNA ubiquitylation in the RPE1 hTERT PCNA K164R cell line in the presence HU and VCPi. As demonstrated in **Figure 26B**, in RPE1 hTERT PCNA K164R cells, PCNA gets neither mono- nor polyubiquitylated. These results highlight the similarity between the PIP-E3^{63} system and the replication stress response and indicate that VCP-mediated extraction of PCNA is a common pathway downstream of PCNA polyubiquitylation.

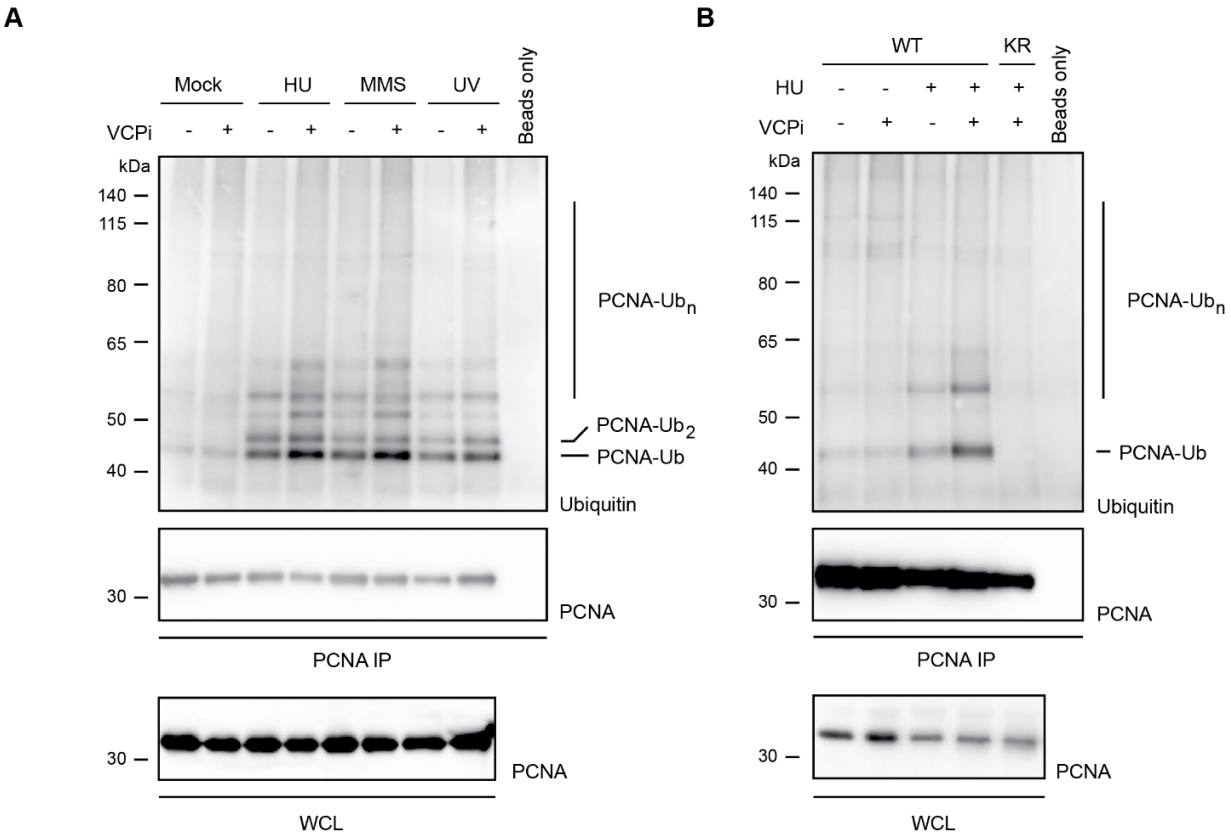

Figure 26: VCP extracts polyubiquitylated PCNA from chromatin under replication stress conditions. (A) RPE1 hTERT cells were left untreated, treated with 4 mM HU for 4,5h, 0.01% MMS for 1 h followed by 4,5h recovery or 40J/m^2 UV followed by 4,5h recovery. During recovery or HU treatment, 5 µM VCPi (NMS-873) or the corresponding amount of DMSO were also added. PCNA polyubiquitylation was analysed by immunoprecipitation from the chromatin fraction and western blotting. **(B)** HU-induced PCNA polyubiquitylation in RPE1 hTERT (WT) or RPE1 hTERT PCNA K164R (KR) was analysed as in panel (A).

3.5.2 Analysing the interactome of polyubiquitylated PCNA upon VCP inhibition

Up until now, it remains unclear what happens to the interactors of polyubiquitylated proteins upon their removal by VCP from different cellular compartments. If polyubiquitylated PCNA is removed from chromatin, its binders will likely leave it as well. Therefore, some interactions could be lost in our MS-based experiment. Also, although K48 and K11 linkages were identified in the interactome, they showed no enrichment after PCNA polyubiquitylation. As these linkage types are well-characterised substrates for VCP-dependent extraction, VCP inhibition would be necessary in order to analyse their presence on chromatin upon polyubiquitylation of PCNA. For that reason, I performed an

analogous mass spectrometry-based experiment as described in **section 3.4**, except that VCP was inhibited for 6 h both during PIP-E3^{63}ΔRING or PIP-E3^{63} expression. Preparation of samples for mass-spectrometry analysis as well as subsequent data analysis was carried out by Ivan Mikicic (Petra Beli laboratory). **Figure 27A** shows the results of the experiment as a volcano plot, with factors preferentially interacting with PCNA upon PIP-E3^{63} expression positioned on the right half of the plot. I reproducibly observe WRNIP1 and HUWE1 as interactors of polyubiquitylated PCNA. The DNA translocase ERCC6L (PICH), which has been shown to catalyse processive fork reversal (Tian *et al.,* 2021), is also enriched upon PCNA polyubiquitylation. No other proteins with known functions in DNA replication or repair were enriched in the condition of PIP-E3^{63} expression. Interestingly, analysis of the ubiquitin linkages in the described experiment reveals an increase not only of K63 but also of K48 and K11 linkages after K63-linked PCNA polyubiquitylation (**Figure 27B**). In the following sections, I will discuss the origin of these linkages and their impact on VCP-dependent PCNA extraction.

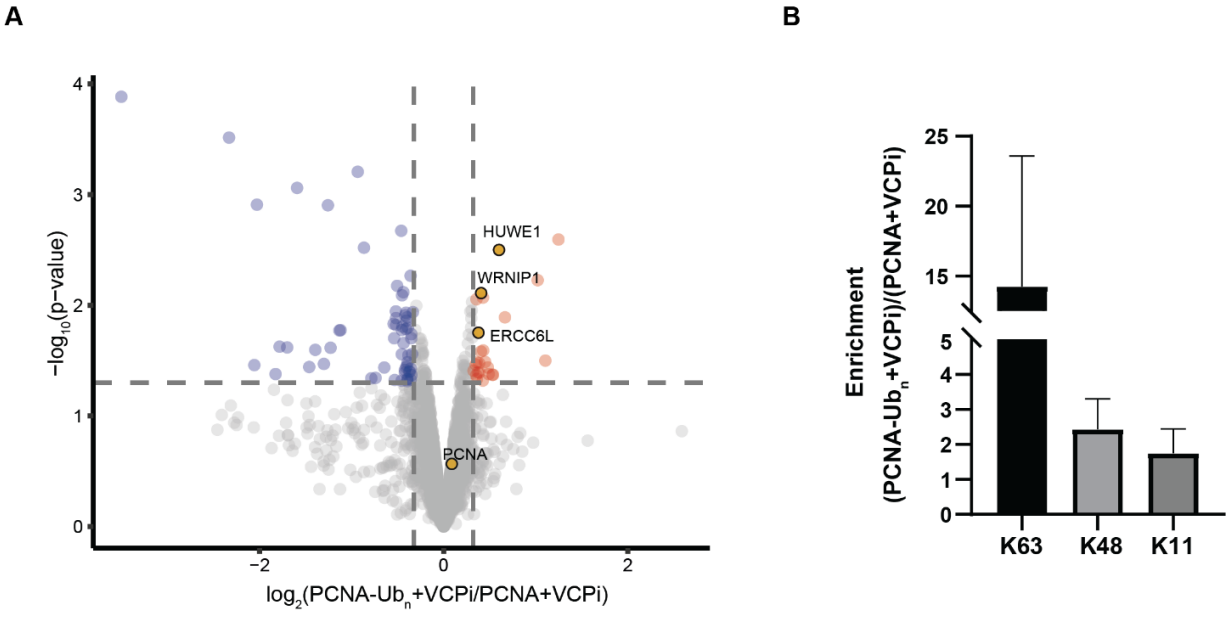

Figure 27: Interactome of polyubiquitylated PCNA upon VCP inhibition. (A) Volcano plot showing interactors of PCNA upon expression of PIP-E3^{63}ΔRING (left) or PIP-E3^{63} after 6 h treatment with VCPi (NMS-873). Proteins with known functions in replication or DNA repair are highlighted in yellow. **(B)** Enrichment of ubiquitin linkages in the conditions described in panel (A).

3.5.3 K63-linked chains on PCNA are converted into branched K63-K48 conjugates

3.5.3.1 UBICREST assay

It was intriguing to observe that polyubiquitylation of PCNA with K63-linked chains leads to an increase of K48- and K11-linked ubiquitin chains that co-immunoprecipitate with PCNA. As immunoprecipitation of PCNA is performed under non-denaturing conditions, there are three scenarios that can explain these results (**Figure 28**):

1. K48 and K11 linkages are assembled on top of K63-linked chains (branched ubiquitin chains)
2. K63-linked chain remains intact. However, PCNA lysines other than K164 undergo K48- or K11-linked polyubiquitylation
3. K48 and K11-linked chains reside on PCNA interactors and therefore are not covalently attached to (polyubiquitylated) PCNA

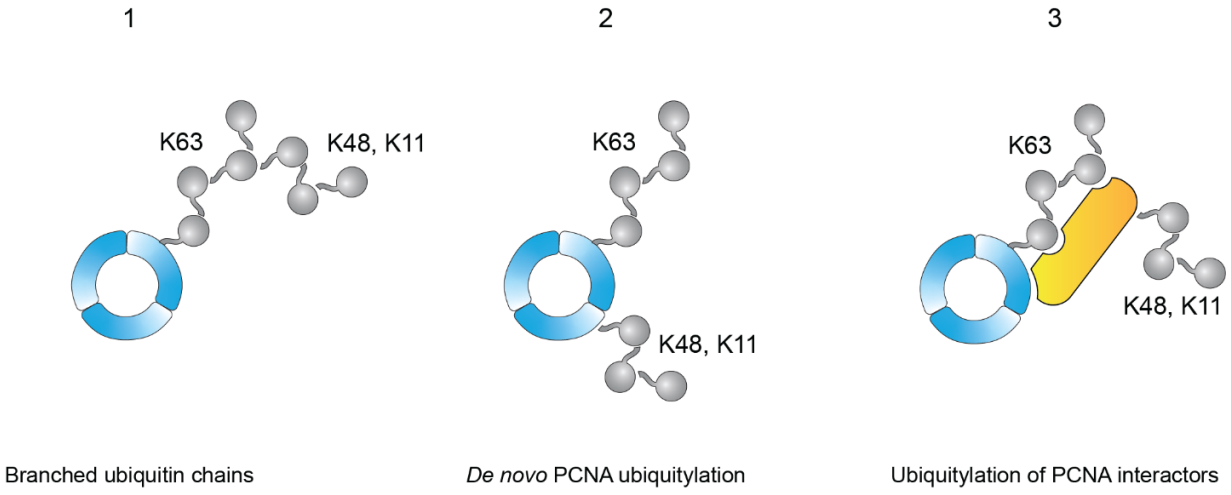

Figure 28: Scenarios explaining accumulation of K48 and K11 linkages in PCNA immunoprecipitates. From left to right: K48 and K11 linkages are assembled on top of K63-linked chains, on PCNA (except K164) or on PCNA interactors.

To discriminate between the first scenario and the latter two, I employed a deubiquitinase-based assay called UBICREST (Ubiquitin Chain Restriction) (Hospenthal *et al.,* 2015) to determine the precise architecture of ubiquitin chains on PCNA. In the following experiments, I focus mainly on K48 linkages due to the availability of a high-quality linkage-specific antibody and established UBICREST assays for this linkage type.

The experimental set-up required immunoprecipitation of PCNA from cellular extracts, followed by treatment with linkage-selective deubiquitinating enzymes (hereafter called DUBs) and analysis of the ubiquitylation status of PCNA ('elution from beads') or soluble ubiquitin forms that are released into solution upon DUBs cleavage ('supernatant'). This discrimination between soluble and insoluble (coupled to beads via PCNA) ubiquitin forms explains whether K48 linkages were assembled on top of K63-linked chains or have another attachment site. If a K63-linked chain on PCNA remains intact and is not further modified with other linkages, its cleavage by the K63-selective DUB AMSH (McCullough *et al.,* 2006) should produce ubiquitin in the soluble fraction. Concomitantly, monoubiquitylated PCNA should remain on the beads, as AMSH is not able to cleave the first ubiquitin attached to a substrate. At the same time, if ubiquitin units in a K63-linked chain are further modified with other linkages, AMSH will not be able to cleave them, and they will appear in the soluble fraction as di-ubiquitin, tri-ubiquitin or higher conjugates depending on the length of branched units in an initial chain. This reaction is possible if AMSH activity towards K63-linked chains is unaffected by chain branching, which is most likely the case (Ohtake *et al.,* 2016). We can also expect a loss of K48 linkages from the beads, which should be released into the supernatant. However, if a non-K63 linkage resides on a ubiquitin closest to PCNA, this linkage will not be targeted by AMSH cleavage and, therefore, should remain coupled to PCNA (**Figure 29A**).

Firstly, I applied UBICREST-AMSH to the chains generated by PIP-E3^{63}. Four conditions were compared: mock treatment (DMSO), expression of PIP-E3^{63}, VCP inhibition or a combination of both. As demonstrated in **Figure 29B**, VCP inhibition alone does not lead to PCNA polyubiquitylation, whereas expression of PIP-E3^{63} results in the robust formation of chains on PCNA, which are further stabilised by VCP inhibition. Consistent with the linkage specificity of PIP-E3^{63}, almost all ubiquitin signal on the beads disappears after incubation with AMSH. In striking contrast to the total ubiquitin signal, an anti-K48 linkage-selective antibody reveals the presence of K48 linkages only if both PIP-E3^{63} is expressed and VCP is inhibited, but in neither of these conditions alone. This may indicate that once formed, K48 linkages are promptly removed from chromatin by VCP and therefore are undetectable in the chromatin fraction. Similarly to total ubiquitin, the anti-K48 signal is lost upon AMSH treatment. As AMSH is unable to cleave K48 linkages, this suggests that K48 linkages are assembled on top of K63-linked chains. Analysis of

the ubiquitin forms released in the soluble fraction after AMSH treatment reveals the presence of low-intensity chain branching even in unperturbed cells, which is mainly limited to di-ubiquitin. This chain branching increases with PIP-E3^{63} expression and is strongly stabilised by concomitant VCP inhibition. Interestingly, in the latter condition, the chain branching pattern shows more di-ubiquitin and tri-ubiquitin forms than monoubiquitin. Although precise quantification of the degree of chain branching from this experiment is difficult, we can roughly estimate that approximately every second ubiquitin in a chain is modified with non-K63 linkages. It is also worth pointing out that inhibition of VCP mainly affects uncleaved linkages but not monoubiquitin, indicating that branched chains are a better substrate for VCP than homotypic K63 linkages.

To understand the nature of the branched chains on PCNA, I applied DUBs with different linkage selectivities to PCNA polyubiquitylated *in vivo* by PIP-E3^{63}. Suppose ubiquitin linkages released into the supernatant upon treatment with AMSH are conjugated through K48. In that case, co-treatment with the K48-selective DUB OTUB1 (Wang *et al.,* 2009) should decrease their amount, whereas treatment with a non-selective DUB USP2 should result in only monoubiquitin in the soluble fraction (**Figure 30A**). As shown in **Figure 30B**, amounts of di- to tetraubiquitin in the soluble fraction after AMSH cleavage are reduced when OTUB1 is added to the reaction. Some chains may remain upon combined treatment with AMSH + OTUB1 due to incomplete digestion by OTUB1 or because other linkages are present (for example, K11, as their mobility in a gel is similar to that of K48-linked chains (Michel *et al.,* 2018)). Surprisingly, reaction with OTUB1 alone also releases a chain in the supernatant, which is absent when both AMSH and OTUB1 are used together. This indicates that the architecture of the chains may be more complex than initially anticipated: K48 linkages, assembled on top of the K63-linked chain, are further modified by K63 linkages, likely due to the presence of PIP-E3^{63}. As predicted, USP2 releases monoubiquitin as the only soluble form. Taken together, these data confirm that K63 chains on PCNA are branched *in vivo* and that these branched chains consist, at least partially, of K48 ones.

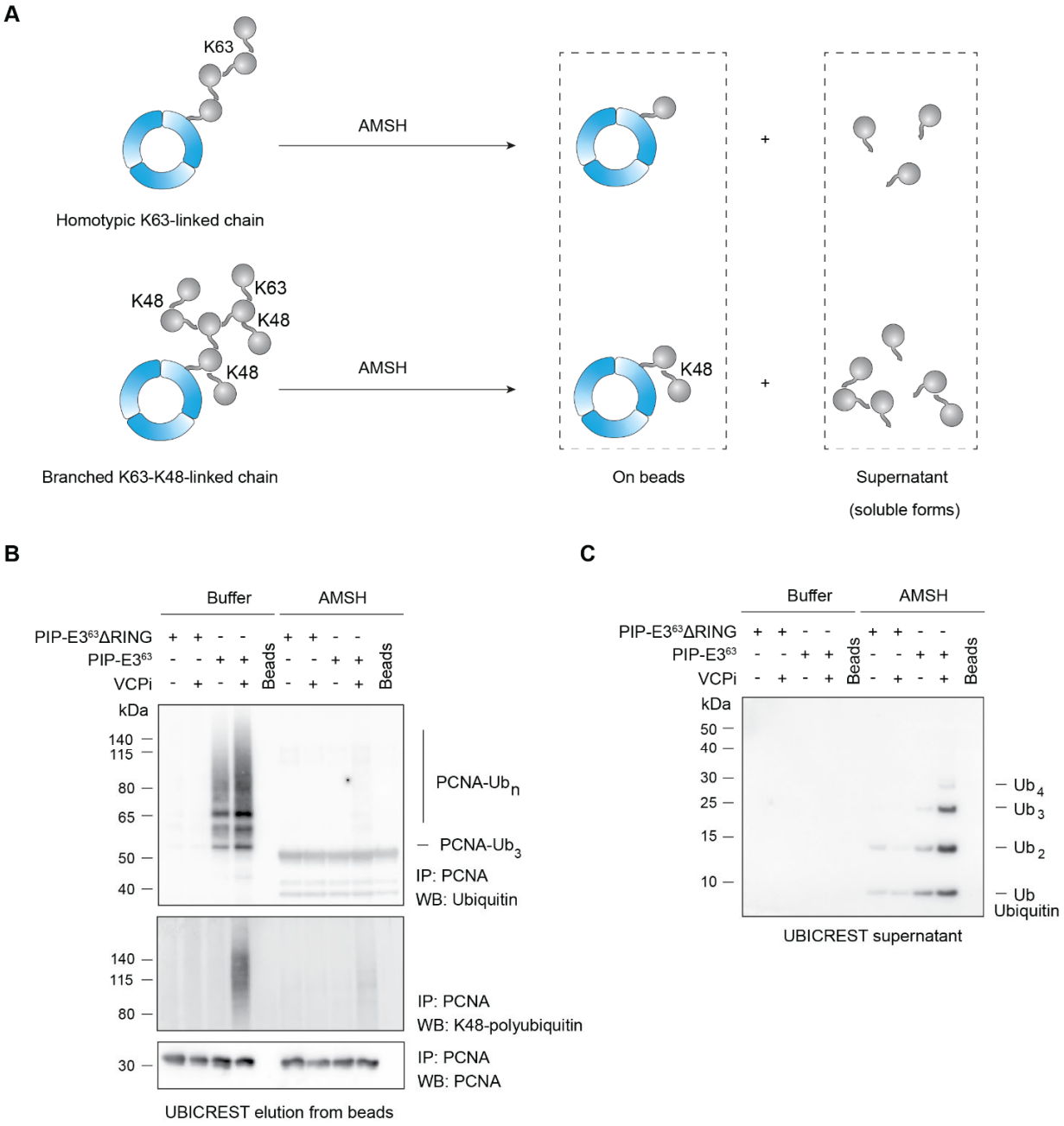

Figure 29: The UBICREST assay reveals ubiquitin chain branching on PCNA. (A) Schematic representation of a UBICREST assay applied to a homotypic (top) or branched ubiquitin conjugates (bottom). **(B)** On-beads fraction of the UBICREST assay applied to PCNA ubiquitylated via transfection of HEK 293T cells with PIP-E3^{63} and, if indicated, treatment with 5 µM VCPi (NMS-873) for 6 h. **(C)** Supernatant fraction of the UBICREST assay described in (B). Ubiquitin was detected with the VU1 monoclonal antibody.

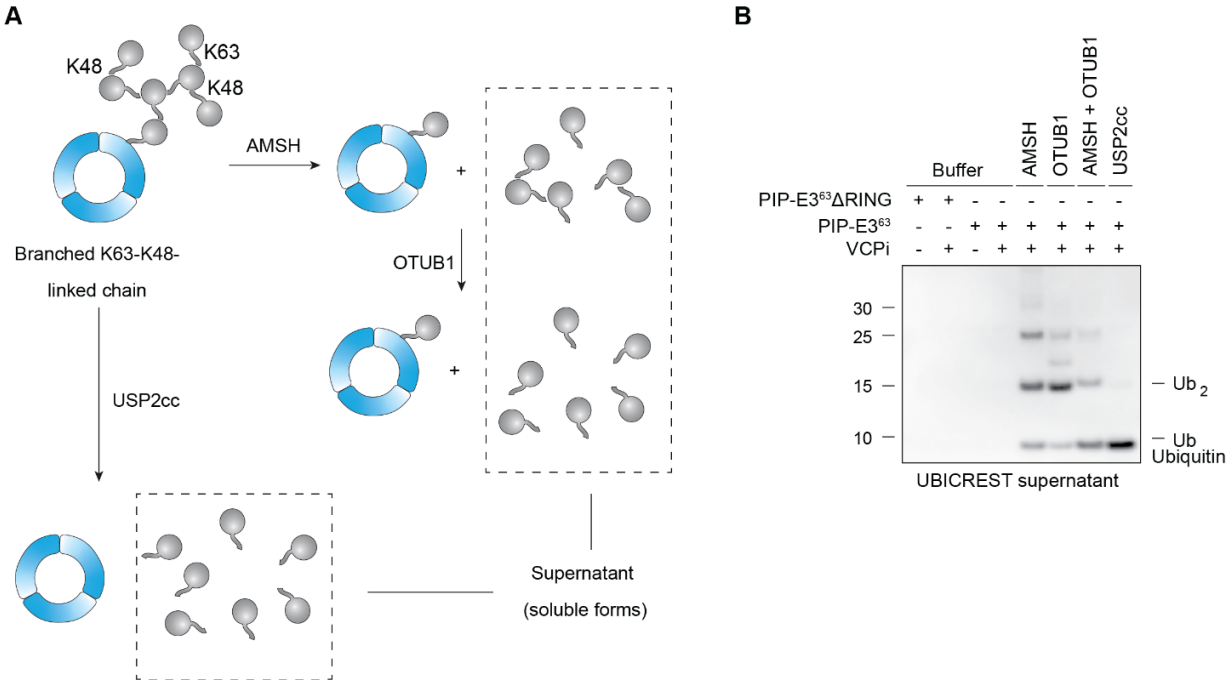

Figure 30: K63-linked chains on PCNA are branched with K48 linkages. (A) Schematic representation of the UBICREST assay with the K63-selective DUB AMSH, the K48-selective DUB OTUB1 and the linkage non-selective DUB USP2 (cc = catalytic centre). **(B)** Supernatant fraction of the UBICREST assay applied to PCNA ubiquitylated via transfection of HEK 293T cells with PIP-E3^{63} and, if indicated, treatment with 5 µM VCPi (NMS-873) for 6 h. Ubiquitin was detected with the VU1 anti-ubiquitin antibody.

Finally, I applied the UBICREST assay to analyse the architecture of ubiquitin chains formed on PCNA upon replication stress independently of PIP-E3^{63}. HU, MMS and UV light were used as replication stress-inducing agents, and VCP was inhibited to increase the amount of chromatin-bound polyubiquitylated PCNA. Similar to the PIP-E3^{63} system, AMSH cleavage releases ubiquitin chains into the soluble fraction, indicating that branching of K63-linked chains takes place (**Figure 31**). Interestingly, among all three treatments, adding HU together with VCP inhibition results in the highest amount of both total K63 linkages, as indicated by the strong accumulation of monoubiquitin in the supernatant, and branched conjugates. One possible explanation for these differences between the three genotoxins may lie in their mechanism of action: MMS and UV directly damage DNA bases, and PCNA ubiquitylation is triggered once a replisome encounters damaged DNA. On the contrary, hydroxyurea affects all the active replication forks due to

the depletion of the dNTP pool and, therefore, may affect more replication forks at a given time, thus inducing stronger PCNA polyubiquitylation. Altogether, both the PIP-E3^{63} system and replication stress produce similar ubiquitin architectures on PCNA, which suggests that they should trigger similar downstream mechanisms *in vivo*.

3.5.3.2 Targeted deubiquitylation of PCNA *in vivo* recapitulates the UBICREST assay

In a UBICREST assay, DUBs are applied to polyubiquitylated PCNA immunoprecipitated from cell extracts. I aimed to understand whether targeting the K48-selective DUB OTUB1 to PCNA can interfere with chain branching *in vivo*. A similar strategy has been employed in the DUBTAC method, where OTUB1 is targeted to substrates via heterobifunctional small molecules to promote substrate stabilisation (Henning *et al.,* 2022). To promote the interaction of OTUB1 with PCNA, I fused a PIP-box N-terminally to OTUB1, analogously to the architecture of tailor-made ubiquitin ligases (**Figure 32A**). An N-terminal Flag tag was used for the detection of the enzyme. Furthermore, since OTUB1 has been shown to directly bind and inhibit UBC13 and, therefore, may cause side effects upon its overexpression, the catalytically inactive OTUB1 mutant C91S was used as a control (hereafter referred to as “CS“). **Figure 32B** shows the expression levels of WT and CS PIP-OTUB1. This fusion protein is expressed at drastically higher levels than PIP-E3^{63}, which may be due to the codon usage of the constructs or the higher stability of OTUB1 in comparison to E3^{63}. Inhibition of VCP reduces the levels of PIP-OTUB1, possibly due to the general toxic effects of VCPi. **Figure 32C** demonstrates the effects of PIP-OTUB1 expression on PIP-E3^{63}-induced PCNA polyubiquitylation. Surprisingly, expression of PIP-E3^{63} alone or in combination with PIP-OTUB1 CS results in similar levels of PCNA polyubiquitylation despite much higher levels of PIP-OTUB1 CS compared to PIP-E3^{63}, which I expected to have a dominant-negative effect. When catalytically active PIP-OTUB1 is used, polyubiquitin chains on PCNA, visualised by total ubiquitin antibody, become shorter. At the same time, the K48-linked polyubiquitin signal is reduced in PCNA immunoprecipitates. Thus, similarly to the *in vitro* assays, PIP-OTUB1 can de-branch K63-K48 chains on PCNA. Interestingly, the increase

in PCNA-Ub and PCNA-Ub_2 levels in the condition of PIP-$E3^{63}$ and PIP-OTUB1 co-expression likely indicates that these PCNA forms (and potentially others) are further modified with K48 linkages *in vivo*. These data confirm the results of the *in vitro* UBICREST assay, which suggested that not only distant but also the first ubiquitin in a K63-linked chain, can be a substrate for K48-linked ubiquitylation. Altogether, the consequences of targeting OTUB1 to PCNA *in vivo* confirm the results of the UBICREST assay and validate the approach as a tool to interfere with the branching of K63-linked chains *in vivo*.

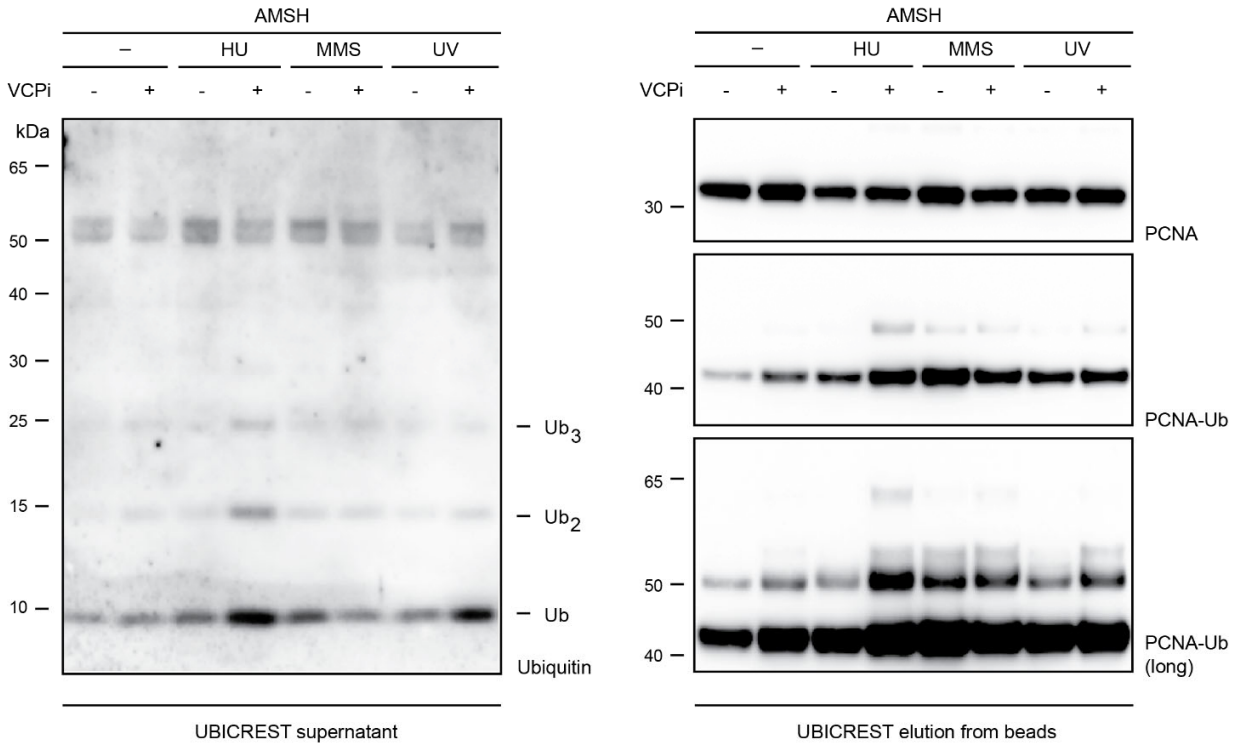

Figure 31: Replication stress induces formation of K63-K48 branched chains on PCNA. RPE1 hTERT WT cells were mock-treated, treated with 4 mM HU for 2 h, 0.01% MMS for 1 h followed by 2 h recovery or 40 J/m^2 UV followed by 2 h recovery. In all cases, NMS-873 (VCPi) or the corresponding amount of DMSO were added to a final concentration of 5 µM during the last 2 h of treatments. Soluble (left) and bead (right) fractions of the UBICREST assay are shown

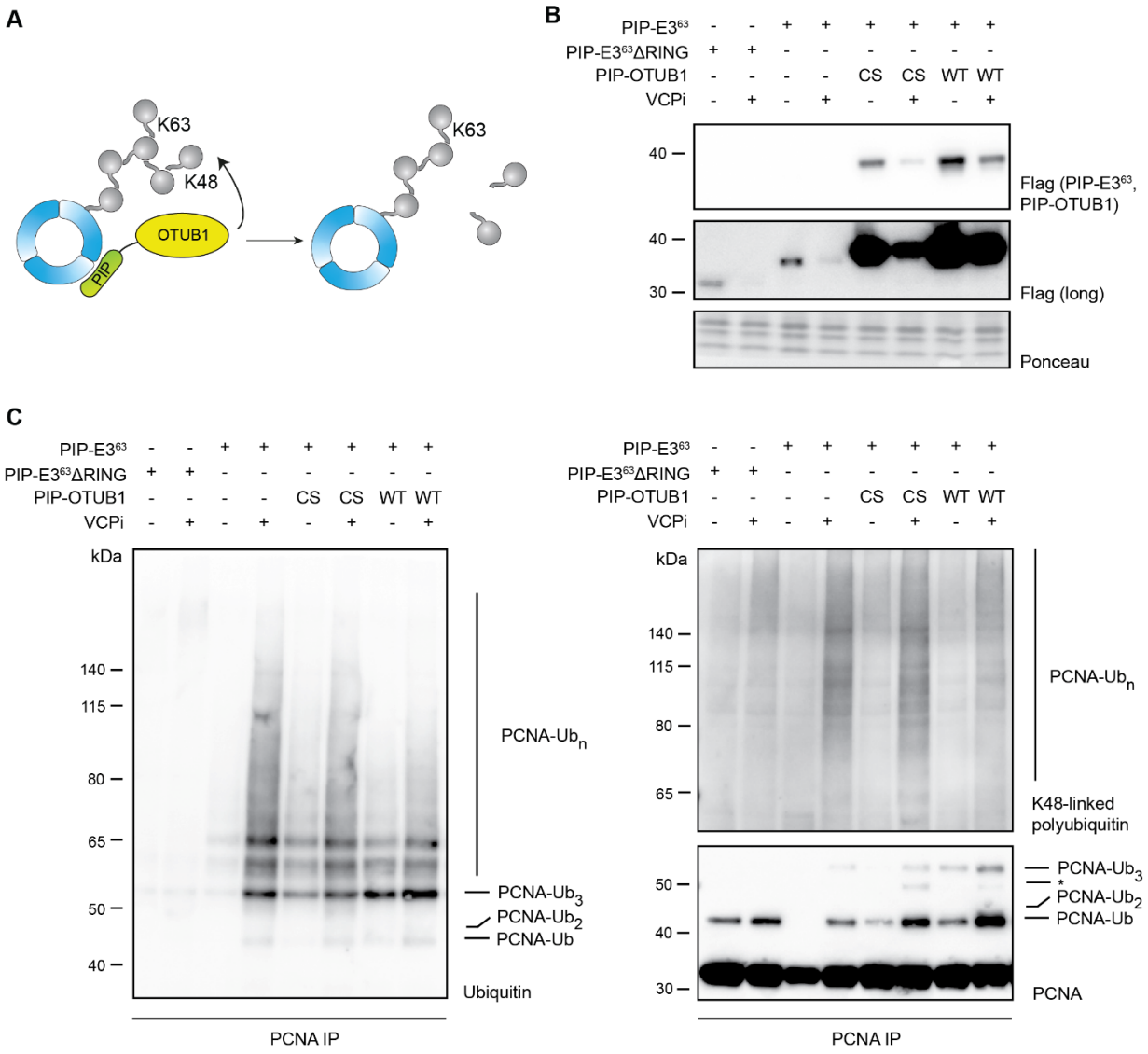

Figure 32: Targeting of OTUB1 to PCNA interferes with chain branching *in vivo*. (A) Scheme of the PIP-OTUB1 construct and its activity towards PCNA modified with branched ubiquitin chains. **(B)** Western blot analysis of whole cell extracts from HEK 293T cells, transfected with the specified constructs and, if indicated, treated with 5 µM VCPi (NMS-873) for 6 h. Ponceau S staining serves as a loading control. **(C)** PCNA polyubiquitylation in HEK 293T cells, transfected and treated as described in (B). Asterisk indicates PCNA modified with a K48-linked di-ubiquitin.

3.5.3.3 K63-linked chains on PCNA are branched via K48 and K11

The UBICREST assay and the *in vivo* targeting of the K48-selective DUB OTUB1 to PCNA reveal that the K63-linked chains built by PIP-E3^{63} or by cellular enzymes upon replication stress are further modified with K48 linkages. At the same time, MS-based interactome analysis suggests that the build-up of not only K48 but also K11-linked chains is induced by PIP-E3^{63} expression upon inhibited VCP activity. Because linkages other than K63, K48 and K11 were not identified in this experiment, they cannot be quantified, yet they may still be involved in the branching of K63-linked chains on PCNA. The involvement of specific ubiquitin lysines in certain cellular pathways can be conveniently analysed by expressing the corresponding ubiquitin mutants. In yeast, ubiquitin replacement strains, in which exogenous ubiquitin mutants are expressed upon the knock-out of endogenous ubiquitin genes, have found widespread use (Meza Gutierrez *et al.,* 2018). Although a similar strategy exists for mammalian cells, it involves transient knock-down of ubiquitin genes (Xu *et al.,* 2009), which is highly labour-consuming and may cause unwanted side effects due to changes in total ubiquitin levels. Another commonly used approach in human cells relies on overexpressing a tagged ubiquitin mutant without depleting its endogenous pool. Subsequent tag-based pulldown allows for the enrichment of proteins that incorporated the overexpressed ubiquitin. To analyse which of the six ubiquitin lysine residues are involved in the branching of the K63-linked chains on PCNA, I created the following panel of His$_{10}$-tagged ubiquitin mutants: K48R, K11R/K48R and K6R/K11R/K27R/K29R/K33R/K48R ("K63-only"-Ubiquitin). In addition, for each ubiquitin variant (including the wild-type), I added the K63R mutation. This modification acts as a negative control as it does not support the assembly of K63-linked chains. The addition of this mutation to the "K63-only"-Ubiquitin results in a "K0-Ubiquitin" that lacks any lysines and can modify proteins only as a single unit. My hypothesis regarding the effects of the ubiquitin mutants on PIP-E3^{63}-induced PCNA polyubiquitylation is graphically represented in **Figure 33A**. In the case of wild-type ubiquitin overexpression, branching of K63-linked chains should occur, leading to the degradation of the polyubiquitylated PCNA forms. On the contrary, the K48R mutation should protect K63-linked chains from branching via K48, stabilising polyubiquitylated PCNA. If additional lysines are involved in chain branching, their mutation may lead to even further stabilisation of polyubiquitylated PCNA. Adding a

K63R mutation should inhibit PCNA polyubiquitylation by PIP-E3^{63} in all cases. **Figure 33B** shows the ubiquitylated PCNA forms that were enriched with the Ni-NTA pulldown and therefore were ubiquitylated with His-tagged ubiquitin. Without PIP-E3^{63}, only a single prominent band is present, corresponding to monoubiquitylated PCNA. Interestingly, upon expression of PIP-E3^{63}, I do not observe ubiquitin chains but rather the disappearance of monoubiquitylated PCNA. The same effect was observed for PIP-E3^{48} (**Figure 13**). These observations indicate that, upon overexpression of ubiquitin, the pathway is accelerated, and equilibrium is shifted towards PCNA degradation. As expected, accumulation of chains takes place when the K48R ubiquitin mutant is used. Strikingly, even further stabilisation is observed upon overexpression of the double K11R/K48R mutant, whereas mutation of all lysines except K63 (K63-only form) does not further increase the amount of detected polyubiquitylated PCNA. As expected, the K0-Ubiquitin mutant abolishes chain formation for all chain types, therefore confirming that the observed polyubiquitylated PCNA forms contain K63 linkages. This clearly pinpoints K48 and K11 as the two substrate lysines for branching of a K63-linked polyubiquitin chain on PCNA.

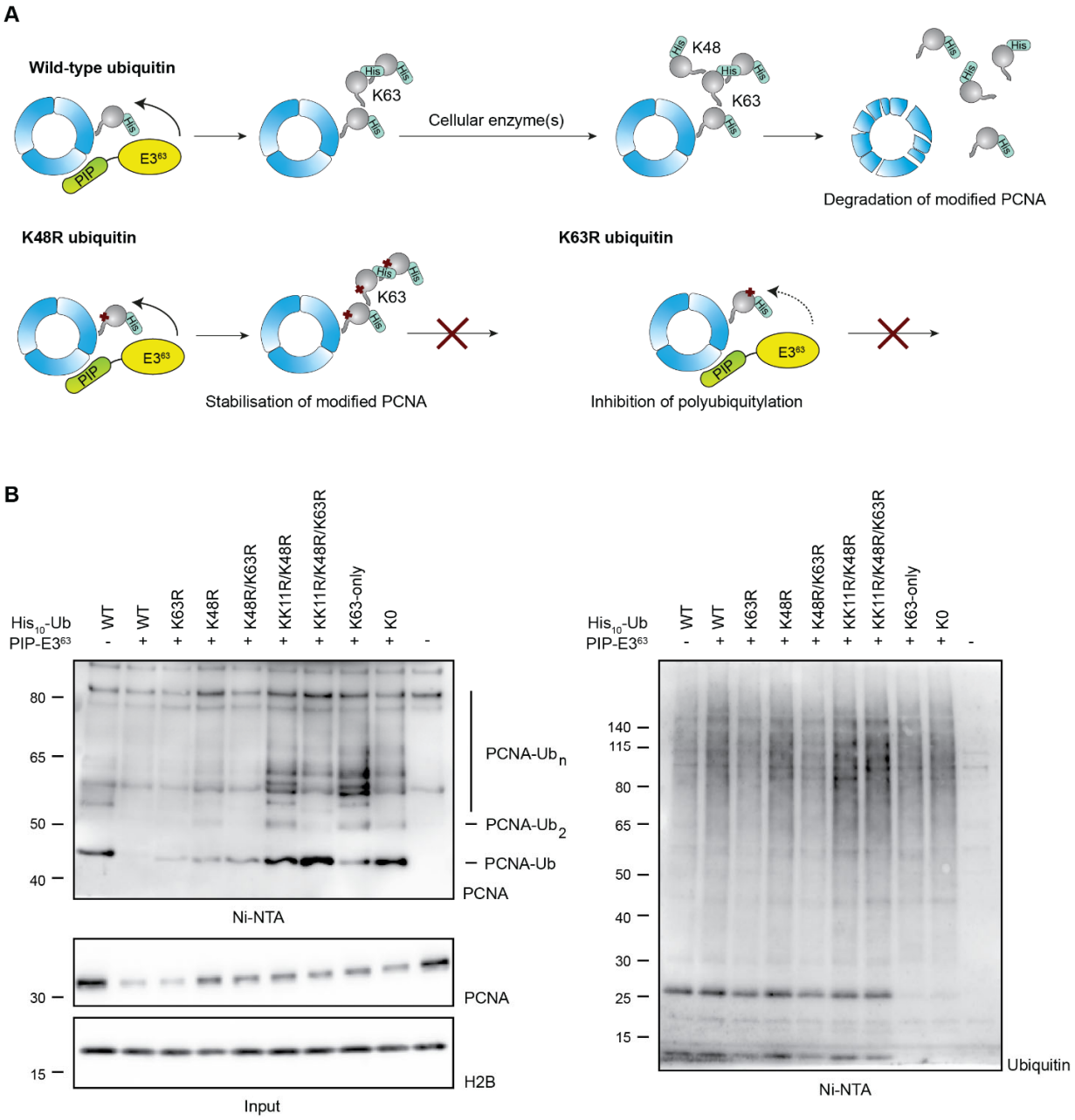

Figure 33: K63-linked chains on PCNA are branched via K48 and K11. (A) Schematic representation of the chain architecture analysis by overexpression of ubiquitin mutants. **(B)** Indicated ubiquitin mutants were expressed in HEK 293T cells together with PIP-E3^{63}, followed by Ni-NTA pulldown and analysis of PCNA ubiquitylation by western blotting.

3.5.4 UBE2K is involved in the build-up of branched chains on PCNA

One of the important characteristics of PIP-E3^{63} is its exclusive linkage selectivity, as proven *in vitro* and *in vivo* in *S. cerevisiae* (Wegmann *et al.,* 2022). Therefore, it is reasonable to envision that certain cellular enzymes use K63-linked chains on PCNA as a substrate and extend them via lysines K48 and K11, into branched conjugates. This would also explain the appearance of branched chains on PCNA upon replication stress in the absence of PIP-E3^{63}, when K63-linked polyubiquitylation is carried out by cellular enzymes. Several enzymes have been reported to exhibit chain branching activity towards K63-linked ubiquitin chains. The first is the ubiquitin-conjugating (E2) enzyme UBE2K and its yeast homologue UBC1. In addition to a UBC domain, characteristic of all E2 enzymes (Stewart *et al.,* 2016), it possesses a highly K63 linkage-selective UBA domain (**Figure 34A**). This specificity is demonstrated by the ability of this UBA domain to discriminate between K63-linked and conformationally similar M1-linked ubiquitin chains (Pluska *et al.,* 2021). Upon binding to a K63-linked ubiquitin dimer, UBE2K ubiquitylates K48 of the proximal ubiquitin. Importantly, UBE2K is much more processive in creating a single K48 linkage on a K63-linked dimer than in synthesising long K48-linked chains. The second ligase with chain branching activity is the HECT-type E3 HUWE1, which was also identified as a binder of polyubiquitylated PCNA in our mass-spectrometry-based interactome analysis. HUWE1 turns homotypic K63-linked chains on TRAF6 into branched structures and, in cooperation with UBR4 and UBR5, branches K63-linked chains on TXNIP (Ohtake *et al.,* 2016; Ohtake *et al.,* 2018). In order to understand whether UBE2K and HUWE1 are involved in chain branching in the PIP-E3^{63} system, these enzymes were depleted in RPE1 hTERT PIP-E3^{63} cells. As shown in **Figure 34B**, depletion of UBE2K almost completely abolishes checkpoint activation after the expression of PIP-E3^{63}. Depletion of HUWE1 leads to a moderate decrease in checkpoint activation, and co-depletion of both enzymes behaves like depletion of UBE2K alone. Importantly, the knockdown of UBE2K does not affect the expression levels of PIP-E3^{63}, which means that the deleterious effects of excessive PCNA polyubiquitylation depend on the enzymatic activity of UBE2K.

Next, I analysed whether UBE2K can branch ubiquitin chains on PCNA *in vitro* (these reactions were performed by Nils Krapoth, Ulrich Laboratory). As demonstrated in

Figure 34C, when unmodified PCNA or PCNA monoubiquitylated on K164 were used as substrates, UBE2K does not display any significant activity. However, when K63-linked polyubiquitylated PCNA is used as a substrate, the addition of UBE2K drastically changes the chain pattern. Anti-ubiquitin and anti-K63-polyubiquitin signals shift to the high molecular weight range, and the anti-K48 signal appears only when PCNA is pre-polyubiquitylated with K63 linkages and UBE2K is added to the reaction. At the same time, there is a reduction in shorter ubiquitylated PCNA forms, thus suggesting that they are converted into heavier conjugates due to UBE2K activity. This experiment confirms the specificity of UBE2K towards K63-linked chains in comparison to monoubiquitin and non-ubiquitylated substrates.

To prove that UBE2K also affects PCNA polyubiquitylation *in vivo* in the PIP-E3^{63} system, the tailor-made ligase was expressed in RPE1 hTERT cells transfected with an siRNA against UBE2K or a corresponding control siRNA, and VCP was inhibited to further accumulate chains on chromatin-bound PCNA. As expected, the knockdown of UBE2K leads to a decrease in both anti-ubiquitin and anti-K48-linked polyubiquitin signal after PCNA immunoprecipitation, whereas the levels of PCNA monoubiquitylation in whole cell extracts appear to slightly increase upon loss of UBE2K (**Figure 35**). This indicates that the above-described drop in PCNA polyubiquitylation is not the result of lower levels of monoubiquitylated PCNA but rather confirms the chain branching activity of UBE2K. The UBICREST assay also confirms this hypothesis: when UBE2K is depleted, less di- and tri-ubiquitin forms are released into the soluble fraction after AMSH-mediated cleavage of polyubiquitylated PCNA without significantly affecting the amount of cleaved monoubiquitin (**Figure 36A**). Overall, these observations show that UBE2K is involved in the formation of short K48 linkages on top of PCNA-conjugated K63-linked chains. Yet, it is also clear that a significant amount of chain branching in the PIP-E3^{63} system takes place even in the absence of UBE2K, thus suggesting that ubiquitin ligases may be involved in this pathway.

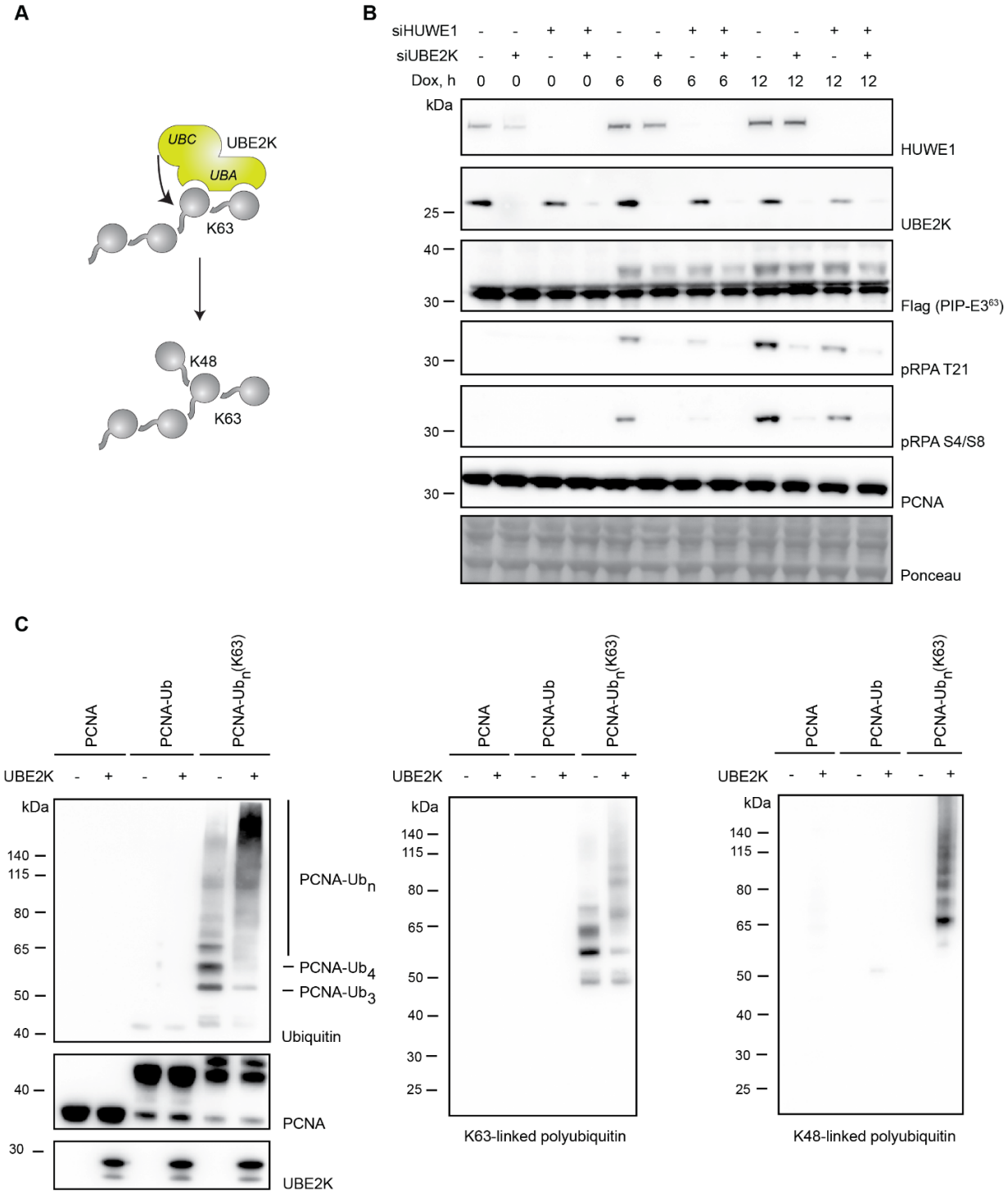

Figure 34: UBE2K forms K63-K48 branched ubiquitin chains in the PIP-E3^{63} system. (A) Schematic representation of the UBE2K domain structure and catalytic activity. **(B)** Checkpoint activation in RPE1 hTERT PIP-E3^{63} cells after depletion of HUWE1 and UBE2K and doxycycline-induced expression of the ligase for the indicated times. **(C)** *In vitro* ubiquitylation assay with UBE2K as a ligase and PCNA, PCNA-Ub and PCNA-Ub$_n$(K63) as substrates.

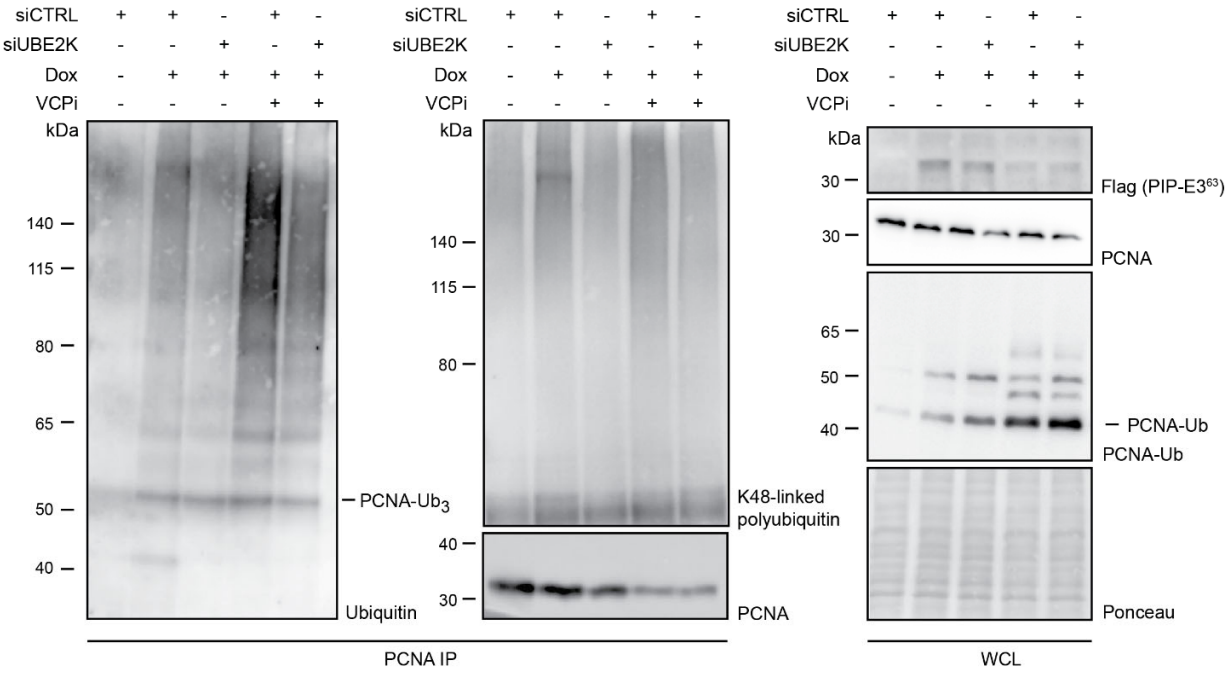

Figure 35: Effects of UBE2K on PCNA polyubiquitylation *in vivo*. RPE1 hTERT PIP-E3^{63} cells were depleted of UBE2K and treated with 1 µg/ml doxycycline and 5 µM NMS-873 (VCPi) for 6 h. PCNA ubiquitylation was analysed after PCNA immunoprecipitation from the chromatin fraction or in total cell extracts. Ponceau S staining serves as a loading control.

Finally, I analysed the impact of UBE2K on PCNA polyubiquitylation upon replication stress. I compared different replication stress-inducing agents: HU (2 h and 4 h), MMS and UV. As shown in **Figure 36B**, MMS and UV induce stronger PCNA mono- and polyubiquitylation than HU, and depletion of UBE2K leads to a reduction in some polyubiquitylated forms of PCNA. Although the UBICREST assay is needed to strictly prove that these forms represent branched chains on PCNA, the first evidence suggests that UBE2K is active on K63-linked chains on PCNA independently of the enzyme(s) that create them. Interestingly, checkpoint signalling is unaffected by UBE2K depletion. In the case of MMS and UV, it is likely that a significant portion of the checkpoint signalling originates from the nucleotide excision repair and gap resection outside of the S phase (Balogun *et al.,* 2013), and for all tested damaging agents, PCNA polyubiquitylation seems to play a minor role in checkpoint activation in wild-type RPE1 cells.

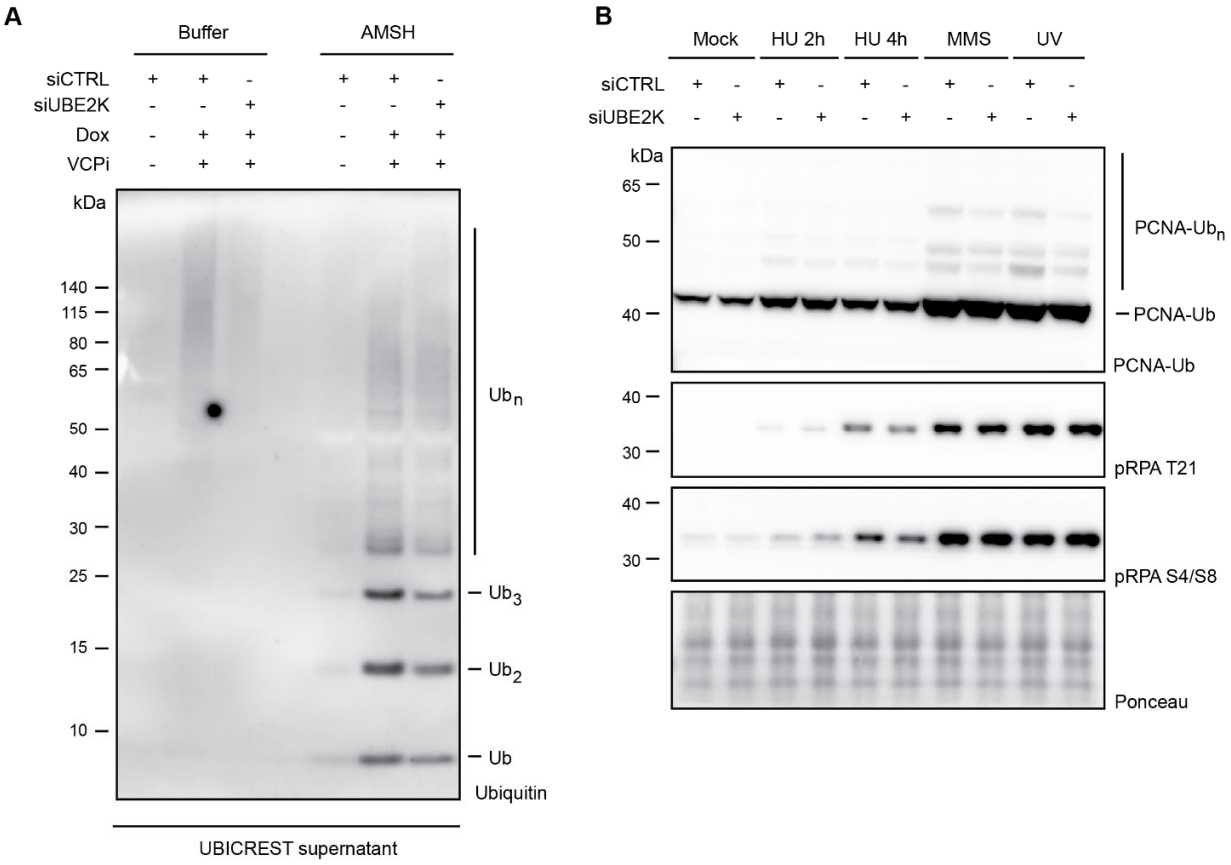

Figure 36: UBE2K affects PCNA polyubiquitylation both in the PIP-E3^{63} system and during endogenous damage response. (A) The UBICREST assay was performed on PCNA, immunoprecipitated from RPE1 hTERT PIP-E3^{63} cells treated with 1 µg/ml doxycycline and 5 µM NMS-873 (VCPi). Soluble ubiquitin forms were visualised by western blotting with the VU1 ubiquitin antibody. **(B)** RPE1 hTERT cells were mock-treated, treated with 4 mM HU for 2 h or 4h, with 0.01% MMS for 4h or with 40J/m^2 UV followed by a 4h recovery in complete growth medium. PCNA ubiquitylation and checkpoint signalling were analysed in total cell extracts by western blotting with the indicated antibodies. Ponceau S staining serves as a loading control.

3.6 Analysing the significance of polyubiquitin linkage type on PCNA in triggering replication collapse

K63- and K48-linked polyubiquitin chains are the most studied polyubiquitin conjugates. The difference between these chain types is unambiguously demonstrated by their different effects on DNA damage bypass in *S. cerevisiae* (Wegmann *et al.,* 2022). In the human PIP-E3^{63} system, I observe the downstream modification of the K63-linked chain

on PCNA with K48 linkages, leading to VCP recruitment and extraction of the polyubiquitylated PCNA from chromatin. Therefore, unlike the situation in budding yeast, in human cells one would expect that modifying PCNA with a K48-linked chain should lead to a similar, rather than opposite, phenotype, as both VCP and the proteasome have a high affinity towards K48-linked chains. I decided to test whether polyubiquitylation of PCNA with K48-linked chains leads to checkpoint activation in a manner similar to K63-linked chains and, if so, which chain type is more efficient in recruiting VCP and promoting replication catastrophe.

3.6.1 Establishment of a cell line with inducible K48-linked polyubiquitylation of PCNA

Our initial optimisation of PIP-E3^{48} in HEK 293T cells showed that maximal activity towards PCNA requires co-overexpression of the yeast E2 Ubc7, optimised in terms of codon usage for *H. sapiens*. PIP-E3^{48} construct contains a VSV and a Flag tag at its N-terminus, and Ubc7 is additionally N-terminally tagged with a triple Flag sequence. For the sake of simplicity, in the following sections, I will omit the tags from the construct names. In order to create a cell line that expresses both PIP-E3^{48} and Ubc7, I created a single fusion protein containing both enzymes separated by a self-cleavable P2A peptide. The latter consists of 22 amino acids and is co-translationally cleaved between the C-terminal glycine and proline (Ryan *et al.,* 1991). Upon expression and self-cleavage of a fusion protein, the first enzyme (PIP-E3^{48}) receives 21 additional amino acids on its C-terminus, and the second protein (Ubc7) starts with a proline just upstream of its genuine initiator methionine (**Figure 37A**). The fusion construct, hereafter called PIP-E3^{48}-P2A-Ubc7, was integrated into RPE1 hTERT FlpIn cells in a manner analogous to the RPE1 hTERT PIP-E3^{63} cell line. A cell line that carries PIP-E3^{48} without the P2A-Ubc7 extension was used as a control. **Figure 37B** shows the expression of the enzymes in the described cell lines after the addition of doxycycline and VCP inhibition. As expected, only PIP-E3^{48} is expressed in the RPE1 hTERT PIP-E3^{48} cell line. An additional species can be observed in the RPE1 hTERT PIP-E3^{48}-P2A-Ubc7 cell line, corresponding to P2A-cleaved Ubc7. Notably, the apparent molecular weight of PIP-E3^{48}, originating from the fusion construct,

is slightly higher than that of the enzyme expressed in RPE1 hTERT PIP-E3^{48} cells, reflecting the presence of the post-cleavage peptide remnant of P2A at the C-terminus of the ligase. Consistently with results obtained in HEK 293T cells upon transient overexpression of the enzymes, efficient polyubiquitylation of PCNA requires co-overexpression of Ubc7 together with PIP-E3^{48} (**Figure 37C**). Interestingly, even upon co-expression of Ubc7 and PIP-E3^{48}, the levels of polyubiquitylated PCNA are quite low if VCP is not inhibited. This indicates that even single K48 linkages on PCNA, along with longer chains, trigger efficient VCP-mediated removal from chromatin.

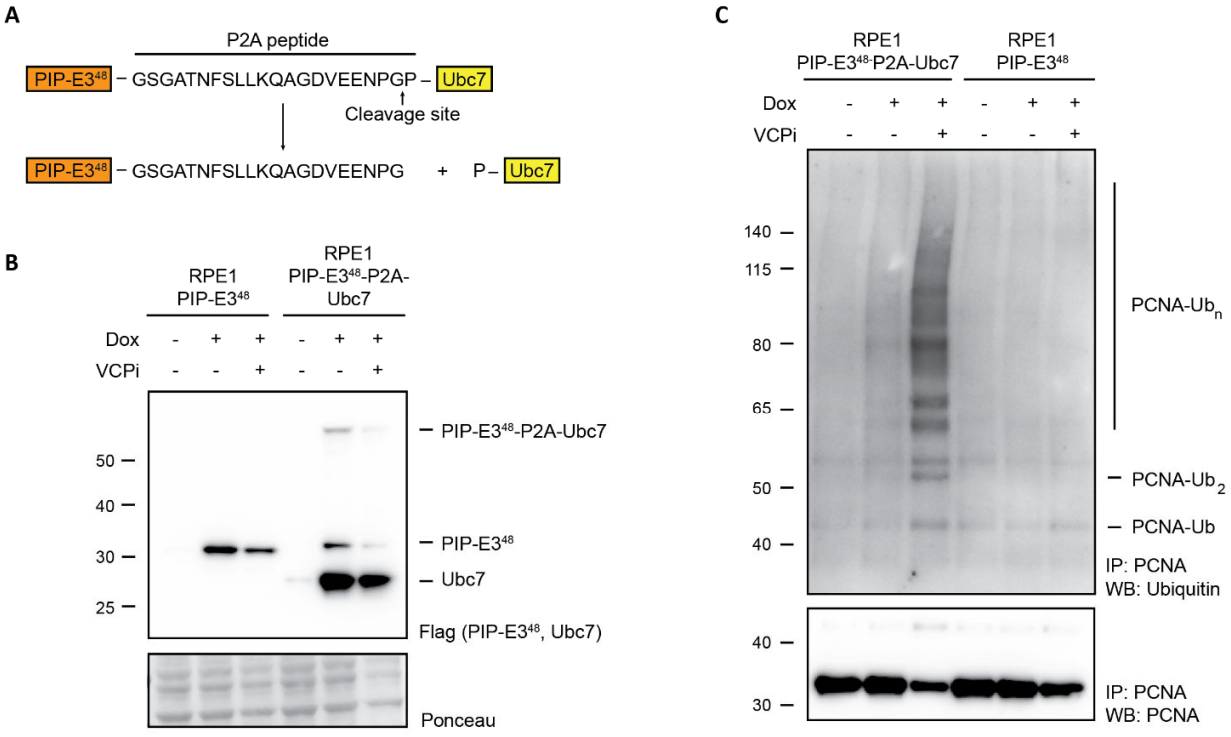

Figure 37: Design and creation of a cell line with inducible K48-linked polyubiquitylation of PCNA. (A) Schematic representation of a self-cleavable fusion of PIP-E3^{48} to Ubc7 via a P2A peptide. The full amino acid P2A sequence as well as the cleavage site are shown. **(B)** Cell lines with doxycycline-inducible expression of PIP-E3^{48} or its self-cleavable fusion with Ubc7 were treated for 6 h with 1 µg/ml doxycycline or 5 µM VCPi (NMS-873). Enzyme levels were analysed by western blotting of cell lysates against the Flag tag. Ponceau S staining serves as a loading control. **(C)** Indicated cell lines were treated as in (B), followed by PCNA immunoprecipitation from the chromatin fraction and western blotting with the indicated antibodies. Note that the order of samples is opposite of those in (B).

A certain proportion of the PIP-E3^{48}-P2A-Ubc7 construct in RPE1 hTERT cells remains uncleaved and appears as a ~50 kDa product (**Figure 37B**). Since this permanent fusion could be more active than co-expressed but separate E3 and E2 enzymes, I investigated whether rendering the P2A peptide uncleavable could further boost the activity of the system. Provided that the four last amino acids of the P2A peptide are critical for the self-cleavage (Hahn and Palmenberg 1996), I created a mutant version with the C-terminal NPGP sequence mutated to KLAS sequence (hereafter referred to as P2A*, **Figure 38A**). As expected, the mutant version appears in a western blot as a ~ 50 kDa protein with no detectable free PIP-E3^{48} or Ubc7 (**Figure 38B)**. Interestingly, permanent fusion of Ubc7 to PIP-E3^{48} via P2A* leads to a similar level of PCNA polyubiquitylation as making the E3 and E2 enzymes from the self-cleavable precursor. Consistently with the experiments described above, K48-linked ubiquitin chains produced by the uncleavable mutant on chromatin-bound PCNA can be detected only upon VCP inhibition (**Figure 38C**).

On the one hand, these results could indicate that head-to-tail fusion of the E2 to E3 results in their optimal orientation for the ubiquitin transfer. On the other hand, the amount of polyubiquitin chains on PCNA depends on the level of PCNA monoubiquitylation, which may become a limiting factor for the reaction. Therefore, for the PCNA system, I did not pursue using the permanent fusion of PIP-E3^{48} to Ubc7 because it does not display any additional activity beyond that provided by the self-cleavable fusion. However, for the future development of tailor-made enzymes, for example, for the 'Ubiquiton' technology (**section 3.8**), these constructs may be of practical use.

3.6.2 Direct comparison of K63- versus K48-linked PCNA polyubiquitylation

The data described above suggest that K63- and K48-linked PCNA polyubiquitylation may similarly affect cell replication, as they both are substrates for VCP activity. In order to directly compare these chain types on PCNA, they were induced in RPE1 hTERT cells by expressing PIP-E3^{63} or PIP-E3^{48}-P2A-Ubc7 (**Figure 39**). I observed that K63- and K48-linked ubiquitin chains on PCNA behave differently with respect to VCP inhibition. For K63-linked chains, VCP does not extract oligo-ubiquitylated (containing 2-4 ubiquitin units) PCNA from chromatin but is rather active towards heavily

polyubiquitylated forms, likely consisting of branched ubiquitin conjugates. This is different for K48-linked chains, where all ubiquitin conjugates on PCNA, including a single K48 linkage, are substrates of VCP. Yet, K63-linked polyubiquitylation of PCNA leads to a much stronger checkpoint activation than K48-linked one, as demonstrated by higher levels of RPA phosphorylation 6 h after the expression of the corresponding E3 enzymes for the former. Remarkably, for both chain types, checkpoint activation is dependent on VCP activity. Altogether, these data indicate that although both chain types lead to the activation of checkpoint signalling, probably due to the removal of PCNA from chromatin, K63-linked chains are significantly more active in triggering this pathway.

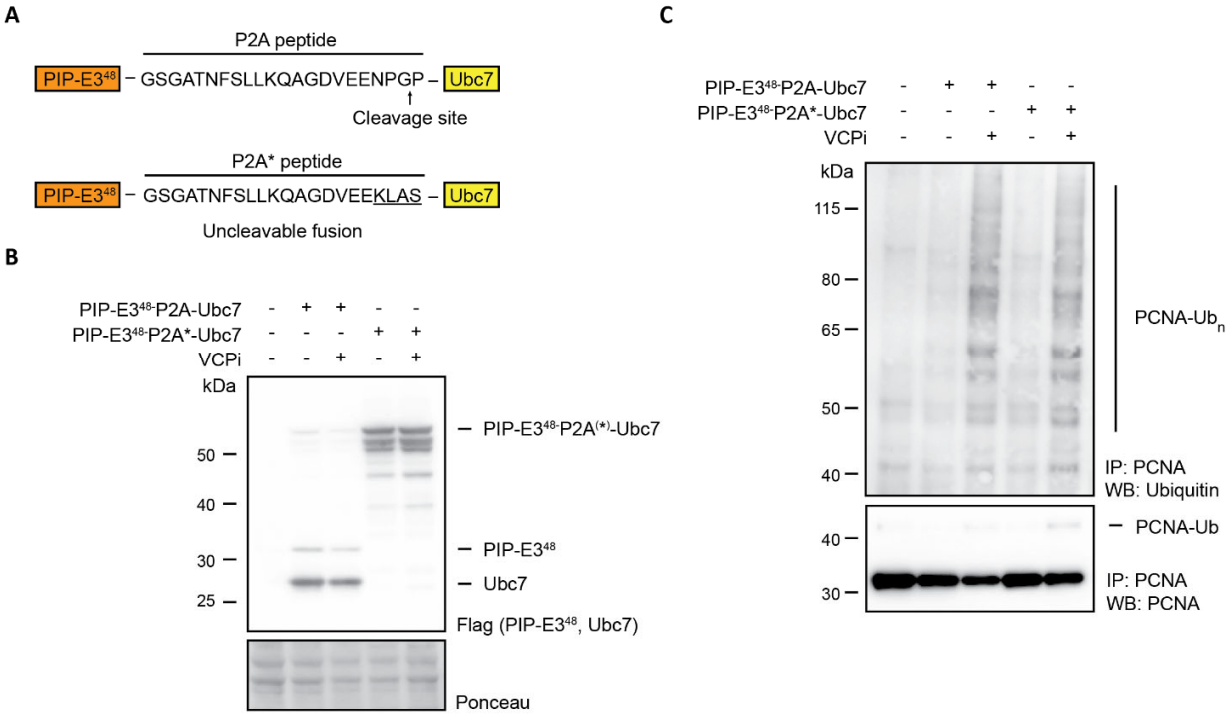

Figure 38: Self-cleavable and uncleavable fusions of PIP-E3^{48} to Ubc7 display similar activity towards PCNA *in vivo*. (A) Schematic representation of the self-cleavable construct PIP-E3^{48}-P2A-Ubc7 in comparison to its uncleavable version PIP-E3^{48}-P2A*-Ubc7. **(B)** HEK 293T cells were transfected with the indicated constructs and harvested after 24 h. If stated, VCPi (NMS-873) was added to growth medium to a final concentration of 5 µM 6 h prior to cell harvesting. Cell lysates were analysed by western blotting against the Flag tag. Ponceau S staining serves as a loading control. **(C)** HEK 293T cells were treated as described in (B), followed by PCNA immunoprecipitation from the chromatin fraction and western blotting with the indicated antibodies.

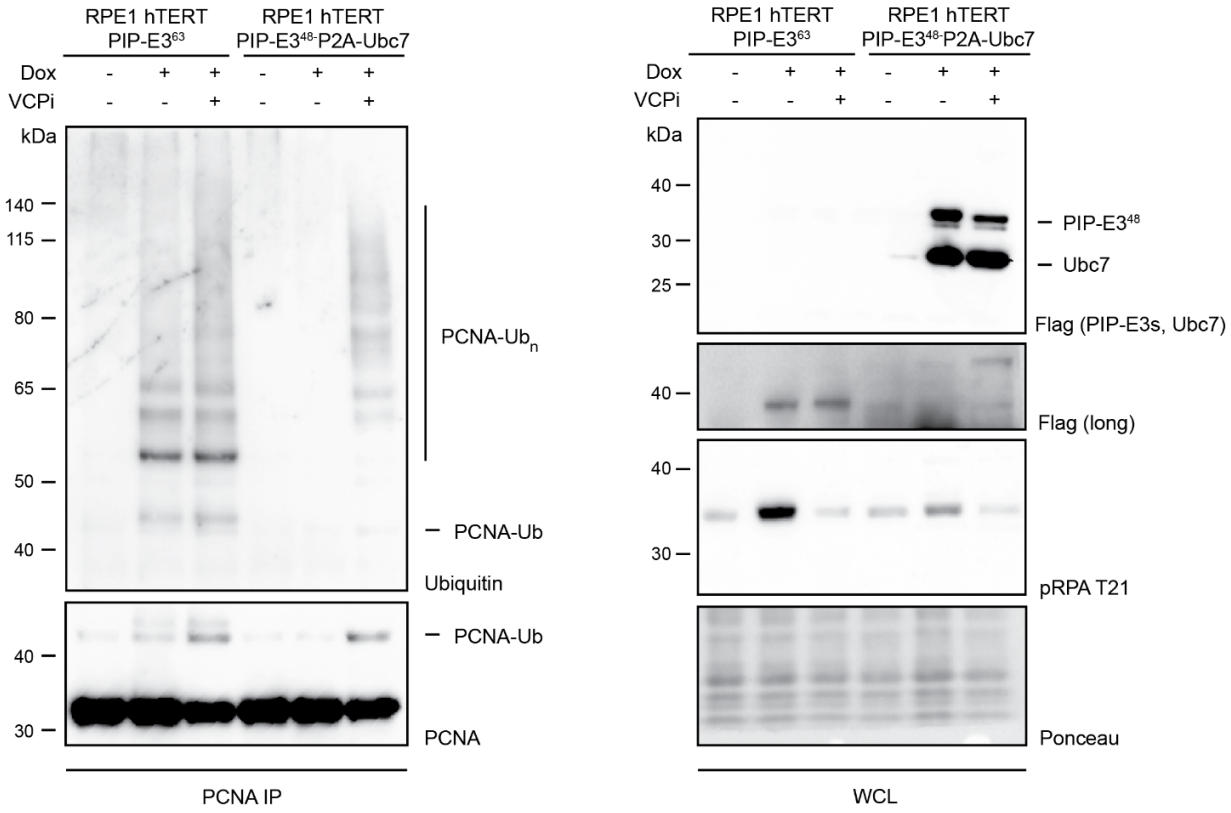

Figure 39: Comparison of K63- and K48-linked PCNA polyubiquitylation. RPE1 hTERT PIP-E3^{63} or PIP-E3^{48}-P2A-Ubc7 cells were treated with 1 µg/ml doxycycline or 5 µM VCPi (NMS-873) for 6 h, followed by chromatin fractionation and PCNA immunoprecipitation (left) or lysis and western blotting analysis with the indicated antibodies. Ponceau S staining serves as a loading control.

One possible explanation for why K63-linked chains trigger stringer checkpoint activation could be that branched ubiquitin chains, originating from K63 ones, are a better substrate for VCP than homotypic K48-linked chains. Despite the fact that it has not directly been investigated for K63 chains, this effect has been demonstrated for K48 and K11 linkages: branched conjugates have higher affinity to VCP (and its adaptors) than homotypic chains (Yau *et al.,* 2017). I previously demonstrated that UBE2K is at least partially responsible for the branching of K63-linked chains in the PIP-E3^{63} system. If our mechanistic understanding of the pathway is correct, UBE2K depletion should not affect checkpoint activation in the PIP-E3^{48} system because UBE2K cannot branch K48-linked chains. As demonstrated in **Figure 40**, this is indeed the case. While checkpoint activation by PIP-E3^{63} largely depends on UBE2K, PIP-E3^{48}-induced checkpoint activation is significantly less intense and does not depend on the levels of UBE2K. Interestingly, if

DNA damage is directly induced by MMS, I do not observe a significant dependency of checkpoint activation on UBE2K. This indicates that in the presence of exogenous DNA damage, most checkpoint signalling originates from sources other than polyubiquitylated PCNA.

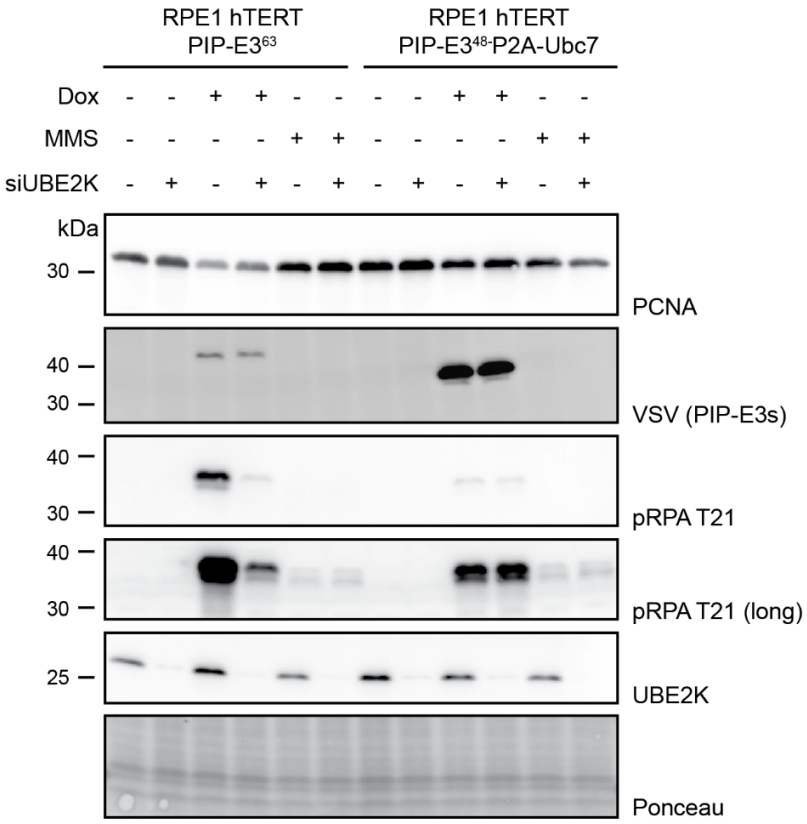

Figure 40: UBE2K mediates checkpoint activation after K63-, but not K48-linked PCNA polyubiquitylation. RPE1 hTERT cells inducibly expressing PIP-E3^{63} or PIP-E3^{48}-P2A-Ubc7 were transfected with an siRNA against UBE2K or a non-targeting siRNA for 72 h and treated, if indicated, with 1 µg/ml doxycycline for 24 h. 90 min treatment with 0.01% MMS was used as a positive control for checkpoint activation. The levels of the E3s, UBE2K and phosphorylated RPA were analysed in total cell extracts by western blotting. Ponceau S staining serves as a loading control.

3.7 Analysing the physiological relevance of ubiquitin chain branching on PCNA

3.7.1 Introduction to the synthetic lethal relationship between BRCA1 and USP1

In human cells, the endogenous levels of PCNA monoubiquitylation are sufficient to support PIP-E3^{63} activity. Due to the elongation specificity of the tailor-made E3s, the amount of polyubiquitylated PCNA must be governed by the availability of the monoubiquitylated form. The ubiquitin ligases HLTF and SHPRH display activities similar to PIP-E3^{63}: they directly interact with PCNA and can extend a monoubiquitin moiety into a K63-linked chain (Seelinger and Otterlei, 2020; Motegi *et al.,* 2008; Unk *et al.,* 2006). Nevertheless, contrary to the endogenously expressed HLTF and SHPRH, PIP-E3^{63} expression can lead to a replication catastrophe. Therefore, I hypothesised that certain mechanisms may counteract the activity of HLTF and SHPRH but not PIP-E3^{63}. One of these mechanisms could rely on recruiting the DUB USP1, which deubiquitylates monoubiquitylated PCNA and FANCD2 (Huang *et al.,* 2006; Nijman *et al.,* 2005). The tonicity-responsive enhancer-binding protein TonEBP has been shown to recruit both SHPRH and USP1 to the sites of DNA damage, preventing persistent PCNA polyubiquitylation (Kang *et al.,* 2019). Therefore, I investigated whether inhibition of USP1 activity can, in certain cellular backgrounds, phenocopy the expression of PIP-E3^{63}. Recently, USP1 and BRCA1 were shown to be in a synthetic lethal relationship: inhibition or depletion of USP1 in BRCA1-deficient cells results in cell death concomitantly with a drastic decrease in total PCNA levels. This synthetic lethality depends on RAD18 and UBE2K, suggesting that PCNA, rather than FANCD2 ubiquitylation underlies the observed phenotypes (Simoneau *et al.,* 2023). The reported effects of USP1 inhibition in BRCA1-deficient cells resemble the phenotypes of PIP-E3^{63} expression, including impaired cell growth, accumulation of cells in the S phase and a lower replication speed. Dependency of these phenotypes on UBE2K makes it tempting to imply that chain branching could be the underlying pathway. Additionally, inhibition of USP1 in a BRCA1-deficient background leads to deprotection of replication forks, as observed by the degradation of nascent DNA after blocking replication with hydroxyurea. Although fork deprotection has been demonstrated to depend on RAD18 activity, other details of the pathway remain unknown

(Lim *et al.,* 2018). In the following sections, I will investigate whether the replication problems in BRCA1-deficient cells where USP1 is also inhibited have the same origin as those in PIP-E3^{63}-expressing cells.

3.7.2 VCP mediates PCNA degradation upon inhibition of USP1 in BRCA1-deficient cells

As a model cell line lacking functional BRCA1, I used breast cancer MDA-MB-436 cells (kind gift from Petra Beli Laboratory, IMB). These cells contain a mutation in exon 20 of BRCA1, resulting in a truncated protein (Elstrodt *et al.,* 2006). If inhibition of USP1 in the background of BRCA1 deficiency is indeed functionally similar to overexpression of PIP-E3^{63} in wild-type cells, VCP inhibition should reverse these effects because polyubiquitylated PCNA cannot be removed from chromatin and subsequently degraded. Since inducing significant PCNA degradation requires 24 h of USP1 inhibition (Simoneau *et al.,* 2023), and inhibition of VCP for too long is cytotoxic, in order to further boost PCNA monoubiquitylation and therefore accelerate the pathway, I treated the cells with a high dose of hydroxyurea (HU). Indeed, although 4 h treatment with hydroxyurea alone does not lead to a significant loss of PCNA in total cell extracts, the addition of the USP1 inhibitor ML-323 (hereafter USP1i) induces PCNA degradation (**Figure 41**). The observed degradation is VCP-dependent, as it can be reversed upon co-treatment with the VCP inhibitor. A long exposure of the western blot for PCNA reveals the presence of short degradation products when hydroxyurea is used together with the USP1 inhibitor, likely originating from incomplete proteasomal degradation of PCNA. Given that inhibition of VCP not only stabilises PCNA but also prevents the formation of partially degraded PCNA forms, this means that, as for the artificially modified PCNA in the PIP-E3^{63} system, extraction of natively polyubiquitylated PCNA from chromatin by VCP is a prerequisite for its proteasomal degradation. Notably, checkpoint activation, as represented by levels of RPA phosphorylation, correlates with PCNA levels, pinpointing the role of PCNA in checkpoint activation in this system. Time course analysis reveals consistent PCNA degradation 0-6 h after the addition of both HU and USP1 inhibitor in both total cell extracts

(**Figure 41B**) and the chromatin fraction (**Figure 41C**), which can be rescued by VCP inhibition.

The behaviour of monoubiquitylated PCNA in this experiment is surprising: although co-treatment with VCPi, HU and USP1i massively stabilises total PCNA levels, the levels of the monoubiquitylated form remain relatively unchanged. This could be explained if constant recycling of PCNA takes place at the HU-induced replication intermediates. Once polyubiquitylated, PCNA is removed from chromatin and degraded by the proteasome. If new PCNA trimers replace the removed ones, they should undergo the same process as forks remain in a compromised state. In this scenario, the total amount of PCNA should drop due to continuous proteasomal degradation, but the levels its monoubiquitylated form should be determined by the number of stressed forks or other replication intermediates and therefore remain similar in a given timescale.

.

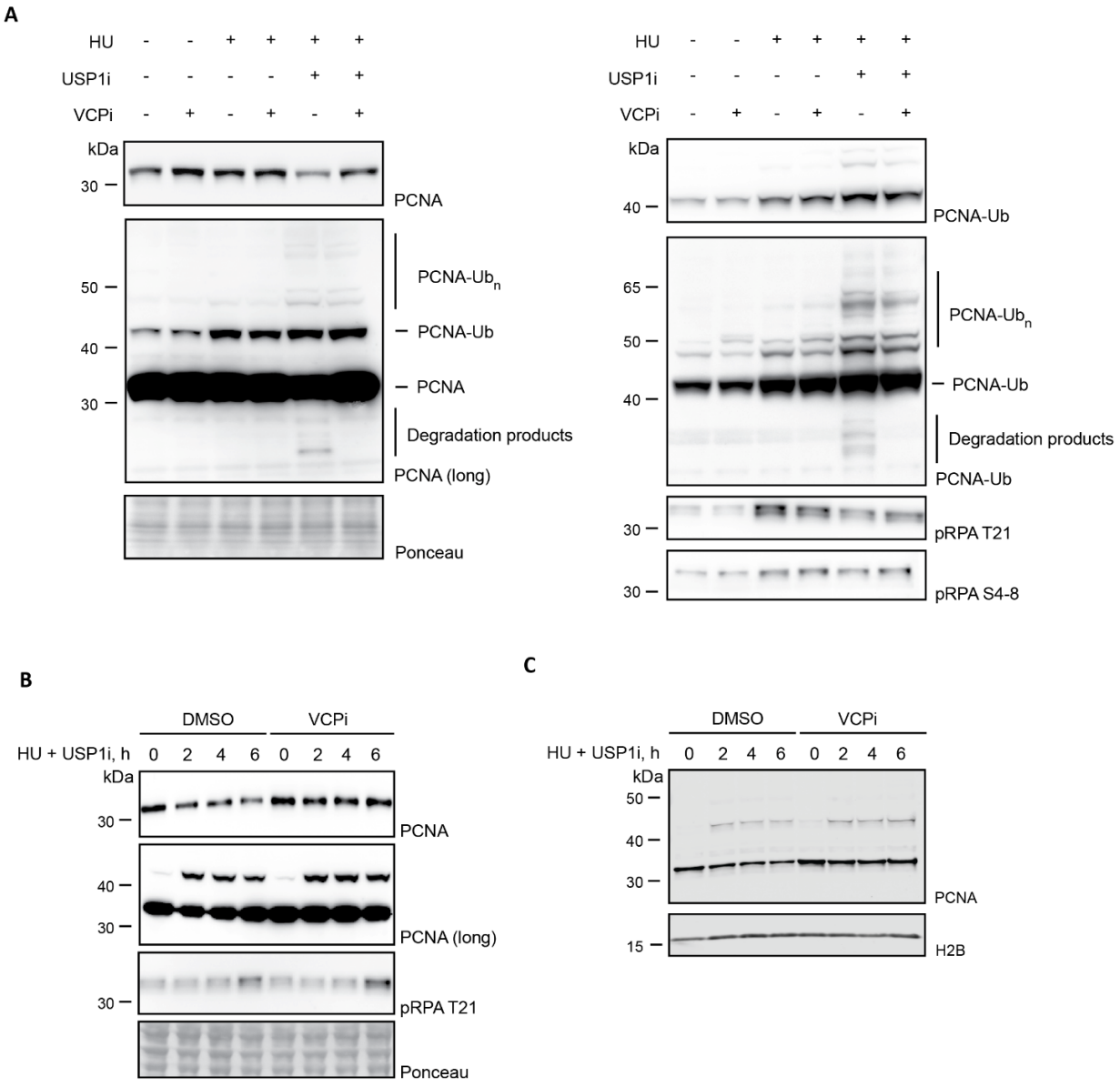

Figure 41: HU- and USP1i-dependent PCNA degradation in BRCA1-deficient cells. (A) MDA-MB-436 cells were treated with 4 mM HU, 30 µM ML323 (USP1i) or 5 µM NMS-873 (VCPi) for 4 h, followed by western blotting with the indicated antibodies. Ponceau S serves as a loading control. **(B)** MDA-MB-436 cells were treated with 4 mM HU, 30 µM ML323 (USP1i) or 5 µM NMS-873 (VCPi) for the indicated time periods followed by western blotting with the indicated antibodies. **(C)** MDA-MB-436 cells were treated as in (B) followed by isolation of the chromatin fraction and western blotting with the indicated antibodies.

3.7.3 Ubiquitin chain branching underlies the synthetic lethality between BRCA1 and USP1

The synthetic lethality between BRCA1 and USP1 was shown to originate from a massive loss of PCNA and to be dependent on RAD18 and UBE2K (Simoneau *et al.,* 2023). According to the *in vitro* data and the PIP-E3^{63} system, UBE2K is unlikely to act on monoubiquitylated PCNA but rather on polyubiquitylated one. As the ubiquitin ligase RFWD3 promotes PCNA polyubiquitylation without significantly affecting monoubiquitylated PCNA levels (Moore *et al.,* 2023), I tested whether depletion of RFWD3 would prevent USP1i toxicity in BRCA1-deficient cells. As shown in **Figure 42A**, the USP1 inhibitor ML-323 affects MDA-MB-436 cell viability in a dose-dependent manner. Importantly, depletion of RAD18, UBE2K or RFWD3 completely prevents ML-323 toxicity. Furthermore, treatment of MDA-MB-436 cells with increasing ML-323 concentrations for 72 h results in bulk PCNA degradation, which is prevented if RAD18, UBE2K or (partially) RFWD3 are depleted (**Figure 42B**). Knocking down RAD18 prevents the ML-323-induced increase in PCNA monoubiquitylation, which is consistent with the role of RAD18 in monoubiquitylating PCNA. Depleting UBE2K does not prevent PCNA monoubiquitylation but still reverts PCNA degradation. This is consistent with our model, where I propose that UBE2K acts on polyubiquitylated PCNA without affecting its monoubiquitylation. Furthermore, I observe RAD18-, UBE2K- and RFWD3-dependent activation of checkpoint signalling, as demonstrated by an increase in phospho-RPA T21 levels, concomitantly with PCNA degradation. Thus, inhibiting USP1 in a BRCA1-deficient background affects cells in the same way as expressing PIP-E3^{63} in wild-type cells. Thus, I propose that chain branching on PCNA is the pathway that mediates the degradation of this protein in MDA-MB-436 cells and underlies BRCA1-USP1 synthetic lethality.

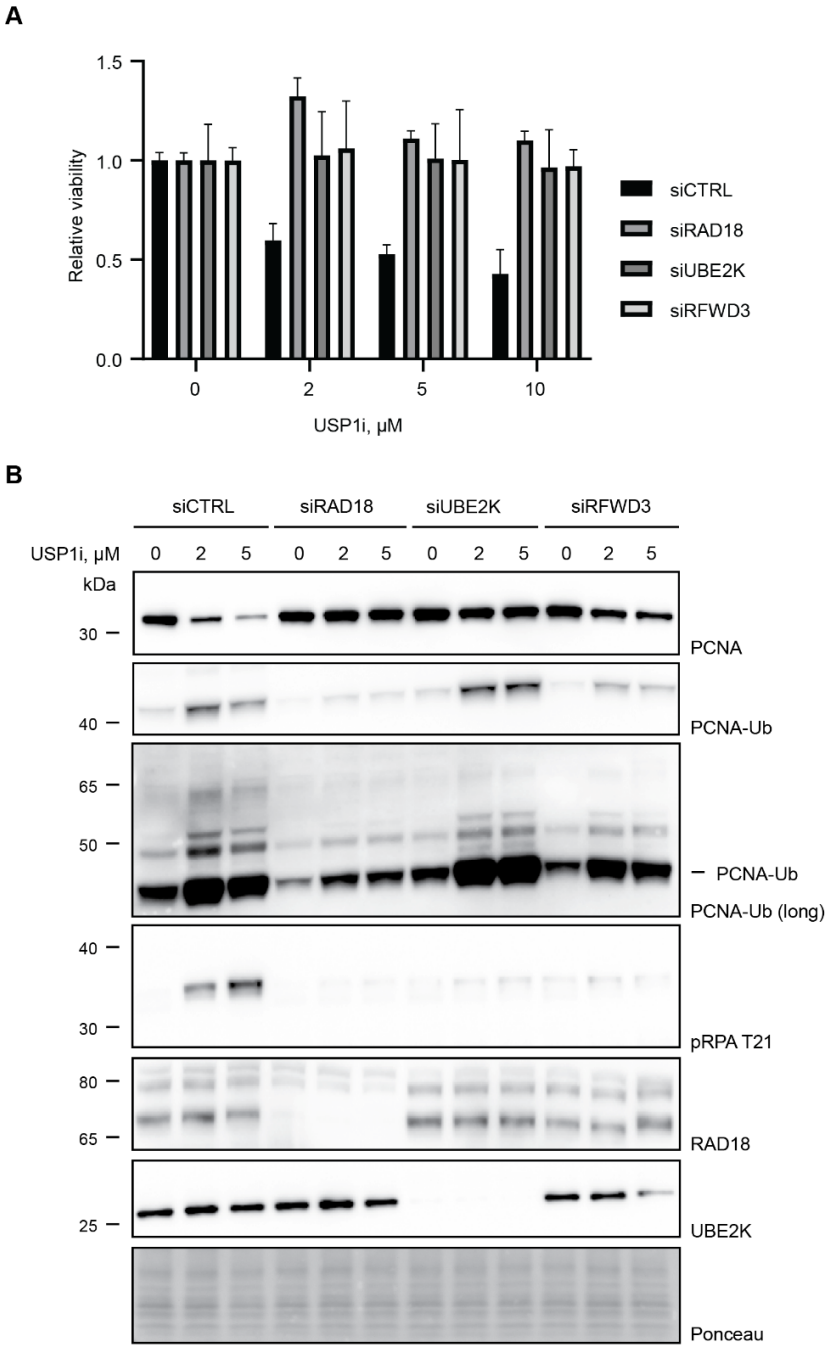

Figure 42: Toxic effects of USP1 inhibition in BRCA1-deficient cells is dependent on RAD18, UBE2K and RFWD3. (A) MTT cell viability assay performed on MDA-MB-436 cells, transfected with the indicated siRNAs for 48 h and cultured for 96 h in the presence of indicated concentrations of the USP1 inhibitor ML-323. **(B)** MDA-MB-436 cells were transfected and treated as described in (A). USP1 was inhibited for 72 h. The levels of PCNA and phosphorylated RPA were analysed by western blotting. Ponceau S staining serves as a loading control.

3.7.4 Removal of PCNA impacts the damage bypass pathway in BRCA1-deficient cells

K63-linked PCNA polyubiquitylation in human cells has been functionally linked to the pathway of replication fork reversal (Vujanovic *et al.,* 2017). Formation of reversed forks during replication over damaged DNA is thought to protect forks from collapse (Mutreja *et al.,* 2018) and simultaneously transfer damaged bases into the parental DNA duplex, where they can be repaired by the base or the nucleotide excision repair machinery. In terms of replication speed, fork reversal slows down replication: interfering with the pathway results in higher replication rates upon replication stress. Potentially, branching of K63-linked chains on PCNA can affect replication over damaged DNA in at least three different ways. First, removal of PCNA from replication forks is important for the completion of fork reversal (Park *et al.,* 2019). Second, if this reaction takes place before ZRANB3 recruitment, it can rather prevent fork reversal as it should remove K63-linked polyubiquitylated PCNA, which is necessary for ZRANB3 recruitment, from stressed forks. In this case, alternative pathways, such as TLS at the fork or repriming, should be favoured. Third, the branching could impact the interactions of polyubiquitylated PCNA with ZRANB3 or WRNIP1, or there may be specific readers of the branched chains.

To gain insights into the roles of UBE2K-VCP pathway in DNA damage bypass, I used the MDA-MB-436 cell line and analysed how well it replicates over damaged DNA in the presence of the USP1 inhibitor, which should lead to excessive chain branching on PCNA. As a replication stress-inducing agent I used hydroxyurea, which induces oxidative damage of DNA bases and simultaneous depletion of the dNTP pool, and analysed the speed of replication by means of the DNA fibre assay. As shown in **Figure 43A**, inhibition of USP1 results in faster replication in the presence of hydroxyurea. The observed effect is likely due to PCNA removal from chromatin, as it does not take place if VCP is inhibited.

Another assay that has been extensively used to study DNA transactions at stressed forks is the nascent DNA degradation (NDD) assay. It is based on the observation that in certain conditions, newly synthesised DNA is degraded by nucleases upon prolonged fork stalling, which can be visualised as a shortening of the replication tracts. These conditions typically involve depleting or inhibiting certain proteins, collectively termed “fork protectors”. BRCA1 is one of the best-characterised fork

protectors: knock-down of BRCA1 or loss-of-function BRCA1 mutants result in MRE11-dependent DNA degradation upon prolonged HU treatment. This degradation is thought to originate from reversed forks, and the elimination of the fork reversal pathway rescues nascent DNA degradation in BRCA1 mutants. As shown in **Figure 43B**, I could reproduce the above-described phenotype in MDA-MB-436 cells: shortening of newly synthesised DNA takes place when HU is added for 5 h after cell labelling. At the same time, simultaneous inhibition of USP1 rescues this phenotype.

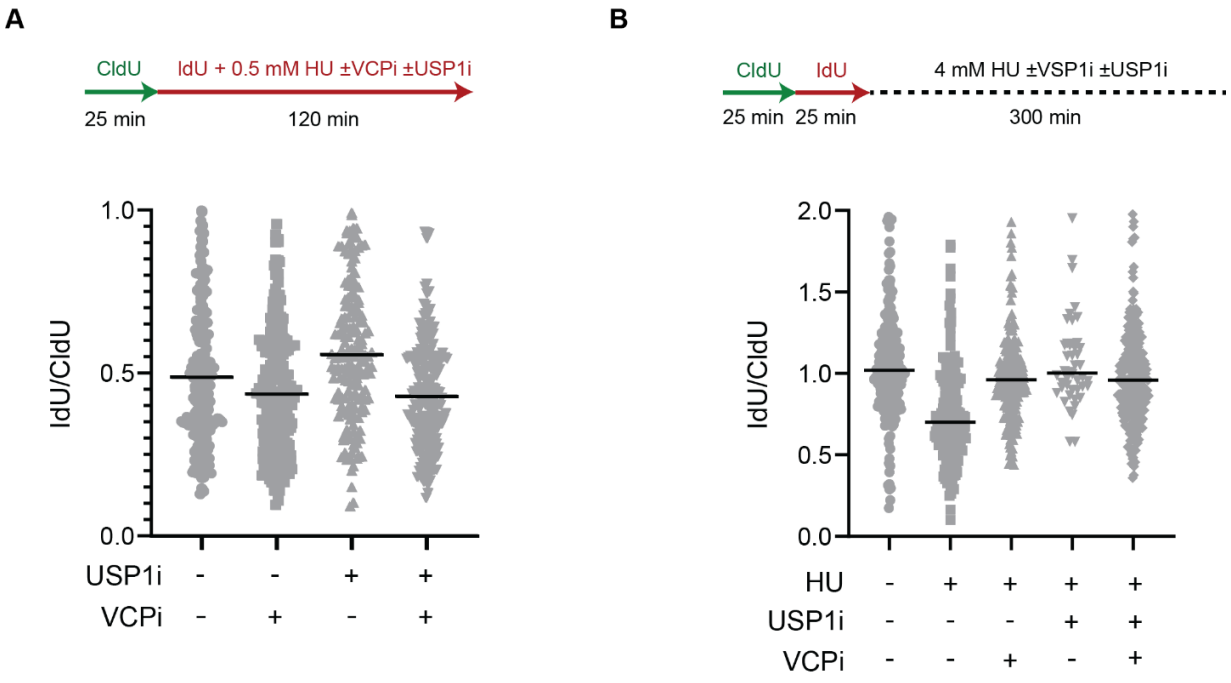

Figure 43: USP1 inhibition in MDA-MD-436 cells affects replication upon replication stress. **(A)** DNA fibre assay performed in MDA-MD-436 cells treated as depicted in the scheme, following DNA spreading and staining. At least 100 fibres per condition were quantified. **(B)** Nascent DNA degradation assay in MDA-MD-436 cells, treated as indicated in the scheme. At least 100 fibres per condition were quantified.

In this assay, I cannot conclude whether the effects observed following USP1 inhibition take place due to PCNA extraction because even VCP inhibition alone rescues nascent DNA degradation, and the simultaneous treatment with both inhibitors acts no differently. At this moment, I do not know precisely why VCP inhibition rescues nascent DNA degradation in MDA-MB-436 cells: possible scenarios and experiments to address this question are described in the **Discussion**. Nevertheless, the presented data indicate that excessive chain branching and VCP-dependent removal of PCNA interfere with fork reversal, favouring higher replication speeds upon replication stress and preventing the degradation of nascent DNA upon prolonged fork stalling. Future experiments will be needed to analyse which pathways compensate for the loss of fork reversal in these conditions and whether this could affect the long-term survival of cancer cells.

3.8 Expanding the technology beyond PCNA: the "Ubiquiton" system

3.8.1 Design of the "Ubiquiton" system

Tailor-made ubiquitin ligases represent a powerful tool to study ubiquitin signalling, as they allow direct manipulation of ubiquitin chain linkage. PCNA is one of the few proteins for which mono- and polyubiquitylation with different linkage types have been shown to fulfil different functions. Nevertheless, the DNA damage response alone involves ubiquitylation of numerous substrates (García-Rodríguez *et al.,* 2016), for which the significance of chain linkage is not understood. Therefore, the development of a system that would allow applying linkage-selective E3s to any substrate would be of great practical use. The catalytic domains of the $E3^{63}$, $E3^{48}$ and $E3^{1}$ highly prefer ubiquitin as a substrate (**Section 3.1**). In the PIP-E3 system, the first ubiquitin is provided to PCNA *in vivo* by RAD18/RAD6 upon replication stress in yeast. In human cells, it is present in significant amounts even without exogenous sources of damage. Although for certain proteins, such as histones, FANCD2 and RAD18, monoubiquitylation is a well-characterised modification, for many others this is not the case and generalising the PIP-E3 system would require solving the problem of chain initiation. Furthermore, a general dimerisation strategy is needed to bring the substrate and ligases in close proximity. The "Ubiquiton" technology provides a solution for these challenges; it allows the application of linkage-specific E3s to any protein of interest (**Figure 44A**). Chain initiation in this system is achieved using the split-ubiquitin principle, which is based on the ability of two ubiquitin halves (containing amino acids 1-34 and 35-76, respectively) to refold when brought in close proximity (Johnsson and Varshavsky 1994). Upon refolding, the ubiquitin halves mimic the tertiary structure of a wild-type ubiquitin and, therefore, can be recognised by the ubiquitylation machinery. When one half of ubiquitin is fused to a substrate and the other to a ligase, ubiquitin refolds when the interaction between the substrate and the ligase is induced, allowing for polyubiquitylation by an E3. In addition to splitting ubiquitin into two halves, two point mutations were also introduced: G76V in the C-terminal moiety of the split-ubiquitin to make it resistant to DUB cleavage and I13A in the N-terminal half to reduce background interaction of ubiquitin halves in the absence of a dimerisation signal (Pratt *et al.,* 2007). Finally, the FKBP-FRB dimerisation system is used to bring the E3s and the substrates together. These two domains come from

immunophilin FKBP12 and the protein kinase mTOR and interact in the presence of the small molecule drug rapamycin (Chen *et al.,* 1995). In the resulting system, a fusion of an N-terminal ubiquitin half to the FRB domain (hereafter called NUbo) and a fusion of the FKBP domain to a C-terminal ubiquitin half (hereafter called CUbo) are appended to substrates and E3s as single tags. Addition of rapamycin induces interaction between FKBP and FRB, which is followed by the re-folding of ubiquitin from its two halves. The E3s then extend the reformed ubiquitin in a linkage-specific manner. **Figure 44B** shows how the Ubiquiton system works for K63, K48 and M1-linked polyubiquitylation. Importantly, for K63- and K48-Ubiquiton, NUbo tags are applied to E3s and the CUbo tag to a substrate. In this case, the resulting chains are covalently attached to a substrate. Since, unlike K63 and K48, ubiquitin's M1 residue is located in an NUbo tag, for the M1-Ubiquiton, the NUbo tag is applied to a substrate and the CUbo tag to the E3s.

3.8.2 Application of the Ubiquiton system to human histone H2B

Histone mono- and polyubiquitylation is an essential cellular response to DNA damage. Nevertheless, the role of ubiquitin chain linkage in histone-coupled chains is not yet well investigated. Therefore, I used human histone H2B as a model substrate for the Ubiquiton system. All constructs were cloned under the control of a CMV promoter and, if not originating from *H. sapiens*, codon-optimised for human cells. The $E3^{1}$ sequence was partially codon-optimised, as described in **section 3.2.3**.

For the K63-Ubiquiton, N-terminally His_8-tagged H2B-CUbo was used as the substrate and NUbo-$E3^{63}$ as the ligase. Additionally, we co-expressed yeast Ubc13 and Mms2 to boost the $E3^{63}$ activity. Isolation of the substrate under denaturing conditions reveals robust polyubiquitylation upon the addition of rapamycin (**Figure 45A**). As expected, given the underlying properties of the Ubiquiton system, mutation of the K63 acceptor lysine in the CUbo tag prevents rapamycin-induced polyubiquitylation.

Because both K63 and K48 are located at the C-terminal half of a split-ubiquitin, the same substrate as for the K63-Ubiquiton was used for the K48-Ubiquiton. Similarly to the PIP-$E3^{48}$ system, Ubc7 was co-expressed with NUbo-$E3^{48}$. **Figure 45B** shows a rapamycin-inducible build-up of K48-linked chains on H2B-CUbo, which depends on the availability of K48 of ubiquitin.

Finally, the activity of $E3^1$-CUbo was detected in total cell extracts with the LUB9 antibody, which detects linear ubiquitin linkages and the NUbo tag and, therefore, the unmodified NUbo-H2B as well. **Figure 46** shows the polyubiquitylation of NUbo-H2B by $E3^1$-CUbo in the presence of rapamycin. An N-terminally blocked substrate (His_6-NUbo-H2B-His_8) is a negative control for this system, similar to the K63R and K48R mutations in the previous experiments. It is important to note that blocking the N terminus of ubiquitin prevents the LUB9 antibody from recognising this protein, which complicates the interpretation of this control. Therefore, in order to make sure that the observed polyubiquitylation results from the $E3^1$ catalytic activity, I utilised the catalytic point mutant (C885A) of the $E3^1$. As expected, no build-up of chains is observed when this mutant is used. Thus, all three chain types can be assembled on a model H2B substrate, which validates the use of the Ubiquiton system to study ubiquitin signalling in human cells.

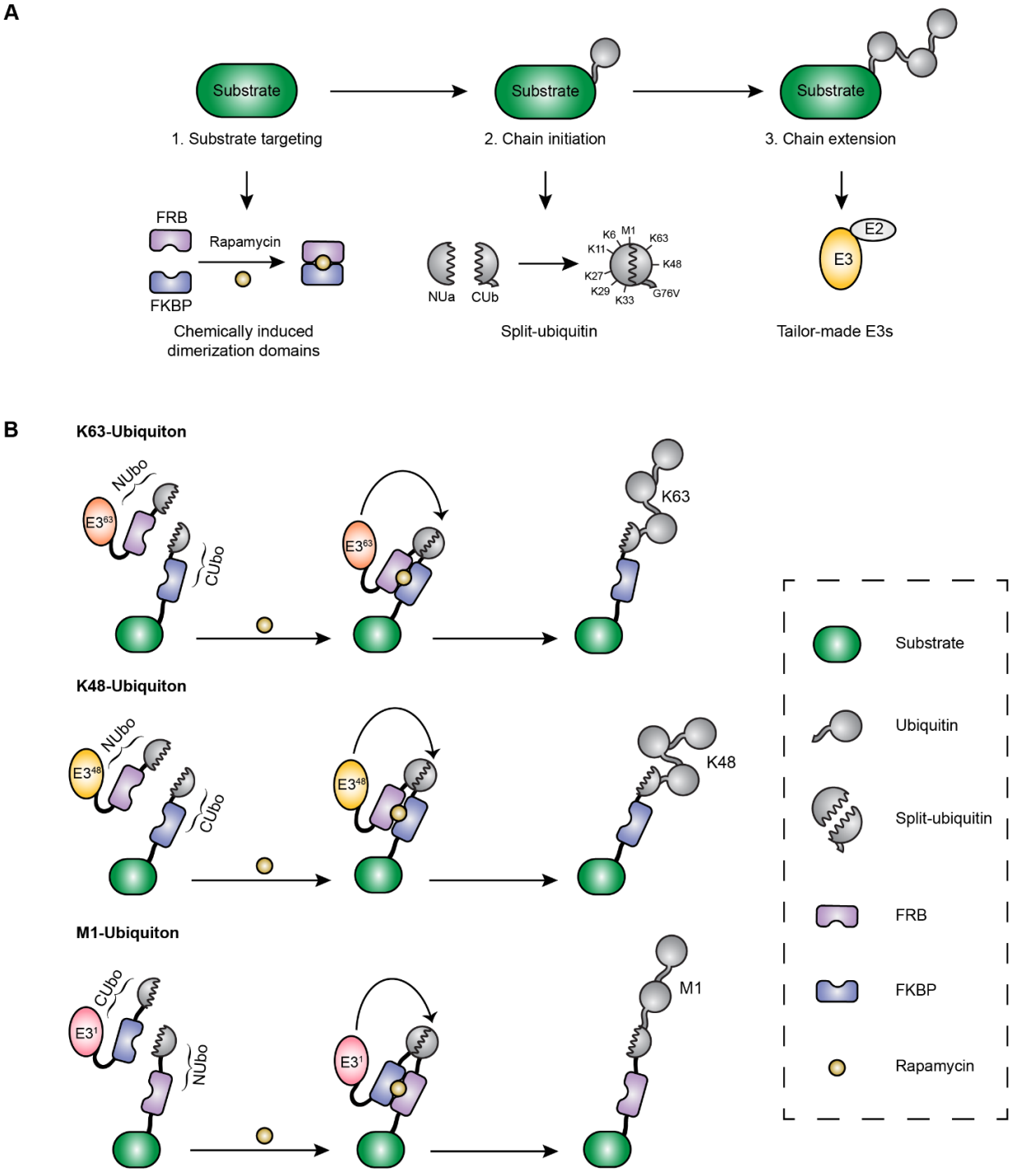

Figure 44 – Design of the Ubiquiton system. (A) Three principal components of the Ubiquiton system. **(B)** Schematic representation of the Ubiquiton system for the three chain types.

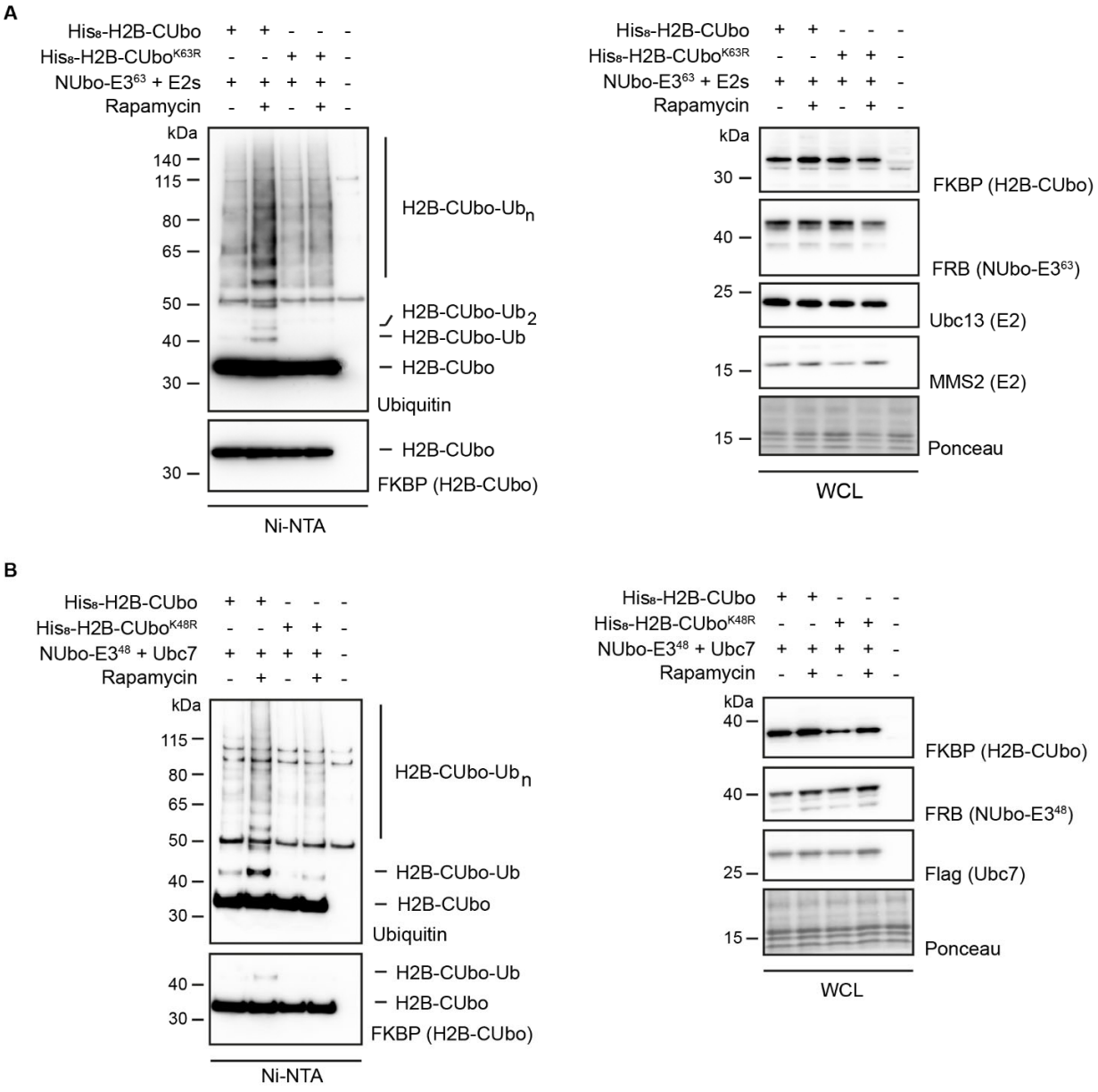

Figure 45: K63- and K48-Ubiquiton applied to human H2B. (A) The indicated constructs for K63-Ubiquiton were expressed in HEK 293T cells for 24 h. Cells were treated, if indicated, with 1 µM rapamycin for 30 min, followed by a Ni-NTA pulldown under denaturing conditions. Substrate polyubiquitylation and expression of the constructs was analysed by western blotting of the Ni-NTA pulldown (left) and whole-cell extracts (right). Ponceau S serves as a loading control. **(B)** Cells were treated as in panel (A), but the K48-Ubiquiton constructs were used.

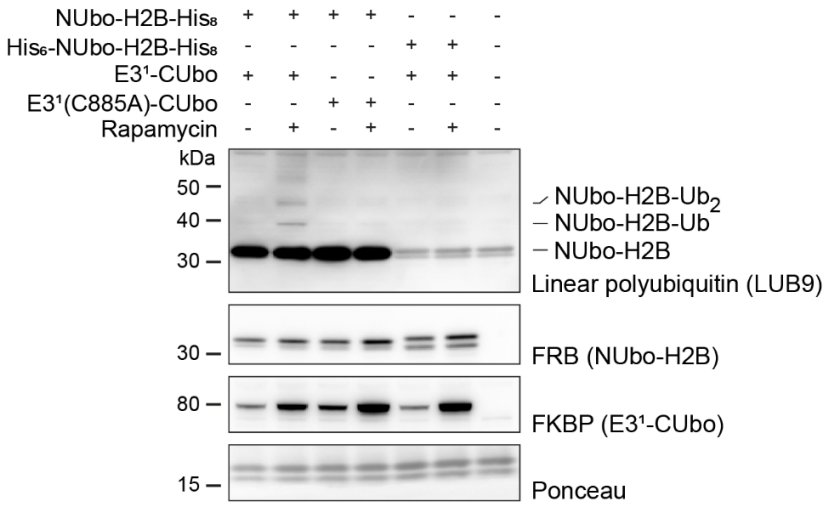

Figure 46: M1-Ubiquiton applied to human H2B. Indicated constructs were expressed in HEK 293T cells for 24 h. Cells were treated, if indicated, with 1 µM rapamycin for 240 min, followed by western blotting of whole-cell extracts with the indicated antibodies. Ponceau S staining serves as a loading control.

Chapter 4

Discussion

4.1 Tailor made E3s as a new engineering approach to study the ubiquitin code

There are several approaches to studying the ubiquitin code. The majority of them rely on the analysis of the existing ubiquitin conjugates. These include mass-spectrometry, linkage-selective binders and a deubiquitylase-based approach UBICREST. All these methods allow to unravel the architecture of the ubiquitin coat on a given substrate without providing information on how important each particular element of the ubiquitin code is. Indeed, in order to understand the significance of the ubiquitin code, one has to be able to directly manipulate it – change the ubiquitin architecture on a substrate and analyse the physiological consequences of this manipulation. The task is challenging because the writers of the ubiquitin code are often unknown. In addition, ubiquitin ligases often have multiple functions and, therefore, cannot be depleted without severe side effects for a cell. Therefore, protein engineering approaches, which allow to re-create specific ubiquitin structures, are of great importance. There are a lot of known examples where permanent fusions of ubiquitin to a protein successfully mimic monoubiquitylation events (Asimaki *et al.,* 2022). This approach, however, has relatively limited scope in mimicking polyubiquitylation. Whereas conformations of head-to-tail ubiquitin functions can be similar to that of K63-linked chains, other linkage types are unlikely to be functionally replaced by linear polyubiquitin fusions. The present work focuses on two protein engineering-based systems, which allow polyubiquitylation of desired substrates with K63-, K48- or M1-linked polyubiquitin chains. The first system – PIP-E3s – is specific for PCNA and was successfully implemented before in *S. cerevisiae*. In this study, PIP-E3s were optimised for human cells. Whereas PIP-E3^{63} did not require further optimisation steps except for optimisation of codon usage, I observed that the activity of PIP-E3^{48} drastically increased in the presence of its cognate E2 Ubc7, which can be co-overexpressed or produced as a self-cleavable or a permanent fusion with PIP-E3^{48}. Unlike PIP-E3^{63} and PIP-E3^{48}, the activity of PIP-E3^{1} was detectable only in

denaturing conditions and upon overexpression of ubiquitin. This may reflect that linear chains are more prone to DUB cleavage in human cells or that this enzyme needs further optimisation to become as active as K63- and K48-specific E3s. The fundamental difference between PIP-E3s and other approaches, where E3s are targeted to the substrates, is their elongation specificity and, therefore, reliance on PCNA monoubiquitylation. One can envision the development of similar tailor-made E3s by means of fusing linkage-selective E3s to substrate binding domains for substrates other than PCNA. In order to promote the activity of E3s, the substrates need to be monoubiquitylated *in vivo*, which limits the scope of potential candidates. The second system I used in this study is the Ubiquiton technology, which can be applied to any desired protein and overcomes the abovementioned problem of chain initiation. While catalytic domains remain the same as in PIP-E3s, several advances have been implemented in the system: the FKBP-FRB dimerisation system as a means of substrate targeting and the split ubiquitin approach for chain initiation. In this thesis, I demonstrate the applicability of the Ubiquiton system to the human histone H2B, and my co-workers Evrydiki Asimaki and Christian Renz have successfully used it to polyubiquitylate human EGFR and GFP as a proof-of-concept substrate. Unlike PIP-E3s, overexpression of E2s was needed for both 'K63' and 'K48'-Ubiquiton. One possible explanation for this phenomenon could lie in the different availability of the substrates in these systems. While PIP-E3s can only act on monoubiquitylated PCNA, which is a relatively rare PCNA modification in unchallenged conditions, the substrate for the Ubiquiton system was overexpressed. In this case, more components of the ubiquitylation machinery may be needed to support the ubiquitylation of the substrate, explaining the need for E2 overexpression.

There are several described approaches, where ubiquitin ligases are targeted to the substrates of interest. One well-known example is proteolysis-targeting chimaeras (PROTACs) – heterobifunctional molecules, which bring the desired substrate and the E3 enzyme in close proximity. A wide range of ubiquitin ligases has been used as a 'degrader' component of the PROTAC system (Békés *et al.,* 2022). In contrast PROTACs, the Ubiquiton system allows not only to degrade proteins but also to study numerous non-degradative functions of K63- and M1- polyubiquitin chains. Even in the context of protein degradation, the Ubiquiton system provides an alternative way for targeted protein

degradation based on the addition of rapamycin, thereby allowing, in combination with other technologies, independent degradation of several cellular proteins.

Another example of a technology which is based on the targeted protein ubiquitylation is the ProxE3 system: catalytic domain of the HECT-type K63-selective E3 NEDD4 was in an inducible manner targeted to the mitochondria-localised substrate (Richard *et al.,* 2020). The authors demonstrate that the activity of the E3 results in the sequestration of mitochondria but not mitophagy induction. However, although the catalytic domain of NEDD4 is predominantly K63-selective, it also multi-monoubiquitylates the substrate, making it difficult to differentiate between multi-mono and polyubiquitylation. In the Ubiquiton system, this is achieved by the split ubiquitin system: mutation of the acceptor lysine on a Ubiquiton tag prevents chain formation while retaining the re-folding of the first ubiquitin. Thus, tailor-made E3s and, in particular, the Ubiquiton system provide a series of conceptual advances over the existing ubiquitin technologies and have a great potential to explore the function of the ubiquitin code.

4.2 Exploring the roles of PCNA polyubiquitylation by means of PIP-E3s

4.2.1 Which biological questions are addressed by the PIP-E3 system in yeast and human cells?

Despite the same mechanism of PIP-E3s' activity in yeast in human cells, fundamental biological questions addressed by the expression of these artificial enzymes are different. The underlying reason is the extent of PCNA monoubiquitylation in cycling cells in undamaged conditions. In yeast, this modification is damage-inducible. Therefore, DNA damage is a prerequisite for PIP-E3 activity in this organism. Thus, a biological question for this system can be whether PIP-E3^{63} can functionally act as Rad5 – an E3 enzyme responsible for PCNA modification with K63-linked chains in the DNA damage bypass. Enzymes with alternative linkage specificity (PIP-E3^{48} and PIP-E3^{1}) provide insight into the relevance of K63 linkage in the pathway. As demonstrated by Wegmann *et al.,* PIP-E3^{63} and PIP-E3^{1} can functionally replace Rad5 in the DNA damage bypass pathway, whereas PIP-E3^{48} counteracts damage bypass owing to PCNA degradation and exerts dominant-negative effects.

In human cells, PCNA is modified with monoubiquitin during normal S-phase progression, whereas polyubiquitylation becomes evident only upon substantial replication stress. The activity of PIP-E3s is therefore not damage-inducible: endogenous levels of PCNA monoubiquitylation are sufficient to support the activity of PIP-E3s, which, in the case of PIP-E3^{63}, leads to replication catastrophe as early as 6 h after the induction of the ligase. Therefore, it is impossible to utilize PIP-E3s to address the same biological question as in budding yeast. Instead, the activity of PIP-E3^{63} simulates a damage response in a cell without 'real' DNA damage. This experimental setup is conceptually similar to tethering DNA damage markers to chromatin without any exogenous damage (Soutoglou and Misteli, 2008). As demonstrated by Soutoglou *et al.,* forced recruitment of DSB repair proteins NBS1, MRE11, MDC1, and ATM to chromatin leads to G2/M arrest of cells, although 'real' DSBs are not present. In this sense, polyubiquitylation of PCNA by PIP-E3^{63} in otherwise unchallenged cells creates a signal, which would typically appear in cells that experience replication stress. In theory, cells can either ignore this unscheduled PCNA modification or undergo a response to it. My results show that the second scenario is the case: human cells respond to PIP-E3^{63}-induced PCNA polyubiquitylation as if they would replicate over damaged DNA: they activate checkpoint signalling and arrest in the S phase. Moreover, PIP-E3^{48}, albeit less efficient, leads to the same phenotype, highlighting the differences in the damage response pathway in yeast and human cells.

4.2.2 Expression of PIP-E3^{63} phenocopies HU-induced replication stress and USP1 inhibition in BRCA1-deficient cells

One of the first observed phenotypes of PIP-E3^{63} expression was S phase arrest and activation of checkpoint signalling. Whereas checkpoint activation begins as early as 6 h post PIP-E3^{63} induction, cells exhibit S-phase accumulation starting from 12 h after expression of PIP-E3^{63}. Alongside S-phase arrest, late (> 24 h) response to PIP-E3^{63} expression includes reduced EdU incorporation, reduced replication speed and formation of double-strand breaks, visualised by the appearance of γH2AX signal. Notably, at early time points, ATR activity prevents the formation of DNA breaks, as ATR inhibition by VE-821 leads to increase of γH2AX 6 h after PIP-E3^{63} expression. All the observed

phenotypes are common for cells experiencing replication stress. Indeed, treatment of cells with high-dose hydroxyurea leads to activation of checkpoint signalling due to exposure of single-stranded DNA, reduced replication speed, S-phase arrest and formation of DSBs upon prolonged treatment. Moreover, at early time points, ATR prevents the formation of DSBs by preventing excessive origin firing and RPA exhaustion. This similarity between PIP-E3^{63} and HU treatment is surprising: treatment with HU affects all replication forks simultaneously, whereas PIP-E3^{63} creates a chain only at the sites where PCNA is monoubiquitylated. As monoubiquitylated PCNA levels are relatively low, it suggests that K63-linked polyubiquitylation is a potent signal for checkpoint activation. One crucial difference between HU-induced replication stress and PIP-E3^{63} expression is PCNA levels: activation of checkpoint signalling in PIP-E3^{63} occurs concomitantly with a drastic decrease in total PCNA levels, whereas massive PCNA degradation upon HU treatment has not been reported.

Another situation which affects cells in a way similar to PIP-E3^{63} expression is the inhibition of USP1 in BRCA1-deficient cells: this treatment results in RAD18-dependent S phase arrest and checkpoint activation, ultimately leading to cell death. Although the importance of BRCA1 deficiency in this scenario is poorly understood and will be discussed in **section 4.2.6**, USP1 inhibition leads to an increase in PCNA monoubiquitylation. As monoubiquitylated PCNA is a substrate for subsequent polyubiquitylation, inhibition of USP1 in a BRCA1-deficient background is likely to induce replication collapse via the same mechanism as PIP-E3^{63} expression. Thus, expression of PIP-E3^{63} leads to similar effects as replication stress triggered by at least two different sources.

4.2.3 Effects of PIP-E3^{63} expression are on-target

In the course of the work, I performed a series of controls to prove that the observed effects are PCNA-specific. PIP-E3^{63}-induced checkpoint activation and cell cycle arrest do not take place if:

1. PIP-box of the ligase is deleted, interaction with UBC13 is compromised via a point mutation of a RING domain, or the catalytic domain is completely deleted

2. PCNA K164R cell line is used, deficient in PCNA ubiquitylation
3. RAD18 is depleted, preventing PCNA monoubiquitylation

Taken together, these data demonstrate that unscheduled PCNA polyubiquitylation with K63-linked chains leads to replication catastrophe.

Results from HEK293T-based cell lines (George-Lucian Moldovan laboratory) provide additional information about the nature of the adverse effects of PIP-E3^{63} expression. Whereas HEK293T WT cells do, and HEK293T PCNA K164R do not activate checkpoint upon expression of PIP-E3^{63}, cells expressing both wild-type and mutant PCNA forms behave like full mutant cells. One possible explanation could be that multiple subunits of the same PCNA trimer need to be polyubiquitylated to lead to the observed phenotype. Several studies indicate that simultaneous ubiquitylation of multiple PCNA subunits of the same trimer may be essential for damage tolerance in human cells. First, human cells expressing two different PCNA forms – WT and PCNA K164R – are sensitive to UV and cisplatin, suggesting that heterotrimeric PCNA forms interfere with damage bypass (Kanao and Masutani, 2017). Second, HLTF preferentially polyubiquitylates PCNA trimers, pre-monoubiquitylated on all three subunits (Masuda *et al.,* 2018). Finally, HUWE1, identified in this study as an interactor of polyubiquitylated PCNA, was shown to amplify the ubiquitin signal various of substrates in different cellular compartments (Zhou *et al.,* 2023). One could also speculate that the activity of HUWE1 would include the propagation of ubiquitin signalling from one PCNA subunit onto others. This needs to be, however, further investigated.

4.2.4 Ubiquitylated PCNA is a VCP substrate

Depletion of the two factors that have been previously shown to interact preferentially with polyubiquitylated PCNA – ZRANB3 and WRNIP1 – do not prevent checkpoint activation by PIP-E3^{63}. Moreover, as there might be redundancy between ZRANB3 and other fork remodellers, I tested whether HLTF and SMARCAL1, as well as the interactor of K63-linked polyubiquitin chains RAP80, are responsible for the harmful effects of PIP-E3^{63} expression. However, none of these factors seems to be involved in the pathway, suggesting the presence of other readers of PCNA polyubiquitylation. This

was a reason to conduct a mass-spectrometry-based identification of factors that preferentially interact with polyubiquitylated PCNA *in vivo*. Alongside WRNIP1, which serves as a positive control, I identified components of a VCP-proteasome system enriched in polyubiquitylated PCNA conditions. Importantly, VCP has been shown to regulate the disassembly of replisomes upon replication termination, and several studies suggest an involvement of VCP in the process of DSB repair (Meerang *et al.,* 2011). However, the functions of VCP in the DNA damage bypass pathway have not yet been reported. VCP inhibition by NMS-873 indeed prevents checkpoint signalling after PIP-E3^{63} expression. Moreover, one can observe a massive accumulation of polyubiquitylated PCNA on chromatin upon VCP inhibition. These data pinpoint VCP activity towards polyubiquitylated PCNA as the reason for replication collapse after PCNA polyubiquitylation. Importantly, this pathway is not an artefact of the PIP-E3^{63} system and also operates when PCNA polyubiquitylation is induced by HU, MMS or UV light, suggesting that removal of polyubiquitylated PCNA from chromatin is a general response to replication stress.

4.2.5 PCNA is modified with branched ubiquitin chains

Mass-spectrometry-based analysis of PCNA, immunoprecipitated from PIP-E3^{63}-expressing cells upon VCP inhibition, reveals upregulation of K63, K48 and K11 linkages. Interestingly, this combination of ubiquitin linkages on a single substrate has already been reported for several proteins. For example, the ubiquitin coat, consisting of K63, K48 and K11 chains, is created by the APC/C complex on the cyclin B1, mediating its rapid degradation at the anaphase onset (Kirkpatrick *et al.,* 2006). Similar ubiquitin architecture is present on the secretory factor EVI/WLS, the responsible ubiquitin-conjugating enzymes being UBE2N, UBE2K and UBE2J2 (Wolf *et al.,* 2021). As UBE2N and UBE2K are highly K63- and K48-linkage specific, UBE2J2 is likely responsible for generating the K11 component of the ubiquitin code. CRISPR screen also identified that UBE2K, UBE2J2 and a K63-specific ubiquitin ligase MARCH5 are responsible for the degradation of the pro-apoptotic factor NOXA. Importantly, UBE2K and UBE2J2 do not mediate NOXA degradation in MARCH5-deficient cells, suggesting that a K63-linked chain serves as a basis for the build-up of a complex branched K63-K48-K11 architecture (Nakao *et al.,*

2023). The same pathway likely underlies the mechanism of action of cIAP-based degraders: a K63-linked chain is further modified with K48- and K11-linkages, leading to rapid degradation of a target protein (Akizuki *et al.,* 2023). Therefore, the branching of K63-linked chains on PCNA may not be specific to PCNA but rather represent a particular case of a general pathway initiated by K63-linked chains.

The model that K48 ubiquitin linkages on PCNA after PIP-E3^{63} expression are assembled on top of K63-linked chains was further confirmed by means of the UBICREST assay, where linkage-selective DUBs are used to delineate the architecture of the ubiquitin conjugates. Treatment of PCNA, immunoprecipitated from PIP-E3^{63}-expressing cells, with a K63-linkage selective DUB AMSH leads to the removal of both K63 and K48 linkages from PCNA. Analysis of soluble ubiquitin forms after AMSH cleavage confirmed that PCNA is decorated with K63-K48 branched ubiquitin chains. I further demonstrate that ubiquitin-conjugating enzyme UBE2K is at least partially responsible for the branching of K63-linked chains on PCNA *in vitro* (collaboration with Nils Krapoth) and *in vivo*. Transient depletion of UBE2K diminishes the amount of branched ubiquitin chains on PCNA and completely prevents checkpoint activation by PIP-E3^{63}. The latter observation is quite interesting because it suggests that a certain amount of ubiquitin chain branching on PCNA can be tolerated by cells; however, its excessive amount results in a replication collapse. By directly comparing the consequences of K63- versus K48-linked PCNA polyubiquitylation, I observed that both chain types lead to VCP-dependent replication collapse. However, due to UBE2K-dependent branching, K63-linked chains lead to much more substantial adverse effects than K48-linked chains (**Figure 47**). This suggests that branched K63-K48 chains are a better substrate for VCP-mediated extraction than homotypic chains, which agrees with similar findings for the branched K11-K48 chains (Yau *et al.,* 2017). A recent study suggests that branched K63-K48 chains play a role in VCP metabolism: several VCP-interacting proteins (ATXN3, ZFAND2B, RHBDD1) preferentially bind to branched K63-K48 conjugates compared to homotypic K63 and K48-linked chains. It is worth pointing out, that in the same study, VCP itself was found to preferentially bind to K48-linked chains. Therefore, it is likely that certain branched chain-specific VCP adaptors are involved in the removal of PCNA from chromatin. As none of them was identified in the MS experiment, alternative approaches, such as crosslinking

MS or siRNA/CRISPR screens, are needed to identify VCP adaptors involved in removing polyubiquitylated PCNA from DNA.

Another remaining question is the nature of identified K11 linkages on PCNA. Theoretically, these linkages can be assembled either on top of K63-linked or K48-linked chains. This can be understood in the future by performing a UBICREST assay with K63- or K48-selective DUBs and analysing the presence of K11 linkages in soluble and PCNA-bound fractions by K11-selective antibodies or mass spectrometry. K11-selective DUB Cezanne and branched K48-K11 selective antibody may also be of great use in this direction.

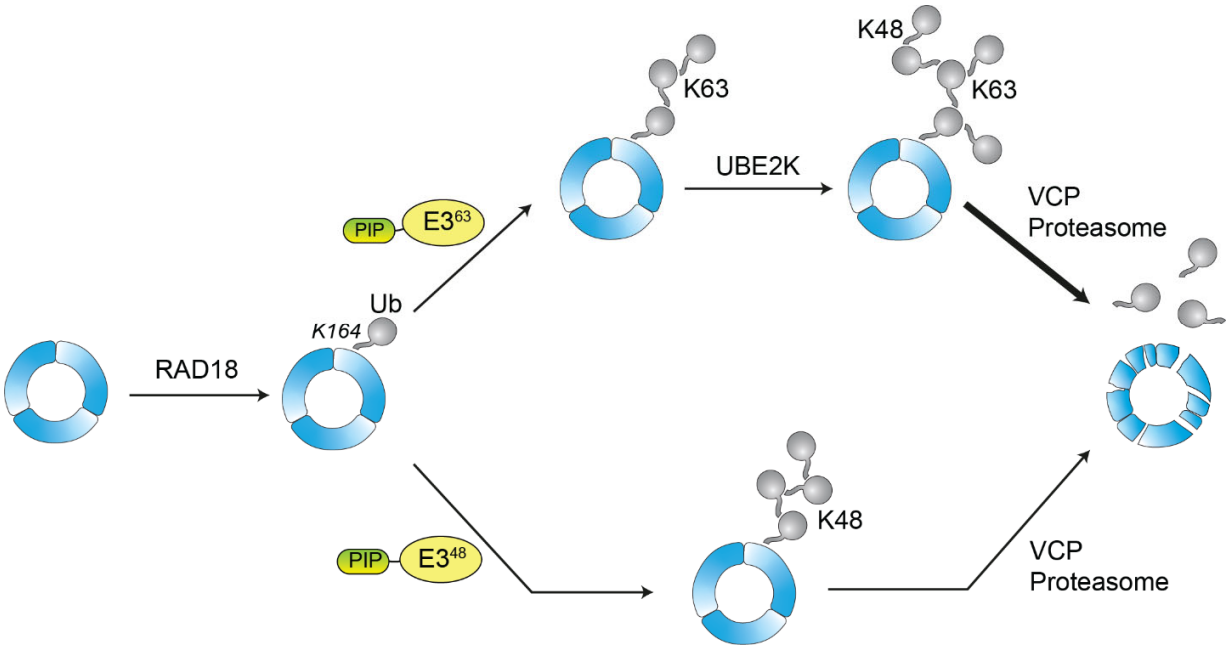

Figure 47: Schematic representation of the pathway, initiated by PCNA polyubiquitylation in the PIP-E3^{63} and PIP-E3^{48} systems

4.2.6 Ubiquitin chain branching underlies synthetic lethality between BRCA1 and USP1

Why does inhibition of USP1 in BRCA1-deficient cells phenocopy overexpression of PIP-E3[63]? Whereas USP1 inhibition increases the levels of mono- and, consequently, polyubiquitylated PCNA, the role of BRCA1 deficiency in this pathway is unclear. The difference between BRCA1-proficient and -deficient cells is evident even during otherwise unchallenged replication, as BRCA1-deficient cells tend to accumulate single-strand DNA gaps, which likely originate from PRIMPOL repriming at DNA lesions or difficult-to-replicate structures (Cong *et al.,* 2021; Quinet *et al.,* 2020). A recent study suggests BRCA1 monoubiquitylates PCNA during unperturbed replication, promoting continuous DNA synthesis (Salas-Lloret *et al.,* 2023). A similar phenotype, namely accumulation of daughter strand gaps, is exhibited by PCNA K164R cells, confirming the proposed role of BRCA1-mediated PCNA ubiquitylation in gap suppression. Studies in yeast suggest that PCNA can remain at the 3' of a gap while the replisome further continues DNA synthesis (Daigaku *et al.,* 2010). Increased formation of DNA gaps may result in more PCNA trimers being loaded on DNA at any time point: in addition to active replication forks, PCNA is likely to be present at the gaps in BRCA1-deficient cells, increasing DNA-bound PCNA pool, which can be a substrate for ubiquitylation. Once PCNA is sequentially monoubiquitylated, polyubiquitylated, undergone chain branching by UBE2K, extracted from DNA by VCP and degraded, a new PCNA trimer can be loaded on the same daughter-strand gap by RFC clamp loader, and the cycle can repeat (Schrecker *et al.,* 2022). In this scenario, total PCNA levels will be a trade-off between degradation of chromatin-bound PCNA and PCNA translation in the cytoplasm. Due to the presence of DNA gaps, the rate of chromatin-bound PCNA degradation should be higher in BRCA1-deficient cells, explaining the observed rapid degradation of PCNA (**Figure 48**). Proof of this hypothesis would require performing the experiments described in **section 3.7.3** upon depletion of PRIMPOL when the formation of ssDNA gaps, at least on the leading DNA strand, is prevented. Alternatively, if the hypothesis is correct, inhibition of VCP or depletion of UBE2K should prevent excessive gap formation, which can be visualised by DNA fibre assay with S1 nuclease treatment (Quinet *et al.,* 2017).

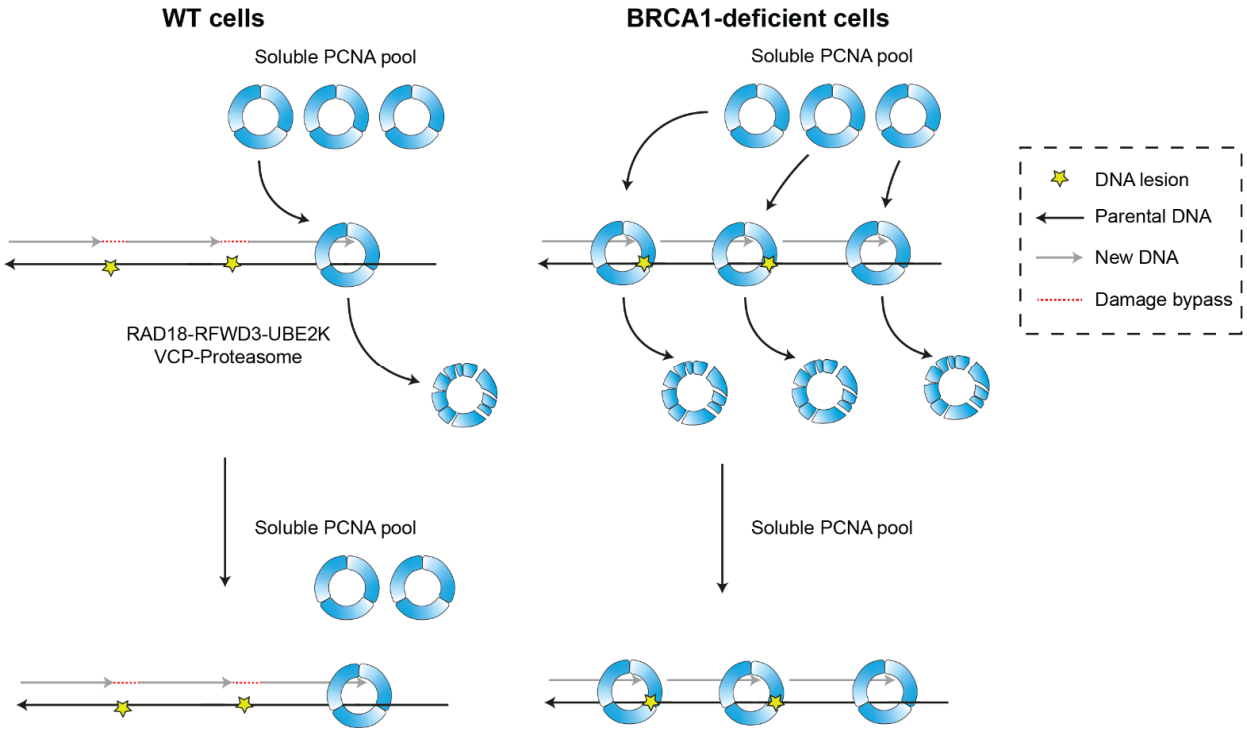

Figure 48: A model explaining rapid PCNA degradation upon USP1 inhibition in BRCA1-deficient compared to wild-type cells. Excessive formation of daughter-strand gaps may lead to more PCNA being loaded onto DNA and undergo ubiquitylation and degradation. More detail in the main text.

4.2.7 USP1 slows down replication under stressed conditions in BRCA1-deficient cells

Inhibition of USP1 in BRCA1-deficient cells for 24 – 72 h results in bulk PCNA degradation and cell death. I hypothesised that this treatment may also affect replication on a shorter timescale. As described in **section 1.2.3.4**, once a replication fork stalls due to encountering a lesion or nucleotide starvation, there are multiple ways to solve this issue, the main ones being translesion synthesis, fork reversal and repriming. Of these three, only repriming is favoured upon the conditions of PCNA depletion, as both TLS and fork reversal require PCNA ubiquitylation. Indeed, my results suggest that fork reversal is impaired in BRCA1-deficient cells, as nascent DNA degradation in this cell line is prevented by USP1 inhibition. Previously, depletion of USP1 was shown to further aggravate, rather than rescue, nascent DNA degradation upon BRCA1 deficiency (Lim *et*

al., 2018). However, it should be noted that there is no discrepancy between these data. Conditions for DNA fibre assay in the Lim *et al.* study include either siRNA-mediated depletion of USP1 or long-term (24 h) treatment with a USP1 inhibitor. These conditions already induce significant PCNA degradation, which may alter the composition or structure of replication forks when HU is applied, enhancing the effects of BRCA1 deficiency (Simoneau *et al.,* 2023). On the contrary, I applied the USP1 inhibitor together with HU, ensuring that USP1 inhibition would not affect the replication forks before they encountered stress conditions. In addition, excessive repriming in BRCA1-deficient cells upon USP1 inhibition is supported by higher replication speed in these conditions. This acceleration of forks upon USP1 inhibition does not take place if VCP activity is inhibited, confirming the proposed role of PCNA extraction from DNA in counteracting TLS and fork reversal and facilitating repriming. Although strict proof of USP1 influence on fork reversal would require performing electron microscopy of the replication intermediates, the rescue of the nascent DNA degradation upon BRCA1 deficiency has been widely used as a proxy for impaired fork reversal. Rescue of the nascent DNA degradation in BRCA1-deficient cells can happen even in the presence of a functional fork reversal pathway, for example, if MRE11 nuclease activity is compromised. However, there is no known connection between USP1 and MRE11, so the hypothesis that USP1 inhibition impairs fork reversal in BRCA1-deficient cells seems more plausible.

4.2.8 Potential clinical significance of the findings

As PCNA is an essential factor in DNA replication and repair, compromising its functions may be a promising approach to inhibit the growth of tumour cells. Chang *et al.* describe a system for targeted PCNA degradation based on a CRL adaptor SPOP fused to a PCNA-targeting peptide Con1 (Chang *et al.,* 2022). Once delivered into cells, Con1-SPOP induces robust PCNA degradation, resulting in mitotic defects, mitochondria dysregulation and overall complete inhibition of tumour growth *in vivo*. These effects depend on PCNA degradation, as they are not observed upon stoichiometric inhibition of PCNA. In this study, I demonstrated that PCNA decoration with K63-linked chains leads to more efficient PCNA degradation than K48-linked polyubiquitylation. Therefore, there is a possibility that the PIP-E3^{63} construct may be even more efficient in inhibiting tumour

growth than Con1-SPOP fusion. As cancer cells often experience replication stress and may have elevated levels of ubiquitylated PCNA at replication forks and daughter-strand gaps, PIP-E3^{63} may preferentially inhibit the proliferation of cancer cells. More research is needed to assess the viability of this approach.

Moreover, the results obtained in this study highlight the toxicity of PCNA ubiquitylation in BRCA1-deficient cells. Analysis of mutations in the factors involved in the pathway (RAD18, UBC13, RFWD3, UBE2K, VCP adaptors and others) may serve as a basis for prediction of how BRCA1-deficient tumours react to USP1, VCP or TLS inhibition or treatment with HU. The results may also be expanded beyond BRCA1-deficient tumours, as discussed in **section 4.3.1**.

4.3 Future perspectives

4.3.1 PCNA polyubiquitylation

Excessive PCNA polyubiquitylation with K63-linked chains, induced either by the expression of PIP-E3^{63} or by USP1 inhibition in a BRCA1-deficient background, results in replication collapse. As this effect is potentially helpful for drug discovery applications, it is crucial to explore whether it also occurs in other cellular backgrounds. My results suggest that ubiquitin chain branching on PCNA and its removal from chromatin take place even in wild-type cells as a part of a replication stress response. However, unlike BRCA1-deficient, wild-type cells do not experience substantial PCNA degradation upon treatment with genotoxins. As mentioned in **section 4.2.6**, an increased presence of daughter-strand gaps in BRCA1-deficient cells can be a reason for a higher PCNA degradation rate in this genetic background. However, there are other conditions that lead to increased formation of gaps during DNA replication. One example is the inhibition of PARP, which leads to an increase in replication speed due to the excessive accumulation of daughter-strand gaps (Maya-Mendoza *et al.,* 2018). As this situation is similar to BRCA1 deficiency, it is worth investigating whether co-treatment of wild-type cells with PARP and USP1 inhibitors would lead to PCNA degradation and checkpoint activation.

Another open question is whether the PCNA-Ub_n – UBE2K – VCP pathway protects replication forks from DNA2-mediated degradation. Indeed, the reason for the fork deprotection in PCNA K164R cell line or upon depletion of RAD18 or UBC13 is not yet identified. One possible explanation could be that VCP-dependent removal of PCNA from stressed replication forks is required for the proper fork reversal and protection. PCNA unloading by ATAD5 is essential for the fork reversal pathway *in vitro*. It is possible that PCNA unloading *in vivo* may involve other factors, such as VCP.

Finally, since the translesion synthesis polymerase Polκ preferentially associates with PCNA modified with K48 ubiquitin linkages, it is tempting to speculate that ubiquitin chain branching by UBE2K may serve as a recruitment signal for this polymerase, facilitating fork restart after prolonged HU treatment. Future research is needed to address this question and investigate the timely coordination between the signalling functions of PCNA-conjugated ubiquitin chains and VCP-dependent termination of the signalling.

4.3.2 The Ubiquiton technology

The Ubiquiton system generalises the PIP-E3 technology, allowing the polyubiquitylation of any protein of interest with one of three (M1-, K63-, K48-linked) chain types. Although the ubiquitin chains in the Ubiquiton system are assembled on the respective tags instead of native attachment sites, there are no known cases where an attachment site of a polyubiquitin chain would impact its functions on a substrate. I demonstrated that the Ubiquiton system can be applied to polyubiquitylate human histone H2B with three different linkage types. This experiment not only serves as a proof-of-concept for the Ubiquiton technology in human cells but also allows to explore the role of ubiquitin signalling in the DSB response. Future experiments can include the modification of histones with polyubiquitin chains in the absence of ‘real’ DNA damage and analysing of a cellular response to this chromatin modification. Should this approach be unsuccessful, one can target the Ubiquiton components to chromatin by other means, such as the TetO-TetR tethering system or non-catalytic Cas9. Since ubiquitin signalling is involved in all major cellular pathways, the Ubiquiton technology will likely find applications beyond DNA damage signalling. It will be useful to study the roles of polyubiquitylation of those substrates that are known to be decorated with different

linkages. Examples are p53, RIPK1 and IRAK1 (Guo *et al.,* 2021; Newton *et al.,* 2008). Combining the Ubiquiton system with the proximity labelling mass spectrometry approach will allow to identify the interactors of the polyubiquitylated substrates.

Another possible application of the Ubiquiton system originates from the results of this work, namely the branching of K63-linked chains on PCNA. The apparent absence of a PCNA-targeting domain in UBE2K suggests that K63-linked chains on other substrates may also be decorated by UBE2K with K48 linkages. Indeed, nearly one-fifth of K63 linkages are branched at K48, although the contribution of UBE2K to the 'bulk' branching of K63-linked chains is yet unknown. This question can be answered with the help of the Ubiquiton system: by assembling K63-linked chains on a panel of substrates (including non-physiological ones, e.g., GFP) and analysing their modification *in vivo*, one can explore the substrate specificity of UBE2K and other chain-branching enzymes.

The expansion of the Ubiquiton technology in terms of other non-canonical linkages is one of the priorities of our laboratory. Several promising candidates will be characterised *in vitro* and *in vivo*, aiming to cover all 8 linkage types in the future.

Finally, the Ubiquiton technology can be combined with the Sortase-based approach in order to site-specifically polyubiquitylate a protein of interest. Sortase-mediated ubiquitylation, in combination with genetic code expansion, has been successfully applied to attach ubiquitin to the internal residues of target proteins (Fottner *et al.,* 2019). Subsequent recruitment of tailor-made E3s would allow site-specific attachment of polyubiquitin chains, eliminating the need to attach tags to proteins. Thus, we anticipate further development of the Ubiquiton technology, leading to its broader applicability to different cellular pathways.

Chapter 5

Appendix

5.1 Abbreviations

aa	Amino acid
ADP	Adenosine-5’-diphosphate
APC	Anaphase-promoting complex
ATM	Ataxia-telangiectasia mutated
ATP	Adenosine-5’-diphosphate
ATR	Ataxia telangiectasia and Rad3 related
AQUA	Absolute quantification
BER	Base excision repair
bp	Base pair
BPDE	Benzo[a]pyrene dihydrodiol epoxide
BRCA	Breast cancer
BrdU	5-Bromo-2'-deoxyuridine
BSA	Bovine serum albumine
CHIP	Chromatin immunoprecipitation
CldU	5-Chloro-2′-deoxyuridine
CMV	Cytomegalovirus
CPD	Cyclobutane pyrimidine dimer
DMEM	Dulbecco's Modified Eagle Medium
DNA	Deoxyribonucleic acid
dNTP	Deoxynucleotide triphosphate
Dox	Doxycycline
DPC	DNA-protein crosslink
DSB	Double-strand break
dsDNA	Double-stranded deoxyribonucleic acid

DUB	Deubiquitylating enzyme
EDTA	Ethylenediaminetetraacetic acid
EdU	5-Ethynyl-2'-deoxyuridine
hco	Human codon-optimised
HECT	Homologous to E6-AP carboxyl terminus
HIRAN	HIP116 Rad5p N-terminal
HLTF	Helicase-like transcription factor
HR	Homologous recombination
hTERT	Human telomerase reverse transcriptase
HU	Hydroxyurea
ICL	Interstrand crosslink
IdU	5-Iodo-2′-deoxyuridine
IF	Immunofluorescence
LDD	Linear chain determination domain
LUBAC	Linear ubiquitin chain assembly complex
MCM	Minichromosome maintenance protein complex
MMS	Methyl methanesulfonate
MNNG	N-Methyl-N'-nitro-N-nitrosoguanidin
MVB	Multivesicular body
NEMO	NF-κB essential modulator
NER	Nucleotide excision repair
NF-κB	Nuclear factor kappa-light-chain-enhancer of activated B cells
NHEJ	Non-homologous end joining
nt	Nucleotide
NTA	Nitrilotriacetic acid
NZF	Npl4 zinc finger
ORC	Origin recognition complex
PARP	Poly (ADP-Ribose) Polymerase
PBS	Phosphate-buffered saline
PCNA	Proliferating cell nuclear antigen

PEI	Polyethyleneimine
PRIMPOL	Primase and DNA directed polymerase
PROTAC	Proteolysis targeting chimera
PTM	Post-translational modification
RBR	RING-between-RING
RING	Really interesting new gene
RNA	Ribonucleic acid
ROS	Reactive oxygen species
RPA	Replication protein A
RPE	Retinal pigment epithelium
SDS	Sodium dodecyl sulfate
SHPRH	SNF2 Histone Linker PHD RING Helicase
siRNA	Small interfering ribonucleic acid
SSB	Single-strand break
ssDNA	Single-stranded deoxyribonucleic acid
TLS	Translesion synthesis
TRC	Transcription-replication conflict
TS	Template switching
UBAN	Ubiquitin-binding domain in ABIN proteins and NEMO
UBD	Ubiquitin-binding domain
UBICREST	Ubiquitin chain restriction
UBLs	Ubiquitin-like proteins
UBZ	Ubiquitin-binding zinc finger
UIM	Ubiquitin-interacting motif
UPS	Ubiquitin-Proteasome system
UV	Ultraviolet light
VCP	Valosin-containing protein
VSV	Vesicular stomatitis virus

5.2 Publications

Asimaki, Evrydiki**; Petriukov, Kirill**; Renz, Christian; Meister, Cindy; Ulrich, Helle D. (2022): Fast friends - Ubiquitin-like modifiers as engineered fusion partners. In Seminars in cell & developmental biology 132, pp. 132–145. DOI: 10.1016/j.semcdb.2021.11.013.

Golovina, Anna Y.; Dzama, Margarita M.; **Petriukov, Kirill S.**; Zatsepin, Timofei S.; Sergiev, Petr V.; Bogdanov, Alexey A.; Dontsova, Olga A. (2014): Method for site-specific detection of m6A nucleoside presence in RNA based on high-resolution melting (HRM) analysis. In Nucleic acids research 42 (4), e27. DOI: 10.1093/nar/gkt1160.

Oo, James A.; Pálfi, Katalin; Warwick, Timothy; Wittig, Ilka; Prieto-Garcia, Cristian; Matkovic, Vigor; Tomaskovic, Ines; Boos, Frederike; Ponce, Judit Izquierdo; Teichmann, Tom; **Petriukov, Kirill** *et al.,* (2022): Long non-coding RNA PCAT19 safeguards DNA in quiescent endothelial cells by preventing uncontrolled phosphorylation of RPA2. In Cell reports 41 (7), p. 111670. DOI: 10.1016/j.celrep.2022.111670.

Sergiev, Petr V.; Golovina, Anna Ya; Osterman, Ilya A.; Nesterchuk, Michail V.; Sergeeva, Olga V.; Chugunova, Anastasia A.; Evfratov, Sergey A.; Andreianova, Ekaterina S.; Pletnev, Philipp P.; Laptev, Ivan G.; **Petriukov, Kirill S**. *et al.,* (2016): N6-Methylated Adenosine in RNA: From Bacteria to Humans. In Journal of molecular biology 428 (10 Pt B), pp. 2134–2145. DOI: 10.1016/j.jmb.2015.12.013.

Wong, Ronald P.; **Petriukov, Kirill**; Ulrich, Helle D. (2021): Daughter-strand gaps in DNA replication - substrates of lesion processing and initiators of distress signalling. In DNA repair 105, p. 103163. DOI: 10.1016/j.dnarep.2021.103163.

5.3 Curriculum Vitae

Personal information

Name:	Kirill Petriukov
Address:	Josefsstrasse 1, 55118 Mainz
E-mail:	k.petriukov@imb-mainz.de
Date of birth:	30.05.1995
Place of birth:	Saint-Petersburg, Russian Federation

Education

Since 08/2018	PhD student, Institute of Molecular Biology (IMB), Mainz
	Research group of Prof. Dr. Helle Ulrich
	Research topic: Analysing polyubiquitin chain signalling by means of tailor-made ubiquitin ligases
09/2012 – 07/2018	Specialist in Chemistry (equivalent of M.Sc.)
	Final grade: 1.0
	Master thesis: Search for targets of the putative methyltransferase NSUN7
09/2001 – 07/2012	High school diploma, Gymnasium 526 Saint-Petersburg
	Final grade: 1.0

Bibliography

Achar, Yathish Jagadheesh; Balogh, David; Neculai, Dante; Juhasz, Szilvia; Morocz, Monika; Gali, Himabindu et al. (2015): Human HLTF mediates postreplication repair by its HIRAN domain-dependent replication fork remodelling. In *Nucleic acids research* 43 (21), pp. 10277–10291. DOI: 10.1093/nar/gkv896.

Acharya, Narottam; Yoon, Jung-Hoon; Gali, Himabindu; Unk, Ildiko; Haracska, Lajos; Johnson, Robert E. et al. (2008): Roles of PCNA-binding and ubiquitin-binding domains in human DNA polymerase eta in translesion DNA synthesis. In *Proceedings of the National Academy of Sciences of the United States of America* 105 (46), pp. 17724–17729. DOI: 10.1073/pnas.0809844105.

Ahlstedt, Brittany A.; Ganji, Rakesh; Raman, Malavika (2022): The functional importance of VCP to maintaining cellular protein homeostasis. In *Biochemical Society transactions* 50 (5), pp. 1457–1469. DOI: 10.1042/BST20220648.

Akizuki, Yoshino; Morita, Mai; Mori, Yuki; Kaiho-Soma, Ai; Dixit, Shivani; Endo, Akinori et al. (2023): cIAP1-based degraders induce degradation via branched ubiquitin architectures. In *Nature chemical biology* 19 (3), pp. 311–322. DOI: 10.1038/s41589-022-01178-1.

Al-Hakim, Abdallah K.; Zagorska, Anna; Chapman, Louise; Deak, Maria; Peggie, Mark; Alessi, Dario R. (2008): Control of AMPK-related kinases by USP9X and atypical Lys(29)/Lys(33)-linked polyubiquitin chains. In *The Biochemical journal* 411 (2), pp. 249–260. DOI: 10.1042/BJ20080067.

Ali, Ammar A. E.; Timinszky, Gyula; Arribas-Bosacoma, Raquel; Kozlowski, Marek; Hassa, Paul O.; Hassler, Markus et al. (2012): The zinc-finger domains of PARP1 cooperate to recognize DNA strand breaks. In *Nature structural & molecular biology* 19 (7), pp. 685–692. DOI: 10.1038/nsmb.2335.

An, Ran; Jia, Yu; Wan, Baihui; Zhang, Yanfang; Dong, Ping; Li, Jing; Liang, Xingguo (2014): Non-enzymatic depurination of nucleic acids: factors and mechanisms. In *PloS one* 9 (12), e115950. DOI: 10.1371/journal.pone.0115950.

Asimaki, Evrydiki; Petriukov, Kirill; Renz, Christian; Meister, Cindy; Ulrich, Helle D. (2022): Fast friends - Ubiquitin-like modifiers as engineered fusion partners. In *Seminars in cell & developmental biology* 132, pp. 132–145. DOI: 10.1016/j.semcdb.2021.11.013.

Bagola, Katrin; Delbrück, Maximilian von; Dittmar, Gunnar; Scheffner, Martin; Ziv, Inbal; Glickman, Michael H. et al. (2013): Ubiquitin binding by a CUE domain regulates ubiquitin chain formation by ERAD E3 ligases. In *Molecular Cell* 50 (4), pp. 528–539. DOI: 10.1016/j.molcel.2013.04.005.

Bai, Gongshi; Kermi, Chames; Stoy, Henriette; Schiltz, Carl J.; Bacal, Julien; Zaino, Angela M. et al. (2020): HLTF Promotes Fork Reversal, Limiting Replication Stress Resistance and Preventing Multiple Mechanisms of Unrestrained DNA Synthesis. In *Molecular Cell* 78 (6), 1237-1251.e7. DOI: 10.1016/j.molcel.2020.04.031.

Bai, Wenya; Huo, Siying; Li, Junjie; Shao, Jianlin (2022): Advances in the Study of the Ubiquitin-Editing Enzyme A20. In *Frontiers in pharmacology* 13, p. 845262. DOI: 10.3389/fphar.2022.845262.

Balogun, Fiyinfolu O.; Truman, Andrew W.; Kron, Stephen J. (2013): DNA resection proteins Sgs1 and Exo1 are required for G1 checkpoint activation in budding yeast. In *DNA repair* 12 (9), pp. 751–760. DOI: 10.1016/j.dnarep.2013.06.003.

Bannister, Andrew J.; Kouzarides, Tony (2011): Regulation of chromatin by histone modifications. In *Cell research* 21 (3), pp. 381–395. DOI: 10.1038/cr.2011.22.

Baris, Yasemin; Taylor, Martin R. G.; Aria, Valentina; Yeeles, Joseph T. P. (2022): Fast and efficient DNA replication with purified human proteins. In *Nature* 606 (7912), pp. 204–210. DOI: 10.1038/s41586-022-04759-1.

Bębenek, Anna; Ziuzia-Graczyk, Izabela (2018): Fidelity of DNA replication-a matter of proofreading. In *Current genetics* 64 (5), pp. 985–996. DOI: 10.1007/s00294-018-0820-1.

Beck, Halfdan; Nähse-Kumpf, Viola; Larsen, Marie Sofie Yoo; O'Hanlon, Karen A.; Patzke, Sebastian; Holmberg, Christian et al. (2012): Cyclin-dependent kinase suppression by WEE1 kinase protects the genome through control of replication initiation and nucleotide consumption. In *Molecular and cellular biology* 32 (20), pp. 4226–4236. DOI: 10.1128/MCB.00412-12.

Békés, Miklós; Langley, David R.; Crews, Craig M. (2022): PROTAC targeted protein degraders: the past is prologue. In *Nature reviews. Drug discovery* 21 (3), pp. 181–200. DOI: 10.1038/s41573-021-00371-6.

Ben-Saadon, Ronen; Fajerman, Ifat; Ziv, Tamar; Hellman, Ulf; Schwartz, Alan L.; Ciechanover, Aaron (2004): The tumor suppressor protein p16(INK4a) and the human papillomavirus oncoprotein-58 E7 are naturally occurring lysine-less proteins that are degraded by the ubiquitin system. Direct evidence for ubiquitination at the N-terminal residue. In *The Journal of biological chemistry* 279 (40), pp. 41414–41421. DOI: 10.1074/jbc.M407201200.

Ben-Saadon, Ronen; Zaaroor, Daphna; Ziv, Tamar; Ciechanover, Aaron (2006): The polycomb protein Ring1B generates self atypical mixed ubiquitin chains required for its in vitro histone H2A ligase activity. In *Molecular Cell* 24 (5), pp. 701–711. DOI: 10.1016/j.molcel.2006.10.022.

Bergoglio, V.; Magnaldo, T. (2006): Nucleotide excision repair and related human diseases. In *Genome dynamics* 1, pp. 35–52. DOI: 10.1159/000092499.

Bienko, Marzena; Green, Catherine M.; Crosetto, Nicola; Rudolf, Fabian; Zapart, Grzegorz; Coull, Barry et al. (2005): Ubiquitin-binding domains in Y-family polymerases regulate translesion synthesis. In *Science (New York, N.Y.)* 310 (5755), pp. 1821–1824. DOI: 10.1126/science.1120615.

Bjelland, S.; Bjørås, M.; Seeberg, E. (1993): Excision of 3-methylguanine from alkylated DNA by 3-methyladenine DNA glycosylase I of Escherichia coli. In *Nucleic acids research* 21 (9), pp. 2045–2049. DOI: 10.1093/nar/21.9.2045.

Blastyák, András; Pintér, Lajos; Unk, Ildiko; Prakash, Louise; Prakash, Satya; Haracska, Lajos (2007): Yeast Rad5 protein required for postreplication repair has a DNA helicase activity specific for replication fork regression. In *Molecular Cell* 28 (1), pp. 167–175. DOI: 10.1016/j.molcel.2007.07.030.

Boone, Julien J. M.; Bhosle, Jaishree; Tilby, Mike J.; Hartley, John A.; Hochhauser, Daniel (2009): Involvement of the HER2 pathway in repair of DNA damage produced by chemotherapeutic agents. In *Molecular cancer therapeutics* 8 (11), pp. 3015–3023. DOI: 10.1158/1535-7163.MCT-09-0219.

Boughton, Andrew J.; Krueger, Susan; Fushman, David (2020): Branching via K11 and K48 Bestows Ubiquitin Chains with a Unique Interdomain Interface and Enhanced Affinity for Proteasomal Subunit Rpn1. In *Structure (London, England : 1993)* 28 (1), 29-43.e6. DOI: 10.1016/j.str.2019.10.008.

Branzei, Dana; Szakal, Barnabas (2016): DNA damage tolerance by recombination: Molecular pathways and DNA structures. In *DNA repair* 44, pp. 68–75. DOI: 10.1016/j.dnarep.2016.05.008.

Branzei, Dana; Vanoli, Fabio; Foiani, Marco (2008): SUMOylation regulates Rad18-mediated template switch. In *Nature* 456 (7224), pp. 915–920. DOI: 10.1038/nature07587.

Caldecott, Keith W. (2008): Single-strand break repair and genetic disease. In *Nature reviews. Genetics* 9 (8), pp. 619–631. DOI: 10.1038/nrg2380.

Ceccaldi, Raphael; Rondinelli, Beatrice; D'Andrea, Alan D. (2016): Repair Pathway Choices and Consequences at the Double-Strand Break. In *Trends in cell biology* 26 (1), pp. 52–64. DOI: 10.1016/j.tcb.2015.07.009.

Centore, Richard C.; Yazinski, Stephanie A.; Tse, Alice; Zou, Lee (2012): Spartan/C1orf124, a reader of PCNA ubiquitylation and a regulator of UV-induced DNA damage response. In *Molecular Cell* 46 (5), pp. 625–635. DOI: 10.1016/j.molcel.2012.05.020.

Champoux, J. J. (2001): DNA topoisomerases: structure, function, and mechanism. In *Annual review of biochemistry* 70, pp. 369–413. DOI: 10.1146/annurev.biochem.70.1.369.

Chan, Kin; Resnick, Michael A.; Gordenin, Dmitry A. (2013): The choice of nucleotide inserted opposite abasic sites formed within chromosomal DNA reveals the polymerase activities participating in translesion DNA synthesis. In *DNA repair* 12 (11), pp. 878–889. DOI: 10.1016/j.dnarep.2013.07.008.

Chang, Howard H. Y.; Pannunzio, Nicholas R.; Adachi, Noritaka; Lieber, Michael R. (2017): Non-homologous DNA end joining and alternative pathways to double-strand break repair. In *Nature reviews. Molecular cell biology* 18 (8), pp. 495–506. DOI: 10.1038/nrm.2017.48.

Chang, Shih Chieh; Gopal, Pooja; Lim, Shuhui; Wei, Xiaona; Chandramohan, Arun; Mangadu, Ruban et al. (2022): Targeted degradation of PCNA outperforms stoichiometric inhibition to result in programed cell death. In *Cell chemical biology* 29 (11), 1601-1615.e7. DOI: 10.1016/j.chembiol.2022.10.005.

Chen, J.; Zheng, X. F.; Brown, E. J.; Schreiber, S. L. (1995): Identification of an 11-kDa FKBP12-rapamycin-binding domain within the 289-kDa FKBP12-rapamycin-associated protein and characterization of a critical serine residue. In *Proceedings of the National Academy of Sciences of the United States of America* 92 (11), pp. 4947–4951. DOI: 10.1073/pnas.92.11.4947.

Chen, Li; Madura, Kiran (2002): Rad23 promotes the targeting of proteolytic substrates to the proteasome. In *Molecular and cellular biology* 22 (13), pp. 4902–4913. DOI: 10.1128/MCB.22.13.4902-4913.2002.

Chen, Xiaoqing; Paudyal, Sharad C.; Chin, Re-I; You, Zhongsheng (2013): PCNA promotes processive DNA end resection by Exo1. In *Nucleic acids research* 41 (20), pp. 9325–9338. DOI: 10.1093/nar/gkt672.

Chiu, Roland K.; Brun, Jan; Ramaekers, Chantal; Theys, Jan; Weng, Lin; Lambin, Philippe et al. (2006): Lysine 63-polyubiquitination guards against translesion synthesis-induced mutations. In *PLoS genetics* 2 (7), e116. DOI: 10.1371/journal.pgen.0020116.

Choe, Katherine N.; Nicolae, Claudia M.; Constantin, Daniel; Imamura Kawasawa, Yuka; Delgado-Diaz, Maria Rocio; De, Subhajyoti et al. (2016): HUWE1 interacts with PCNA to alleviate replication stress. In *EMBO reports* 17 (6), pp. 874–886. DOI: 10.15252/embr.201541685.

Choi, Koyi; Batke, Sabrina; Szakal, Barnabas; Lowther, Jonathan; Hao, Fanfan; Sarangi, Prabha et al. (2015): Concerted and differential actions of two enzymatic domains underlie Rad5 contributions to DNA damage tolerance. In *Nucleic acids research* 43 (5), pp. 2666–2677. DOI: 10.1093/nar/gkv004.

Ciccia, Alberto; Nimonkar, Amitabh V.; Hu, Yiduo; Hajdu, Ildiko; Achar, Yathish Jagadheesh; Izhar, Lior et al. (2012): Polyubiquitinated PCNA recruits the ZRANB3 translocase to maintain genomic integrity after replication stress. In *Molecular Cell* 47 (3), pp. 396–409. DOI: 10.1016/j.molcel.2012.05.024.

Ciechanover, A.; Heller, H.; Elias, S.; Haas, A. L.; Hershko, A. (1980): ATP-dependent conjugation of reticulocyte proteins with the polypeptide required for protein degradation. In *Proceedings of the National Academy of Sciences of the United States of America* 77 (3), pp. 1365–1368. DOI: 10.1073/pnas.77.3.1365.

Ciechanover, Aaron (2005): N-terminal ubiquitination. In *Methods in molecular biology (Clifton, N.J.)* 301, pp. 255–270. DOI: 10.1385/1-59259-895-1:255.

Cipolla, Lina; Bertoletti, Federica; Maffia, Antonio; Liang, Chih-Chao; Lehmann, Alan R.; Cohn, Martin A.; Sabbioneda, Simone (2019): UBR5 interacts with the replication fork and protects DNA replication from DNA polymerase η toxicity. In *Nucleic acids research* 47 (21), pp. 11268–11283. DOI: 10.1093/nar/gkz824.

Cong, Ke; Peng, Min; Kousholt, Arne Nedergaard; Lee, Wei Ting C.; Lee, Silviana; Nayak, Sumeet et al. (2021): Replication gaps are a key determinant of PARP inhibitor synthetic lethality with BRCA deficiency. In *Molecular Cell* 81 (15), 3128-3144.e7. DOI: 10.1016/j.molcel.2021.06.011.

Cooney, Ian; Han, Han; Stewart, Michael G.; Carson, Richard H.; Hansen, Daniel T.; Iwasa, Janet H. et al. (2019): Structure of the Cdc48 segregase in the act of unfolding an authentic substrate. In *Science (New York, N.Y.)* 365 (6452), pp. 502–505. DOI: 10.1126/science.aax0486.

Couch, Frank B.; Bansbach, Carol E.; Driscoll, Robert; Luzwick, Jessica W.; Glick, Gloria G.; Bétous, Rémy et al. (2013): ATR phosphorylates SMARCAL1 to prevent replication fork collapse. In *Genes & development* 27 (14), pp. 1610–1623. DOI: 10.1101/gad.214080.113.

Courtot, Lilas; Hoffmann, Jean-Sébastien; Bergoglio, Valérie (2018): The Protective Role of Dormant Origins in Response to Replicative Stress. In *International journal of molecular sciences* 19 (11). DOI: 10.3390/ijms19113569.

Cui, Lun; Bikard, David (2016): Consequences of Cas9 cleavage in the chromosome of Escherichia coli. In *Nucleic acids research* 44 (9), pp. 4243–4251. DOI: 10.1093/nar/gkw223.

Daigaku, Yasukazu; Davies, Adelina A.; Ulrich, Helle D. (2010): Ubiquitin-dependent DNA damage bypass is separable from genome replication. In *Nature* 465 (7300), pp. 951–955. DOI: 10.1038/nature09097.

Dalgaard, Jacob Z. (2012): Causes and consequences of ribonucleotide incorporation into nuclear DNA. In *Trends in genetics : TIG* 28 (12), pp. 592–597. DOI: 10.1016/j.tig.2012.07.008.

Davis, Emily J.; Lachaud, Christophe; Appleton, Paul; Macartney, Thomas J.; Näthke, Inke; Rouse, John (2012): DVC1 (C1orf124) recruits the p97 protein segregase to sites of DNA damage. In *Nature structural & molecular biology* 19 (11), pp. 1093–1100. DOI: 10.1038/nsmb.2394.

Deans, Andrew J.; West, Stephen C. (2011): DNA interstrand crosslink repair and cancer. In *Nature reviews. Cancer* 11 (7), pp. 467–480. DOI: 10.1038/nrc3088.

Deng, L.; Wang, C.; Spencer, E.; Yang, L.; Braun, A.; You, J. et al. (2000): Activation of the IkappaB kinase complex by TRAF6 requires a dimeric ubiquitin-conjugating enzyme complex and a unique polyubiquitin chain. In *Cell* 103 (2), pp. 351–361. DOI: 10.1016/s0092-8674(00)00126-4.

Dewar, James M.; Walter, Johannes C. (2017): Mechanisms of DNA replication termination. In *Nature reviews. Molecular cell biology* 18 (8), pp. 507–516. DOI: 10.1038/nrm.2017.42.

Dittmar, Gunnar; Winklhofer, Konstanze F. (2019): Linear Ubiquitin Chains: Cellular Functions and Strategies for Detection and Quantification. In *Frontiers in chemistry* 7, p. 915. DOI: 10.3389/fchem.2019.00915.

Dolan, M. E.; Moschel, R. C.; Pegg, A. E. (1990): Depletion of mammalian O6-alkylguanine-DNA alkyltransferase activity by O6-benzylguanine provides a means to evaluate the role of this protein in protection against carcinogenic and therapeutic alkylating agents. In *Proceedings of the National Academy of Sciences of the United States of America* 87 (14), pp. 5368–5372. DOI: 10.1073/pnas.87.14.5368.

Donnianni, Roberto A.; Symington, Lorraine S. (2013): Break-induced replication occurs by conservative DNA synthesis. In *Proceedings of the National Academy of Sciences of the United States of America* 110 (33), pp. 13475–13480. DOI: 10.1073/pnas.1309800110.

Dynek, Jasmin N.; Goncharov, Tatiana; Dueber, Erin C.; Fedorova, Anna V.; Izrael-Tomasevic, Anita; Phu, Lilian et al. (2010): c-IAP1 and UbcH5 promote K11-linked polyubiquitination of RIP1 in TNF signalling. In *The EMBO journal* 29 (24), pp. 4198–4209. DOI: 10.1038/emboj.2010.300.

Edmunds, Charlotte E.; Simpson, Laura J.; Sale, Julian E. (2008): PCNA ubiquitination and REV1 define temporally distinct mechanisms for controlling translesion synthesis in the avian cell line DT40. In *Molecular Cell* 30 (4), pp. 519–529. DOI: 10.1016/j.molcel.2008.03.024.

Elia, Andrew E. H.; Boardman, Alexander P.; Wang, David C.; Huttlin, Edward L.; Everley, Robert A.; Dephoure, Noah et al. (2015): Quantitative Proteomic Atlas of Ubiquitination and Acetylation in the DNA Damage Response. In *Molecular Cell* 59 (5), pp. 867–881. DOI: 10.1016/j.molcel.2015.05.006.

Elstrodt, Fons; Hollestelle, Antoinette; Nagel, Jord H. A.; Gorin, Michael; Wasielewski, Marijke; van den Ouweland, Ans et al. (2006): BRCA1 mutation analysis of 41 human breast cancer cell lines reveals three new deleterious mutants. In *Cancer research* 66 (1), pp. 41–45. DOI: 10.1158/0008-5472.CAN-05-2853.

Emmerich, Christoph H.; Ordureau, Alban; Strickson, Sam; Arthur, J. Simon C.; Pedrioli, Patrick G. A.; Komander, David; Cohen, Philip (2013): Activation of the canonical IKK complex by K63/M1-linked hybrid ubiquitin chains. In *Proceedings of the National Academy of Sciences of the United States of America* 110 (38), pp. 15247–15252. DOI: 10.1073/pnas.1314715110.

Erenpreisa, Jekaterina; Cragg, Mark S. (2013): Three steps to the immortality of cancer cells: senescence, polyploidy and self-renewal. In *Cancer cell international* 13 (1), p. 92. DOI: 10.1186/1475-2867-13-92.

Fei, Cong; Li, Zhenfei; Li, Chen; Chen, Yuelei; Chen, Zhangcheng; He, Xiaoli et al. (2013): Smurf1-mediated Lys29-linked nonproteolytic polyubiquitination of axin negatively regulates Wnt/β-catenin signaling. In *Molecular and cellular biology* 33 (20), pp. 4095–4105. DOI: 10.1128/MCB.00418-13.

Fennell, Lilian M.; Rahighi, Simin; Ikeda, Fumiyo (2018): Linear ubiquitin chain-binding domains. In *The FEBS journal* 285 (15), pp. 2746–2761. DOI: 10.1111/febs.14478.

Finley, D.; Sadis, S.; Monia, B. P.; Boucher, P.; Ecker, D. J.; Crooke, S. T.; Chau, V. (1994): Inhibition of proteolysis and cell cycle progression in a multiubiquitination-deficient yeast mutant. In *Molecular and cellular biology* 14 (8), pp. 5501–5509. DOI: 10.1128/mcb.14.8.5501-5509.1994.

Fottner, Maximilian; Brunner, Andreas-David; Bittl, Verena; Horn-Ghetko, Daniel; Jussupow, Alexander; Kaila, Ville R. I. et al. (2019): Site-specific ubiquitylation and SUMOylation using genetic-code expansion and sortase. In *Nature chemical biology* 15 (3), pp. 276–284. DOI: 10.1038/s41589-019-0227-4.

Freudenthal, Bret D.; Gakhar, Lokesh; Ramaswamy, S.; Washington, M. Todd (2010): Structure of monoubiquitinated PCNA and implications for translesion synthesis and DNA polymerase exchange. In *Nature structural & molecular biology* 17 (4), pp. 479–484. DOI: 10.1038/nsmb.1776.

Fumasoni, Marco; Zwicky, Katharina; Vanoli, Fabio; Lopes, Massimo; Branzei, Dana (2015): Error-free DNA damage tolerance and sister chromatid proximity during DNA replication rely on the Polα/Primase/Ctf4 Complex. In *Molecular Cell* 57 (5), pp. 812–823. DOI: 10.1016/j.molcel.2014.12.038.

Galan, J. M.; Haguenauer-Tsapis, R. (1997): Ubiquitin lys63 is involved in ubiquitination of a yeast plasma membrane protein. In *The EMBO journal* 16 (19), pp. 5847–5854. DOI: 10.1093/emboj/16.19.5847.

Gallina, Irene; Hendriks, Ivo A.; Hoffmann, Saskia; Larsen, Nicolai B.; Johansen, Joachim; Colding-Christensen, Camilla S. et al. (2021): The ubiquitin ligase RFWD3 is required for translesion DNA synthesis. In *Molecular Cell* 81 (3), 442-458.e9. DOI: 10.1016/j.molcel.2020.11.029.

Gallo, David; Kim, TaeHyung; Szakal, Barnabas; Saayman, Xanita; Narula, Ashrut; Park, Yoona et al. (2019): Rad5 Recruits Error-Prone DNA Polymerases for Mutagenic Repair of ssDNA Gaps on Undamaged Templates. In *Molecular Cell* 73 (5), 900-914.e9. DOI: 10.1016/j.molcel.2019.01.001.

García-Rodríguez, Néstor; Morawska, Magdalena; Wong, Ronald P.; Daigaku, Yasukazu; Ulrich, Helle D. (2018a): Spatial separation between replisome- and template-induced replication stress signaling. In *The EMBO journal* 37 (9). DOI: 10.15252/embj.201798369.

García-Rodríguez, Néstor; Wong, Ronald P.; Ulrich, Helle D. (2016): Functions of Ubiquitin and SUMO in DNA Replication and Replication Stress. In *Frontiers in genetics* 7, p. 87. DOI: 10.3389/fgene.2016.00087.

García-Rodríguez, Néstor; Wong, Ronald P.; Ulrich, Helle D. (2018b): The helicase Pif1 functions in the template switching pathway of DNA damage bypass. In *Nucleic acids research* 46 (16), pp. 8347–8356. DOI: 10.1093/nar/gky648.

Gatti, Marco; Pinato, Sabrina; Maiolica, Alessio; Rocchio, Francesca; Prato, Maria Giulia; Aebersold, Ruedi; Penengo, Lorenza (2015): RNF168 promotes noncanonical K27 ubiquitination to signal DNA damage. In *Cell reports* 10 (2), pp. 226–238. DOI: 10.1016/j.celrep.2014.12.021.

Giannattasio, Michele; Zwicky, Katharina; Follonier, Cindy; Foiani, Marco; Lopes, Massimo; Branzei, Dana (2014): Visualization of recombination-mediated damage bypass by template switching. In *Nature structural & molecular biology* 21 (10), pp. 884–892. DOI: 10.1038/nsmb.2888.

Gómez-Pinto, Irene; Cubero, Elena; Kalko, Susana G.; Monaco, Vania; van der Marel, Gijs; van Boom, Jacques H. et al. (2004): Effect of bulky lesions on DNA: solution structure of a DNA duplex containing a cholesterol adduct. In *The Journal of biological chemistry* 279 (23), pp. 24552–24560. DOI: 10.1074/jbc.M311751200.

Gonzalez-Santamarta, Maria; Ceccato, Laurie; Carvalho, Ana Sofia; Rain, Jean-Christophe; Matthiesen, Rune; Rodriguez, Manuel S. (2023): Isolation and Mass Spectrometry Identification of K48 and K63 Ubiquitin Proteome Using Chain-Specific Nanobodies. In *Methods in molecular biology (Clifton, N.J.)* 2602, pp. 125–136. DOI: 10.1007/978-1-0716-2859-1_9.

Grabbe, Caroline; Dikic, Ivan (2009): Functional roles of ubiquitin-like domain (ULD) and ubiquitin-binding domain (UBD) containing proteins. In *Chemical reviews* 109 (4), pp. 1481–1494. DOI: 10.1021/cr800413p.

Gudjonsson, Thorkell; Altmeyer, Matthias; Savic, Velibor; Toledo, Luis; Dinant, Christoffel; Grøfte, Merete et al. (2012): TRIP12 and UBR5 suppress spreading of chromatin ubiquitylation at damaged chromosomes. In *Cell* 150 (4), pp. 697–709. DOI: 10.1016/j.cell.2012.06.039.

Guilliam, Thomas A.; Brissett, Nigel C.; Ehlinger, Aaron; Keen, Benjamin A.; Kolesar, Peter; Taylor, Elaine M. et al. (2017): Molecular basis for PrimPol recruitment to replication forks by RPA. In *Nature Communications* 8, p. 15222. DOI: 10.1038/ncomms15222.

Guo, Caixia; Sonoda, Eiichiro; Tang, Tie-Shan; Parker, Joanne L.; Bielen, Aleksandra B.; Takeda, Shunichi et al. (2006): REV1 protein interacts with PCNA: significance of the REV1 BRCT domain in vitro and in vivo. In *Molecular Cell* 23 (2), pp. 265–271. DOI: 10.1016/j.molcel.2006.05.038.

Guo, Yafei; Li, Qin; Zhao, Gang; Zhang, Jie; Yuan, Hang; Feng, Tianyu et al. (2021): Loss of TRIM31 promotes breast cancer progression through regulating K48- and K63-linked ubiquitination of p53. In *Cell death & disease* 12 (10), p. 945. DOI: 10.1038/s41419-021-04208-3.

Haas, A. L.; Bright, P. M. (1985): The immunochemical detection and quantitation of intracellular ubiquitin-protein conjugates. In *The Journal of biological chemistry* 260 (23), pp. 12464–12473.

Hagai, Tzachi; Levy, Yaakov (2010): Ubiquitin not only serves as a tag but also assists degradation by inducing protein unfolding. In *Proceedings of the National Academy of Sciences of the United States of America* 107 (5), pp. 2001–2006. DOI: 10.1073/pnas.0912335107.

Haglund, Kaisa; Sigismund, Sara; Polo, Simona; Szymkiewicz, Iwona; Di Fiore, Pier Paolo; Dikic, Ivan (2003): Multiple monoubiquitination of RTKs is sufficient for their endocytosis and degradation. In *Nature cell biology* 5 (5), pp. 461–466. DOI: 10.1038/ncb983.

Hahn, H.; Palmenberg, A. C. (1996): Mutational analysis of the encephalomyocarditis virus primary cleavage. In *Journal of virology* 70 (10), pp. 6870–6875. DOI: 10.1128/JVI.70.10.6870-6875.1996.

Halder, Swagata; Ranjha, Lepakshi; Taglialatela, Angelo; Ciccia, Alberto; Cejka, Petr (2022): Strand annealing and motor driven activities of SMARCAL1 and ZRANB3 are stimulated by RAD51 and the paralog complex. In *Nucleic acids research* 50 (14), pp. 8008–8022. DOI: 10.1093/nar/gkac583.

Hanada, Katsuhiro; Budzowska, Magda; Davies, Sally L.; van Drunen, Ellen; Onizawa, Hideo; Beverloo, H. Berna et al. (2007): The structure-specific endonuclease Mus81 contributes to replication restart by generating double-strand DNA breaks. In *Nature structural & molecular biology* 14 (11), pp. 1096–1104. DOI: 10.1038/nsmb1313.

Heidelberger, Jan B.; Voigt, Andrea; Borisova, Marina E.; Petrosino, Giuseppe; Ruf, Stefanie; Wagner, Sebastian A.; Beli, Petra (2018): Proteomic profiling of VCP substrates links VCP to K6-linked ubiquitylation and c-Myc function. In *EMBO reports* 19 (4). DOI: 10.15252/embr.201744754.

Hendel, Ayal; Ziv, Omer; Gueranger, Quentin; Geacintov, Nicholas; Livneh, Zvi (2008): Reduced efficiency and increased mutagenicity of translesion DNA synthesis across a TT cyclobutane pyrimidine dimer, but not a TT 6-4 photoproduct, in human cells lacking DNA polymerase eta. In *DNA repair* 7 (10), pp. 1636–1646. DOI: 10.1016/j.dnarep.2008.06.008.

Henning, Nathaniel J.; Boike, Lydia; Spradlin, Jessica N.; Ward, Carl C.; Liu, Gang; Zhang, Erika et al. (2022): Deubiquitinase-targeting chimeras for targeted protein stabilization. In *Nature chemical biology* 18 (4), pp. 412–421. DOI: 10.1038/s41589-022-00971-2.

Hergeth, Sonja P.; Schneider, Robert (2015): The H1 linker histones: multifunctional proteins beyond the nucleosomal core particle. In *EMBO reports* 16 (11), pp. 1439–1453. DOI: 10.15252/embr.201540749.

Hershko, A.; Ciechanover, A.; Heller, H.; Haas, A. L.; Rose, I. A. (1980): Proposed role of ATP in protein breakdown: conjugation of protein with multiple chains of the polypeptide of ATP-dependent proteolysis. In *Proceedings of the National Academy of Sciences of the United States of America* 77 (4), pp. 1783–1786. DOI: 10.1073/pnas.77.4.1783.

Hess, M. T.; Gunz, D.; Luneva, N.; Geacintov, N. E.; Naegeli, H. (1997): Base pair conformation-dependent excision of benzoapyrene diol epoxide-guanine adducts by human nucleotide excision repair enzymes. In *Molecular and cellular biology* 17 (12), pp. 7069–7076. DOI: 10.1128/MCB.17.12.7069.

Hibbert, Richard G.; Sixma, Titia K. (2012): Intrinsic flexibility of ubiquitin on proliferating cell nuclear antigen (PCNA) in translesion synthesis. In *The Journal of biological chemistry* 287 (46), pp. 39216–39223. DOI: 10.1074/jbc.M112.389890.

Hicke, L. (2001): Protein regulation by monoubiquitin. In *Nature reviews. Molecular cell biology* 2 (3), pp. 195–201. DOI: 10.1038/35056583.

Hodge, Curtis D.; Spyracopoulos, Leo; Glover, J. N. Mark (2016): Ubc13: the Lys63 ubiquitin chain building machine. In *Oncotarget* 7 (39), pp. 64471–64504. DOI: 10.18632/oncotarget.10948.

Hoege, Carsten; Pfander, Boris; Moldovan, George-Lucian; Pyrowolakis, George; Jentsch, Stefan (2002): RAD6-dependent DNA repair is linked to modification of PCNA by ubiquitin and SUMO. In *Nature* 419 (6903), pp. 135–141. DOI: 10.1038/nature00991.

Hospenthal, Manuela K.; Mevissen, Tycho E. T.; Komander, David (2015): Deubiquitinase-based analysis of ubiquitin chain architecture using Ubiquitin Chain Restriction (UbiCRest). In *Nature protocols* 10 (2), pp. 349–361. DOI: 10.1038/nprot.2015.018.

Hu, Yiduo; Scully, Ralph; Sobhian, Bijan; Xie, Anyong; Shestakova, Elena; Livingston, David M. (2011): RAP80-directed tuning of BRCA1 homologous recombination function at ionizing radiation-induced nuclear foci. In *Genes & development* 25 (7), pp. 685–700. DOI: 10.1101/gad.2011011.

Huang, Haining; Jeon, Myung-Shin; Liao, Lujian; Yang, Chun; Elly, Chris; Yates, John R. 3rd; Liu, Yun-Cai (2010): K33-linked polyubiquitination of T cell receptor-zeta regulates proteolysis-independent T cell signaling. In *Immunity* 33 (1), pp. 60–70. DOI: 10.1016/j.immuni.2010.07.002.

Huang, Tony T.; Nijman, Sebastian M. B.; Mirchandani, Kanchan D.; Galardy, Paul J.; Cohn, Martin A.; Haas, Wilhelm et al. (2006): Regulation of monoubiquitinated PCNA by DUB autocleavage. In *Nature cell biology* 8 (4), pp. 339–347. DOI: 10.1038/ncb1378.

Husnjak, Koraljka; Dikic, Ivan (2012): Ubiquitin-binding proteins: decoders of ubiquitin-mediated cellular functions. In *Annual review of biochemistry* 81, pp. 291–322. DOI: 10.1146/annurev-biochem-051810-094654.

Igoucheva, O.; Alexeev, V.; Yoon, K. (2006): Differential cellular responses to exogenous DNA in mammalian cells and its effect on oligonucleotide-directed gene modification. In *Gene therapy* 13 (3), pp. 266–275. DOI: 10.1038/sj.gt.3302643.

Izhar, Lior; Ziv, Omer; Cohen, Isadora S.; Geacintov, Nicholas E.; Livneh, Zvi (2013): Genomic assay reveals tolerance of DNA damage by both translesion DNA synthesis and homology-dependent repair in mammalian cells. In *Proceedings of the National Academy of Sciences of the United States of America* 110 (16), E1462-9. DOI: 10.1073/pnas.1216894110.

Jha, Vikash; Bian, Chuanbing; Xing, Guangxin; Ling, Hong (2016): Structure and mechanism of error-free replication past the major benzoapyrene adduct by human DNA polymerase κ. In *Nucleic acids research* 44 (10), pp. 4957–4967. DOI: 10.1093/nar/gkw204.

Johnson, E. S.; Ma, P. C.; Ota, I. M.; Varshavsky, A. (1995): A proteolytic pathway that recognizes ubiquitin as a degradation signal. In *The Journal of biological chemistry* 270 (29), pp. 17442–17456. DOI: 10.1074/jbc.270.29.17442.

Johnsson, N.; Varshavsky, A. (1994): Split ubiquitin as a sensor of protein interactions in vivo. In *Proceedings of the National Academy of Sciences of the United States of America* 91 (22), pp. 10340–10344. DOI: 10.1073/pnas.91.22.10340.

Jones, R. M.; Mortusewicz, O.; Afzal, I.; Lorvellec, M.; García, P.; Helleday, T.; Petermann, E. (2013): Increased replication initiation and conflicts with transcription underlie Cyclin E-induced replication stress. In *Oncogene* 32 (32), pp. 3744–3753. DOI: 10.1038/onc.2012.387.

Kaiho-Soma, Ai; Akizuki, Yoshino; Igarashi, Katsuhide; Endo, Akinori; Shoda, Takuji; Kawase, Yasuko et al. (2021): TRIP12 promotes small-molecule-induced degradation through K29/K48-branched ubiquitin chains. In *Molecular Cell* 81 (7), 1411-1424.e7. DOI: 10.1016/j.molcel.2021.01.023.

Kanao, Rie; Masutani, Chikahide (2017): Regulation of DNA damage tolerance in mammalian cells by post-translational modifications of PCNA. In *Mutation research* 803-805, pp. 82–88. DOI: 10.1016/j.mrfmmm.2017.06.004.

Kang, Hyun Je; Park, Hyun; Yoo, Eun Jin; Lee, Jun Ho; Choi, Soo Youn; Lee-Kwon, Whaseon et al. (2019): TonEBP Regulates PCNA Polyubiquitination in Response to DNA Damage through Interaction with SHPRH and USP1. In *iScience* 19, pp. 177–190. DOI: 10.1016/j.isci.2019.07.021.

Kanu, N.; Zhang, T.; Burrell, R. A.; Chakraborty, A.; Cronshaw, J.; DaCosta, C. et al. (2016): RAD18, WRNIP1 and ATMIN promote ATM signalling in response to replication stress. In *Oncogene* 35 (30), pp. 4009–4019. DOI: 10.1038/onc.2015.427.

Kelsall, Ian R.; Zhang, Jiazhen; Knebel, Axel; Arthur, J. Simon C.; Cohen, Philip (2019): The E3 ligase HOIL-1 catalyses ester bond formation between ubiquitin and components of the Myddosome in mammalian cells. In *Proceedings of the National Academy of Sciences of the United States of America* 116 (27), pp. 13293–13298. DOI: 10.1073/pnas.1905873116.

Khoury, George A.; Baliban, Richard C.; Floudas, Christodoulos A. (2011): Proteome-wide post-translational modification statistics: frequency analysis and curation of the swiss-prot database. In *Scientific reports* 1. DOI: 10.1038/srep00090.

Kim, Woong; Bennett, Eric J.; Huttlin, Edward L.; Guo, Ailan; Li, Jing; Possemato, Anthony et al. (2011): Systematic and quantitative assessment of the ubiquitin-modified proteome. In *Molecular Cell* 44 (2), pp. 325–340. DOI: 10.1016/j.molcel.2011.08.025.

Kirisako, Takayoshi; Kamei, Kiyoko; Murata, Shigeo; Kato, Michiko; Fukumoto, Hiromi; Kanie, Masato et al. (2006): A ubiquitin ligase complex assembles linear polyubiquitin chains. In *The EMBO journal* 25 (20), pp. 4877–4887. DOI: 10.1038/sj.emboj.7601360.

Kirkpatrick, Donald S.; Hathaway, Nathaniel A.; Hanna, John; Elsasser, Suzanne; Rush, John; Finley, Daniel et al. (2006): Quantitative analysis of in vitro ubiquitinated cyclin B1 reveals complex chain topology. In *Nature cell biology* 8 (7), pp. 700–710. DOI: 10.1038/ncb1436.

Koegl, M.; Hoppe, T.; Schlenker, S.; Ulrich, H. D.; Mayer, T. U.; Jentsch, S. (1999): A novel ubiquitination factor, E4, is involved in multiubiquitin chain assembly. In *Cell* 96 (5), pp. 635–644. DOI: 10.1016/s0092-8674(00)80574-7.

Komander, David; Rape, Michael (2012): The ubiquitin code. In *Annual review of biochemistry* 81, pp. 203–229. DOI: 10.1146/annurev-biochem-060310-170328.

Komander, David; Reyes-Turcu, Francisca; Licchesi, Julien D. F.; Odenwaelder, Peter; Wilkinson, Keith D.; Barford, David (2009): Molecular discrimination of structurally equivalent Lys 63-linked and linear polyubiquitin chains. In *EMBO reports* 10 (5), pp. 466–473. DOI: 10.1038/embor.2009.55.

Krieg, Adam J.; Hammond, Ester M.; Giaccia, Amato J. (2006): Functional analysis of p53 binding under differential stresses. In *Molecular and cellular biology* 26 (19), pp. 7030–7045. DOI: 10.1128/MCB.00322-06.

Krokan, Hans E.; Bjørås, Magnar (2013): Base excision repair. In *Cold Spring Harbor perspectives in biology* 5 (4), a012583. DOI: 10.1101/cshperspect.a012583.

Lai, Z.; Ferry, K. V.; Diamond, M. A.; Wee, K. E.; Kim, Y. B.; Ma, J. et al. (2001): Human mdm2 mediates multiple mono-ubiquitination of p53 by a mechanism requiring enzyme isomerization. In *The Journal of biological chemistry* 276 (33), pp. 31357–31367. DOI: 10.1074/jbc.M011517200.

Lange, Sven M.; McFarland, Matthew R.; Lamoliatte, Frederic; Kwaśna, Dominika; Shen, Linnan; Wallace, Iona et al. (2023): Comprehensive approach to study branched ubiquitin chains reveals roles for K48-K63 branches in VCP/p97-related processes. In *Biorxiv*, Article https://doi.org/10.1101/2023.01.10.523363.

Lanz, Michael Charles; Dibitetto, Diego; Smolka, Marcus Bustamante (2019): DNA damage kinase signaling: checkpoint and repair at 30 years. In *The EMBO journal* 38 (18), e101801. DOI: 10.15252/embj.2019101801.

Lau, Wilson C. Y.; Li, Yinyin; Zhang, Qinfen; Huen, Michael S. Y. (2015): Molecular architecture of the Ub-PCNA/Pol η complex bound to DNA. In *Scientific reports* 5, p. 15759. DOI: 10.1038/srep15759.

Lechtenberg, Bernhard C.; Rajput, Akhil; Sanishvili, Ruslan; Dobaczewska, Małgorzata K.; Ware, Carl F.; Mace, Peter D.; Riedl, Stefan J. (2016): Structure of a HOIP/E2~ubiquitin complex reveals RBR E3 ligase mechanism and regulation. In *Nature* 529 (7587), pp. 546–550. DOI: 10.1038/nature16511.

Lee, D. H.; Goldberg, A. L. (1998): Proteasome inhibitors: valuable new tools for cell biologists. In *Trends in cell biology* 8 (10), pp. 397–403. DOI: 10.1016/s0962-8924(98)01346-4.

Lee, Sangho; Tsai, Yien Che; Mattera, Rafael; Smith, William J.; Kostelansky, Michael S.; Weissman, Allan M. et al. (2006): Structural basis for ubiquitin recognition and autoubiquitination by Rabex-5. In *Nature structural & molecular biology* 13 (3), pp. 264–271. DOI: 10.1038/nsmb1064.

Lemaçon, Delphine; Jackson, Jessica; Quinet, Annabel; Brickner, Joshua R.; Li, Shan; Yazinski, Stephanie et al. (2017): MRE11 and EXO1 nucleases degrade reversed forks and elicit MUS81-dependent fork rescue in BRCA2-deficient cells. In *Nature Communications* 8 (1), p. 860. DOI: 10.1038/s41467-017-01180-5.

Lerner, Leticia K.; Francisco, Guilherme; Soltys, Daniela T.; Rocha, Clarissa R. R.; Quinet, Annabel; Vessoni, Alexandre T. et al. (2017): Predominant role of DNA polymerase eta and p53-dependent translesion synthesis in the survival of ultraviolet-irradiated human cells. In *Nucleic acids research* 45 (3), pp. 1270–1280. DOI: 10.1093/nar/gkw1196.

Leuzzi, Giuseppe; Marabitti, Veronica; Pichierri, Pietro; Franchitto, Annapaola (2016): WRNIP1 protects stalled forks from degradation and promotes fork restart after replication stress. In *The EMBO journal* 35 (13), pp. 1437–1451. DOI: 10.15252/embj.201593265.

Li, Yanchang; Dammer, Eric B.; Gao, Yuan; Lan, Qiuyan; Villamil, Mark A.; Duong, Duc M. et al. (2019): Proteomics Links Ubiquitin Chain Topology Change to Transcription Factor Activation. In *Molecular Cell* 76 (1), 126-137.e7. DOI: 10.1016/j.molcel.2019.07.001.

Liang, Ruei-Yue; Chen, Li; Ko, Bo-Ting; Shen, Yu-Han; Li, Yen-Te; Chen, Bo-Rong et al. (2014): Rad23 interaction with the proteasome is regulated by phosphorylation of its ubiquitin-like (UbL) domain. In *Journal of molecular biology* 426 (24), pp. 4049–4060. DOI: 10.1016/j.jmb.2014.10.004.

Lim, Kah Suan; Li, Heng; Roberts, Emma A.; Gaudiano, Emily F.; Clairmont, Connor; Sambel, Larissa Alina et al. (2018): USP1 Is Required for Replication Fork Protection in BRCA1-Deficient Tumors. In *Molecular Cell* 72 (6), 925-941.e4. DOI: 10.1016/j.molcel.2018.10.045.

Lindström, Mikael S.; Jurada, Deana; Bursac, Sladana; Orsolic, Ines; Bartek, Jiri; Volarevic, Sinisa (2018): Nucleolus as an emerging hub in maintenance of genome stability and cancer pathogenesis. In *Oncogene* 37 (18), pp. 2351–2366. DOI: 10.1038/s41388-017-0121-z.

Liu, Shengqin; Opiyo, Stephen O.; Manthey, Karoline; Glanzer, Jason G.; Ashley, Amanda K.; Amerin, Courtney et al. (2012): Distinct roles for DNA-PK, ATM and ATR in RPA phosphorylation and checkpoint activation in response to replication stress. In *Nucleic acids research* 40 (21), pp. 10780–10794. DOI: 10.1093/nar/gks849.

Liu, W.; Krishnamoorthy, A.; Zhao, R.; Cortez, D. (2020): Two replication fork remodeling pathways generate nuclease substrates for distinct fork protection factors. In *Science advances* 6 (46). DOI: 10.1126/sciadv.abc3598.

Liu, Xiaoping; Xu, Bosen; Yang, Jianguo; He, Lin; Zhang, Zihan; Cheng, Xiao et al. (2021): UHRF2 commissions the completion of DNA demethylation through allosteric activation by 5hmC and K33-linked ubiquitination of XRCC1. In *Molecular Cell* 81 (14), 2960-2974.e7. DOI: 10.1016/j.molcel.2021.05.022.

Lu, Chunwan; Yang, Dafeng; Sabbatini, Maria E.; Colby, Aaron H.; Grinstaff, Mark W.; Oberlies, Nicholas H. et al. (2018): Contrasting roles of H3K4me3 and H3K9me3 in regulation of apoptosis and gemcitabine resistance in human pancreatic cancer cells. In *BMC cancer* 18 (1), p. 149. DOI: 10.1186/s12885-018-4061-y.

Lu, Ying; Lee, Byung-Hoon; King, Randall W.; Finley, Daniel; Kirschner, Marc W. (2015): Substrate degradation by the proteasome: a single-molecule kinetic analysis. In *Science (New York, N.Y.)* 348 (6231), p. 1250834. DOI: 10.1126/science.1250834.

MacDougall, Christina A.; Byun, Tony S.; Van, Christopher; Yee, Muh-ching; Cimprich, Karlene A. (2007): The structural determinants of checkpoint activation. In *Genes & development* 21 (8), pp. 898–903. DOI: 10.1101/gad.1522607.

Maga, G.; Villani, G.; Tillement, V.; Stucki, M.; Locatelli, G. A.; Frouin, I. et al. (2001): Okazaki fragment processing: modulation of the strand displacement activity of DNA polymerase delta by the concerted action of replication protein A, proliferating cell nuclear antigen, and flap endonuclease-1. In *Proceedings of the National Academy of Sciences of the United States of America* 98 (25), pp. 14298–14303. DOI: 10.1073/pnas.251193198.

Magnaghi, Paola; D'Alessio, Roberto; Valsasina, Barbara; Avanzi, Nilla; Rizzi, Simona; Asa, Daniela et al. (2013): Covalent and allosteric inhibitors of the ATPase VCP/p97 induce cancer cell death. In *Nature chemical biology* 9 (9), pp. 548–556. DOI: 10.1038/nchembio.1313.

Markkanen, Enni (2017): Not breathing is not an option: How to deal with oxidative DNA damage. In *DNA repair* 59, pp. 82–105. DOI: 10.1016/j.dnarep.2017.09.007.

Martin, Sara K.; Wood, Richard D. (2019): DNA polymerase ζ in DNA replication and repair. In *Nucleic acids research* 47 (16), pp. 8348–8361. DOI: 10.1093/nar/gkz705.

Martinez-Fonts, Kirby; Davis, Caroline; Tomita, Takuya; Elsasser, Suzanne; Nager, Andrew R.; Shi, Yuan et al. (2020): The proteasome 19S cap and its ubiquitin receptors provide a versatile recognition platform for substrates. In *Nature Communications* 11 (1), p. 477. DOI: 10.1038/s41467-019-13906-8.

Masuda, Yuji; Mitsuyuki, Satoshi; Kanao, Rie; Hishiki, Asami; Hashimoto, Hiroshi; Masutani, Chikahide (2018): Regulation of HLTF-mediated PCNA polyubiquitination by RFC and PCNA monoubiquitination levels determines choice of damage tolerance pathway. In *Nucleic acids research* 46 (21), pp. 11340–11356. DOI: 10.1093/nar/gky943.

Matsumoto, Marissa L.; Dong, Ken C.; Yu, Christine; Phu, Lilian; Gao, Xinxin; Hannoush, Rami N. et al. (2012): Engineering and structural characterization of a linear polyubiquitin-specific antibody. In *Journal of molecular biology* 418 (3-4), pp. 134–144. DOI: 10.1016/j.jmb.2011.12.053.

Matsumoto, Marissa L.; Wickliffe, Katherine E.; Dong, Ken C.; Yu, Christine; Bosanac, Ivan; Bustos, Daisy et al. (2010): K11-linked polyubiquitination in cell cycle control revealed by a K11

linkage-specific antibody. In *Molecular Cell* 39 (3), pp. 477–484. DOI: 10.1016/j.molcel.2010.07.001.

Maxwell, Brian A.; Gwon, Youngdae; Mishra, Ashutosh; Peng, Junmin; Nakamura, Haruko; Zhang, Ke et al. (2021): Ubiquitination is essential for recovery of cellular activities after heat shock. In *Science (New York, N.Y.)* 372 (6549), eabc3593. DOI: 10.1126/science.abc3593.

Maya-Mendoza, Apolinar; Moudry, Pavel; Merchut-Maya, Joanna Maria; Lee, MyungHee; Strauss, Robert; Bartek, Jiri (2018): High speed of fork progression induces DNA replication stress and genomic instability. In *Nature* 559 (7713), pp. 279–284. DOI: 10.1038/s41586-018-0261-5.

McClellan, Amie J.; Laugesen, Sophie Heiden; Ellgaard, Lars (2019): Cellular functions and molecular mechanisms of non-lysine ubiquitination. In *Open biology* 9 (9), p. 190147. DOI: 10.1098/rsob.190147.

McCullough, John; Row, Paula E.; Lorenzo, Oscar; Doherty, Mary; Beynon, Robert; Clague, Michael J.; Urbé, Sylvie (2006): Activation of the endosome-associated ubiquitin isopeptidase AMSH by STAM, a component of the multivesicular body-sorting machinery. In *Current biology : CB* 16 (2), pp. 160–165. DOI: 10.1016/j.cub.2005.11.073.

Meerang, Mayura; Ritz, Danilo; Paliwal, Shreya; Garajova, Zuzana; Bosshard, Matthias; Mailand, Niels et al. (2011): The ubiquitin-selective segregase VCP/p97 orchestrates the response to DNA double-strand breaks. In *Nature cell biology* 13 (11), pp. 1376–1382. DOI: 10.1038/ncb2367.

Meyer, Hemmo; Bug, Monika; Bremer, Sebastian (2012): Emerging functions of the VCP/p97 AAA-ATPase in the ubiquitin system. In *Nature cell biology* 14 (2), pp. 117–123. DOI: 10.1038/ncb2407.

Meyer, Hemmo; van den Boom, Johannes (2023): Targeting of client proteins to the VCP/p97/Cdc48 unfolding machine. In *Frontiers in molecular biosciences* 10, p. 1142989. DOI: 10.3389/fmolb.2023.1142989.

Meyer, Hemmo; Weihl, Conrad C. (2014): The VCP/p97 system at a glance: connecting cellular function to disease pathogenesis. In *Journal of cell science* 127 (Pt 18), pp. 3877–3883. DOI: 10.1242/jcs.093831.

Meyer, Hermann-Josef; Rape, Michael (2014): Enhanced protein degradation by branched ubiquitin chains. In *Cell* 157 (4), pp. 910–921. DOI: 10.1016/j.cell.2014.03.037.

Meza Gutierrez, Fernando; Simsek, Deniz; Mizrak, Arda; Deutschbauer, Adam; Braberg, Hannes; Johnson, Jeffrey et al. (2018): Genetic analysis reveals functions of atypical polyubiquitin chains. In *eLife* 7. DOI: 10.7554/eLife.42955.

Michel, Martin A.; Komander, David; Elliott, Paul R. (2018): Enzymatic Assembly of Ubiquitin Chains. In *Methods in molecular biology (Clifton, N.J.)* 1844, pp. 73–84. DOI: 10.1007/978-1-4939-8706-1_6.

Michel, Martin A.; Swatek, Kirby N.; Hospenthal, Manuela K.; Komander, David (2017): Ubiquitin Linkage-Specific Affimers Reveal Insights into K6-Linked Ubiquitin Signaling. In *Molecular Cell* 68 (1), 233-246.e5. DOI: 10.1016/j.molcel.2017.08.020.

Moore, Chandler E.; Yalcindag, Selin E.; Czeladko, Hanna; Ravindranathan, Ramya; Wijesekara Hanthi, Yodhara; Levy, Juliana C. et al. (2023): RFWD3 promotes ZRANB3 recruitment to regulate the remodeling of stalled replication forks. In *The Journal of cell biology* 222 (5). DOI: 10.1083/jcb.202106022.

Moreno, Olga María; Paredes, Angela Camila; Suarez-Obando, Fernando; Rojas, Adriana (2021): An update on Fanconi anemia: Clinical, cytogenetic and molecular approaches (Review). In *Biomedical reports* 15 (3), p. 74. DOI: 10.3892/br.2021.1450.

Morris, Joanna R.; Solomon, Ellen (2004): BRCA1 : BARD1 induces the formation of conjugated ubiquitin structures, dependent on K6 of ubiquitin, in cells during DNA replication and repair. In *Human molecular genetics* 13 (8), pp. 807–817. DOI: 10.1093/hmg/ddh095.

Motegi, Akira; Liaw, Hung-Jiun; Lee, Kyoo-Young; Roest, Henk P.; Maas, Alex; Wu, Xiaoli et al. (2008): Polyubiquitination of proliferating cell nuclear antigen by HLTF and SHPRH prevents genomic instability from stalled replication forks. In *Proceedings of the National Academy of Sciences of the United States of America* 105 (34), pp. 12411–12416. DOI: 10.1073/pnas.0805685105.

Murakumo, Y.; Ogura, Y.; Ishii, H.; Numata, S.; Ichihara, M.; Croce, C. M. et al. (2001): Interactions in the error-prone postreplication repair proteins hREV1, hREV3, and hREV7. In *The Journal of biological chemistry* 276 (38), pp. 35644–35651. DOI: 10.1074/jbc.M102051200.

Mutreja, Karun; Krietsch, Jana; Hess, Jeannine; Ursich, Sebastian; Berti, Matteo; Roessler, Fabienne K. et al. (2018): ATR-Mediated Global Fork Slowing and Reversal Assist Fork Traverse and Prevent Chromosomal Breakage at DNA Interstrand Cross-Links. In *Cell reports* 24 (10), 2629-2642.e5. DOI: 10.1016/j.celrep.2018.08.019.

Nakao, Fumihiko; Setoguchi, Kiyoko; Semba, Yuichiro; Yamauchi, Takuji; Nogami, Jumpei; Sasaki, Kensuke et al. (2023): Targeting a mitochondrial E3 ubiquitin ligase complex to overcome AML cell-intrinsic Venetoclax resistance. In *Leukemia* 37 (5), pp. 1028–1038. DOI: 10.1038/s41375-023-01879-z.

Newton, Kim; Matsumoto, Marissa L.; Wertz, Ingrid E.; Kirkpatrick, Donald S.; Lill, Jennie R.; Tan, Jenille et al. (2008): Ubiquitin chain editing revealed by polyubiquitin linkage-specific antibodies. In *Cell* 134 (4), pp. 668–678. DOI: 10.1016/j.cell.2008.07.039.

Nibe, Yoichi; Oshima, Shigeru; Kobayashi, Masanori; Maeyashiki, Chiaki; Matsuzawa, Yu; Otsubo, Kana et al. (2018): Novel polyubiquitin imaging system, PolyUb-FC, reveals that K33-linked polyubiquitin is recruited by SQSTM1/p62. In *Autophagy* 14 (2), pp. 347–358. DOI: 10.1080/15548627.2017.1407889.

Niikura, Yohei; Kitagawa, Risa; Fang, Lei; Kitagawa, Katsumi (2019): CENP-A Ubiquitylation Is Indispensable to Cell Viability. In *Developmental cell* 50 (6), 683-689.e6. DOI: 10.1016/j.devcel.2019.07.015.

Nijman, Sebastian M. B.; Huang, Tony T.; Dirac, Annette M. G.; Brummelkamp, Thijn R.; Kerkhoven, Ron M.; D'Andrea, Alan D.; Bernards, René (2005): The deubiquitinating enzyme USP1 regulates the Fanconi anemia pathway. In *Molecular Cell* 17 (3), pp. 331–339. DOI: 10.1016/j.molcel.2005.01.008.

Nowotny, Marcin (2019): Crosslink and shield: protecting abasic sites from error-prone repair. In *Nature structural & molecular biology* 26 (7), pp. 530–532. DOI: 10.1038/s41594-019-0264-4.

Ohashi, Eiji; Murakumo, Yoshiki; Kanjo, Naoko; Akagi, Jun-Ichi; Masutani, Chikahide; Hanaoka, Fumio; Ohmori, Haruo (2004): Interaction of hREV1 with three human Y-family DNA polymerases. In *Genes to cells : devoted to molecular & cellular mechanisms* 9 (6), pp. 523–531. DOI: 10.1111/j.1356-9597.2004.00747.x.

Ohtake, Fumiaki; Saeki, Yasushi; Ishido, Satoshi; Kanno, Jun; Tanaka, Keiji (2016): The K48-K63 Branched Ubiquitin Chain Regulates NF-κB Signaling. In *Molecular Cell* 64 (2), pp. 251–266. DOI: 10.1016/j.molcel.2016.09.014.

Ohtake, Fumiaki; Tsuchiya, Hikaru; Saeki, Yasushi; Tanaka, Keiji (2018): K63 ubiquitylation triggers proteasomal degradation by seeding branched ubiquitin chains. In *Proceedings of the National Academy of Sciences of the United States of America* 115 (7), E1401-E1408. DOI: 10.1073/pnas.1716673115.

Okatsu, Kei; Koyano, Fumika; Kimura, Mayumi; Kosako, Hidetaka; Saeki, Yasushi; Tanaka, Keiji; Matsuda, Noriyuki (2015): Phosphorylated ubiquitin chain is the genuine Parkin receptor. In *The Journal of cell biology* 209 (1), pp. 111–128. DOI: 10.1083/jcb.201410050.

Oltion, Keely; Carelli, Jordan D.; Yang, Tangpo; See, Stephanie K.; Wang, Hao-Yuan; Kampmann, Martin; Taunton, Jack (2023): An E3 ligase network engages GCN1 to promote the degradation of translation factors on stalled ribosomes. In *Cell* 186 (2), 346-362.e17. DOI: 10.1016/j.cell.2022.12.025.

Ong, Shao-En; Mann, Matthias (2006): A practical recipe for stable isotope labeling by amino acids in cell culture (SILAC). In *Nature protocols* 1 (6), pp. 2650–2660. DOI: 10.1038/nprot.2006.427.

Ordureau, Alban; Heo, Jin-Mi; Duda, David M.; Paulo, Joao A.; Olszewski, Jennifer L.; Yanishevski, David et al. (2015): Defining roles of PARKIN and ubiquitin phosphorylation by PINK1 in mitochondrial quality control using a ubiquitin replacement strategy. In *Proceedings of the National Academy of Sciences of the United States of America* 112 (21), pp. 6637–6642. DOI: 10.1073/pnas.1506593112.

Orlando, V. (2000): Mapping chromosomal proteins in vivo by formaldehyde-crosslinked-chromatin immunoprecipitation. In *Trends in biochemical sciences* 25 (3), pp. 99–104. DOI: 10.1016/s0968-0004(99)01535-2.

Panzarino, Nicholas J.; Krais, John J.; Cong, Ke; Peng, Min; Mosqueda, Michelle; Nayak, Sumeet U. et al. (2021): Replication Gaps Underlie BRCA Deficiency and Therapy Response. In *Cancer research* 81 (5), pp. 1388–1397. DOI: 10.1158/0008-5472.CAN-20-1602.

Park, Su Hyung; Kang, Nalae; Song, Eunho; Wie, Minwoo; Lee, Eun A.; Hwang, Sunyoung et al. (2019): ATAD5 promotes replication restart by regulating RAD51 and PCNA in response to replication stress. In *Nature Communications* 10 (1), p. 5718. DOI: 10.1038/s41467-019-13667-4.

Park, Yoon; Yoon, Sungjoo Kim; Yoon, Jong-Bok (2009): The HECT domain of TRIP12 ubiquitinates substrates of the ubiquitin fusion degradation pathway. In *The Journal of biological chemistry* 284 (3), pp. 1540–1549. DOI: 10.1074/jbc.M807554200.

Parker, Matthew W.; Botchan, Michael R.; Berger, James M. (2017): Mechanisms and regulation of DNA replication initiation in eukaryotes. In *Critical reviews in biochemistry and molecular biology* 52 (2), pp. 107–144. DOI: 10.1080/10409238.2016.1274717.

Peng, Junmin; Schwartz, Daniel; Elias, Joshua E.; Thoreen, Carson C.; Cheng, Dongmei; Marsischky, Gerald et al. (2003): A proteomics approach to understanding protein ubiquitination. In *Nature biotechnology* 21 (8), pp. 921–926. DOI: 10.1038/nbt849.

Petermann, Eva; Orta, Manuel Luís; Issaeva, Natalia; Schultz, Niklas; Helleday, Thomas (2010): Hydroxyurea-stalled replication forks become progressively inactivated and require two different

RAD51-mediated pathways for restart and repair. In *Molecular Cell* 37 (4), pp. 492–502. DOI: 10.1016/j.molcel.2010.01.021.

Piberger, Ann Liza; Bowry, Akhil; Kelly, Richard D. W.; Walker, Alexandra K.; González-Acosta, Daniel; Bailey, Laura J. et al. (2020): PrimPol-dependent single-stranded gap formation mediates homologous recombination at bulky DNA adducts. In *Nature Communications* 11 (1), p. 5863. DOI: 10.1038/s41467-020-19570-7.

Pickart, C. M. (1997): Targeting of substrates to the 26S proteasome. In *FASEB journal : official publication of the Federation of American Societies for Experimental Biology* 11 (13), pp. 1055–1066. DOI: 10.1096/fasebj.11.13.9367341.

Pluska, Lukas; Jarosch, Ernst; Zauber, Henrik; Kniss, Andreas; Waltho, Anita; Bagola, Katrin et al. (2021): The UBA domain of conjugating enzyme Ubc1/Ube2K facilitates assembly of K48/K63-branched ubiquitin chains. In *The EMBO journal* 40 (6), e106094. DOI: 10.15252/embj.2020106094.

Porebski, Bartlomiej; Wild, Sebastian; Kummer, Sandra; Scaglione, Sarah; Gaillard, Pierre-Henri L.; Gari, Kerstin (2019): WRNIP1 Protects Reversed DNA Replication Forks from SLX4-Dependent Nucleolytic Cleavage. In *iScience* 21, pp. 31–41. DOI: 10.1016/j.isci.2019.10.010.

Postow, Lisa; Funabiki, Hironori (2013): An SCF complex containing Fbxl12 mediates DNA damage-induced Ku80 ubiquitylation. In *Cell cycle (Georgetown, Tex.)* 12 (4), pp. 587–595. DOI: 10.4161/cc.23408.

Powers, Kyle T.; Lavering, Emily D.; Washington, M. Todd (2018): Conformational Flexibility of Ubiquitin-Modified and SUMO-Modified PCNA Shown by Full-Ensemble Hybrid Methods. In *Journal of molecular biology* 430 (24), pp. 5294–5303. DOI: 10.1016/j.jmb.2018.10.017.

Pratt, Matthew R.; Schwartz, Edmund C.; Muir, Tom W. (2007): Small-molecule-mediated rescue of protein function by an inducible proteolytic shunt. In *Proceedings of the National Academy of Sciences of the United States of America* 104 (27), pp. 11209–11214. DOI: 10.1073/pnas.0700816104.

Przetocka, Sara; Porro, Antonio; Bolck, Hella A.; Walker, Christina; Lezaja, Aleksandra; Trenner, Anika et al. (2018): CtIP-Mediated Fork Protection Synergizes with BRCA1 to Suppress Genomic Instability upon DNA Replication Stress. In *Molecular Cell* 72 (3), 568-582.e6. DOI: 10.1016/j.molcel.2018.09.014.

Qian, Shu-Bing; Ott, David E.; Schubert, Ulrich; Bennink, Jack R.; Yewdell, Jonathan W. (2002): Fusion proteins with COOH-terminal ubiquitin are stable and maintain dual functionality in vivo. In *The Journal of biological chemistry* 277 (41), pp. 38818–38826. DOI: 10.1074/jbc.M205547200.

Qin, Weihua; Steinek, Clemens; Kolobynina, Ksenia; Forné, Ignasi; Imhof, Axel; Cardoso, M. Cristina; Leonhardt, Heinrich (2022): Probing protein ubiquitination in live cells. In *Nucleic acids research* 50 (21), e125. DOI: 10.1093/nar/gkac805.

Qin, Zhoushuai; Bai, Zhiqiang; Sun, Ying; Niu, Xiaohong; Xiao, Wei (2016): PCNA-Ub polyubiquitination inhibits cell proliferation and induces cell-cycle checkpoints. In *Cell cycle (Georgetown, Tex.)* 15 (24), pp. 3390–3401. DOI: 10.1080/15384101.2016.1245247.

Quinet, Annabel; Carvajal-Maldonado, Denisse; Lemacon, Delphine; Vindigni, Alessandro (2017): DNA Fiber Analysis: Mind the Gap! In *Methods in enzymology* 591, pp. 55–82. DOI: 10.1016/bs.mie.2017.03.019.

Quinet, Annabel; Tirman, Stephanie; Cybulla, Emily; Meroni, Alice; Vindigni, Alessandro (2021): To skip or not to skip: choosing repriming to tolerate DNA damage. In *Molecular Cell* 81 (4), pp. 649–658. DOI: 10.1016/j.molcel.2021.01.012.

Quinet, Annabel; Tirman, Stephanie; Jackson, Jessica; Šviković, Saša; Lemaçon, Delphine; Carvajal-Maldonado, Denisse et al. (2020): PRIMPOL-Mediated Adaptive Response Suppresses Replication Fork Reversal in BRCA-Deficient Cells. In *Molecular Cell* 77 (3), 461-474.e9. DOI: 10.1016/j.molcel.2019.10.008.

Raducanu, Vlad-Stefan; Tehseen, Muhammad; Al-Amodi, Amani; Joudeh, Luay I.; Biasio, Alfredo de; Hamdan, Samir M. (2022): Mechanistic investigation of human maturation of Okazaki fragments reveals slow kinetics. In *Nature Communications* 13 (1), p. 6973. DOI: 10.1038/s41467-022-34751-2.

Ravid, Tommer; Hochstrasser, Mark (2007): Autoregulation of an E2 enzyme by ubiquitin-chain assembly on its catalytic residue. In *Nature cell biology* 9 (4), pp. 422–427. DOI: 10.1038/ncb1558.

Ren, Xingjie; Yang, Zhihao; Mao, Decai; Chang, Zai; Qiao, Huan-Huan; Wang, Xia et al. (2014): Performance of the Cas9 nickase system in Drosophila melanogaster. In *G3 (Bethesda, Md.)* 4 (10), pp. 1955–1962. DOI: 10.1534/g3.114.013821.

Renz, Christian; Albanèse, Véronique; Tröster, Vera; Albert, Thomas K.; Santt, Olivier; Jacobs, Susan C. et al. (2020): Ubc13-Mms2 cooperates with a family of RING E3 proteins in budding yeast membrane protein sorting. In *Journal of cell science* 133 (10). DOI: 10.1242/jcs.244566.

Richard, Thibaud J. C.; Herzog, Laura K.; Vornberger, Julia; Rahmanto, Aldwin Suryo; Sangfelt, Olle; Salomons, Florian A.; Dantuma, Nico P. (2020): K63-linked ubiquitylation induces global sequestration of mitochondria. In *Scientific reports* 10 (1), p. 22334. DOI: 10.1038/s41598-020-78845-7.

Ryan, M. D.; King, A. M.; Thomas, G. P. (1991): Cleavage of foot-and-mouth disease virus polyprotein is mediated by residues located within a 19 amino acid sequence. In *The Journal of general virology* 72 (Pt 11), pp. 2727–2732. DOI: 10.1099/0022-1317-72-11-2727.

Sakano, K.; Oikawa, S.; Hasegawa, K.; Kawanishi, S. (2001): Hydroxyurea induces site-specific DNA damage via formation of hydrogen peroxide and nitric oxide. In *Japanese journal of cancer research : Gann* 92 (11), pp. 1166–1174. DOI: 10.1111/j.1349-7006.2001.tb02136.x.

Salas-Lloret, Daniel; García-Rodríguez, Néstor; Giebel, Lisanne; Ru, Arnoud de; van Veelen, Peter; Huertas, Pablo et al. (2023): BRCA1/BARD1 ubiquitinates PCNA in unperturbed conditions to promote replication fork stability and continuous DNA synthesis. DOI: 10.1101/2023.01.12.523782.

Salvador, J-Pablo; Vilaplana, Lluïsa; Marco, M-Pilar (2019): Nanobody: outstanding features for diagnostic and therapeutic applications. In *Analytical and bioanalytical chemistry* 411 (9), pp. 1703–1713. DOI: 10.1007/s00216-019-01633-4.

Sato, Yusuke; Fujita, Hiroaki; Yoshikawa, Azusa; Yamashita, Masami; Yamagata, Atsushi; Kaiser, Stephen E. et al. (2011): Specific recognition of linear ubiquitin chains by the Npl4 zinc finger (NZF) domain of the HOIL-1L subunit of the linear ubiquitin chain assembly complex. In *Proceedings of the National Academy of Sciences of the United States of America* 108 (51), pp. 20520–20525. DOI: 10.1073/pnas.1109088108.

Saugar, Irene; Parker, Joanne L.; Zhao, Shengkai; Ulrich, Helle D. (2012): The genome maintenance factor Mgs1 is targeted to sites of replication stress by ubiquitylated PCNA. In *Nucleic acids research* 40 (1), pp. 245–257. DOI: 10.1093/nar/gkr738.

Schärer, Orlando D. (2013): Nucleotide excision repair in eukaryotes. In *Cold Spring Harbor perspectives in biology* 5 (10), a012609. DOI: 10.1101/cshperspect.a012609.

Schrecker, Marina; Castaneda, Juan C.; Devbhandari, Sujan; Kumar, Charanya; Remus, Dirk; Hite, Richard K. (2022): Multistep loading of a DNA sliding clamp onto DNA by replication factor C. In *eLife* 11. DOI: 10.7554/eLife.78253.

Schwertman, Petra; Bekker-Jensen, Simon; Mailand, Niels (2016): Regulation of DNA double-strand break repair by ubiquitin and ubiquitin-like modifiers. In *Nature reviews. Molecular cell biology* 17 (6), pp. 379–394. DOI: 10.1038/nrm.2016.58.

Sedgwick, Barbara; Lindahl, Tomas (2002): Recent progress on the Ada response for inducible repair of DNA alkylation damage. In *Oncogene* 21 (58), pp. 8886–8894. DOI: 10.1038/sj.onc.1205998.

Seelinger, Mareike; Otterlei, Marit (2020): Helicase-Like Transcription Factor HLTF and E3 Ubiquitin Ligase SHPRH Confer DNA Damage Tolerance through Direct Interactions with Proliferating Cell Nuclear Antigen (PCNA). In *International journal of molecular sciences* 21 (3). DOI: 10.3390/ijms21030693.

Shachar, Sigal; Ziv, Omer; Avkin, Sharon; Adar, Sheera; Wittschieben, John; Reissner, Thomas et al. (2009): Two-polymerase mechanisms dictate error-free and error-prone translesion DNA synthesis in mammals. In *The EMBO journal* 28 (4), pp. 383–393. DOI: 10.1038/emboj.2008.281.

Sharma, Sudha (2011): Non-B DNA Secondary Structures and Their Resolution by RecQ Helicases. In *Journal of nucleic acids* 2011, p. 724215. DOI: 10.4061/2011/724215.

Shi, Jie; Hauschulte, Kristine; Mikicic, Ivan; Maharjan, Srijana; Arz, Valerie; Strauch, Tina et al. (2023): Nuclear myosin VI maintains replication fork stability. In *Nature Communications* 14 (1), p. 3787. DOI: 10.1038/s41467-023-39517-y.

Shin, Ji Yeong; Muniyappan, Srinivasan; Tran, Non-Nuoc; Park, Hyeonjeong; Lee, Sung Bae; Lee, Byung-Hoon (2020): Deubiquitination Reactions on the Proteasome for Proteasome Versatility. In *International journal of molecular sciences* 21 (15). DOI: 10.3390/ijms21155312.

Shin, M. E.; Ogburn, K. D.; Varban, O. A.; Gilbert, P. M.; Burd, C. G. (2001): FYVE domain targets Pib1p ubiquitin ligase to endosome and vacuolar membranes. In *The Journal of biological chemistry* 276 (44), pp. 41388–41393. DOI: 10.1074/jbc.M105665200.

Simoneau, Antoine; Engel, Justin L.; Bandi, Madhavi; Lazarides, Katherine; Liu, Shangtao; Meier, Samuel R. et al. (2023): Ubiquitinated PCNA Drives USP1 Synthetic Lethality in Cancer. In *Molecular cancer therapeutics* 22 (2), pp. 215–226. DOI: 10.1158/1535-7163.MCT-22-0409.

Sims, Joshua J.; Cohen, Robert E. (2009): Linkage-specific avidity defines the lysine 63-linked polyubiquitin-binding preference of rap80. In *Molecular Cell* 33 (6), pp. 775–783. DOI: 10.1016/j.molcel.2009.02.011.

Sims, Joshua J.; Scavone, Francesco; Cooper, Eric M.; Kane, Lesley A.; Youle, Richard J.; Boeke, Jef D.; Cohen, Robert E. (2012): Polyubiquitin-sensor proteins reveal localization and linkage-type dependence of cellular ubiquitin signaling. In *Nature methods* 9 (3), pp. 303–309. DOI: 10.1038/nmeth.1888.

Singer, B.; Hang, B. (1997): What structural features determine repair enzyme specificity and mechanism in chemically modified DNA? In *Chemical research in toxicology* 10 (7), pp. 713–732. DOI: 10.1021/tx970011e.

Smit, Judith J.; Monteferrario, Davide; Noordermeer, Sylvie M.; van Dijk, Willem J.; van der Reijden, Bert A; Sixma, Titia K. (2012): The E3 ligase HOIP specifies linear ubiquitin chain assembly through its RING-IBR-RING domain and the unique LDD extension. In *The EMBO journal* 31 (19), pp. 3833–3844. DOI: 10.1038/emboj.2012.217.

Smit, Judith J.; van Dijk, Willem J.; El Atmioui, Dris; Merkx, Remco; Ovaa, Huib; Sixma, Titia K. (2013): Target specificity of the E3 ligase LUBAC for ubiquitin and NEMO relies on different minimal requirements. In *The Journal of biological chemistry* 288 (44), pp. 31728–31737. DOI: 10.1074/jbc.M113.495846.

Socha, Anna; Di Yang; Bulsiewicz, Alicja; Yaprianto, Kelvin; Kupculak, Marian; Liang, Chih-Chao et al. (2020): WRNIP1 Is Recruited to DNA Interstrand Crosslinks and Promotes Repair. In *Cell reports* 32 (1), p. 107850. DOI: 10.1016/j.celrep.2020.107850.

Sogo, José M.; Lopes, Massimo; Foiani, Marco (2002): Fork reversal and ssDNA accumulation at stalled replication forks owing to checkpoint defects. In *Science (New York, N.Y.)* 297 (5581), pp. 599–602. DOI: 10.1126/science.1074023.

Somyajit, Kumar; Spies, Julian; Coscia, Fabian; Kirik, Ufuk; Rask, Maj-Britt; Lee, Ji-Hoon et al. (2021): Homology-directed repair protects the replicating genome from metabolic assaults. In *Developmental cell* 56 (4), 461-477.e7. DOI: 10.1016/j.devcel.2021.01.011.

Soutoglou, Evi; Misteli, Tom (2008): Activation of the cellular DNA damage response in the absence of DNA lesions. In *Science (New York, N.Y.)* 320 (5882), pp. 1507–1510. DOI: 10.1126/science.1159051.

Srinivasan, Seetha V.; Dominguez-Sola, David; Wang, Lily C.; Hyrien, Olivier; Gautier, Jean (2013): Cdc45 is a critical effector of myc-dependent DNA replication stress. In *Cell reports* 3 (5), pp. 1629–1639. DOI: 10.1016/j.celrep.2013.04.002.

Stelter, Philipp; Ulrich, Helle D. (2003): Control of spontaneous and damage-induced mutagenesis by SUMO and ubiquitin conjugation. In *Nature* 425 (6954), pp. 188–191. DOI: 10.1038/nature01965.

Stewart, Mikaela D.; Ritterhoff, Tobias; Klevit, Rachel E.; Brzovic, Peter S. (2016): E2 enzymes: more than just middle men. In *Cell research* 26 (4), pp. 423–440. DOI: 10.1038/cr.2016.35.

Stingele, Julian; Bellelli, Roberto; Boulton, Simon J. (2017): Mechanisms of DNA-protein crosslink repair. In *Nature reviews. Molecular cell biology* 18 (9), pp. 563–573. DOI: 10.1038/nrm.2017.56.

Taglialatela, Angelo; Alvarez, Silvia; Leuzzi, Giuseppe; Sannino, Vincenzo; Ranjha, Lepakshi; Huang, Jen-Wei et al. (2017): Restoration of Replication Fork Stability in BRCA1- and BRCA2-Deficient Cells by Inactivation of SNF2-Family Fork Remodelers. In *Molecular Cell* 68 (2), 414-430.e8. DOI: 10.1016/j.molcel.2017.09.036.

Takahashi, Tomio S.; Wollscheid, Hans-Peter; Lowther, Jonathan; Ulrich, Helle D. (2020): Effects of chain length and geometry on the activation of DNA damage bypass by polyubiquitylated PCNA. In *Nucleic acids research* 48 (6), pp. 3042–3052. DOI: 10.1093/nar/gkaa053.

Tanaka, Keiji (2009): The proteasome: overview of structure and functions. In *Proceedings of the Japan Academy. Series B, Physical and biological sciences* 85 (1), pp. 12–36. DOI: 10.2183/pjab.85.12.

Temviriyanukul, Piya; van Hees-Stuivenberg, Sandrine; Delbos, Frédéric; Jacobs, Heinz; Wind, Niels de; Jansen, Jacob G. (2012): Temporally distinct translesion synthesis pathways for ultraviolet light-induced photoproducts in the mammalian genome. In *DNA repair* 11 (6), pp. 550–558. DOI: 10.1016/j.dnarep.2012.03.007.

Thakar, Tanay; Leung, Wendy; Nicolae, Claudia M.; Clements, Kristen E.; Shen, Binghui; Bielinsky, Anja-Katrin; Moldovan, George-Lucian (2020): Ubiquitinated-PCNA protects replication forks from DNA2-mediated degradation by regulating Okazaki fragment maturation and chromatin assembly. In *Nature Communications* 11 (1), p. 2147. DOI: 10.1038/s41467-020-16096-w.

Thrower, J. S.; Hoffman, L.; Rechsteiner, M.; Pickart, C. M. (2000): Recognition of the polyubiquitin proteolytic signal. In *The EMBO journal* 19 (1), pp. 94–102. DOI: 10.1093/emboj/19.1.94.

Tian, Tian; Bu, Min; Chen, Xu; Ding, Linli; Yang, Yulan; Han, Jinhua et al. (2021): The ZATT-TOP2A-PICH Axis Drives Extensive Replication Fork Reversal to Promote Genome Stability. In *Molecular Cell* 81 (1), 198-211.e6. DOI: 10.1016/j.molcel.2020.11.007.

Tiede, Christian; Bedford, Robert; Heseltine, Sophie J.; Smith, Gina; Wijetunga, Imeshi; Ross, Rebecca et al. (2017): Affimer proteins are versatile and renewable affinity reagents. In *eLife* 6. DOI: 10.7554/eLife.24903.

Tirman, Stephanie; Quinet, Annabel; Wood, Matthew; Meroni, Alice; Cybulla, Emily; Jackson, Jessica et al. (2021): Temporally distinct post-replicative repair mechanisms fill PRIMPOL-dependent ssDNA gaps in human cells. In *Molecular Cell* 81 (19), 4026-4040.e8. DOI: 10.1016/j.molcel.2021.09.013.

Tokunaga, Fuminori; Iwai, Kazuhiro (2012): LUBAC, a novel ubiquitin ligase for linear ubiquitination, is crucial for inflammation and immune responses. In *Microbes and infection* 14 (7-8), pp. 563–572. DOI: 10.1016/j.micinf.2012.01.011.

Tokunaga, Fuminori; Nishimasu, Hiroshi; Ishitani, Ryuichiro; Goto, Eiji; Noguchi, Takuya; Mio, Kazuhiro et al. (2012): Specific recognition of linear polyubiquitin by A20 zinc finger 7 is involved in NF-κB regulation. In *The EMBO journal* 31 (19), pp. 3856–3870. DOI: 10.1038/emboj.2012.241.

Toledo, Luis Ignacio; Altmeyer, Matthias; Rask, Maj-Britt; Lukas, Claudia; Larsen, Dorthe Helena; Povlsen, Lou Klitgaard et al. (2013): ATR prohibits replication catastrophe by preventing global exhaustion of RPA. In *Cell* 155 (5), pp. 1088–1103. DOI: 10.1016/j.cell.2013.10.043.

Tonzi, Peter; Yin, Yandong; Lee, Chelsea Wei Ting; Rothenberg, Eli; Huang, Tony T. (2018): Translesion polymerase kappa-dependent DNA synthesis underlies replication fork recovery. In *eLife* 7. DOI: 10.7554/eLife.41426.

Tornaletti, S.; Pfeifer, G. P. (1996): UV damage and repair mechanisms in mammalian cells. In *BioEssays : news and reviews in molecular, cellular and developmental biology* 18 (3), pp. 221–228. DOI: 10.1002/bies.950180309.

Tubbs, Anthony; Nussenzweig, André (2017): Endogenous DNA Damage as a Source of Genomic Instability in Cancer. In *Cell* 168 (4), pp. 644–656. DOI: 10.1016/j.cell.2017.01.002.

Turner, M. K.; Abrams, R.; Lieberman, I. (1966): Meso-alpha, beta-diphenylsuccinate and hydroxyurea as inhibitors of deoxycytidylate synthesis in extracts of Ehrlich ascites and L cells. In *The Journal of biological chemistry* 241 (24), pp. 5777–5780.

Ulrich, Helle D.; Takahashi, Diane T. (2013): Readers of PCNA modifications. In *Chromosoma* 122 (4), pp. 259–274. DOI: 10.1007/s00412-013-0410-4.

Unk, Ildiko; Hajdú, Ildikó; Fátyol, Károly; Szakál, Barnabás; Blastyák, András; Bermudez, Vladimir et al. (2006): Human SHPRH is a ubiquitin ligase for Mms2-Ubc13-dependent polyubiquitylation of proliferating cell nuclear antigen. In *Proceedings of the National Academy of Sciences of the United States of America* 103 (48), pp. 18107–18112. DOI: 10.1073/pnas.0608595103.

Vaz, Bruno; Halder, Swagata; Ramadan, Kristijan (2013): Role of p97/VCP (Cdc48) in genome stability. In *Frontiers in genetics* 4, p. 60. DOI: 10.3389/fgene.2013.00060.

Vijay-Kumar, S.; Bugg, C. E.; Cook, W. J. (1987): Structure of ubiquitin refined at 1.8 A resolution. In *Journal of molecular biology* 194 (3), pp. 531–544. DOI: 10.1016/0022-2836(87)90679-6.

Villamil, Mark; Xiao, Weidi; Yu, Clinton; Huang, Lan; Xu, Ping; Kaiser, Peter (2022): The Ubiquitin Interacting Motif-Like Domain of Met4 Selectively Binds K48 Polyubiquitin Chains. In *Molecular & cellular proteomics : MCP* 21 (1), p. 100175. DOI: 10.1016/j.mcpro.2021.100175.

Vina-Vilaseca, Arnau; Sorkin, Alexander (2010): Lysine 63-linked polyubiquitination of the dopamine transporter requires WW3 and WW4 domains of Nedd4-2 and UBE2D ubiquitin-conjugating enzymes. In *The Journal of biological chemistry* 285 (10), pp. 7645–7656. DOI: 10.1074/jbc.M109.058990.

Vujanovic, Marko; Krietsch, Jana; Raso, Maria Chiara; Terraneo, Nastassja; Zellweger, Ralph; Schmid, Jonas A. et al. (2017): Replication Fork Slowing and Reversal upon DNA Damage Require PCNA Polyubiquitination and ZRANB3 DNA Translocase Activity. In *Molecular Cell* 67 (5), 882-890.e5. DOI: 10.1016/j.molcel.2017.08.010.

Wagner, Sebastian A.; Beli, Petra; Weinert, Brian T.; Nielsen, Michael L.; Cox, Jürgen; Mann, Matthias; Choudhary, Chunaram (2011): A proteome-wide, quantitative survey of in vivo ubiquitylation sites reveals widespread regulatory roles. In *Molecular & cellular proteomics : MCP* 10 (10), M111.013284. DOI: 10.1074/mcp.M111.013284.

Wajant, Harald; Scheurich, Peter (2011): TNFR1-induced activation of the classical NF-κB pathway. In *The FEBS journal* 278 (6), pp. 862–876. DOI: 10.1111/j.1742-4658.2011.08015.x.

Wang, Qiang; Liu, Xing; Cui, Ye; Tang, Yijun; Chen, Wei; Li, Senlin et al. (2014): The E3 ubiquitin ligase AMFR and INSIG1 bridge the activation of TBK1 kinase by modifying the adaptor STING. In *Immunity* 41 (6), pp. 919–933. DOI: 10.1016/j.immuni.2014.11.011.

Wang, Qing; Song, Changcheng; Li, Chou-Chi H. (2003): Hexamerization of p97-VCP is promoted by ATP binding to the D1 domain and required for ATPase and biological activities. In *Biochemical and biophysical research communications* 300 (2), pp. 253–260. DOI: 10.1016/s0006-291x(02)02840-1.

Wang, Qinghua; Young, Patrick; Walters, Kylie J. (2005): Structure of S5a bound to monoubiquitin provides a model for polyubiquitin recognition. In *Journal of molecular biology* 348 (3), pp. 727–739. DOI: 10.1016/j.jmb.2005.03.007.

Wang, Tao; Yin, Luming; Cooper, Eric M.; Lai, Ming-Yih; Dickey, Seth; Pickart, Cecile M. et al. (2009): Evidence for bidentate substrate binding as the basis for the K48 linkage specificity of

otubain 1. In *Journal of molecular biology* 386 (4), pp. 1011–1023. DOI: 10.1016/j.jmb.2008.12.085.

Wegmann, Sabrina; Meister, Cindy; Renz, Christian; Yakoub, George; Wollscheid, Hans-Peter; Takahashi, Diane T. et al. (2022): Linkage reprogramming by tailor-made E3s reveals polyubiquitin chain requirements in DNA-damage bypass. In *Molecular Cell* 82 (8), 1589-1602.e5. DOI: 10.1016/j.molcel.2022.02.016.

Wertz, Ingrid E.; O'Rourke, Karen M.; Zhou, Honglin; Eby, Michael; Aravind, L.; Seshagiri, Somasekar et al. (2004): De-ubiquitination and ubiquitin ligase domains of A20 downregulate NF-kappaB signalling. In *Nature* 430 (7000), pp. 694–699. DOI: 10.1038/nature02794.

Wolf, Lucie M.; Lambert, Annika M.; Haenlin, Julie; Boutros, Michael (2021): EVI/WLS function is regulated by ubiquitylation and is linked to ER-associated degradation by ERLIN2. In *Journal of cell science* 134 (16). DOI: 10.1242/jcs.257790.

Wong, Ronald P.; García-Rodríguez, Néstor; Zilio, Nicola; Hanulová, Mária; Ulrich, Helle D. (2020): Processing of DNA Polymerase-Blocking Lesions during Genome Replication Is Spatially and Temporally Segregated from Replication Forks. In *Molecular Cell* 77 (1), 3-16.e4. DOI: 10.1016/j.molcel.2019.09.015.

Wright, Joshua D.; Mace, Peter D.; Day, Catherine L. (2016): Noncovalent Ubiquitin Interactions Regulate the Catalytic Activity of Ubiquitin Writers. In *Trends in biochemical sciences* 41 (11), pp. 924–937. DOI: 10.1016/j.tibs.2016.08.003.

Wright, William Douglass; Shah, Shanaya Shital; Heyer, Wolf-Dietrich (2018): Homologous recombination and the repair of DNA double-strand breaks. In *The Journal of biological chemistry* 293 (27), pp. 10524–10535. DOI: 10.1074/jbc.TM118.000372.

Wu, Xiao; Liu, Shichang; Sagum, Cari; Chen, Jianji; Singh, Rajesh; Chaturvedi, Apurva et al. (2019): Crosstalk between Lys63- and Lys11-polyubiquitin signaling at DNA damage sites is driven by Cezanne. In *Genes & development* 33 (23-24), pp. 1702–1717. DOI: 10.1101/gad.332395.119.

Xu, Ming; Skaug, Brian; Zeng, Wenwen; Chen, Zhijian J. (2009): A ubiquitin replacement strategy in human cells reveals distinct mechanisms of IKK activation by TNFalpha and IL-1beta. In *Molecular Cell* 36 (2), pp. 302–314. DOI: 10.1016/j.molcel.2009.10.002.

Yamano, Koji; Kikuchi, Reika; Kojima, Waka; Hayashida, Ryota; Koyano, Fumika; Kawawaki, Junko et al. (2020): Critical role of mitochondrial ubiquitination and the OPTN-ATG9A axis in mitophagy. In *The Journal of cell biology* 219 (9). DOI: 10.1083/jcb.201912144.

Yang, Kailin; Moldovan, George-Lucian; D'Andrea, Alan D. (2010): RAD18-dependent recruitment of SNM1A to DNA repair complexes by a ubiquitin-binding zinc finger. In *The Journal of biological chemistry* 285 (25), pp. 19085–19091. DOI: 10.1074/jbc.M109.100032.

Yau, Richard G.; Doerner, Kerstin; Castellanos, Erick R.; Haakonsen, Diane L.; Werner, Achim; Wang, Nan et al. (2017): Assembly and Function of Heterotypic Ubiquitin Chains in Cell-Cycle and Protein Quality Control. In *Cell* 171 (4), 918-933.e20. DOI: 10.1016/j.cell.2017.09.040.

Yewdell, J. W. (2001): Not such a dismal science: the economics of protein synthesis, folding, degradation and antigen processing. In *Trends in cell biology* 11 (7), pp. 294–297. DOI: 10.1016/s0962-8924(01)02030-x.

Yoon, Jung-Hoon; Acharya, Narottam; Park, Jeseong; Basu, Debashree; Prakash, Satya; Prakash, Louise (2014): Identification of two functional PCNA-binding domains in human DNA polymerase κ. In *Genes to cells : devoted to molecular & cellular mechanisms* 19 (7), pp. 594–601. DOI: 10.1111/gtc.12156.

Yoon, Jung-Hoon; Bhatia, Gita; Prakash, Satya; Prakash, Louise (2010): Error-free replicative bypass of thymine glycol by the combined action of DNA polymerases kappa and zeta in human cells. In *Proceedings of the National Academy of Sciences of the United States of America* 107 (32), pp. 14116–14121. DOI: 10.1073/pnas.1007795107.

You-Wei Zhang; Diane M. Otterness; Gary G. Chiang; Weilin Xie; Yun-Cai Liu; Frank Mercurio; Robert T. Abraham (2005): Genotoxic Stress Targets Human Chk1 for Degradation by the Ubiquitin-Proteasome Pathway. In *Molecular Cell* 19 (5), pp. 607–618. DOI: 10.1016/j.molcel.2005.07.019.

Yu, Guimei; Bai, Yunpeng; Li, Kunpeng; Amarasinghe, Ovini; Jiang, Wen; Zhang, Zhong-Yin (2021): Cryo-electron microscopy structures of VCP/p97 reveal a new mechanism of oligomerization regulation. In *iScience* 24 (11), p. 103310. DOI: 10.1016/j.isci.2021.103310.

Yuan, Wei-Chien; Lee, Yu-Ru; Lin, Shu-Yu; Chang, Li-Ying; Tan, Yen Pei; Hung, Chin-Chun et al. (2014): K33-Linked Polyubiquitination of Coronin 7 by Cul3-KLHL20 Ubiquitin E3 Ligase Regulates Protein Trafficking. In *Molecular Cell* 54 (4), pp. 586–600. DOI: 10.1016/j.molcel.2014.03.035.

Yun, Maximina H.; Hiom, Kevin (2009): CtIP-BRCA1 modulates the choice of DNA double-strand-break repair pathway throughout the cell cycle. In *Nature* 459 (7245), pp. 460–463. DOI: 10.1038/nature07955.

Zellweger, Ralph; Dalcher, Damian; Mutreja, Karun; Berti, Matteo; Schmid, Jonas A.; Herrador, Raquel et al. (2015): Rad51-mediated replication fork reversal is a global response to genotoxic treatments in human cells. In *The Journal of cell biology* 208 (5), pp. 563–579. DOI: 10.1083/jcb.201406099.

Zeman, Michelle K.; Cimprich, Karlene A. (2014): Causes and consequences of replication stress. In *Nature cell biology* 16 (1), pp. 2–9. DOI: 10.1038/ncb2897.

Zeman, Michelle K.; Lin, Jia-Ren; Freire, Raimundo; Cimprich, Karlene A. (2014): DNA damage-specific deubiquitination regulates Rad18 functions to suppress mutagenesis. In *The Journal of cell biology* 206 (2), pp. 183–197. DOI: 10.1083/jcb.201311063.

Zhang, Meng; Wang, Lijuan; Zhong, Dongping (2017): Photolyase: Dynamics and Mechanisms of Repair of Sun-Induced DNA Damage. In *Photochemistry and photobiology* 93 (1), pp. 78–92. DOI: 10.1111/php.12695.

Zhang, Shuwen; Zou, Shitao; Yin, Deyao; Zhao, Lihong; Finley, Daniel; Wu, Zhaolong; Mao, Youdong (2022): USP14-regulated allostery of the human proteasome by time-resolved cryo-EM. In *Nature* 605 (7910), pp. 567–574. DOI: 10.1038/s41586-022-04671-8.

Zhang, Tianpeng; Rawal, Yashpal; Jiang, Haoyang; Kwon, Youngho; Sung, Patrick; Greenberg, Roger A. (2023): Break-induced replication orchestrates resection-dependent template switching. In *Nature*. DOI: 10.1038/s41586-023-06177-3.

Zhao, Shengkai; Ulrich, Helle D. (2010): Distinct consequences of posttranslational modification by linear versus K63-linked polyubiquitin chains. In *Proceedings of the National Academy of*

Sciences of the United States of America 107 (17), pp. 7704–7709. DOI: 10.1073/pnas.0908764107.

Zheng, Ning; Shabek, Nitzan (2017): Ubiquitin Ligases: Structure, Function, and Regulation. In *Annual review of biochemistry* 86, pp. 129–157. DOI: 10.1146/annurev-biochem-060815-014922.

Zhou, Mengying; Fang, Rui; Colson, Louis; Donovan, Katherine; Hunkeler, Moritz; Song, Yuyu et al. (2023): HUWE1 Amplifies Ubiquitin Modifications to Broadly Stimulate Clearance of Proteins and Aggregates. In *Biorxiv*. DOI: 10.1101/2023.05.30.542866.

Zhu, Lu; Jorgensen, Jeff R.; Li, Ming; Chuang, Ya-Shan; Emr, Scott D. (2017): ESCRTs function directly on the lysosome membrane to downregulate ubiquitinated lysosomal membrane proteins. In *eLife* 6. DOI: 10.7554/eLife.26403.

Zucchelli, Silvia; Codrich, Marta; Marcuzzi, Federica; Pinto, Milena; Vilotti, Sandra; Biagioli, Marta et al. (2010): TRAF6 promotes atypical ubiquitination of mutant DJ-1 and alpha-synuclein and is localized to Lewy bodies in sporadic Parkinson's disease brains. In *Human molecular genetics* 19 (19), pp. 3759–3770. DOI: 10.1093/hmg/ddq290.

Zuin, Alice; Isasa, Marta; Crosas, Bernat (2014): Ubiquitin signaling: extreme conservation as a source of diversity. In *Cells* 3 (3), pp. 690–701. DOI: 10.3390/cells3030690.